



HEINRICH HEINE
UNIVERSITÄT DÜSSELDORF

Uptake of the dipeptide-like antibiotic negamycin into bacterial cells

Inaugural-Dissertation

zur Erlangung des Doktorgrades

der Mathematisch-Naturwissenschaftlichen Fakultät

der Heinrich-Heine-Universität Düsseldorf

vorgelegt von

Catherine Schumacher

aus

Darmstadt

Düsseldorf, 18.12.2015

Aus dem Institut für pharmazeutische Biologie und Biotechnologie
der Heinrich-Heine-Universität Düsseldorf

Gedruckt mit der Genehmigung der
Mathematisch-Naturwissenschaftlichen Fakultät der
Heinrich-Heine-Universität Düsseldorf

Referent: Prof. Dr. Heike Brötz-Oesterhelt

Korreferent: Prof. Dr. Peter Proksch

Tag der mündlichen Prüfung: 11.02.2016

„So eine Arbeit wird eigentlich nie fertig, man muss sie für fertig erklären, wenn man nach der Zeit und den Umständen das möglichste getan hat.“
Johann Wolfgang von Goethe (*1749, †1832)

Eidesstattliche Erklärung

Ich versichere an Eides Statt, dass die Dissertation von mir selbständig und ohne unzulässige fremde Hilfe unter Beachtung der „Grundsätze zur Sicherung guter wissenschaftlicher Praxis an der Heinrich-Heine-Universität Düsseldorf“ erstellt worden ist. Diese Dissertation wurde in der vorgelegten oder einer ähnlichen Form noch bei keiner anderen Institution eingereicht und es wurden bisher keine erfolglosen Promotionsversuche von mir unternommen.

Düsseldorf, den 18.12.2015

List of Content

Eidesstattliche Erklärung	IV
List of Abbreviations.....	VIII
Zusammenfassung.....	XI
Abstract	XIII
1 Introduction	15
1.1 <i>Antibiotics and antibiotic resistance</i>	15
1.2 <i>Cell wall and cell membranes-permeability barriers</i>	17
1.2.1 The bacterial cell wall.....	18
1.2.1.1 The Gram-negative outer membrane	18
1.2.1.1.1 Porins	19
1.2.2 The cytoplasmic membrane.....	20
1.2.2.1 The membrane potential, the pH-gradient and the proton motive force	21
1.2.2.2 ABC transporter (ATP-binding cassette transporter).....	23
1.2.2.2.1 Oligopeptide permease Opp	24
1.2.2.2.2 Dipeptide Permease Dpp	25
1.2.2.2.3 Sap (Sensitive to antimicrobial peptides) transporter	25
1.2.2.3 Proton-dependent oligopeptide transporter (POT).....	26
1.3 <i>Antibiotic uptake</i>	27
1.3.1 Different uptake mechanisms.....	27
1.3.1.1 Aminoglycoside uptake.....	27
1.3.1.2 Tetracycline uptake	28
1.3.1.3 Quinolone uptake	29
1.4 <i>Negamycin - an underexplored peptide-like antibiotic</i>	30
1.4.1 Sperabillin – an antibacterial agent structurally related to negamycin	32
1.5 <i>Escherichia coli as a model organism</i>	33
1.6 <i>Goal of the thesis</i>	34
2 Results	35
2.1 <i>Characterization of negamycin activity</i>	35
2.1.1 Negamycin activity in different strains and media	35
2.1.2 Azidonegamycin activity in different strains and media	36
2.1.3 Bactericidal activity of negamycin	37
2.1.4 Mode of action.....	38
2.2 <i>Side-project: Sperabillin activity</i>	40
2.2.1 Sperabillin activity in different strains and media	40
2.2.2 Sperabillins: Mode of action	42
2.3 <i>Negamycin passage across the outer membrane</i>	43
2.3.1 The outer membrane as a rate-limiting barrier	44
2.3.2 Involvement of porins in negamycin uptake.....	44
2.3.3 Susceptibility of the LPS-mutant “rough-phenotype”	45
2.4 <i>Negamycin passage across the cytoplasmic membrane</i>	47
2.4.1 Uptake via peptide transporter.....	47
2.4.1.1 Complementation of JW3513 (Δ dppA).....	55
2.4.1.2 Construction of periplasmic binding protein double- and triple-knockouts in E. coli JW351356	

2.4.1.3	Characterization of the constructed double and triple knockouts (Δ dppA- Δ oppA, Δ dppA- Δ sapA, and Δ dppA- Δ sapA- Δ oppA).....	60
2.4.1.4	Comparison of strains with intact and deleted resistance cassette	64
2.4.1.5	Expression of different ABC transporter periplasmic-binding proteins in <i>E. coli</i> JW3513 (Δ dppA), JW1235 (Δ oppA), JW1287 (Δ sapA).....	66
2.4.2	Uptake of negamycin via lysine-uptake systems	67
2.4.3	Isolation and characterization of negamycin resistant clones	69
2.4.3.1	Susceptibility profile	70
2.4.3.2	Growth and morphology studies	74
2.4.3.3	Sequencing of the dpp-operon	77
2.5	<i>Influence of salts on negamycin activity</i>	79
2.5.1	Complexation of divalent cations	80
2.5.2	Localization of the Ca^{2+} -effect.....	82
2.6	<i>Influence of pH on negamycin activity</i>	84
2.6.1	Growth of <i>E. coli</i> BW25113 under different pH conditions	85
2.6.2	Negamycin killing in relation to pH	86
2.6.3	Negamycin distribution between charged and uncharged species depending on pH.....	87
2.6.4	Influence of CCCP on negamycin activity	90
2.6.5	Negamycin activity in membrane energy mutants	92
2.7	<i>Negamycin as a possible efflux-substrate</i>	94
3	Discussion	96
3.1	<i>Negamycin and sperabillin activity</i>	96
3.2	<i>Passage of negamycin across the outer membrane</i>	97
3.3	<i>Passage of negamycin across the cytoplasmic membrane</i>	99
3.4	<i>Ca^{2+}-complexation by negamycin</i>	103
3.5	<i>Alkaline pH increases negamycin activity</i>	105
3.6	<i>Negamycin: a substrate of the TolC-efflux pump</i>	106
4	Conclusion and proposed negamycin uptake-model	107
5	Material and Methods	111
5.1	<i>Material</i>	111
5.1.1	Chemicals	111
5.1.2	Antibiotics	114
5.1.3	Kits	115
5.1.4	Enzymes	115
5.1.5	DNA-Ladder.....	116
5.1.6	Bacterial Strains	117
5.1.7	Synthetic Oligonucleotides	124
5.1.8	Plasmids	130
5.1.9	Media	131
5.1.10	Solutions and Buffers	135
5.1.11	Laboratory equipment	137
5.1.11.1	Software	138
5.2	<i>Methods</i>	139
5.2.1	Microbiology methods	139
5.2.1.1	Culturing of bacteria	139
5.2.1.2	Minimal inhibition concentration (MIC) determination	139

5.2.1.2.1	Broth Microdilution method	139
5.2.1.2.2	Agar dilution method	140
5.2.1.3	Growth curves	140
5.2.1.4	Killing curves	141
5.2.1.5	Resistance rate determination	141
5.2.2	Molecular Biology Methods	141
5.2.2.1	DNA isolation	141
5.2.2.2	Plasmid isolation	142
5.2.2.3	DNA sequencing	142
5.2.2.4	Computer supported sequence analysis	142
5.2.2.5	DNA amplification via the <u>P</u> olymerase <u>C</u> hain <u>R</u> eaction (PCR)	142
5.2.2.6	Purification of PCR products	144
5.2.2.7	DNA digest with restriction endonucleases	144
5.2.2.8	Agarose gel electrophoresis	145
5.2.2.9	Gel purification	145
5.2.2.10	Dephosphorylation of vectors	145
5.2.2.11	Ligation of two DNA Fragments	146
5.2.2.12	Preparation of electrocompetent cells	146
5.2.2.13	Transformation of electrocompetent cells	146
5.2.2.14	Single-gene knockout (Datsenko & Wanner)	147
5.2.2.15	RNA isolation	148
5.2.2.16	cDNA synthesis	149
5.2.2.17	Quantitative real-time-PCR (qPCR)	149
5.2.3	<i>in vitro</i> Assays	151
5.2.3.1	Promoter assay (Urban et al.)	151
5.2.3.2	Miscoding assay	152
5.2.3.3	Transcription-translation assay (TraLa-Assay)	152
5.2.4	Analytical methods	153
5.2.4.1	Thin layer chromatography (TLC)	153
5.2.4.2	Isothermal titration calorimetry (ITC)	153
List of Tables		154
List of Figures		156
Bibliography		159
Supplements		170
<i>Supplemental Data</i>		170
Alignments of periplasmic binding proteins		170
Plasmid-maps		174
Alignments of constructed knockouts		182
<i>Curriculum vitae</i>		184
<i>Publications</i>		186
<i>Acknowledgements</i>		188

List of Abbreviations

AA	<u>A</u> mino <u>a</u> cids
ABC transporter	<u>A</u> TP- <u>b</u> inding <u>c</u> assette transporter
Amp	<u>A</u> mpicillin
ATP	<u>A</u> denosine 5'- <u>t</u> riphosphate
bp	<u>B</u> ase <u>p</u> air
BSA	<u>B</u> ovine <u>s</u> erum <u>a</u> lbumin
Ca ²⁺	Calcium
CCCP	<u>C</u> arbonyl <u>c</u> yanide <u>m</u> - <u>c</u> hloro <u>p</u> henylhydrazone
CFU	<u>C</u> olony <u>f</u> orming <u>u</u> nits
Cm	<u>C</u> hloro <u>a</u> mphenicol
CoA	<u>C</u> oenzym <u>A</u>
CP	<u>P</u> hospho <u>c</u> reatine
CPK	<u>C</u> reatine <u>p</u> hospho <u>k</u> inase
CTP	<u>C</u> ytidine <u>t</u> riphosphate
DiBAC ₄ (3)	Bis-(1,3-dibutylbarbituric acid) trimethine oxonol
Dpp	<u>D</u> i <u>p</u> eptide <u>p</u> ermease
DTT	<u>D</u> ithio <u>t</u> hreitol
EDPI/II	<u>E</u> nergy- <u>d</u> e <u>p</u> endent- <u>p</u> hase I/II
GTP	<u>G</u> uanosine <u>t</u> riphosphate
h34	<u>H</u> elix <u>34</u>
i.e.	<u>I</u> d <u>e</u> st
IC ₅₀ value	Half maximal inhibitory concentration
ITC	<u>I</u> sothermal <u>t</u> itration <u>c</u> alorimetry
IVTT	<i><u>I</u>n <u>v</u>itro <u>t</u>ranscription <u>t</u>ranslation</i>
KOAc	Potassium acetate
KPO4	Potassium phosphate

LB	<u>L</u> ysogeny <u>b</u> roth
LPS	<u>L</u> ipopolysaccharide
MFS	<u>M</u> ajor <u>f</u> acilitator <u>s</u> uperfamily
Mg ²⁺	Magnesium
MH	<u>M</u> ueller- <u>H</u> inton
MIC	<u>M</u> inimal <u>I</u> nhibition <u>C</u> oncentration
MQ	<u>M</u> illi- <u>Q</u> water (ultrapure water of Type 1)
N ⁺	Sodium
NGS	<u>N</u> ext generation <u>s</u> equencing
NRTC	<u>N</u> o- <u>r</u> everse <u>t</u> ranscription <u>c</u> ontrols
NTC	<u>N</u> o- <u>t</u> emplate <u>c</u> ontrols
Opp	<u>O</u> ligopeptide <u>p</u> ermease
ORF	<u>O</u> pen <u>r</u> eading <u>f</u> rame
PCR	<u>P</u> olymerase <u>C</u> hain <u>R</u> eaction
PEG	<u>P</u> oly <u>e</u> thylene glycol 6000
PEP	<u>P</u> hospho <u>e</u> no <u>l</u> pyruvate
PMBN	<u>P</u> olymyxin- <u>B</u> - <u>n</u> ona <u>p</u> eptide
PMF	<u>P</u> roton <u>M</u> otive <u>F</u> orce
PMSF	<u>P</u> henyl <u>m</u> ethane <u>s</u> ulfonyl <u>f</u> luoride
POT	<u>P</u> roton dependend oligopeptide <u>t</u> ransporter
PP	0.5% <u>p</u> olypeptone
PUT	<u>P</u> utrescine
qPCR	<u>Q</u> uantitative real-time <u>P</u> CR
Rf	<u>R</u> etardation <u>f</u> actor
RND	<u>R</u> esistance-modulation <u>d</u> ivision
ROM	<u>R</u> ead- <u>O</u> ut <u>M</u> ix
RT	<u>R</u> everse <u>T</u> ranscriptase
Sap	<u>S</u> ensitive to <u>a</u> ntimicrobial <u>p</u> eptides

TAE-Buffer	<u>T</u> ris- <u>A</u> cetate- <u>E</u> DTA buffer
TC	<u>T</u> emplate <u>C</u> ontrol
TLC	<u>T</u> hin <u>l</u> ayer <u>c</u> hromatography
TPP ⁺	<u>T</u> etraphenylphosphonium bromide, phenyl-3H
TraLa	<u>T</u> ranscription- <u>T</u> ransl <u>a</u> tion Assay
UTP	<u>U</u> ridine <u>t</u> riphosphate
WHO	<u>W</u> orld <u>H</u> ealth <u>O</u> rganization

Zusammenfassung

Infektionserkrankungen und das ansteigende Vorkommen von Antibiotika-resistenten Keimen zählen zu den größten Gesundheitsproblematiken der heutigen Zeit. Inzwischen gehören sie zu den sechst-häufigsten Todesursachen in Europa [1]. Die Entdeckung und Entwicklung neuer antibakterieller Substanzen ist sehr mühsam und schwer, was dazu führt, dass kaum neue Substanzen in den Pipelines sind [2]. Zwischen 1962 und dem Jahr 2000 wurden keine neue Antibiotikaklassen auf den Markt gebracht, obwohl immer mehr resistente Keime aufkamen [3]. Die größte Herausforderung ist es jedoch neue Antibiotika gegen Gram-negative Bakterien zu finden und zu entwickeln. Neben der Cytoplasmamembran besitzen diese eine zweite Barriere, die äußere Membran. Viele Wirkstoffe, die gegen Gram-positive Keime wirken, sind inaktiv gegen Gram-negative Bakterien. Bei vielen dieser Wirkstoffe ist dies darauf zurück zu führen, dass die Substanzen nicht in der Lage sind, die äußere Membran zu überwinden [2]. Diese alarmierenden Fakten heben hervor, wie dringend und groß der Bedarf an neuen und innovativen Wirkstoffen ist, die sowohl gegen Gram-positive als auch gegen Gram-negative Bakterien wirken.

Eine vielversprechende Substanz, in diesem Zusammenhang, ist das Pseudopeptid Negamycin. Es wurde erstmalig aus dem Kulturfiltrat eines *Streptomyces* isoliert, der dem Stamm *Streptomyces purpeofuscus* sehr ähnlich ist [4]. Es zeigt sowohl gegen Gram-positive als auch gegen Gram-negative Bakterien, zum Beispiel *Escherichia coli*, *Pseudomonas aeruginosa* und *Staphylococcus aureus*, bakterizide Aktivität [4]. Hieraus lässt sich schließen, dass Negamycin in der Lage ist die äußere Membran und die Cytoplasmamembran zu überwinden. Für die Substanz wurde eine geringe Toxizität und vielversprechende pharmakokinetische Eigenschaften beschrieben [4, 5], was sie zu einem interessanten Kandidaten für eine mögliche, therapeutische Anwendung macht. Negamycin hemmt die Protein-Biosynthese, indem es die Ribosomen-Translokation und Polysomen-Stabilisierung inhibiert, sowie „miscoding“ verursacht [6-13]. Über die Aufnahme dieser hydrophilen und geladenen Substanz in die Zelle war jedoch zu Beginn dieser Doktorarbeit nur wenig bekannt.

Das Ziel dieser Arbeit war es den Aufnahmemechanismus von Negamycin zu untersuchen, und Erkenntnisse darüber zu gewinnen, welche Eigenschaften eine Substanz besitzen muss, um effizient in Gram-negative Bakterien zu gelangen. Aus den gewonnenen Ergebnissen und Erkenntnissen konnte ein Negamycin-Aufnahme Modell erstellt werden.

Ein Großteil der Aufnahmestudien wurde in dem Modellorganismus *Escherichia coli* durchgeführt. Es konnte gezeigt werden, dass die Aufnahme von Negamycin in die bakterielle Zelle sehr komplex ist. Negamycin nutzt verschiedene Wege um in die Zelle zu gelangen, was das Risiko der Entstehung von Hochresistenz durch Mutation eines einzelnen Transporters minimiert. Die vergleichsweise geringe Resistenzrate konnte dies bestätigen. Die Penetration der äußeren Membran kann durch verschiedene Wege erfolgen. Zum einen nutzt Negamycin Porine um über die äußere Membran zu gelangen. Die Aufnahme über

Porine erfolgt hauptsächlich über OmpN, ein Porin für das bisher noch keine Beteiligung an Antibiotika-Aufnahme beschrieben wurde [14]. Die Molekülstruktur von Negamycin legt nahe, dass auch "Self-promoted uptake" einen Aufnahmeweg für Negamycin darstellen könnte. Bei pH-Werten um 8,5, bei denen ein nennenswerter Prozentsatz von Negamycin netto neutral (zwitterionisch) vorliegt, trägt möglicherweise auch passive Diffusion zu einem kleinen Anteil der Aufnahme bei. Auch um die zweite Barriere, die Cytoplasmamembran, zu überqueren, nutzt Negamycin verschiedene Routen. In Peptid-freiem Medium ist der Haupttransportweg die Dipeptid Permease Dpp. Auch beobachteten wir bei Deletionsmutanten des Protonen-abhängigen Peptidtransporters YbgH eine verringerte Negamycin Aufnahme. Negamycin gelingt es jedoch sogar in Abwesenheit von Dpp und in Peptid-haltigen Medien, in dem die Nahrungspeptide mit Negamycin um die Aufnahme an Peptidtransportern konkurrieren, in die Zelle zu gelangen. Dies weist darauf hin, dass Negamycin noch mindestens eine weitere Aufnahmeroute, neben den Peptidtransportern, nutzen kann. Es konnte gezeigt werden, dass die Medien-Bedingungen einen großen Einfluss auf die Negamycin-Aktivität haben. In Standard-Testmedien konnte immer nur eine moderate Wirkung gemessen werden. In dieser Arbeit wurde gezeigt, dass die Zugabe von Ca^{2+} die Negamycin-Aktivität stark verbessert. Negamycin und Ca^{2+} formen einen Komplex, was zu einer gesteigerten Interaktion mit negativ geladenen Phospholipiden führt. Des Weiteren ist die Wirkung bei pH 8.5 deutlich besser als bei neutralem pH. Zum einen wird eine Aminoglykosid-ähnliche Aufnahme vermutet, bei der der Proton motive force (pmf) die treibende Kraft ist, und zum anderen eine passive Aufnahme. Überschlagsrechnungen legen nahe, dass etwa zwei Drittel der Negamycin-Moleküle bei diesem pH als Zwitterion vorliegen. Zu einem geringen Teil liegt Negamycin auch ungeladen vor, ein Ladungszustand der grundsätzlich auch eine passive Aufnahme der Substanz möglich macht. Die Kombination beider förderlichen Bedingung, die Zugabe von Ca^{2+} und pH 8.5, führte zu einer 32-fachen Wirkungssteigerung in *E. coli*, und auch in den pathogenen Problemkeimen *P. aeruginosa* und *S. aureus* konnte unter diesen Bedingungen eine minimale Hemmkonzentration von 4 $\mu\text{g}/\text{ml}$ gemessen werden. Die Ergebnisse dieser Arbeit zeigen, dass die antibakterielle Potenz von Negamycin unter Standard-Testbedingungen deutlich unterschätzt wird, und dass insbesondere für intrazellulär wirkende Antibiotika gegen Gram-negative Bakterien ein Verständnis des Aufnahme-Mechanismus unabdingbar ist, um eine Substanz zielgerichtet optimieren zu können.

Abstract

Infectious diseases and the increase of antibiotic resistant strains are one of the main health issues we are facing today. In fact infectious diseases are the sixth major cause of death in Europe [1], and this is aggravated by the fact that discovery and development of novel antibiotics face many challenges and pipelines are empty [2]. Accordingly, between 1962 and 2000 no new antibiotic classes were introduced into the market [3]. The discovery and development of new antibiotics against Gram-negative bacteria is particularly problematic. They carry, besides the cytoplasmic membrane, an additional barrier, the outer-membrane. Consequently, antibiotics active against Gram-positive bacteria are often inactive against Gram-negative bacteria, due to their incapacity of penetrating this additional barrier [2]. In this context the discovery of new antibiotics, active against Gram-positive and Gram-negative bacteria, with new modes of action is an urgent therapeutic need.

A promising antibacterial compound is negamycin, a pseudopeptide that was first obtained from culture filtrates of *Streptomyces* strains, closely related to *Streptomyces purpeofuscus* [4]. Negamycin is active against Gram-positive and Gram-negative bacteria including *Escherichia coli*, *Pseudomonas aeruginosa* and *Staphylococcus aureus* [4], implying that negamycin is able to cross both penetration barriers, the outer membrane and the cytoplasmic membrane. Furthermore it showed low toxicity and promising pharmacokinetic properties [4, 5], which makes it interesting for therapeutic purposes. Negamycin was shown to target protein biosynthesis, by inhibiting ribosome translocation, polysome stabilization and miscoding [6-13]. However, the mechanism of uptake of this hydrophilic, positively charged compound into bacterial cells was scarcely investigated at the start of this PhD project.

The aim of this work was to study the uptake of negamycin and to learn from nature the characteristics that render an antibiotic able to pass both the outer and the cytoplasmic membrane. On the basis of results of this work, a negamycin-uptake model was established. Entry-studies, performed in the model organism *E. coli*, demonstrated that the uptake of negamycin into the bacterial cell is very complex, and that the antibiotic enters the cell, using different uptake routes. This reduces the risk of developing high-level resistance by mutating a single transporter, as the comparatively low resistance rate for negamycin indicates.

The uptake across the outer membrane occurs mainly *via* a porin-mediated route. The molecule structure of negamycin indicates that a “self-promoted-uptake” might be a possible route as well. A passive-diffusion-mediated uptake should be considered too, as a minority of negamycin molecules is uncharged, which allows, in general, a passive uptake of a molecule. It was shown that negamycin can pass the first barrier by using the porin OmpN, a minor porin that was never described as a route for antibiotic-uptake before [14]. The second barrier, the cytoplasmic membrane, negamycin can cross via multiple routes. The dipeptide permease Dpp was identified as the main entry route in peptide-free medium.

Furthermore, reduced negamycin uptake was observed in knock-out mutants of the proton-dependent peptide transporter YbgH. However, negamycin is able to enter the cytoplasm even in the absence of functional Dpp or in pepton broth, which is rich in outcompeting nutrient peptides, indicating an additional entry option besides peptide transporters.

The antibacterial activity of negamycin depends strongly on the culture medium and in standard media only moderate activity was described for negamycin. In this work, the presence of Ca^{2+} was demonstrated to strongly improve the activity of negamycin against both Gram-negative and Gram-positive bacteria. Furthermore, it was shown that Ca^{2+} forms a complex with negamycin and facilitates the interaction with negatively charged phospholipids. The antibacterial activity is also improved at basic pH. An aminoglycoside-like-uptake might be possible. The driving force would be the pmf. Furthermore a small amount of negamycin will enter the cytoplasm via passive diffusion. A simplified equation, which gives a rough estimation of how many molecules are charged at a certain pH, indicates that roughly two-thirds of negamycin molecules are zwitterionic at pH 8.5, which could lead to facilitated passive uptake under this condition. The combination of both beneficial conditions, namely the presence of Ca^{2+} and pH 8.5, resulted in a 32-fold improvement of sensitivity in *E. coli* and led to a minimal inhibitory concentration in the pathogens *P. aeruginosa* and *S. aureus* of 4 $\mu\text{g}/\text{ml}$. These findings show that the antibacterial potency of negamycin is strongly underestimated, when tested under standard MIC assay conditions. The present study also shows that for an antibiotic that acts in the cytoplasm of Gram-negative bacteria understanding the uptake mechanism is crucial towards a rational approach of structure optimization.

1 Introduction

1.1 Antibiotics and antibiotic resistance

“Antibiotics are molecules that stop microbes [...] from growing or kill them outright”[15]. This definition, by C. Walsh, widens the original one, that described antibiotics just as small molecules synthesized by microorganism [16], and includes synthetic and semi-synthetic compounds. Different antibiotic classes can be distinguished, which are active against a variety of targets.

The major target areas for antibacterial actions are: 1. inhibition of cell wall synthesis, 2. inhibition of DNA or RNA synthesis, 3. inhibition of protein synthesis, 4. inhibition of folate synthesis and 5. membrane-activity. β -lactam antibiotics, vancomycin and teicoplanin belong to the first class. They all inhibit cell wall synthesis, by either targeting the transpeptidases (β -lactams) or by targeting the D-Ala-D-Ala termini of peptidoglycan and of lipid II (vancomycin, teicoplanin). Representatives of the second class are fluoroquinolones and the rifamycin group. Fluoroquinolones target either the DNA gyrase (topoisomerase II) or the topoisomerase IV. Representatives of the rifamycin group target the RNA synthesis, by inhibiting the RNA polymerase. Aminoglycosides, macrolides and tetracyclines act by blocking one or more of the protein biosynthesis steps that occur at the 30S and 50S subunits of the bacterial ribosome, and therefore belong to the third class. The folate synthesis is inhibited by trimetoprim and sulfamethoxazole, which target different steps in the biosynthetic pathway from p-amino benzoic acid to tetrahydrofolate [15].

The history of antibiotics goes back to the year 1897, when Ernest Duchesne described in his thesis “antagonism between molds and bacteria”, that *Penicillium notatum* kills other bacteria [17]. In 1909 Salvarsan was synthesized by Paul Ehrlich and was used as the first antibiotic in the treatment of syphilis [18]. Almost ten years later, in 1928, Alexander Flemming discovered and isolated penicillin [19]. Today he is considered as the pioneer in antibiotic research. In the following decades many different antibiotic classes were discovered, in the so called “Golden Age of Discovery” (Figure 1).

Many, formerly lethal infections were treatable and in 1972 the United States Surgeon General, Dr. William H. Stewart (1965-1969) even stated: “It is time to close the book on infectious diseases, and declare the war against pestilence won.”[20] But very soon, it became clear that this assumption was wrong. The first resistant bacteria occurred (Table 1), but at the same time, no new antibiotic classes were introduced. It took almost 40 years, until the next antibiotic class entered the market (Figure 1).

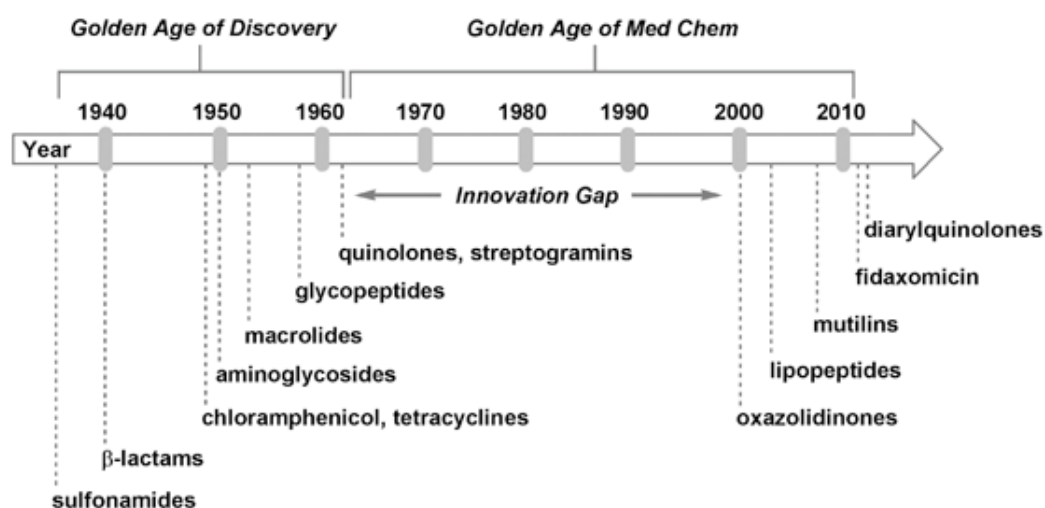


Figure 1: Timeline of the discovery of new antibiotic classes.

The dotted lines represent the year in which the antibiotic was introduced into the market. [21] Between the 1960s and 2000 substantial effort went into structural optimization of known classes. Notably, the market authorizations of the recently discovered pleuromutilin, fidaxomicin and diarylquinolone are limited to narrow bacterial spectra and partly topical treatment.

Walsh describes this gap, and the following years, as the “Golden Age of antibiotic medicinal chemistry” [21], where chemical tailoring of the major antibiotic classes helped to deal with the occurrence of resistant bacterial pathogens.

Table 1: Antibiotic discovery and evolution of resistance

(adapted from Walsh C, *Antibiotics: Actions, origins, resistance*. [15] and Walsh C., *Prospects for new antibiotics: a molecule-centered perspective* [21])

Antibiotic	Year deployed	Resistance observed
Sulfonamides	1930s	1940s
Penicillin	1943	1946
Streptomycin	1943	1959
Chloramphenicol	1947	1959
Tetracycline	1948	1952
Erythromycin	1952	1988
Vancomycin	1956	1988
Methicillin	1960	1961
Ampicillin	1961	1973
Cephalosporins	1960s	late 1960s
Nalidixic acid	1962	1962

Table 1: Antibiotic discovery and evolution of resistance (continued)

Antibiotic	Year deployed	Resistance observed
Fluoroquinolones	1980s	1980s
Linezolid	1999	1999
Daptomycin	2003	2003
Retapamulin	2007	2007
Fidaxomicin	2011	2011
Bedaquiline	2013	2014

Infectious diseases and the increase of resistant strains are one of the main health issues we are facing today. In fact, infectious diseases are the sixth major cause of death in Europe (World health organization, The European health report 2012 [1]). According to the WHO, “an estimated 25 000 people die every year because of infections related to antibiotic resistance, most of them contracted in health care settings” [22].

In this context new antibiotics with new modes of actions are strongly needed. There are two different approaches to address this problem: On the one hand screening for new drugs and synthesis of new chemical core structures, and on the other hand derivatisation of already known antibiotics. Two important goals of the derivatisation process are increasing the target-affinity and reaching higher effective concentrations at the bacterial target. The design of new compounds might help to overcome the permeability barrier in bacteria, which plays a particularly severe role in Gram-negative bacteria. This suggests that it is not only crucial to understand the mode of action but also to understand the uptake mechanism.

1.2 Cell wall and cell membranes-permeability barriers

To enter the cell an antibiotic needs to pass the cell wall and the cytoplasmic membrane. However, the limiting barrier is the cytoplasmic membrane. In the case of Gram-negative bacteria it has to cross an additional barrier, the outer membrane. All barriers have different characteristics, which makes a passage into the cell more difficult and challenging.

1.2.1 The bacterial cell wall

The bacterial cell wall can be defined as the structure that lies outside of the cytoplasmic membrane [23]. Gram-negative as well as Gram-positive bacteria have a peptidoglycan layer, which the layer of Gram-positive bacteria generally being substantially thicker (Figure 2). Its cross-linked structure gives strength and shape to the cells and can withstand a high internal osmotic pressure. The cell wall of Gram-positive bacteria consists of 50-90% peptidoglycan [23, 24]. The other major component is an acidic polymer, which differs from species to species, although it is often a teichoic acid. The acidic character of this polymer gives the cell surface a strongly polar character and a negative charge. The Gram-negative peptidoglycan layer is much thinner and is covalently linked to lipoproteins [23].

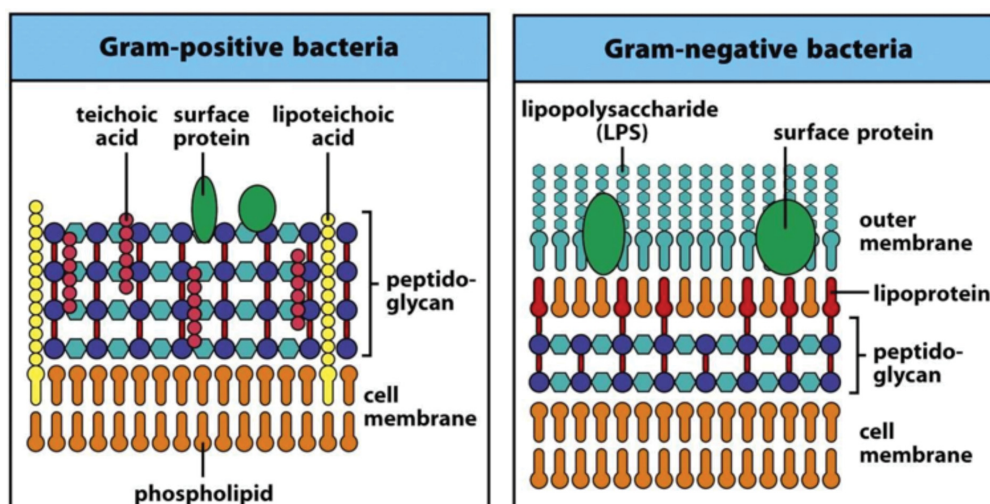


Figure 2: Cell-envelope of Gram-positive and Gram-negative bacteria [25]

1.2.1.1 The Gram-negative outer membrane

Besides the peptidoglycan layer, Gram-negative bacteria have an outer membrane. The outer membrane is an asymmetric lipid bilayer with hydrophilic groups on the outer surface. It mainly consists of lipopolysaccharides (LPS) anchored in the outer leaflet, phospholipids, fatty acids and proteins and it is negatively charged. The LPS, which is the major component of the outer membrane, consists of a hydrophobic lipid section (lipid A), a hydrophilic core polysaccharide and long chain of repeating hydrophilic oligosaccharide units (O-antigen).

The outer membrane is a strong barrier with two pathways a compound can take to cross, a lipid mediated pathway, by passive diffusion, or a porin-mediated pathway [26, 27]. Small, charged and hydrophilic molecules (<600 Da) can pass through water filled channels, the porins [28]. Besides porins, the outer membrane carries solute-specific diffusion channels, which reach into the periplasm. They are involved in the transport of iron-chelator

complexes and Vitamin B₁₂ [28-30]. They allow specific solutes to penetrate and therefore bypass the porin size and charge requirements. Aminoglycosides, make an exception, they use neither of those described pathways, but enter the cell via self-promoted uptake [31, 32]. This mechanism will be described in detail in 1.3.1.1.

1.2.1.1.1 Porins

Porin proteins form small waterfilled channels in the outer membrane of Gram-negative bacteria and consist of a tight and trimeric structure [28] (Figure 3).

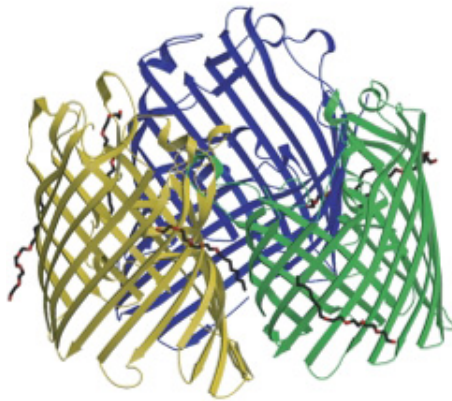


Figure 3: Structure of the OmpF trimer [33].

Porins allow the diffusion of hydrophilic compounds into the periplasmic space. They can be divided in three different types [23, 28].

1. Non-specific or general porins,
2. Selectively permeable channels with internal specific binding sites, and
3. Selectively permeable “gated” channels, which only open upon binding of a specific permeant

All three types allow the passage of compounds with molecular masses <600 Da. *E. coli* produces three main porins OmpF, OmpC and PhoE [26], which belong to the first class of porins. They share a high sequence identity, and are more than 70% homologous in their amino-acid sequence [34] and are known to be involved in the uptake of several antibiotics [26, 35-37]. PhoE is only expressed under phosphate starvation [38], and shows selectivity for anionic compounds, and phosphate and phosphorylated compounds in particular [39]. OmpF and OmpC are generally and high expressed (10^5 copies per cell [40, 41]) [42]. These two porins allow the diffusion over the outer membrane of cationic or zwitterionic compounds [28, 39], including tetracyclines [35], β -lactam antibiotics [37] and quinolones [36]. The uptake of antibiotics via porins was described for other species, too. β -lactam antibiotics, for example, diffuse through the basic amino-acid specific channel OprD of *Pseudomonas aeruginosa* [43]. The major non-specific porin of *P. aeruginosa* is OprF. It differs from the OmpF-class porins, as the influx of compounds is about 100-fold slower, but

it can transport larger substrates, as polysaccharides up to 2000-3000 daltons [44]. Minor porins are generally expressed at a lower level [26, 40, 45]. Two representatives of this class, in *E. coli*, are OmpN and OmpW. OmpN has similar channel properties as OmpC and OmpF, and was described to be expressed at low levels during growth in rich media [45]. So far, this porin has not been shown to participate in the uptake of antibiotics. In fact, in a previous study, the overexpression of OmpN did not show any effect on the susceptibility to a wide range of antibiotics, including compounds as diverse as tetracycline and ciprofloxacin [14]. The same is true for OmpW. So far no antibiotic uptake was described for this channel. Furthermore OmpW was described to function as an ion channel as for example for KCl [46, 47]. Nevertheless, the importance of porins for the influx of antimicrobial compounds is clearly demonstrated, as porin-deficient mutants are less susceptible to a wide range of antibiotics [26, 48, 49].

1.2.2 The cytoplasmic membrane

The cytoplasmic membrane consists of a phospholipid bilayer, hydrophobic in the center of the bilayer and hydrophilic on both surfaces (Figure 4). There are proteins embedded in the membrane (Figure 2, Figure 4). Its main function is to separate the inside of the cell from the surrounding, but it is also involved in further processes such as the transport of molecules, cell signaling and it is the main location of energy generation [24]. The cytoplasmic membrane is selectively permeable and regulates what enters the cell (Figure 4).

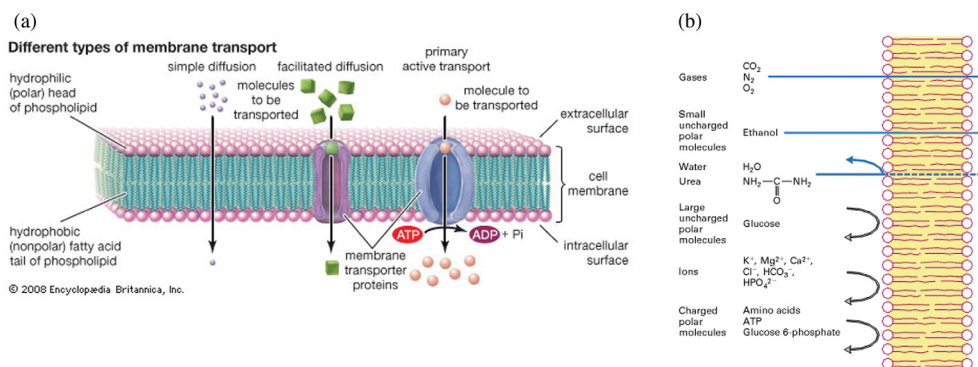


Figure 4: (a) Different types of membrane transport [50] (b) Relative permeability of a pure phospholipid bilayer to various molecules (Lodish 4th edition [51])

The transport can happen either passively or through an active transport. Due to the inner hydrophobic core, only small, electrically neutral, lipophilic molecules can passively diffuse through the phospholipid layer (e.g. CO₂, O₂). Charged and hydrophilic compounds (e.g. amino acids and glucose) need to enter or exit the cell through active transportation (Figure

4), as for example ABC (*ATP-binding cassette*)- or POT (*proton dependent oligopeptide*)-transporters.

1.2.2.1 The membrane potential, the pH-gradient and the proton motive force

The membrane potential is the difference of the electronic charge between inside and outside of the cell, and is described as $\Delta\psi$. This difference is based on the unequal distribution of the ions between cytoplasm and surrounding medium and leads to a voltage across the membrane. $\Delta\psi$ can be defined according to the Nernst equation [52]:

$$\Delta\psi = -\frac{RT}{zF} \ln \frac{[\text{ion inside cell}]}{[\text{ion outside cell}]}$$

z is the number of electrons per mole, R is the ideal gas constant (8.314 J/mol x K) and F the Faraday's constant (96484.56 C/mol).

The membrane potential varies in acidophile, neutrophile and alkaliphile bacteria from + 10 to -180 mV. *E. coli*, for example, has a $\Delta\psi$ of -135 mV ([53], Figure 6). The membrane potential and the pH gradient define the proton motive force (pmf). The pmf, which is an energy currency, can be described as an electrochemical gradient of H^+ across the cytoplasmic membrane (Figure 5).

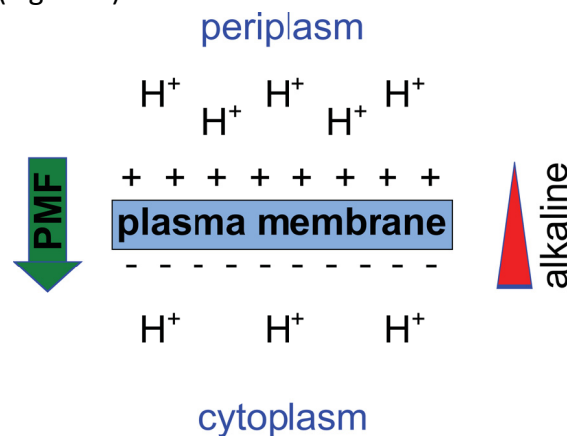


Figure 5: PMF-the electrochemical gradient of H^+

Furthermore, the pmf is the driving force for energy-requiring processes such as solute transport and ATP synthesis [54]. In 1966 Mitchell described the pmf in his chemiosmotic hypothesis as followed [54]:

$$\Delta p \text{ (mV)} = -\frac{\Delta\mu_{H^+}}{F}$$

$\Delta\mu_{H^+}$ (electrochemical proton gradient)= 1 kJ*mol corresponds to Δp (proton motive force)= 10.4 mV. At 25°C this equation takes the form:

$$\Delta p = -\Delta\psi - 59\Delta pH$$

The pH gradient (ΔpH) describes the difference between internal and external pH, and is alkaline inside the cell relative to outside. $\Delta\psi$ is defined as the electrical gradient.

pH homeostasis is crucial for living cells, because most proteins have distinct ranges of pH within which they can function. The pH outside of the cell can vary in the different habitats, and the bacteria must be able to keep a stable pH inside the cell. Neutrophilic bacteria, as for example *E. coli*, can grow at external pH values of 5.5-9.0, but generally maintain, as seen in Figure 6, their cytoplasmic pH in a range of 7.5-7.7 [55]. Numerous adaptations need to be made to maintain a stable pH. These adaptations include changes in transporter and enzyme levels, as well as metabolic and cell surface changes. *E. coli*, for example, changes its gene expression profile when growing at pH 8.7 [56]. Genes encoding the respiratory chain complex are repressed and therefore fewer protons can be pumped outwards. Furthermore the expression of genes encoding the F_1F_0 -ATP synthase, which imports protons during the ATP synthesis and genes encoding the *cyd*- terminal oxidase, that generates a pmf without outward proton pumping, were induced. Furthermore chemotaxis and motility are suppressed [56]. Alkaline pH can even induce an SOS-like response in *E. coli* [57]. Acidic pH has quite the opposite effect. It accelerates proton export and acid consumption and induces stress and heat shock regulons [56].

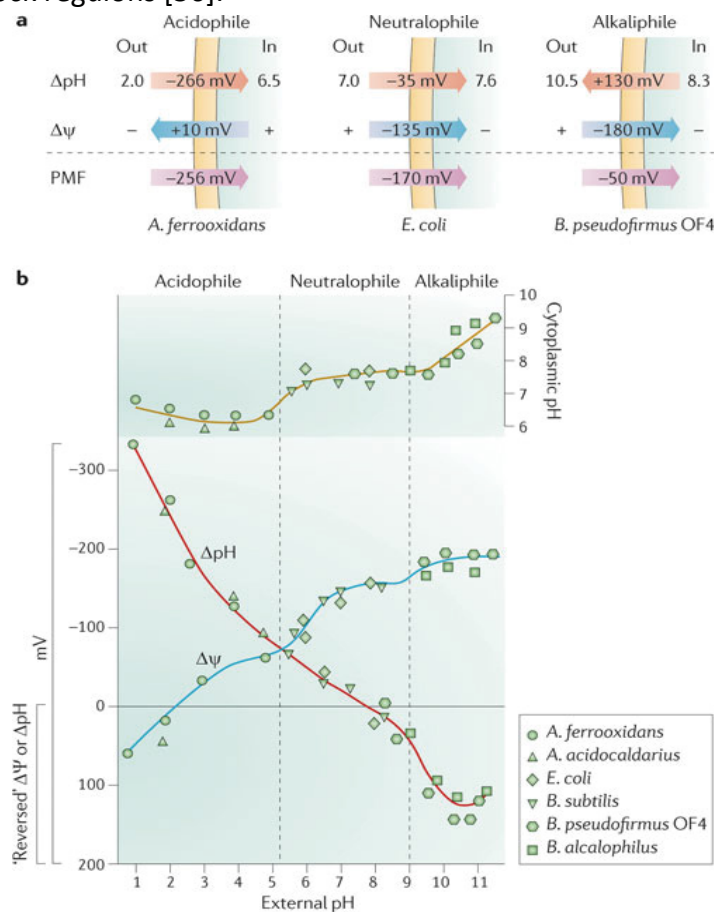


Figure 6: (a) pH-homeostasis for acidophile, neutrophile and alkaliphile bacteria. (b) Pattern of $\Delta\psi$, ΔpH and cytoplasmic pH plotted over a range of external pH values for acidophilic, neutrophilic and alkaliphilic bacteria [53]

1.2.2.2 ABC transporter (ATP-binding cassette transporter)

ABC systems are widespread among living organisms and share a remarkable conservation in the primary sequence of the cassette. They can be classified in three main functional groups: the import system, efflux system and a third category, which is not involved in transport but in translation in mRNA and DNA repair [58]. In total *E. coli* has 69 ABC-systems, of which 57 are transport systems and 44 of those are periplasmic-binding protein dependent [59]. The archetypal ABC transporter consists of two transmembrane domains, two ATP-binding cassette domains and, in the majority, of a binding domain (Figure 7). The substrate is bound by the binding protein, which is then recognized by the integral membrane domains, which form the translocation complex. The accumulation of the substrate is energized by ATP hydrolysis.



Figure 7: General ABC transporter architecture in *E. coli*.

The transporter is embedded in the cytoplasmic membrane (light blue) and comprises five different components: Two homologous transmembrane domains (dark blue), two homologous ATP-binding domains (green) and one periplasmic binding domain (orange) that binds the substrate (red) and guides it to the transporter.

ABC transporters are located in the cytoplasmic membrane. Here the transmembrane domains span the cytoplasmic membrane multiple times. The periplasmic binding domain is most of the times located in the periplasm. It has a very high binding affinity to the substrate and is essential for the transport even when high concentrations of the substrate are present. The range of substrates can be very diverse, including amino acids, short peptides, organic and inorganic ions, sugars, vitamins, metals, cations, opines and siderophores [60]. Most of the transporters are specific for one substrate or one family of substrates (maltose-maltodextrin transporter). There are many well-described import ABC transporters in *E. coli* such as the maltose-maltodextrin transporter MalFGK₂ [61], the oligopeptide transporter Opp [62, 63] and the dipeptide transporter Dpp [64].

ABC transporters are not only involved in import but also in export, as for example in peptides or drug efflux. One of those drug secretion systems is MacAB-TolC (*E. coli*) (Figure 8) [65]. MacAB-TolC represents a specific macrolide pump and consists out of three components, the periplasmic membrane fusion protein MacA, the ABC-type transporter MacB and the outer membrane channel protein TolC [65, 66].

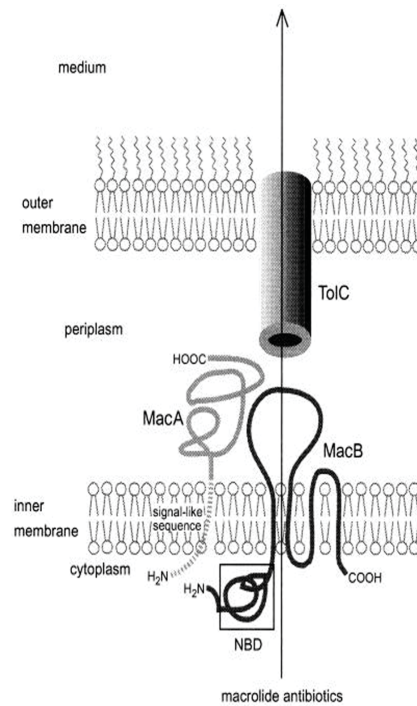


Figure 8: Schematic model of the molecular construction of the ABC-type macrolide-specific drug exporter MacA-MacB system complex with TolC in *E. coli*. NBD indicates the possible nucleotide-binding domain [65].

1.2.2.2.1 Oligopeptide permease *Opp*

The oligopeptide transporter *Opp* is one of the best-studied ABC transporters. It shows the typical ABC transporter structure and consists of five domains (Figure 7): two homologous transmembrane domains (*OppB* and *OppC*), two homologous ATP-binding proteins (*OppD* and *OppF*) and a soluble, periplasmic binding protein (*OppA*) mobile in the periplasmic space. The genes of this transporter are located in an operon [62]. If one of the five genes is knocked out the transporter is not functional anymore [67]. It is localized in the cytoplasmic membrane of both Gram-positive and Gram-negative bacteria, between which it shares a high sequence identity. It represents one of the main peptide transporters, with a high affinity for a broad range of substrates. It specifically transports peptides of two- to five amino acids with no apparent sequence selectivity. Although it was already reported that the periplasmic binding protein *OppA* can bind peptides up to 35 amino acids [60], based on the negatively charged binding pocket of *OppA*, the binding protein has a preference to bind positively charged, basic peptides [68]. *Opp* is furthermore involved in cell-wall recycling [69] even though *OppA* does not facilitate transport of the cell wall component murein tripeptide. The murein tripeptide seems to be bound by another periplasmic binding protein, *MppA*. *MppA* supplies the membrane bound domains of *Opp* with the murein tripeptides [70].

1.2.2.2.2 Dipeptide Permease Dpp

A second main and well-described peptide transporter is the dipeptide permease Dpp. It shares with Opp the same overall transporter structure and its genes are encoded in one operon in *E. coli*. It consists of the periplasmic binding protein DppA, the two transmembrane domains DppB and DppC and the two ATP-binding proteins DppD and DppF. The knockout of one of the five compartments leads to a loss of function of this transporter [71, 72].

It has the highest affinity to dipeptides containing L-amino acids or glycine, but can also translocate tri-, tetra- and hexapeptides [73]. Besides the peptide transport, the periplasmic binding protein DppA is involved in chemotaxis [64, 74]. Substrate-bound DppA interacts with the Tap chemotactic signal transducer and initiates an attractant signal. Peptides are the only attractants reported to elicit a signal through Tap. Furthermore the Dpp transporter is required for heme-uptake [75]. When an outer membrane heme-receptor is expressed, the Dpp transporter is also able to transport heme and the heme-precursor δ aminolevulinic acid [75]. It was shown that peptides compete for binding to DppA with heme [75]. When cells are grown in minimal medium DppA accumulates to high levels [72]. As soon as the medium is supplemented with casamino acids the protein levels of DppA are reduced [72]. A reduction of DppA was observed under glucose limitation and zinc stress too [76, 77].

1.2.2.2.3 Sap (*Sensitive to antimicrobial peptides*) transporter

SapABCDF encodes an ABC transporter of unknown function, which belongs to the subgroup of peptide transporters. The Sap-transporter shows the same structure as Dpp and Opp, and shares a high similarity with those peptide transporters [78]. It was described for being involved in resistance to antimicrobial drugs. Parra-Lopez *et al.* proposed that SapA binds antimicrobial peptides, transports them across the cytoplasmic membrane and into the cytoplasm, and therefore prevent their access to putative targets membrane-standing targets. In the cytoplasm the antimicrobial peptides are either degraded or they initiate a cascade resulting in activation of resistance determinants [78]. Furthermore it was shown that the ATP-binding domain SapD is involved in K^+ -transport via the uptake system TrkH and TrkG [79]. TrkH and TrkG are two closely related potassium ion transporters [80]. It has been implicated that SapD confers ATP dependence to these two K^+ uptake proteins [79]. Furthermore the Sap transporter plays a role, comparable to the dipeptide permease, in heme utilization. SapA can bind heme and it can be translocated into the cytoplasm via the Sap permease [81].

1.2.2.3 Proton-dependent oligopeptide transporter (POT)

POTs are proton-coupled transporters that facilitate the transport of di- and tri-peptides over the cytoplasmic membrane [82]. The transport of the peptides is coupled to an inward directed proton electrochemical gradient. The POTs belong to a subfamily of the functionally vast Major Facilitator Superfamily (MFS). They consist of 12 transmembrane helices, arranged in two 6-helices bundles that assemble together in the membrane to form a 'V'-shaped transporter with a central substrate-binding site between those bundles [83, 84]. Some of the POTs carry two further transmembrane helices (H_A and H_B). They are inserted between the two bundles [84].

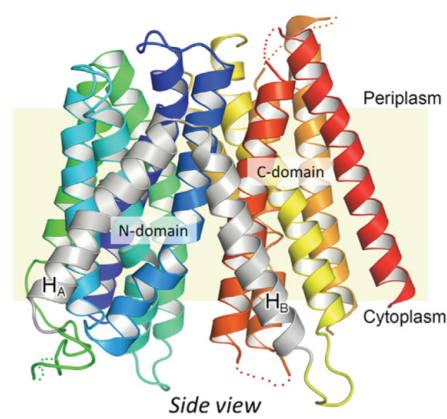


Figure 9: Structure of the *E. coli* POT YbgH.

The 12 helices transmembrane core is colored in a rainbow scheme (N-terminus blue to the red C-terminus). H_A and H_B are colored in grey. The transporter is embedded in the membrane (yellow) [83].

The structure of the transporter changes during the uptake process. One current uptake model proposes the following mechanism:

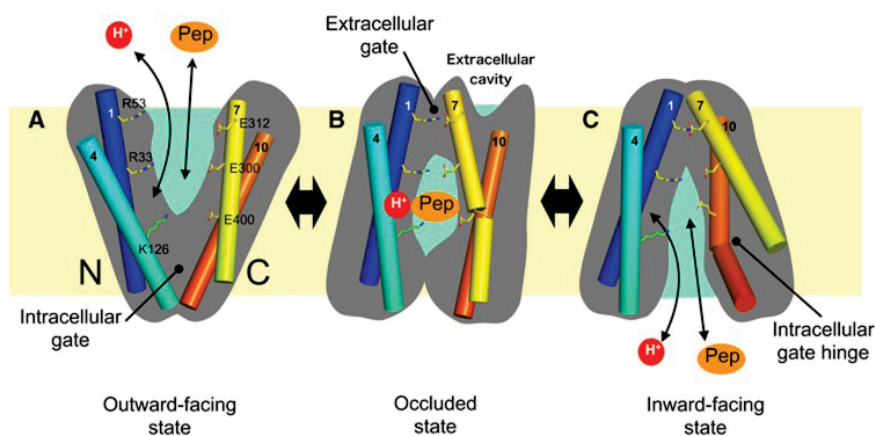


Figure 10: Model for proton-driven peptide symport by PepT_{st} [84]

In the first phase the transporter is in an outward-facing state (Figure 10). The peptide and proton bind from the extracellular side of the membrane. The binding leads to the closure of the extracellular gate and the transporter forms the occluded state. The transition to the

inward state occurs in part through hinge-like movement of two helices that results in release of the intracellular gate. This inward-facing state allows the proton and peptide to exit into the interior of the cell. The different conformations are created and changed through a dynamic salt-bridge network within the molecule [83, 84].

One representative of this transporter class is TppB (also named DtpA or YdgR), which is considered, besides Opp and Dpp, as one of the main peptide transporters of *E. coli*. It shows an affinity to di- and tripeptides composed of L- amino acids [85]. YjdL and YbgH, unlike most other characterized POTs, lack an affinity for tripeptides and show a preference for dipeptides [86, 87].

1.3 Antibiotic uptake

As mentioned before, antibiotics need to pass several barriers, with different characteristics, before they can reach an intracellular target. The mechanism of action of antibiotics was studied intensively in the era of antibiotics, but the uptake mechanism of many antibiotics remained elusive. As resistance mechanism can be based on a decrease in uptake too [31], it is crucial to understand the uptake of an antibacterial compound.

1.3.1 Different uptake mechanisms

Antibiotics can enter the cell via different uptake routes. In Gram-negative bacteria they need to pass even two main barriers with opposing penetration characteristics, the outer membrane and the cytoplasmic membrane (Figure 2). In the following chapter, the uptake mechanism of some selected antibiotics will be described, which were used as comparators in this study.

1.3.1.1 Aminoglycoside uptake

Aminoglycosides are polycationic water-soluble molecules with three to six net positive charges [32]. It was under discussion if aminoglycosides are taken up, at least to some extent, through porin channels [88], but this could never be proven until today. It was shown that aminoglycosides are crossing the outer membrane via so-called “self-promoted uptake” because they force and facilitate their own uptake across this barrier. The first step of this process is based on rapid electrostatic binding. In this phase the positive aminoglycosides bind to the negatively charged sides (lipopolysaccharides) of the outer membrane [89]. For gentamicin it was shown that it binds to the outer membrane, disrupts the Mg^{2+} bridges between the lipopolysaccharide (LPS) molecules and by disturbing the integrity of the LPS barrier promotes its own uptake [31, 32, 90]. These antibiotics are considered as permeabilizers, as the interaction with the outer membrane can permeabilize it to

fluorescence hydrophobic probes [32]. However this effect is rather weak compared to the permeabilizer polymyxin-B-nonapeptide (PMBN) [91].

After aminoglycosides have passed the outer membrane they accumulate to some extent in the periplasm, followed by two energy dependent steps. In EDPI (energy-dependent-phase I), aminoglycosides cross the cytoplasmic membrane in response to the membrane potential, and a slow rate of accumulation takes place [92]. The positively charged aminoglycosides are attracted by the charge gradient across the cytoplasmic membrane (negative inside). The aminoglycoside uptake across the cytoplasmic membrane is an energy requiring process. The cells accumulate them against a concentration gradient and the pmf provides the driving force [88]. It was seen that low pH, which leads to a drop of pmf [93-95], led to a much poorer transport of aminoglycosides, and therefore a lower effective intracellular concentration of the drugs [96]. It was shown that the oligopeptide transport system is involved in the uptake during EDPI [97, 98], but the complete mechanism is not yet understood. In the third phase of aminoglycoside uptake, EDPII, a linear rate of aminoglycoside transport across the cytoplasmic membrane takes place. This is based on a process that uses energy from electron transport and possibly from ATP-hydrolysis [99]. The initiation of the third phase is dependent on ribosomal binding and the binding contributes significantly to the total uptake of aminoglycosides [93]. Once the aminoglycosides cause misreading, the membrane permeabilizes by the insertion of mistranslated proteins, and more aminoglycosides can easily enter the cell [100].

1.3.1.2 Tetracycline uptake

Tetracyclines use two pathways to cross the outer membrane, a lipid-mediated and a porin-mediated pathway. The porin-mediated uptake takes place in the form of a net positive magnesium-bound chelate complex [101]. Tetracyclines cross the outer membrane of Gram-negative bacteria through the porins OmpC and OmpF [35, 101, 102], and they passage preferably via OmpF [101]. The cationic chelate-complex crosses the outer membrane and accumulates in the periplasm. It was shown that in the absence of only OmpF and OmpF/OmpC, accumulation of tetracycline was still detected in the periplasm [101]. This is due to the fact that tetracycline can also pass the outer membrane in the uncharged magnesium-free form, by passive diffusion [103], albeit at lower rates than through the porins. It has a pKa of 7.7, and exists mainly in the protonated form at neutral pH [103]. At a pH 7.4 7% of tetracycline species are uncharged [103].

In the periplasm reversible dissociation of the chelate releases the uncharged and lipophilic tetracycline. In this state tetracycline can passively diffuse through the lipid-bilayer of the cytoplasmic membrane [104]. In the cytoplasm it converts again to an ionic compound as the internal pH and the Mg^{2+} concentration is higher than in the periplasm [105, 106]. The cytoplasmic pH is tightly regulated in the range 7.4-7.8, whereas the periplasmic pH equals the external pH [106, 107]. This leads to the diffusion of more uncharged tetracycline into the cytoplasm to reach equilibrium. The accumulation equilibrium is shown in Figure 11.

Tetracycline accumulates against its concentration gradient and this active process is energized by the pmf. As the pH difference is dependent on the pmf it explains the energy dependence of tetracycline uptake. Only the uncharged, protonated tetracycline can diffuse through the bilayer. The equilibrium between protonated tetracycline and the chelate complex depends on the pH and the magnesium ion concentration. It was shown that tetracycline is able to complex other divalent cations besides magnesium, such as calcium and copper [108]. Each tetracycline molecule can complex two metal ions. Calcium and magnesium give similar interactions with tetracycline, whereas copper binds to different sides of the antibiotic. The association constant showed a correlation of pH and complexation. With increasing pH the complexation was favoured [108], which underlines again the dependency on the pH in tetracycline uptake.

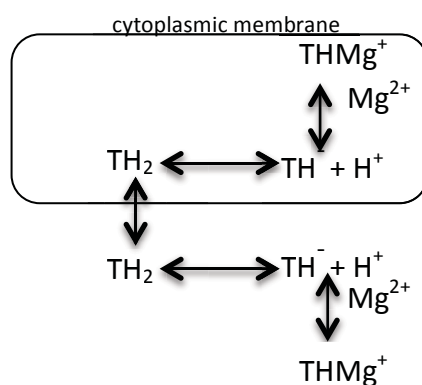


Figure 11: Passage of tetracycline across the bacterial cytoplasmic membrane and accumulation within the cytoplasm

(adapted from Yamaguchi et al., [105]) While fully protonated TH_2 is uncharged, TH^- is negative and net positive when complexing Mg^{2+} . Uptake across the outer membrane is not depicted.

1.3.1.3 Quinolone uptake

Quinolones can pass the outer membrane via two different pathways. They can either use porins or cross it by passive diffusion. In the charged form they pass the outer membrane preferably through OmpF [36]. The ionization of the carboxyl group enables ciprofloxacin to chelate with Mg^{2+} [109]. It was shown that strains lacking OmpF had a reduced accumulation of norfloxacin [110]. At pH 7.4 approximately 10% of hydrophilic quinolones are in their uncharged form [103]. In this form quinolones are able to cross the outer membrane passively [36], as they can diffuse through the lipid bilayer in the protonated form [103].

The chelated complex, which entered through the porins, dissociates again in the periplasm, comparable to the tetracycline- Mg^{2+} complex. Due to the accumulation in the periplasm and the concentration gradient across the cytoplasmic membrane, the uncharged molecule can passively diffuse through the lipid-bilayer [111]. The quinolones distribute across the membrane so that the concentration of uncharged species is identical on both sides of the membrane [103]. There is no evidence that active drug uptake into the cytoplasm takes

place. It is more likely based on the physicochemical properties of the compound and the pH differences in the periplasm and cytoplasm.

1.4 Negamycin - an underexplored peptide-like antibiotic

Negamycin was first discovered in 1970 and obtained from culture filtrates of *Streptomyces* strains, closely related to *Streptomyces purpeofuscus* [4]. Metabolites, as epideoxynegamycin, were also isolated from *Streptomyces goshikiensis* [112] and from a *Micromonospora* strain [113]. Negamycin is a pseudopeptide with a diamino-hydroxyhexonacid (hydroxyl- β -lysine) as a central β -aminoacid (Figure 12).

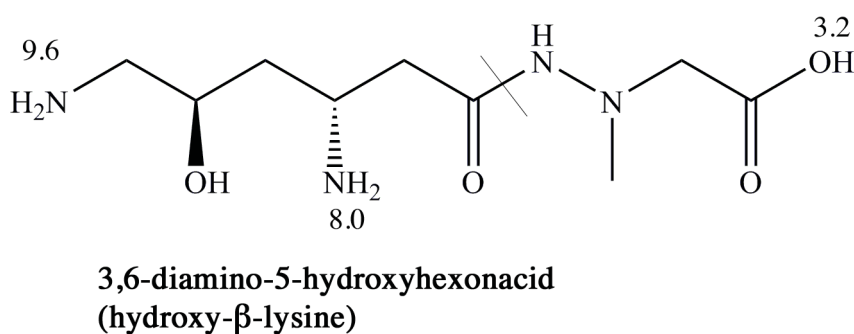


Figure 12: Structure of negamycin with previously published pKa's [114].

Negamycin showed promising activity against Gram-positive and Gram-negative bacteria *in vitro* and in septicemia models of infection [4, 115] and displayed low acute toxicity in rodents [4, 5]. One early report [115] mentioned a toxicity study in dogs where daily administration of negamycin had led to a formation of N-methylhydrazinylacetic acid, which had inhibited glutamate pyruvate transaminase and had led to reversible hepatic coma. In contrast, recent detailed preclinical profiling of negamycin demonstrated low hepatic metabolism and almost complete renal excretion in unchanged form [5]. Only 0.05 to 0.25% of N-methylhydrazinylacetic acid was detected in the urine of rats and dogs, respectively. It is active against clinically relevant strains such as the pathogens *Staphylococcus aureus*, *Pseudomonas aeruginosa* and Enterobacteriaceae. It displays a moderate antibacterial activity with MIC values of: 4 $\mu\text{g/ml}$ (*E. coli*), 32-50 $\mu\text{g/ml}$ (*S. aureus*), 25 $\mu\text{g/ml}$ (*Bacillus subtilis*) and 6-32 $\mu\text{g/ml}$ (*P. aeruginosa*) [4, 116]. Synthesis of analogs and modification of the compound were performed using different approaches [116-119]. Even though some analogs displayed a higher activity in cell-free assays, none of them had an improved activity in whole-cell assays. These observations demonstrate that factors like permeation play a critical role in antimicrobial activity and led to the assumption that negamycin is entering the cell through an active transport mediated event. It was demonstrated that negamycin has stringent requirements with regard to the chemical structure. C-terminal modification resulted in a complete loss of activity and the basicity of the N-terminal amino group was shown to be critical, too. Only one negamycin analog, deoxynegamycin, rendered comparable activities to the original compound [117, 120]. Only recently, McKinney *et al.*

published a new negamycin analogue, N6-(3-aminopropyl)-negamycin, which is showing a 4-fold improvement of antibacterial activity [121].

In conclusion, the transport structure-activity-relationship is not in parallel with the target structure-activity-relationship for negamycin. The activity on the target was studied in several approaches [6-13], whereas the uptake mechanism remained elusive. Only recently it became subject of ongoing studies [114].

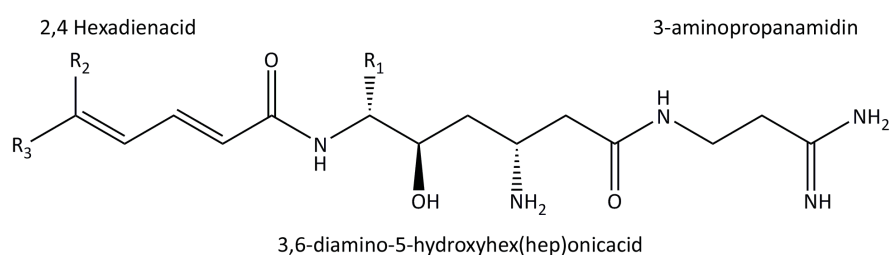
Negamycin targets protein biosynthesis [7, 8]. Early investigation on the mode of action described an inhibition of the initiation step [7]. In recent crystal structures negamycin was detected at 9 independent binding sites at the ribosome, which are distributed over the large and small subunit [13]. Schroeder *et al.* proposed one further binding site, which has not been confirmed so far [122]. It is uncertain, how many of these sites are functionally relevant and which are artefacts of the crystallization procedure. The main binding site, and the one consistent with the mode of action and resistance mutations, is located at the 16S rRNA in the vicinity of the conserved helix 34 (h34). This binding site overlaps with the tetracycline-binding site. Here, negamycin interacts also with the tRNA and stabilizes the binding of the aminoacyl-tRNA to the ribosome. This stimulates miscoding due to prolonged residency time of no-cognate tRNAs at the ribosome and inhibits translocation [12, 13]. Negamycin promotes miscoding in the 5'-terminal and internal position (A→U, C→U and A→G). This spectrum is identical with the miscoding spectrum of streptomycin and kanamycin, even though no ribosomal cross-resistance was detected, in line with different binding sites of the two compound classes at the ribosome [6, 8]. Furthermore negamycin inhibits the termination step. It binds, most likely irreversibly, to polysomal ribosomes and inhibits the release of the peptides [10, 11]. The miscoding effect was utilized in an approach for treating Duchenne muscular dystrophy in a mouse model study [123]. In one-third of the cases, the illness is based on a mutation in the dystrophin gene. This mutation results in a stop codon, which leads to a premature termination of the translation of this gene [124]. Compounds, which cause miscoding have been considered for treating a genetic disease like this. Aminoglycosides would be potential candidates in this regard. The disadvantage of this antibiotic class is the high toxicity and therefore its severe side effects. Negamycin, with predicted lower toxicity is an interesting candidate in the therapy for this genetic illness. In fact, Arakawa *et al.* showed that negamycin was able to restore dystrophin expression [123]. A similar attempt was conducted in a study concerning APC (Adenomatous Polyposis Coli) tumor suppressor gene in human colorectal cancer. In 80% of this cancer the APC gene is mutated. 30% of these mutations are nonsense mutations, which lead to a premature termination. Negamycin was shown to read through the stop-codon and recover the biological activity of APC cancer cell lines [125]. This makes negamycin not only an interesting candidate for treating antibacterial infection, but also for treating genetic illnesses based on a nonsense mutation.

As mentioned before, the uptake mechanism of negamycin remained elusive for a long time. An active transport was suggested by Raju *et al.*, and Uehara *et al.* proposed that negamycin permeates through a lysine-permeation system, but this hypothesis was never proven [116, 120]. Rafanan *et al.* suggested on a poster in 2003 at the ICAAC conference, that negamycin

could be a substrate of the Dipeptide Permease Dpp. The route was confirmed in this work as well as in a publication of McKinney *et al.* from 2015 [114]. Furthermore Rafanan *et al.* pointed out that spontaneous mutants showed complementary cross-resistance to aminoglycosides. Some mutants were deficient in components of the electron transport system [126]. McKinney *et al.* isolated mutants as well, which were deficient in these components [114]. None of these studies investigated uptake across the outer membrane or took effect of ion complexes into account. Clearly negamycin is not entering the cell by using only one uptake route, and the whole mechanism is not understood so far. Goal of this work was to investigate the different uptake routes of negamycin into the bacterial cell, to evaluate previous hypotheses and to complement our knowledge on the complex uptake process.

1.4.1 Sperabillin – an antibacterial agent structurally related to negamycin

The natural products sperabillin A, B, C, D are produced by *Pseudomonas fluorescens* YK-437 [127]. They were first identified as antibacterial compounds in 1985 by Takeda Chemical industries [128]. The chemical characterization and structure determination was published in 1993 by Hida *et al.* [129] and confirmed with the total synthesis by Hashiguchi *et al.* [130] (Figure 13).

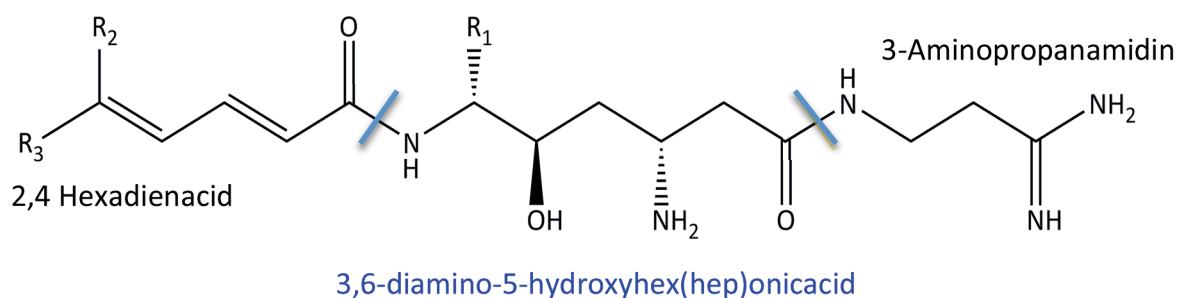


Sperabillin	R1	R2	R3
A	H	CH ₃	H
B	CH ₃	CH ₃	H
C	H	H	CH ₃
D	CH ₃	H	CH ₃
Hexadecyl-	H	H	C ₁₁ H ₂₄ CO

Figure 13: Structure of Sperabillin A, B, C, D and Hexadecyl-Sperabillin.

Sperabillin is, like negamycin, a positively charged pseudopeptide with a 3,6-diamino-5-hydroxyhexanoic acid (Figure 14).

Sperabillin



Negamycin

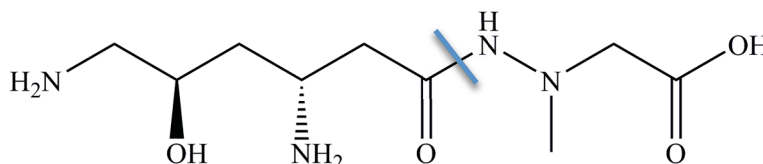


Figure 14: Structure-comparison of sperabillin and negamycin.

Sperabillin has *in vivo* and *in vitro* activity against Gram-positive and Gram-negative bacteria, including antibiotic resistant strains of *P. aeruginosa* and *S. aureus*. Interestingly the *in vivo* activity is stronger than that expected from *in vitro* potencies [127]. An acute toxicity of 500 mg/kg upon subcutaneous injection was described [127]. The *in vitro* activity is strongly dependent on the assay condition and the ionic strength of the media. Therefore the MICs can vary under different conditions, as for example in *E. coli* the MIC ranges from 12.5 $\mu\text{g/ml}$ to >100 $\mu\text{g/ml}$. However, derivatisation of these peptide-antibiotics yielded metabolites with significantly improved activity [131]. But when the amidino moiety was modified, the compound lost its activity. Similar results were described for negamycin [119]. Hida et al. proposed that the amidino group might play an important role in electrostatic binding to the bacterial cell wall. The mode of action is not yet known. Preliminary data showed an inhibition of RNA-, DNA-, protein- and cell wall-biosynthesis in *E. coli*, but the experimental design and selectivity should be questioned [127].

Pre-treatment of mice with sperabillin A had a protective effect against lethal bacterial infections [127]. This prophylactic characteristic of sperabillin was discussed as potentially immunostimulatory. Large sperabillin polymers were shown to activate macrophages, but it is unsure, if this effect is based on particle size or related to monomer activity [132]. Furthermore, these polymers displayed an anti-tumor activity in mice based on proliferation-inhibition and the mentioned immunostimulatory effect [133].

1.5 *Escherichia coli* as a model organism

Escherichia coli is a Gram-negative, rod-shaped, facultative anaerobic bacterium. The genus is named after Theodor Escherich, a doctor who in 1886 discovered this rod-shaped bacterium in the gut-flora of babies [134]. *E. coli* belongs to the family of

Enterobacteriaceae. It is a common inhabitant of the gastrointestinal tract of warm-blooded organisms [135]. The *E. coli* strains, which are part of the gut-flora are commensales, and mostly even beneficial for the host, as they produce vitamin K₂ [136] and prevent the colonization by pathogenic bacteria. Even though most of the *E. coli* strains are harmless, some strains are highly infectious pathogens, and can cause severe intestinal and extraintestinal diseases [137]. Extended spectrum β -lactamases and other resistance factors are increasingly frequent in *E. coli* [138]. Thus, new therapeutic treatment options are also important for this species.

No other bacterial species is as well understood as *E. coli*. It has served in the laboratory as a model organism for more than sixty years. This is due to its easy cultivation and the fast reproduction cycle of 20 minutes under optimal conditions. It plays a major role in the fields of biotechnology and microbiology, where it is used as a host organism for work with recombinant DNA. The first *E. coli* strain that was sequenced was MG1655, an offspring of the commonly used laboratory strain K12 [139]. MG1655 has only been cured of the temperate bacteriophage lambda and F plasmid. The chromosome consists of 4.639.221 basepairs (bp), with 4.288 open reading frames (ORFs), which equal 88% of the genome. 1% encodes for tRNAs and rRNAs, 0.5% for non-coding repeats and 10% for regulatory and other functions [139].

As *E. coli* is so well characterized, easy to handle and because negamycin shows moderate to good activity against this strain, *E. coli* was chosen as the main model organism for this work.

1.6 Goal of the thesis

The main goal of this thesis was to investigate the molecular uptake mechanism of the pseudopeptide negamycin. Negamycin shows a moderate antibacterial activity and optimization approaches of the compound without rational guidance did not yield an improved or more potent antibiotic [116-119]. The observation was made that the permeation factor plays a critical role in antimicrobial activity. Therefore it is not only crucial to understand the mode of action but also the uptake mechanism for goal-oriented compound optimization. As negamycin is active against Gram-positive and Gram-negative bacteria this work focuses on the passage of negamycin through the outer membrane as well as across the cytoplasmic membrane and the influence of external environmental factors on negamycin activity, by using *E. coli* as a Gram-negative model organism. The compound used in this project was synthesized by Squarix GmbH.

A side project of this thesis focused on sperabillin, which is structurally related to negamycin. As mentioned before the mode of action and the uptake of this promising compound remains elusive. Two different derivatives of this antibiotic, sperabillin C [127] and hexadecyl-sperabillin [131], were provided by Squarix GmbH to perform preliminary investigations on the mode of action and uptake mechanism.

2 Results

2.1 Characterization of negamycin activity

2.1.1 Negamycin activity in different strains and media

The first goal of this thesis was to determine the activity and potency-profile of negamycin. Therefore the MIC was determined in Gram-positive and Gram-negative bacteria under different media conditions (Table 2).

Table 2: Negamycin MICs in Gram-positive and Gram-negative bacteria under different test conditions (n.d.: not determined, n.g.: no growth).

MIC [$\mu\text{g/ml}$]					
	<i>E. coli</i> BW25113	<i>E. coli</i> ATCC29522	<i>P. aeruginosa</i> PA01	<i>S. aureus</i> ATCC29213	<i>B. subtilis</i> trpC2
medium					
0.5% polypeptone	16	16	64	>64	>64
Peptone water	n.d.	64	>64	>64	>64
peptone (meat)	n.d.	16	8	64	32-64
M9	4	2	>64	n.g.	n.g.
LB	>64	>64	>64	>64	>64
MH	>64	>64	>64	>64	>64
MH cation adjusted	n.d.	64	>64	>64	>64
Nutrient broth	n.d.	32	64	>64	n.g.
CYG	n.d.	>64	>64	>64	>64
Belitzky	n.d.	4	>64	n.g.	>64

Table 2: Negamycin MICs in Gram-positive and Gram-negative bacteria under different test conditions (continued)

MIC [$\mu\text{g/ml}$]					
	<i>E. coli</i> BW25113	<i>E. coli</i> ATCC29522	<i>P. aeruginosa</i> PA01	<i>S. aureus</i> ATCC29213	<i>B. subtilis</i> trpC2
medium					
Meat extract	n.d.	32-64	64	>64	>64
Agar					
0.5% polypeptone.- Agar	2	n.d.	n.d.	n.d.	n.d.
M9-Agar	8	n.d.	n.d.	n.d.	n.d.

Testing negamycin against different strains in different media showed diverse activity (Table 2). *E. coli*, for example, was not susceptible in rich media, such as LB, MH, MH-cation adjusted and CYG. A moderate activity was determined in 0.5% polypeptone (PP) (16 $\mu\text{g/ml}$), peptone-meat (16 $\mu\text{g/ml}$), Belitzky (4 $\mu\text{g/ml}$) and M9 (2-4 mg/ml). All of these broths are minimal media, which contain either only peptone (PP, peptone meat), salts and glucose (M9) or salts, glucose and amino acids (Belitzky), respectively. In peptone water, which contains peptides and salt, no activity could be determined. Other Gram-positive and Gram-negative bacteria, treated with negamycin, showed only a slight (*P. aeruginosa*) or no inhibition under these conditions. The determined MIC on M9-agar is 2-fold higher than in liquid. Interestingly on PP-agar the MIC is 8 fold lower than in the broth.

These observations align with previously published data [4], and show that negamycin has a higher potential in Gram-negative bacteria. The differences in negamycin activity in different media point to multiple entry routes into the bacterial cytoplasm.

For further investigations, two media with opposing composition, PP and M9, were selected.

2.1.2 Azidonegamycin activity in different strains and media

The derivative azidonegamycin was synthesized by our cooperation partner Squarix GmbH. It carries an azido-group at the N-terminus (Figure 15).

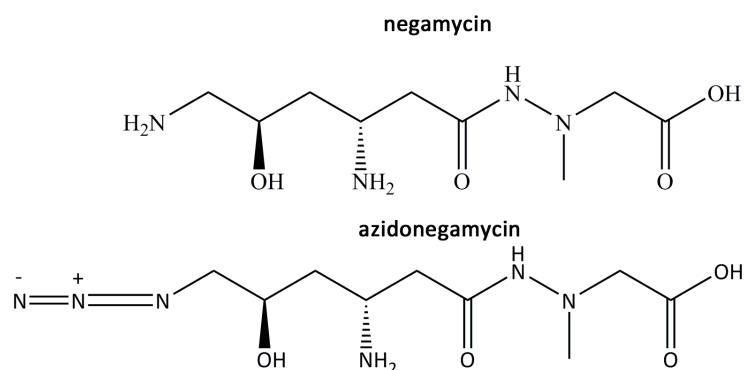


Figure 15: Comparison of the chemical structures of negamycin and azidonegamycin

The activity was tested against Gram-negative and Gram-positive bacteria. The MICs were determined in PP (Table 3), as negamycin, azidonegamycin showed a moderate activity in this medium.

Table 3: Azidonegamycin activity in Gram-negative and Gram-positive bacteria

MIC [$\mu\text{g/ml}$]				
	<i>E. coli</i> ATCC25922	<i>P. aeruginosa</i> PA01	<i>B. subtilis</i> 168	<i>S. aureus</i> ATCC13709
PP	>64	>64	64	>64

Azidonegamycin was inactive in Gram-positive and Gram-negative bacteria. It was demonstrated before that negamycin has stringent requirements with regard to the chemical structure. The basicity of the N-terminal amino-group was shown to be critical [116]. This aligns with our result. As the azidogroup is not basic, the antibacterial activity of negamycin is lost.

2.1.3 Bactericidal activity of negamycin

Antibiotics can either have a bacteriostatic or bactericidal effect. To determine the antibacterial activity of negamycin, killing curves were performed (Figure 16). Over a time course of 25 hours. *E. coli* BW25113 was treated with different concentrations of the antibiotic, plated out and colony-forming-units (CFUs) were counted. As azidonegamycin did not show an antibacterial activity $\leq 64 \mu\text{g/ml}$ in *E. coli* the killing curves were only performed with negamycin.

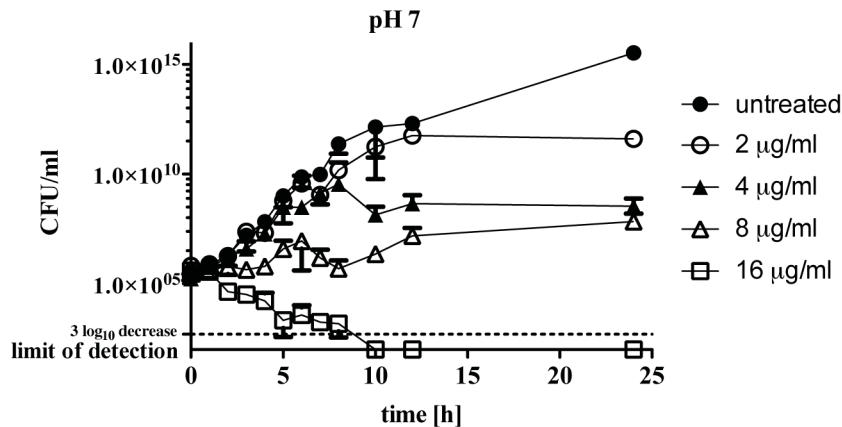


Figure 16: Bactericidal activity of negamycin in PP

Bactericidal activity of an antibiotic is defined as a $\geq 3 \log_{10}$ decrease in cfu/mL (here marked with the dashed line) within 24 hours. The negamycin killing curve showed that this is the case when *E. coli* is treated with 16 $\mu\text{g/ml}$ negamycin (which equals the MIC in this medium) after 8 hours. Therefore the negamycin activity is bactericidal, which aligns with previously published data [10].

2.1.4 Mode of action

Negamycin inhibits different steps of the protein biosynthesis [7, 8]. It inhibits translation by a dual mode of action. On the one hand it causes miscoding and on the other it inhibits termination. Negamycin binds to its main binding site at the 16S rRNA and interacts with the tRNA. This leads to a stabilization of the binding of the aminoacyl-tRNA to the ribosome. This leads to an inhibition of translocation and stimulates miscoding [12, 13]. During the time course of this project, different *in vitro* assays on the mode of action of negamycin were performed. The effect of azidonegamycin on translation was investigated in comparison to negamycin (Figure 17).

The transcription-translation assay showed that azidonegamycin is inhibiting the transcription-translation in *E. coli*, but only when applied in a high concentration (Figure 17 (a)). The half maximal inhibitory concentration (IC_{50}) of azidonegamycin is 32.6 $\mu\text{g/ml}$, compared to the IC_{50} of 0.692 $\mu\text{g/ml}$ of negamycin (b). The uncoupled T7/translation assay can separate between targeting the transcription or the translation. It was performed for negamycin and showed that the inhibition is indeed taking place in the translation process (c).

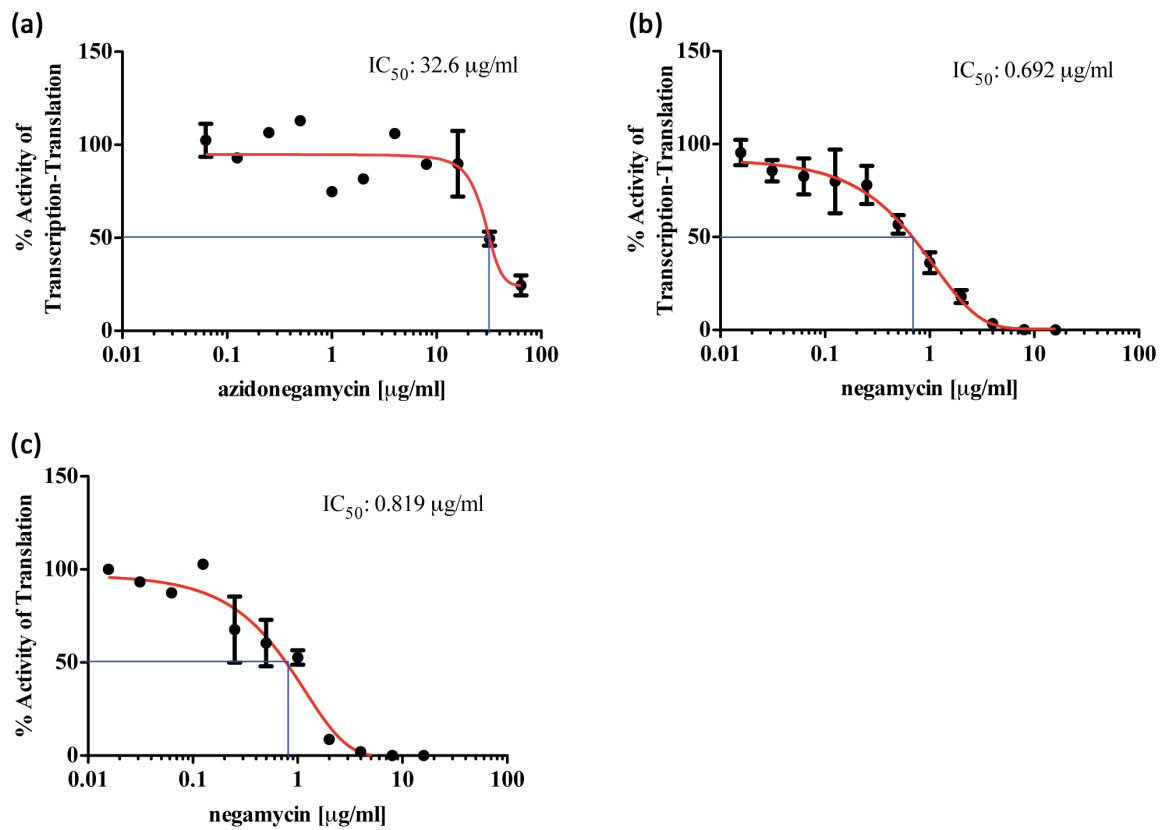


Figure 17: *in vitro* coupled transcription/translation assay with (a) azidonegamycin, (b) negamycin and (c) uncoupled T7/translation assay with negamycin

To investigate the miscoding of a compound an assay can be used which is based on a read-through of a stop-codon by miscoding-causing compounds. This assay was performed with negamycin (Figure 18).

E. coli BW25113 carried the pBestluc-mut plasmid, which carries a stop-codon in the luciferase gene. When a compound causes misreading, the stop-codon is over read and the luciferase can be expressed. Therefore a luminescence signal can be detected.

Streptomycin, an aminoglycoside that causes miscoding, was used as a positive control. Tetracycline, which is inhibiting the binding of the aminoacyl-tRNA to the A-site of the ribosome, was used as a negative control. The assay showed that negamycin, as well as streptomycin, caused miscoding, which led to a read-through of the stop-codon and a detection of luminescence signal (Figure 18). The negative control tetracycline did not show any luminescence induction, which was expected, as it does not cause miscoding.

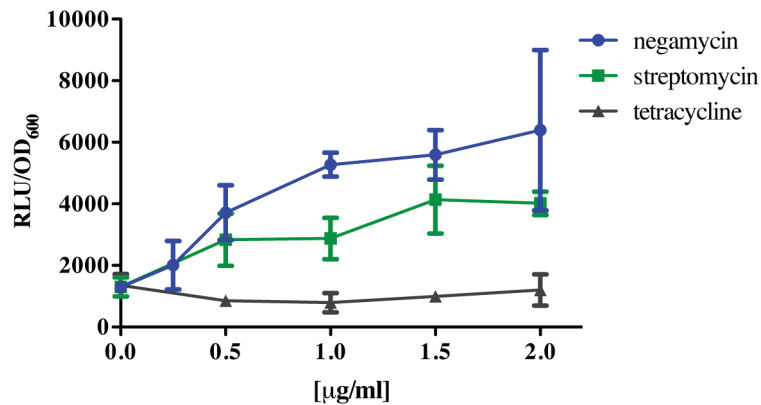


Figure 18: Miscoding-Assay in M9 with negamycin, streptomycin (pos. control) and tetracycline (neg. control)

2.2 Side-project: Sperabillin activity

Sperabillin is a pseudo-peptide and shares structural similarities to negamycin (Figure 14). Therefore the impact of different growth media on its antibacterial activity and the mode of action were investigated and compared to negamycin. Our cooperation partner Squarix GmbH synthesized two different sperabillin derivatives, sperabillin C and hexadecyl-sperabillin.

2.2.1 Sperabillin activity in different strains and media

For negamycin a media-dependent activity was shown (2.1.1). Similar observations were made for sperabillins in literature [127]. Further media conditions were tested for the two derivatives sperabillin C and hexadecyl-sperabillin (Table 4).

Table 4: Sperabillin MICs in Gram-negative and Gram-positive bacteria under different test conditions (n.d.: not determined).

microorganism	medium	MIC [µg/ml]	
		sperabillin C	hexadecyl-sperabillin
<i>E. coli</i>	MH	>64	32
BW25113	NB	>64	n.d.
	½ NB	>64	16 (32)
	DYAB	n.d.	32

Table 4: Sperabillin MICs in Gram-negative and Gram-positive bacteria under different test conditions (continued)

microorganism	medium	MIC [$\mu\text{g/ml}$]	
		sperabillin C	hexadecyl-sperabillin
<i>E. coli</i> BW25113	PP	>64	8
	PP + 25 $\mu\text{g/ml}$ PMBN	>64	n.d.
	M9	>64	32 (64)
<i>B. subtilis</i> IS58	MH	n.d.	16 (32)
	$\frac{1}{2}$ NB	n.d.	16
	DYAB	n.d.	16
	PP	n.d.	4 (8)
	Belitzky	n.d.	16
<i>S. aureus</i> 133	MH	n.d.	16
	NB	>64	n.d.
	$\frac{1}{2}$ NB	>64	16 (32)
	DYAB	n.d.	16
	PP	>64	4(8)
<i>P. aeruginosa</i> PAOI	NB	>64	n.d.
	PP	>64	n.d.
	PP+ 25 $\mu\text{g/ml}$ PMBN	>64	n.d.
	M9	>64	n.d.
<i>A. baumannii</i> 09987	MH	>64	n.d.
	NB	>64	n.d.
	$\frac{1}{2}$ NB	>64	n.d.

Sperabillin C did not show any activity in the different strains tested, in none of the media conditions. This result aligns with previous data, published by Katayama *et al.* [127]. They determined only a moderate to slight activity in one *Pseudomonas aeruginosa* and one *Acinetobacter calcoaceticus* strain. As we did not have the same strains in our laboratory, strains from the same species respectively genus were tested, but they did not show susceptibility to sperabillin C. Hexadecyl-sperabillin, on the other hand, showed moderate activity in Gram-positive and Gram-negative bacteria. Hida *et al.* published a similar activity-profile in DYAB medium [131]. For the other media-conditions no data was published so far.

Hexadecyl-sperabillin showed a slight media dependency. The activity in PP was 4-fold better, compared to the other conditions. Similar results were seen for negamycin, even though for this antibiotic, a medium with only salts and glucose (M9) was beneficial, too (Table 2). This was not seen for sperabillin.

2.2.2 Sperabillins: Mode of action

Next, the mode of action of sperabillins was investigated. Sperabillin C and hexadecyl-sperabillin were both tested in a promoter assay (Figure 19). This assay uses different reporters as a screening tool for novel drug candidates. Based on broad transcriptional profiling 5 promoters had been previously selected [140] that are rather selectively induced upon disturbance of particular metabolic areas or cellular structures: cell-envelope (*ypuA* and *lial*), protein- (*bmrC*), DNA- (*yorB*) and RNA-biosynthesis (*helD*). Five *Bacillus subtilis* strains, each carrying one of these promoters fused to the firefly luciferase reporter gene, were previously generated by Urban *et al.* [140]. When a compound targets one of the biosynthesis pathways, the promoter is activated, the luciferase expressed, and chemoluminescence can be detected.

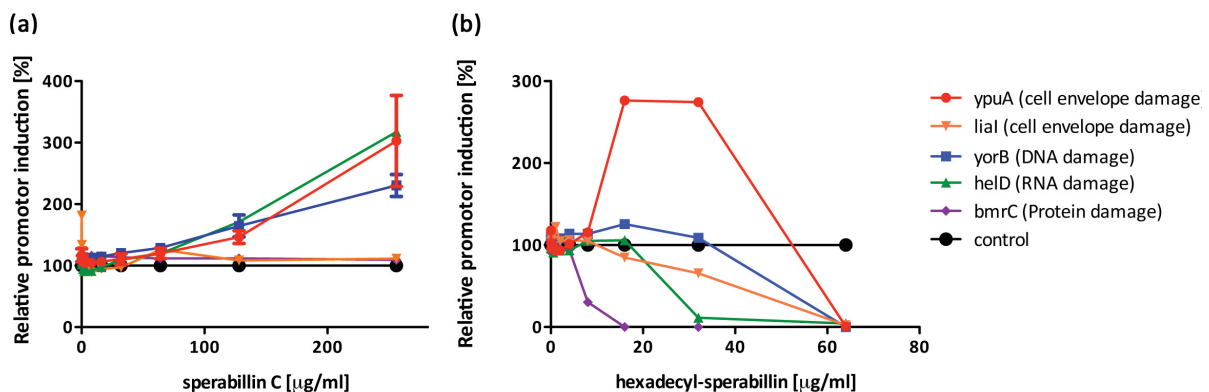


Figure 19: in vitro promoter assay with (a) sperabillin C and (b) hexadecyl-sperabillin

Sperabillin C induced the cell envelope-, DNA- and RNA-damage reporters (Figure 19 a). This two- respectively three-fold induction occurred at a high concentration of 256 µg/ml. This effect on the promoters at such a high concentration, aligns with the MIC >64 µg/ml of

sperabillin C. Katayama *et al.* published data of an incorporation assay, which indicated an inhibition of all four biosynthesis pathways, cell envelope, DNA, RNA and protein biosynthesis, already at a concentration of 25 $\mu\text{g}/\text{ml}$ [127]. However, he performed the experiments with the more potent sperabillin A. An inhibition of protein biosynthesis could not be seen in the promoter assay. Hexadecyl-sperabillin induced only *ypuA*, the promoter, which is activated when cell envelope damage occurs. The induction was seen at 1x MIC and 2x MIC (16 and 32 $\mu\text{g}/\text{ml}$). The different mode of action could be due to the different structure of the two sperabillin derivatives.

As sperabillins are structurally related to negamycin the protein-biosynthesis inhibition through sperabillin was investigated. The inhibition of transcription and translation was tested in the *in vitro* transcription-translation assay (Figure 20).

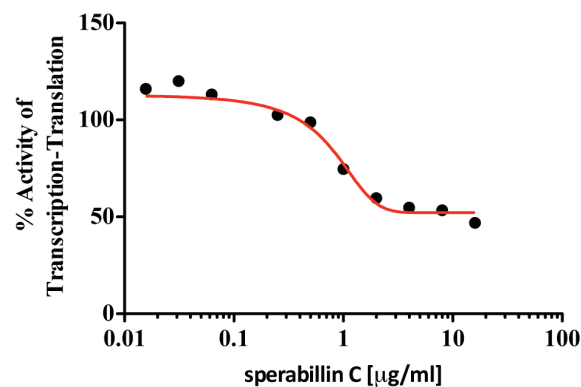


Figure 20: *in vitro* transcription-translation assay with sperabillin C

The assay showed that sperabillin C had a slight, but not conclusive effect, on either transcription or translation or both. This assay should be repeated with a more potent sperabillin, as for example sperabillin A. Hexadecyl-sperabillin was not applied in this assay.

2.3 Negamycin passage across the outer membrane

For entering the cell, antibiotics need to cross several barriers (see chapter 1.2). Gram-negative bacteria even have an additional barrier, the outer membrane (Figure 2). The outer membrane can be approached in different ways. It can be crossed by a self-promoted uptake as described for aminoglycosides (1.3.1.1). Furthermore it can be passed by porin mediated transport, which tetracyclines and quinolones use in their charged form, or passive diffusion, which is described for uncharged tetracyclines and quinolones (see chapters 1.3.1.2, 1.3.1.3.). In this chapter the investigations on the uptake of negamycin over the outer membrane are described.

2.3.1 The outer membrane as a rate-limiting barrier

Negamycin is active in Gram-positive and Gram-negative bacteria. In Gram-negative bacteria it needs to pass the outer membrane as the first barrier. To investigate if the outer membrane is rate-limiting for the uptake of negamycin, polymyxin B nonapeptide (PMBN) was added to the MIC-determinations (Figure 21). PMBN is a small cationic peptide that permeabilizes the outer membrane. Therefore compounds, which are either too big or cannot cross the outer membrane under regular conditions, can diffuse through the membrane upon treatment with PMBN.

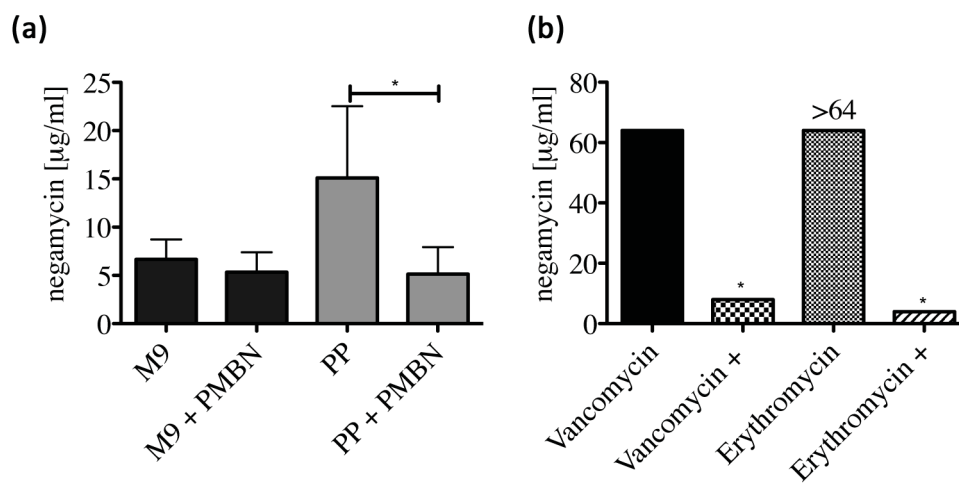


Figure 21: (a) Negamycin and (b) vancomycin and erythromycin activity in M9 and PP with addition of 15 µg/ml PMBN (+ PMBN, or +) in *E. coli* BW25113. (n*=p<0.05)

In M9 the outer membrane is not rate-limiting for negamycin activity, as the treatment with PMBN did not show a significant effect (Figure 21 a). In contrast in PP, the MIC decreased 4 fold, from 16 to 4 µg/ml, indicating that it is a barrier in this medium. To investigate whether the outer membrane is generally no barrier in M9, MICs with erythromycin and vancomycin were performed. Both antibiotics cannot pass the outer membrane, and therefore Gram-negative bacteria are resistant against these two compounds. The addition of PMBN led to a susceptibility of *E. coli* BW25113 towards vancomycin and erythromycin (Figure 21 b). This result shows that the outer membrane is in general a barrier for antibiotics in M9, but not for negamycin.

2.3.2 Involvement of porins in negamycin uptake

In the next step the involvement of porins in negamycin-uptake was investigated. Therefore different porin knockout-strains were tested against negamycin (Table 5). Furthermore it was tested if the outer membrane is rate limiting in porin-knockouts (Figure 22).

Table 5: MIC of different porin-knockout-strains in PP and M9 (n*=p<0.05)

MIC [$\mu\text{g/ml}$]		
<i>E. coli</i> strain	PP	M9
BW25113	16	4
$\Delta ompN$	16/32	8/16*
$\Delta ompC$	16	4
$\Delta ompF$	16	4
$\Delta phoE$	16	4
$\Delta ybfM$	16	4
$\Delta ompA$	16	4
$\Delta ompG$	16	
$\Delta ompL$	16	4

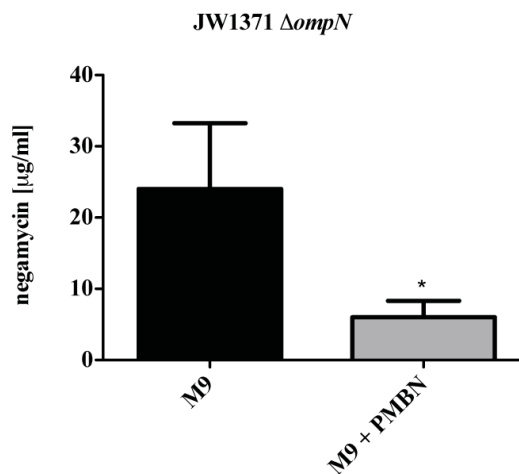


Figure 22: Negamycin activity in JW1371 ($\Delta ompN$) with addition of 15 mg/L PMBN (+ PMBN). (n*=p<0.05)

Only the deletion of *ompN* led to a higher negamycin MIC. This was seen in both media and the effect was stronger in M9. To see if the outer membrane becomes rate-limiting for the uptake in the *ompN*-knockout strain in M9, PMBN was added to the MIC-assay (Figure 22). It was shown that the addition of PMBN increased the negamycin-susceptibility of this knockout strain in M9, in contrast to the effect in the wildtype (Figure 21 and Figure 22).

2.3.3 Susceptibility of the LPS-mutant “rough-phenotype”

Furthermore the susceptibility of a strain with a “deep-rough phenotype” was tested. This strain, JW3606 ($\Delta rfaG$), does not have the outer core region of the LPS (Figure 23). The negative charge of the inner core is exposed and easily accessible. The antibiotic susceptibility of this strain was tested in different media and compared to the wildtype susceptibility (Figure 24).

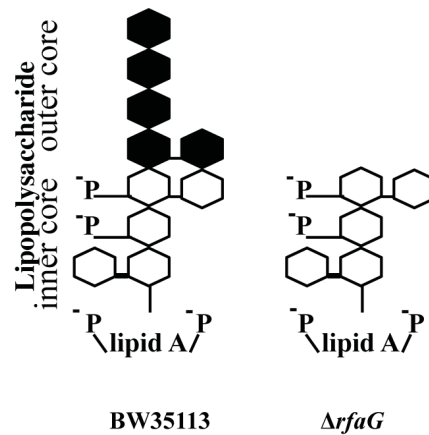


Figure 23: Outer membrane structure of *E. coli* BW25113 and JW3606 (Δ*rfaG*).

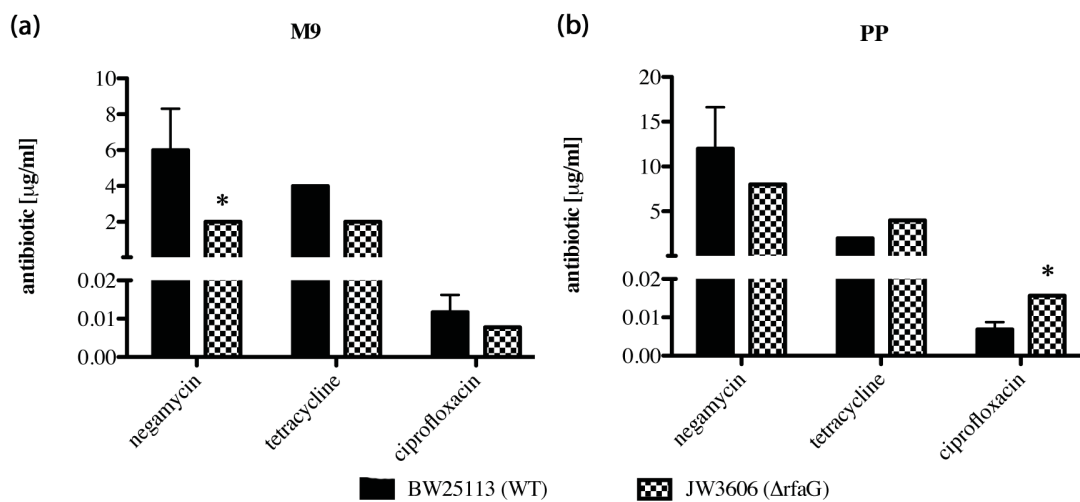


Figure 24: Antibiotic susceptibility of the “deep-rough phenotype” strain JW3606 (Δ*rfaG*) compared to the wildtype (BW25113) in (a) M9 and (b) PP.

The rough phenotype is significantly more susceptible to negamycin in M9 compared to the wildtype (Figure 24a). Tetracycline and ciprofloxacin, which were used as control antibiotics, showed the same trend, even though the difference in the susceptibility was not significant. In PP this effect was not seen for all three antibiotics (Figure 24b). The *rfaG*-knockout and the wildtype showed similar susceptibilities for negamycin and tetracycline. Against ciprofloxacin *rfaG*-knockout seemed more resistant than the wildtype.

To check if the *rfaG*-knockout has a lower fitness in the minimal medium M9 compared to the wildtype, and might therefore be more susceptible to different antibiotics, a growth curve was performed in the microplate reader (Figure 25).

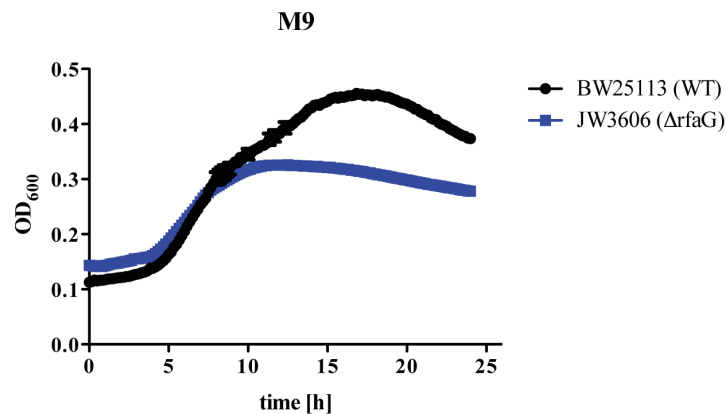


Figure 25: Growth curves of the *E. coli* strains BW25113 (wildtype) and JW3606 (*rfaG*-knockout) in M9 over 24 hours

In the first 10 hours the wildtype and $\Delta rfaG$ grew similarly, as during the lag- and the exponential phase the growth of both strains was comparable. After ten hours the *rfaG*-knockout entered the stationary phase, whereas the wildtype continued growing and reached the stationary phase five hours later. This growth curves show that the “deep-rough-phenotype” $\Delta rfaG$ is growing initially as well as the wildtype in the minimal medium M9, but does not reach the same cell-density. This might be one reason for the increased susceptibility of the strain, although we cannot exclude that the exposed negative surface charge of the $\Delta rfaG$ strain facilitates adhesion of the positively charged negamycin to the Gram-negative cells.

2.4 Negamycin passage across the cytoplasmic membrane

The cytoplasmic membrane is a barrier which has to be crossed in Gram-negative as well as in Gram-positive bacteria (see chapter 1.2.2). The transport can occur either passive or through active transport. Small and electrically neutral molecules can passively diffuse through the phospholipid layer. This uptake route is described for tetracyclines and quinolones in their uncharged form (see chapters 1.3.1.2 and 1.3.1.3). Charged and hydrophilic compounds need to enter via active transporter-mediated uptake. An involvement of the peptide transporter Opp in the uptake of aminoglycosides was described (see chapter 1.3.1.1). In this chapter the investigations on negamycin-uptake over the cytoplasmic membrane are presented.

2.4.1 Uptake via peptide transporter

As negamycin is a pseudopeptide, a possible transport system across the cytoplasmic membrane might be peptide transporters. The negamycin susceptibility of different peptide transporter knockouts of the Keio-collection was tested in M9 and PP (Table 6).

Table 6: Negamycin MICs of different *E. coli* transporter mutants in M9 and PP media.
 (n*=p<0.05, n**= p<0.01) The MIC determination of some strains were performed more often than others.
 This explains why the significance level can differ.

<i>E. coli</i> strain	description	MIC [$\mu\text{g/ml}$]	
		M9	0.5% poylpeptone
BW25113	wildtype	4	16
JW3513 ($\Delta dppA$)	<i>dppA</i> knockout (ABC transporter; periplasmic binding protein)	16**	16
JW3512 ($\Delta dppB$)	<i>dppB</i> knockout (ABC transporter; transmembrane domain)	16*	16
JW3511 ($\Delta dppC$)	<i>dppC</i> knockout (ABC transporter; transmembrane domain)	16*	16
JW35110 ($\Delta dppD$)	<i>dppD</i> knockout (ABC transporter; ATP-binding domain)	16*	16
JW3509 ($\Delta dppF$)	<i>dppF</i> knockout (ABC transporter; ATP binding domain)	16*	16
JW1287 ($\Delta sapA$)	predicted antimicrobial peptide transporter; <i>sapA</i> knockout (ABC transporter; periplasmic binding protein)	8**	32
JW1286 ($\Delta sapB$)	predicted antimicrobial peptide transporter; <i>sapB</i> knockout (ABC transporter; transmembrane domain)	4	16
JW1285 ($\Delta sapC$)	predicted antimicrobial peptide transporter; <i>sapC</i> knockout (ABC transporter; transmembrane domain)	4	16
JW1284 ($\Delta sapD$)	predicted antimicrobial peptide transporter; <i>sapD</i> knockout (ABC transporter; ATP-binding domain)	2 ($p = 0.05152$)	16 (8)
JW1283 ($\Delta sapF$)	predicted antimicrobial peptide transporter; <i>sapF</i> knockout (ABC transporter; ATP-binding domain)	4	16
JW1235 ($\Delta oppA$)	<i>oppA</i> knockout (ABC transporter; periplasmic binding protein)	4	16
JW1236 ($\Delta oppB$)	<i>oppB</i> knockout (ABC transporter; transmembrane domain)	4	16

Table 6: Negamycin MICs of different *E. coli* transporter mutants in M9 and PP media (continued)

<i>E. coli</i> strain	description	MIC [$\mu\text{g/ml}$]	
		M9	0.5% poylpeptone
JW1237 (ΔoppC)	<i>oppC</i> knockout (ABC transporter; transmembrane domain)	4	16
JW1238 (ΔoppD)	<i>oppD</i> knockout (ABC transporter; ATP-binding domain)	4	16
JW1239 (ΔoppF)	<i>oppF</i> knockout (ABC transporter; ATP binding domain)	4	16
JW5240 (ΔddpA)	<i>ddpA</i> knockout (ABC transporter; periplasmic binding protein)	4	16
JW1480 (ΔddpC)	<i>ddpC</i> knockout (ABC transporter; transmembrane domain)	4	16
JW1626 (ΔtppB)	peptide-POT transporter knockout mutant	4	16 (32)
JW0699 (ΔybgH)	POT transporter knockout mutant	4	32*
JW4091 (ΔyjdL)	putative POT transporter knockout mutant	4	16 (8)
JW3463 (ΔyhiP)	putative POT transporter knockout mutant	4	16 (8)
JW1322 (ΔmppA)	<i>mppA</i> -knockout (Component of murein tripeptide ABC transporter; periplasmic binding protein)	4	16
JW2988 (ΔygiS)	<i>ygiS</i> -knockout (putative ABC transporter; predicted periplasmic binding protein)	4	16 (8)
JW2800 (ΔygdQ)	<i>ygdQ</i> -knockout (putative peptide transporter; predicted transmembrane protein)	4	16

The dipeptide permease (Dpp) seems to be a main uptake route of negamycin in M9. The knockout of all different components (*dppA*, *dppB*, *dppC*, *dppD* and *dppF*) led to a 4-fold decrease in susceptibility. This effect was only seen in M9, not in PP. In this medium the knockouts of the dipeptide permease did not show any effect. Another periplasmic binding

protein of an ABC transporter seems to be involved in the negamycin uptake, SapA. The knockout of this periplasmic binding protein led to a two-fold higher resistance in M9. A similar trend was seen in polypeptone, yet it was not significant. Interestingly, the knockout of the other components of this ABC transporter did not have the same effect. In fact, the knockout of *sapD* showed a trend towards higher susceptibility in M9, and the other domain-knockouts did not influence the negamycin activity. The knockout of another main *E. coli* peptide transporter, the oligopeptidase Opp, did not change the susceptibility of the strains. Further mutants of predicted ABC transporters and POT transporters did not have any effect on negamycin activity. In PP only one peptide transporter mutant showed an effect, the knockout of the POT transporter YbgH.

The uptake of negamycin via peptide transporter in *S. aureus* was investigated, too (Table 7). MICs were performed in the *S. aureus* wildtype strain RN6390, and in strains with a knockout in either one of the main oligopeptide transporters *opp-1*, 2, 3 or 4, the combined knockout of all 4 oligopeptide transporters *opp1-4*, knockout in the di/tripeptide permease *dtpT* or the knockout of all four oligopeptide transporter plus the di/tripeptide permease.

Table 7: Negamycin susceptibility in different *S. aureus* transporter mutants in *S. aureus* minimal medium.

<i>S. aureus</i>	description	MIC in <i>S. aureus</i> minimal medium µg/ml
RN6390	wildtype	16
$\Delta opp-1$	<i>opp-1</i> oligopeptide permease knockout	16
$\Delta opp-2$	<i>opp-2</i> oligopeptide permease knockout	16
$\Delta opp-3$	<i>opp-3</i> oligopeptide permease knockout	16
$\Delta opp-4$	<i>opp-4</i> oligopeptide permease knockout	16
$\Delta dtpT$	<i>dtpT</i> dipeptide permease knockout	16
$\Delta opp-1234$	knockout of <i>opp-1</i> , <i>opp-2</i> , <i>opp-3</i> , <i>opp-4</i> permeases	16
$\Delta dtpT-opp-1234$	knockout of the oligopeptide permeases <i>opp-1</i> , <i>opp-2</i> , <i>opp-3</i> , <i>opp-4</i> and the dipeptide permease DtpT	16/32

The peptide transporters in *S. aureus* do not seem to play a substantial role in negamycin uptake in minimal medium (Table 7). The knockout of the oligopeptide- or di/tripeptide transporters did not have any effect on negamycin susceptibility. When all four oligopeptide

transporters and the di/tripeptide transporter were knocked out ($\Delta dtpT\text{-}opp\text{-}1234$), a small, but not significant, change in negamycin activity was observed (16/32 $\mu\text{g/ml}$).

In the next step it was elucidated whether the main peptide transporters are expressed at lower levels in PP compared to M9 in *E. coli*, which could explain that the knockouts of *dppA-F*, *sapA*, *tppB* and *oppA-F* did not show any effect in PP. The expression of the different periplasmic binding proteins and the POT TppB of exponentially grown *E. coli* BW25113 (WT) in PP were compared to the expression in M9 (Figure 26).

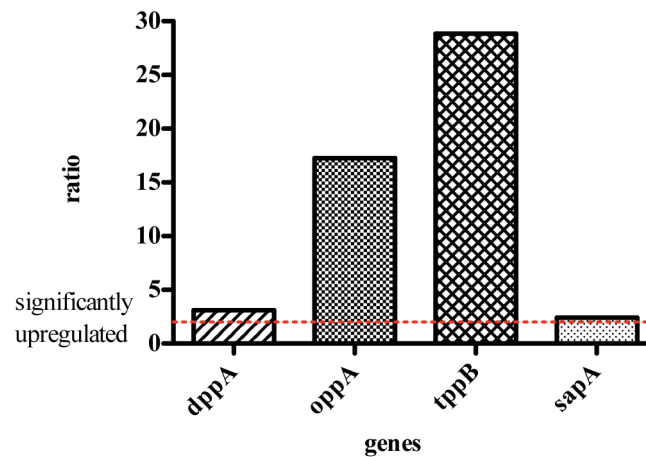


Figure 26: Transporter expression in 0.5 % polypeptone compared to M9 in *E. coli* BW25113. This experiment was performed three times. One is shown as representative. The red line represents the threshold of detection, which indicates a significant upregulation.

The expression analysis showed that all transporters are more highly expressed in PP than in M9 (Figure 26). All measured transporter components were significantly (ratio >2) upregulated in PP. *TppB* is even 30-fold upregulated in polypeptone whereas *dppA* and *sapA* expression was only 2-5 times increased. This result shows that the transporters are present in PP. Knowing that negamycin can use Dpp as an uptake route (see Table 6), one could expect that the knockout of these transporters should lead to a decrease in negamycin-susceptibility.

As this is not the case in PP, another explanation could be that negamycin is competing with peptides for uptake, which are present in PP but not in M9. To investigate this hypothesis, MICs were performed in M9 with addition of casein, peptides and amino acids. Furthermore it was investigated whether the addition of amino acids to M9 had an effect on the transporter expression (Figure 27). To this end, the cells were treated for 30 min with 0.1 mM amino acid-mix (mixture of all 20 proteinogenous amino acids in purified form) and the expression-levels were compared to the untreated cells.

The addition of peptides and single amino acids to M9 led to a decrease in negamycin susceptibility, correlating with increasing concentrations for achieving growth inhibition (Figure 27 (a), (b) and (c)).

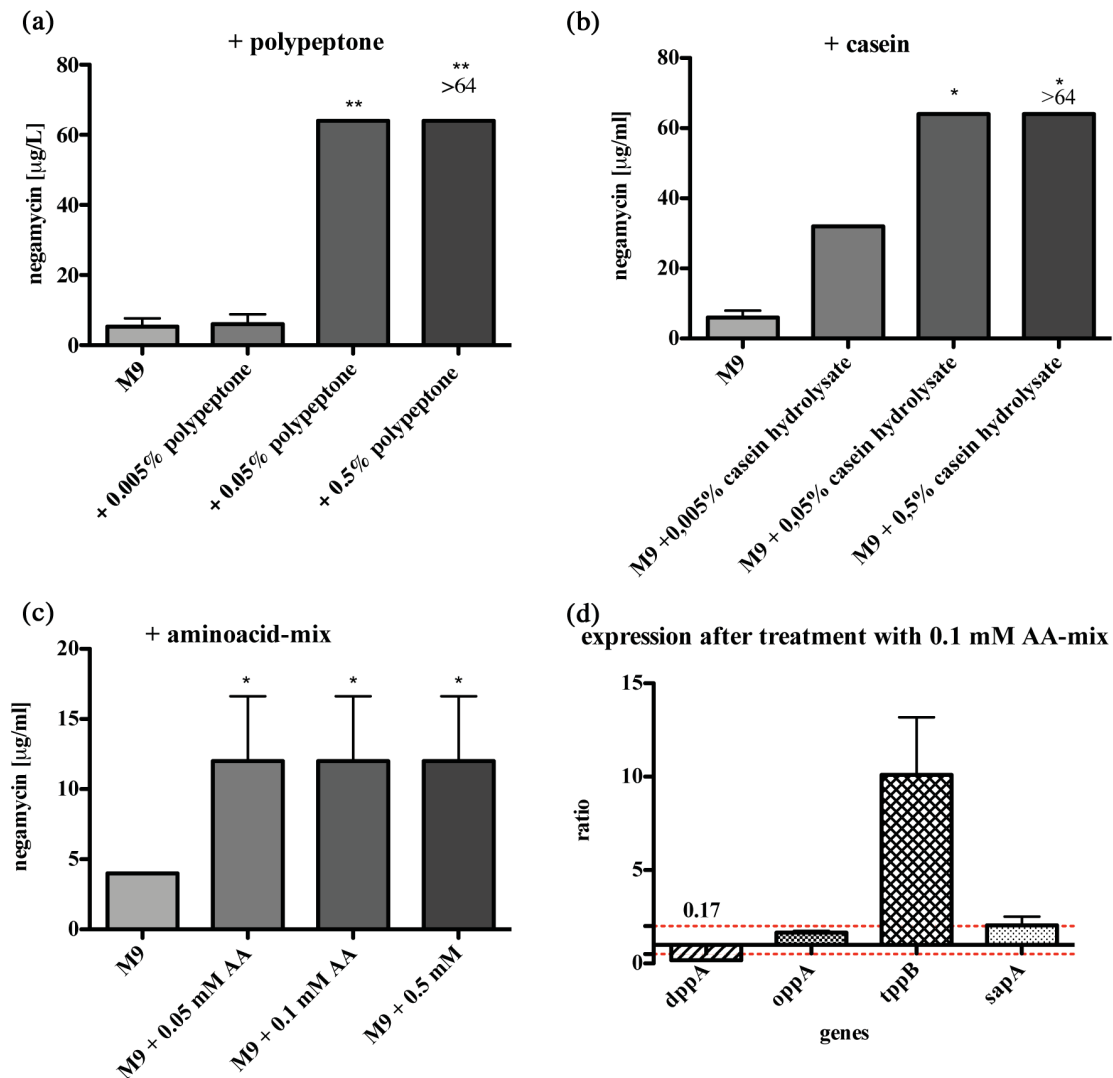


Figure 27: Determination of *E. coli* BW25113 (WT) MICs in M9 with the addition of different concentrations of (a) polypeptone, (b) casein and (c) aminoacid-mix. (d) Transporter expression after 30 minutes treatment with 0.1 mM amino acid-mix (AA-mix) compared to no treatment (M9). (n*=p<0.05, n= p<0.01)**

An increase of MIC above the highest concentration tested (64 $\mu\text{g/ml}$) was seen when PP or 0.5% casein hydrolysate were added to M9. These results point to a competition for uptake with peptides. Furthermore the expression profiles of the transporters, after a 30 minutes treatment with 0.1 mM amino acid-mix (AA-mix) were determined. When the amino acids were added to M9, the expression of *oppA* and *sapA* remained the same compared to the situation in M9 without addition. *TppB*, on the other hand, was 10-fold more highly expressed, and the periplasmic binding protein *dppA* was significantly downregulated.

For comparison, the same MIC-studies, with addition of polypeptone, were performed with bialaphos (Figure 28). Bialaphos is a natural herbicide and a known substrate of *Opp* and *Dpp* [64].

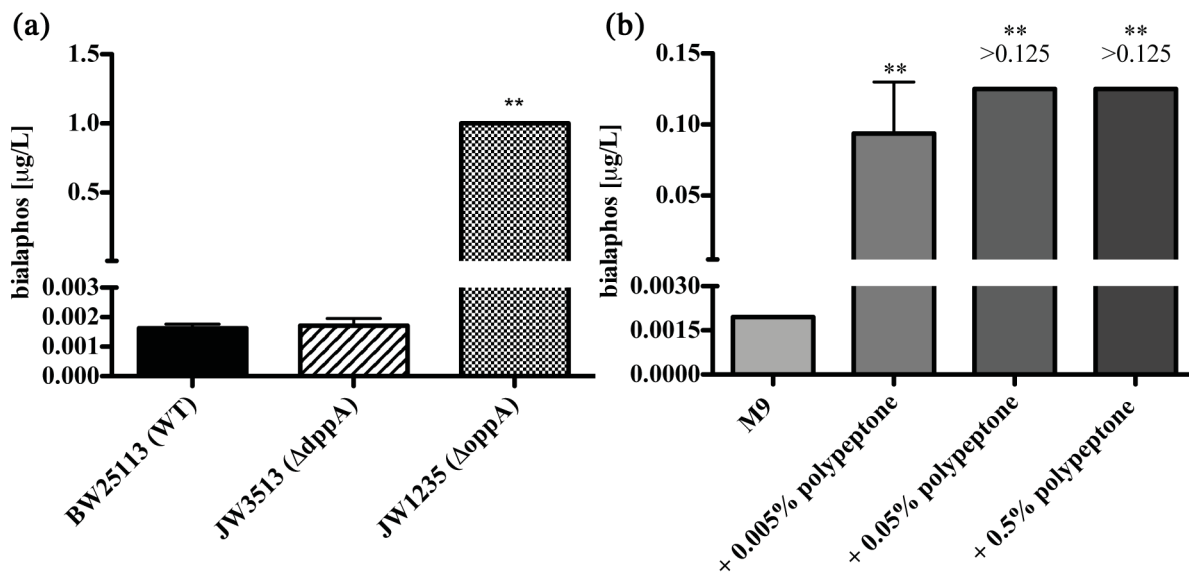


Figure 28: (a) MIC determination of bialaphos in *E. coli* BW25113, $\Delta dppA$ and $\Delta oppA$. (b) Bialaphos MIC determination in M9 with the addition of different concentrations of polypeptone

Bialaphos uses Opp as its main transporter [64]. The MIC determination showed that the knockout of *dppA* did not have any effect on bialaphos susceptibility. When *oppA* was deleted, the MIC increased (Figure 28 (a)). As Opp is the main route of bialaphos, the knockout of Dpp does not seem to have an effect. In further experiments the effect of a double and triple-knockout of different peptide transporters on bialaphos susceptibility was investigated. The results are shown in chapter 2.4.1.3. The addition of polypeptone to M9 had a similar effect for bialaphos as it was seen for negamycin. With increasing concentrations of polypeptone bialaphos activity decreased significantly (Figure 28 (b)).

Another hypothesis was that negamycin induces the expression of peptide transporters in M9. Negamycin is a pseudopeptide and could be recognized as a peptide, which are absent in M9, under the peptide-starvation conditions. Before the qPCR studies were performed, a growth curve was done, to determine a negamycin-concentration that did not kill the cells outright. The experiment was performed in M9 and PP. In the following step the expression of the transporters was measured (Figure 29). *E. coli* BW25113 (WT) cells were grown into the exponential phase, and then treated for 30 minutes with negamycin.

The addition of $\frac{1}{2}$ MIC (2 $\mu\text{g/ml}$) negamycin did almost not affect the growth of the cells in M9 (Figure 29 (a)). In PP the addition of $\frac{1}{2}$ MIC (8 $\mu\text{g/ml}$) negamycin did slightly affect the growth (Figure 29 (b)). The treated cells entered the stationary phase two hours after treatment (timepoint 5 hours). The untreated cells entered the stationary phase after 6 hours and reached a higher OD_{600} than the treated cells (1.3 vs. 1).

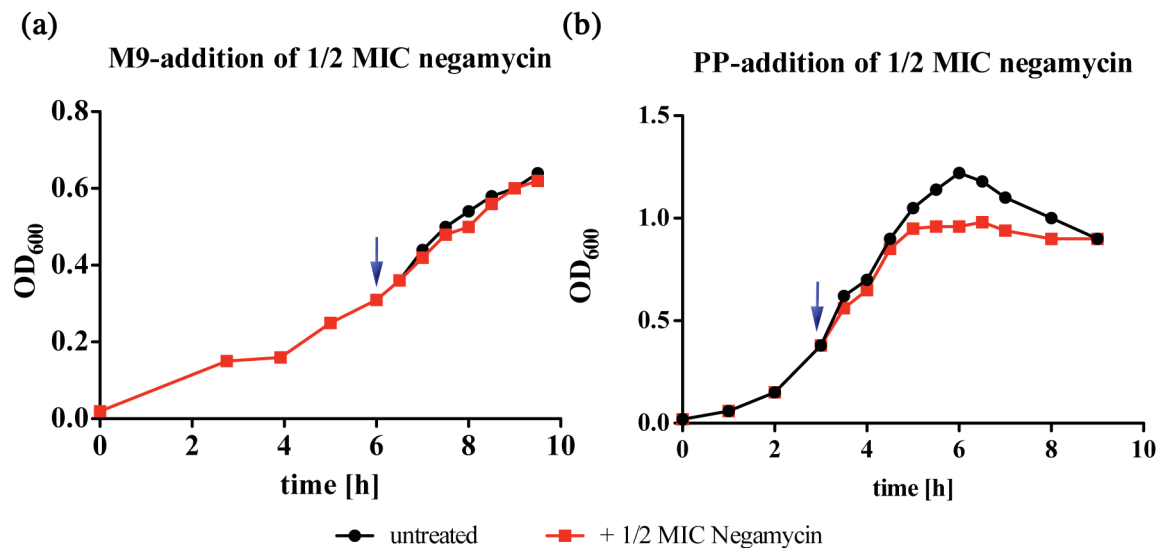


Figure 29: Growth curves of treated and untreated *E. coli* BW25113 (WT) in (a) M9 and (b) PP. Cells were grown to the exponential phase. The timepoint, when negamycin was added, is marked with a blue arrow. The experiment was repeated twice.

As the treatment with this concentration of negamycin did not lead to a strong damage and inhibition of the cells, the expression-analysis was done after treatment with 1/2 MIC negamycin for 30 minutes in M9 (Figure 30), to investigate the changes in transporter expression once the cell senses negamycin.

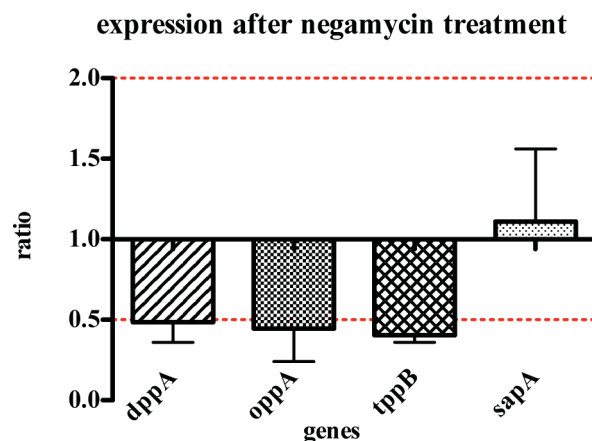


Figure 30: Transporter expression in M9 after 30 minutes treatment with 1/2 MIC negamycin (2 µg/ml).

The qPCR data showed that negamycin does not induce transporter expression (Figure 29 b). In contrary, a trend of downregulation was seen. *TppB* was significantly downregulated

2.4.1.1 Complementation of JW3513 ($\Delta dppA$)

To confirm the effect of the dipeptide permease on negamycin activity the knockout strain was complemented. The cloning was performed by Anne Berscheid (Brötz-Oesterhelt lab). *DppA* was cloned into the vector pASK-IBA 5 plus. JW3513 ($\Delta dppA$) del. was then transformed with the plasmid, and the empty vector. This vector carries a promoter, which can be induced by anhydrotetracycline (ATc).

In the first step, negamycin MICs were performed with different ATc concentrations, to determine the best amount of ATc for induction (Figure 31).

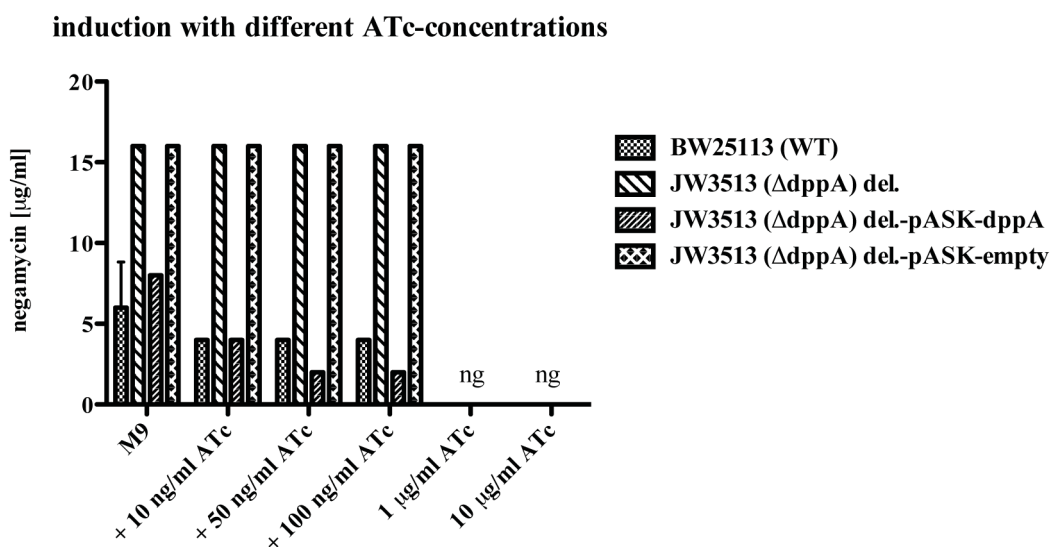


Figure 31: Determination of ATc-concentration for induction of *dppA*-expression in pASK-*dppA*. (ng= no growth could be detected)

When no ATc was added to the MIC assay, the wildtype showed, as expected, a MIC of 4 $\mu\text{g/ml}$ and the *dppA* knockout strain 16 $\mu\text{g/ml}$. The strain, which was transformed with pASK-*dppA* had an MIC of 8 $\mu\text{g/ml}$. This reduced resistance can be due to a leaky promoter. Even though no ATc is added, *dppA* is expressed to a small amount, and leads to an increased susceptibility compared to the *dppA* knockout strain. When 10 ng/ml ATc were added, the complemented strain showed the same susceptibility as the wild type. The strain, transformed with the empty vector, showed the same susceptibility as $\Delta dppA$ del. The same profile was seen when 50 ng/ml ATc were added. At a concentration of 100 ng/ml JW3513 ($\Delta dppA$) del. pASK-*dppA* was even more susceptible than the wildtype. This high concentration of ATc might lead to an overexpression of *dppA*, which explains the increased susceptibility. When higher ATc concentrations were added, the strains could not grow anymore. Based on these results, the MIC was determined in M9 supplemented with 10 ng/ml ATc to induce the expression of *dppA* (Figure 32).

As mentioned before, the *dppA* knockout strain leads to a four-fold increase of negamycin resistance (Table 6). When the knockout was complemented, the strain showed the same susceptibility as the wildtype. As a control the strain was transformed with the empty vector. JW3513 del.-pASK-empty showed an MIC of 16 $\mu\text{g/ml}$, as the knockout of *DppA*. This verifies

that the knockout of *dppA* is responsible for the increased negamycin resistance and not a downstream effect on the *dpp* gene cluster

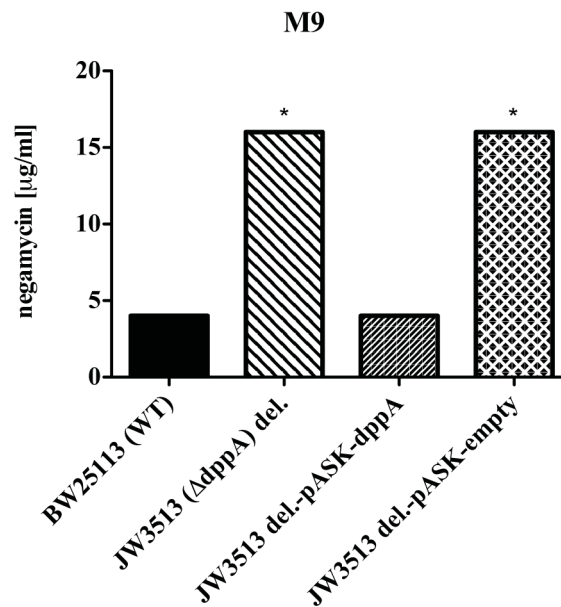


Figure 32: Negamycin susceptibility in BW25113 (WT), the *dppA*-knockout strain JW3513 ($\Delta dppA$) del., the complemented strain JW3513 del. pASK-*dppA* and JW3513 del.-pASK-empty. ($n^*=p<0.05$)

2.4.1.2 Construction of periplasmic binding protein double- and triple-knockouts in *E. coli* JW3513

As the periplasmic binding proteins of the main ABC-peptide transporters (*DppA*, *OppA* and *SapA*) share high amino acid similarity in *E. coli* (*DppA* & *OppA*: 40.6%, *DppA* & *SapA*: 54.7% and *OppA* & *SapA*: 41.1%, see chapter: Alignments of periplasmic binding proteins, Supplemental Data), a cross-talk between the periplasmic binding proteins of the different transporters and binding of the same substrates could be possible. If cross talk occurred in the absence of one periplasmic binding protein, the remaining ones could still bind the substrate, as for example negamycin, and transport it into the cell, regardless that it is not the preferred transporter route. To investigate this hypothesis double and triple-knockout strains of these binding proteins were created.

The knockouts were constructed as described by Datsenko and Wanner [141]. The *dppA-sapA* double knockout containing resistance cassettes in both genes, and $\Delta dppA-\Delta sapA$ del., where the resistance cassettes were removed and only a small scar was left, were constructed within the bachelor thesis of Melanie Dostert. The *dppA-oppA* double knockout, containing resistance cassettes in both genes, and all further cloned strains, were constructed within this work.

In the first step the chloramphenicol-resistance cassette (cm-cassette) was amplified, using primers with homologous ends to *oppA* and *sapA*, respectively. *E. coli* JW3513 was then

transformed with the helper plasmid pKD46, which carries the λ -red genes behind the araBAD promoter for recombination, followed by transformation with the amplified cassette. The cells were then plated on LB Amp/Cm and potential clones were checked for insertion of the cm-cassette by PCR (Figure 33). The expected size of the *oppA*-wildtype PCR fragment was 1852 bp, and the one of the *oppA*-knockout 1379 bp. The expected *sapA*-wildtype fragment was 1813 bp and the one of the knockout 1370 bp.

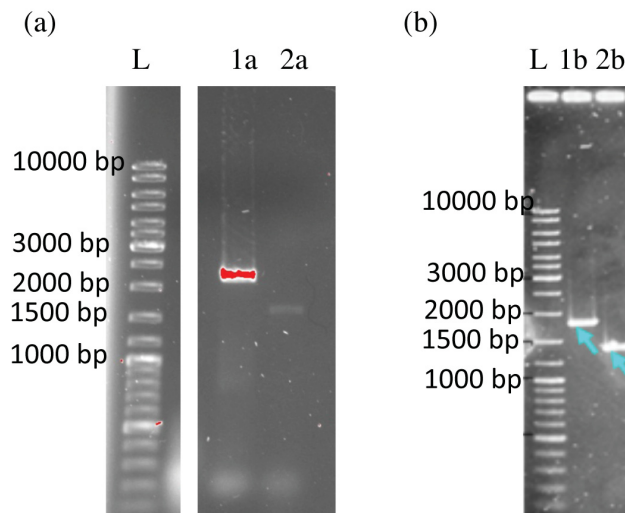


Figure 33: PCR confirmation of the *oppA*-knockout (a) and the *sapA*-knockout (b) in *E. coli* JW3513:
L: ladder, **1a:** *E. coli* JW3513 ($\Delta dppA$) (primer: *oppA* fwd/rev), **2a:** *E. coli* $\Delta dppA$ $-\Delta oppA$ (primer: *oppA* fwd/rev). **1b:** *E. coli* JW3513 ($\Delta dppA$) (primer: *sapA* fwd/rev), **2b:** *E. coli* $\Delta dppA$ $-\Delta sapA$ (primer: *sapA* fwd/rev). (b) was constructed by Melanie Dostert.

The PCR-fragments of the double knockouts showed the expected size. The *oppA*-wildtype had an amplification product with the size of 2000 bp, the product of the putative knockout strain had a size of 1500 bp (Figure 33 a). This correlates with the expected sizes of 1813 and 1370 bp. The same is true for the *dppA-sapA*-knockout. The *sapA*-knockout had an amplification product of around 2000 bp, whereas the putative knockout product was a bit below 1500 bp. Both CR fragments are highlighted with blue arrows (Figure 33 b). The expected sizes were 1813 bp and 1370 bp, which align with the sizes of the obtained PCR products. To confirm the successful knockouts, the amplification products were sent for sequencing, and aligned using Clone Manager (Figure 34, Figure 35).

The alignment of the sequencing results showed that the *oppA* gene in the JW3513 strain is disrupted, after the first 60 bp and before the last 67 bp, and deleted. Therefore the insertion of the chloramphenicol-cassette was successful (Figure 34). The first 60 bp of the *oppA* gene were intact, then the sequence of the inserted resistance cassette, flanked by P1 and P2, followed. The first FRT-element was sequenced too, framing the cm-cassette on the left. The sequence downstream of P2 is not shown in this figure as the obtained sequencing result of the amplification product with the primer *oppA* rev showed a low quality in this region.

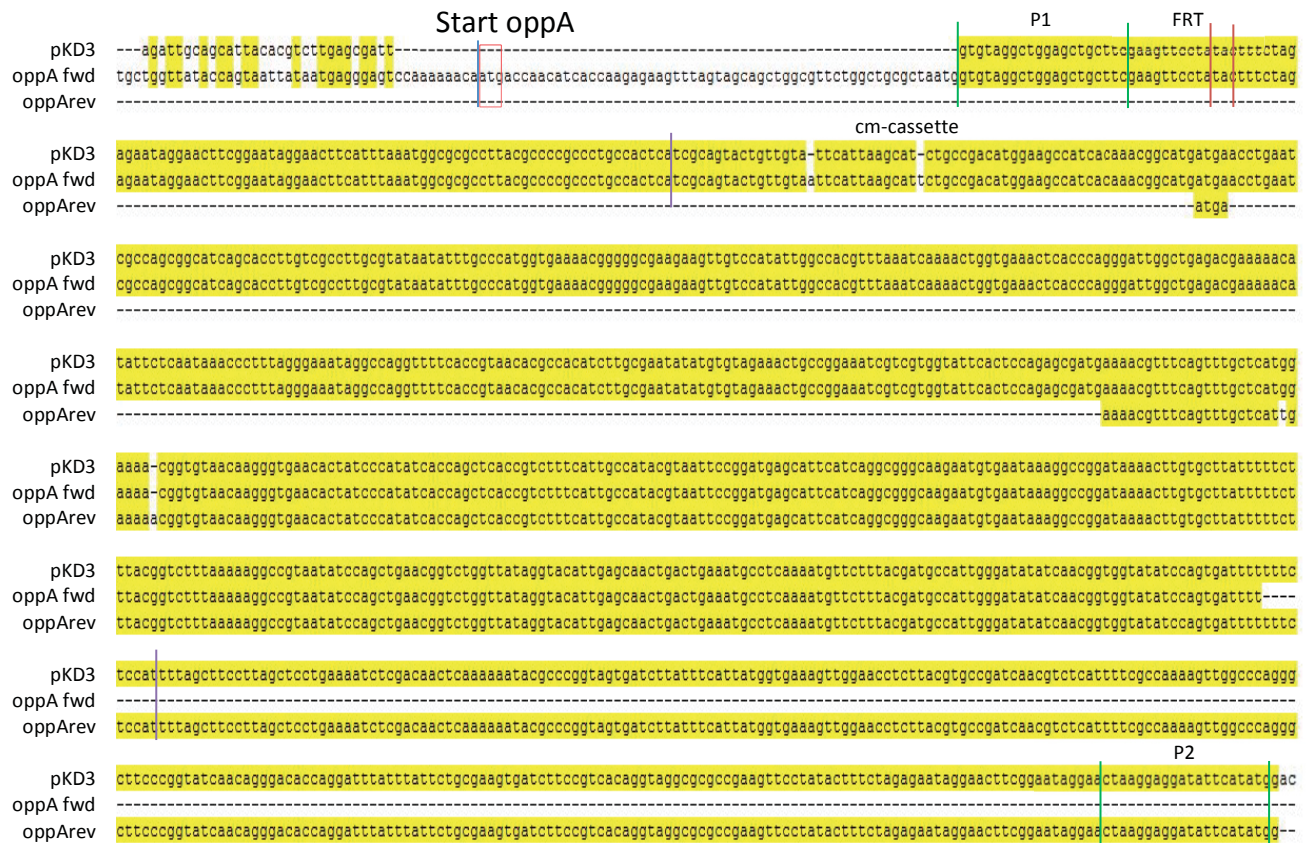


Figure 34: Sequencing result and alignment of the plasmid pKD3 (sequence from database) with obtained sequences with the primers oppA fwd and oppA rev. The sequence from the database is shown in the first row of the alignment. The other two rows show the pKD3 sequences obtained with the different primers (oppA fwd and oppA rev). P1 and P2 (homologous parts of the primer and the resistance cassette), the FRT-elements and the cm-cassette are highlighted in the figure. The obtained sequences are labeled on the left side of the alignment.

The sequencing results of the *sapA*-knockout were aligned with pKD3 too, and showed that the insertion of the cm-cassette was successful (Figure 35). *SapA* was disrupted between the first 106 bp and the last 37 bp. The P1 and P2 and FRT-elements are flanking the cm-cassette and these elements were disrupting the gene. As seen in the sequencing result of the deleted *oppA* gene (see Figure 34), the sequence downstream of P2 is not shown in this figure as the obtained sequencing result of the amplification product with the primer sap rev showed a low quality in this fraction.

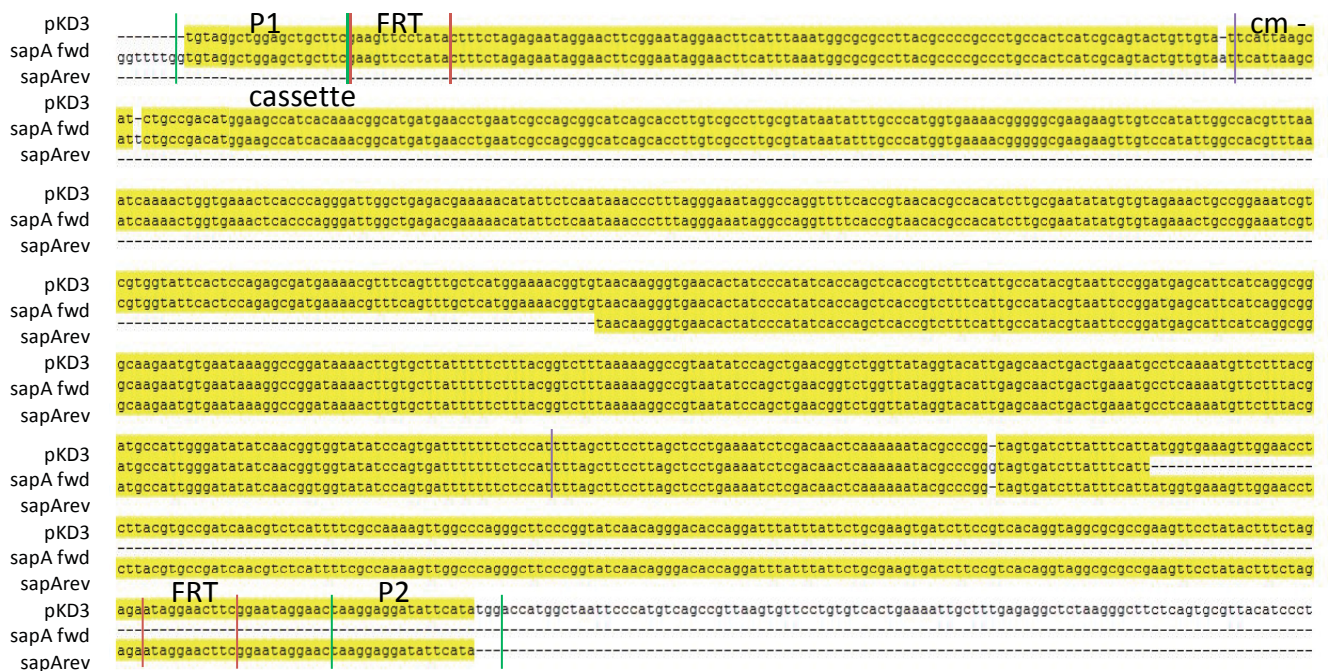


Figure 35: Sequencing result and alignment of the plasmid pKD3 (sequence from database) with obtained sequences with the primers sapA fwd and sapA rev.

The sequence from the database is shown in the first row of the alignment. The other two rows show the pKD3 sequences obtained with the different primers (sapA fwd and sapA rev). P1 and P2 (homologous parts of the primer and the resistance cassette), the FRT-elements and the cm-cassette are highlighted in the figure. The obtained sequences are labeled on the left side of the alignment.

In the next step a triple knockout of the three periplasmic binding proteins, was constructed. To this end the double knockout $\Delta dppA$ - $\Delta sapA$ was used as a starting point. This strain carried two selection markers; the kanamycin cassette in the *dppA*-gene and the chloramphenicol-cassette in the *sapA* gene. To knockout *oppA*, one of these resistance-markers had to be introduced again, therefore the cassettes had to be deleted in the *dppA*-*sapA* double knockout first. To delete the resistance cassette the strain was transformed with the plasmid pCP20 (temperature-sensitive replication and thermal induction of FLP synthesis). Afterwards the strain was tested for the loss of all antibiotic resistance. The scar-areas of the two genes *dppA* and *sapA* were sequenced (alignments are shown in the chapter: Alignments of constructed knockouts, Supplemental Data), and the loss of the selection markers was confirmed. The knockout of *oppA* in the $\Delta dppA$ - $\Delta sapA$ -del. strain was constructed as described before. The cm-cassette was inserted in the *oppA*-gene, and possible clones were checked via PCR and visualized by agarose gel electrophoresis (Figure 36). The expected size of the *oppA*-wildtype fragment was 1852 bp, and the one of the *oppA*-knockout 1379 bp, as described above for the double knockout $\Delta dppA$ - $\Delta oppA$.

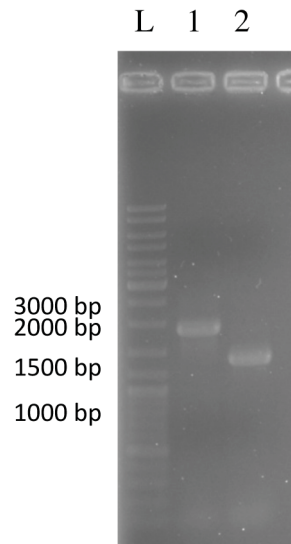


Figure 36: PCR confirmation of the *oppA*-knockout in *E. coli* $\Delta dppA$ - $\Delta sapA$ del.

L: ladder, **1:** *E. coli* $\Delta dppA$ - $\Delta sapA$ del (primer: *oppA* fwd/rev), **2:** *E. coli* $\Delta dppA$ - $\Delta sapA$ - $\Delta oppA$ (primer: *oppA* fwd/rev).

The size of the PCR product of *oppA* in the $\Delta dppA$ - $\Delta sapA$ -del. strain was slightly below 2000 bp. The expected size was 1852 bp, which correlates with this product. The expected size of *oppA* in the $\Delta dppA$ - $\Delta sapA$ - $\Delta oppA$ strain was 1379 bp, which aligns with the PCR product, which is slightly below 1500 bp. The two amplification products were sent for sequencing and aligned with pKD3 and *oppA*, using Clone Manager. In the next step the resistance-cassette in the *oppA* gene was deleted too, so that the strain $\Delta dppA$ - $\Delta sapA$ - $\Delta oppA$ del. did not carry any selection markers. The scar region of *oppA* was sequenced and aligned. The results are shown in the chapter: Alignments of constructed knockouts, Supplemental Data.

2.4.1.3 Characterization of the constructed double and triple knockouts ($\Delta dppA$ - $\Delta oppA$, $\Delta dppA$ - $\Delta sapA$, and $\Delta dppA$ - $\Delta sapA$ - $\Delta oppA$)

Growth curves:

To characterize the constructed double- and triple-knockouts of the periplasmic binding proteins, growth curves were performed in M9 and PP (Figure 37). Growth was measured of BW25113 (WT), JW3513 ($\Delta dppA$), JW1235 ($\Delta oppA$), JW1287 ($\Delta sapA$), $\Delta dppA$ - $\Delta oppA$, $\Delta dppA$ - $\Delta sapA$ and $\Delta dppA$ - $\Delta sapA$ - $\Delta oppA$. The OD_{600} of the cells was adjusted to 0.1 and the growth was measured over 25 hours in the microplate reader. The growth curves of each strain were performed in triplicates.

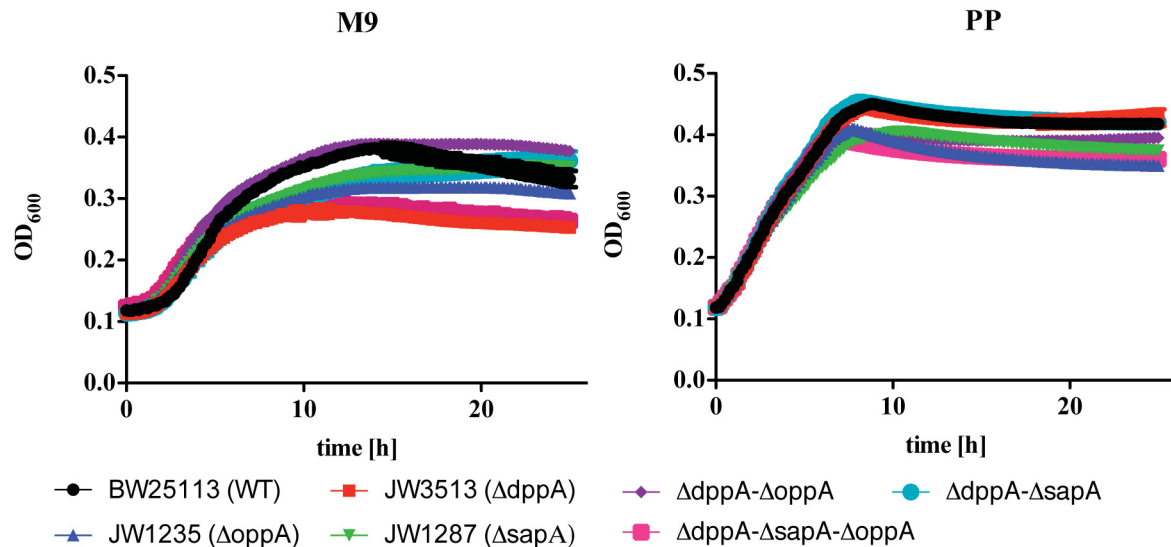


Figure 37: Growth curves of the periplasmic binding protein-single, double- and triple-knockout strains in (a) M9 and (b) PP.

The growth was measured in triplicates over 25 hours in the microplate reader.

In the microplate reader, the strains grew slowly and only to a maximum OD₆₀₀ of 0.4 (M9) and 0.5 (PP) (Figure 37). This is due to the small volume in the 96-well plate (100 μ l) and the lower oxygen conditions in the well, compared to the condition in a flask. In M9 and PP all strains entered the exponential phase at the same time and had a comparable growth rate, with a doubling time of 3 hours in M9 and 2.5 hours in PP. All strains entered the stationary phase in M9 after 6-7 hours and only the maximum OD₆₀₀ differed. The wildtype strain BW25113 (black) and $\Delta dppA-\Delta oppA$ (purple) grew similarly up to an OD₆₀₀ of 0.4. After 15 hours the OD₆₀₀ of the wildtype decreased again, as it entered the death phase. $\Delta sapA$ (green) and the double knockout $\Delta dppA-\Delta sapA$ (turquoise) grew a bit below the maximum OD₆₀₀ of the wildtype (OD₆₀₀ 3.5), but after 23 hours they reached the same OD₆₀₀. The strains $\Delta oppA$ (blue), $\Delta dppA$ (red) and the triple-knockout $\Delta dppA-\Delta sapA-\Delta oppA$ (pink) seemed to have a growth deficiency in this experiment in M9. Even though the exponential phase proceeded parallel with the wildtype strain, the maximum OD₆₀₀ that was reached was 0.3. This effect was seen for the triple knockout (pink) and $\Delta oppA$ (blue) in PP too. These two strains reached an OD₆₀₀ of 0.4, as was seen for $\Delta sapA$ (green), $\Delta dppA-\Delta oppA$ (purple) too. The wildtype (black), $\Delta dppA$ (red) and $\Delta dppA-\Delta sapA$ (turquoise) showed a similar growth, and reached a maximum OD₆₀₀ of 0.5. The growth patterns for all strains were similar and they entered the exponential phase after 1 hour and the stationary phase after 7-7.5 hours.

In summary the knockout of the main oligopeptide transporter Opp (blue) seemed to lead to a growth deficiency in both media. This was seen, in this experiment for the triple knockout (pink), and $\Delta sapA$ (green) too. The double knockout of *dppA* and *oppA* (purple) grew slightly less dense than the wildtype in PP. When Dpp was not functional anymore, the strain seemed to have a growth deficiency in M9 (red). The double knockout of *dppA* and *sapA*

grew comparable to the wildtype (turquoise). As this experiment was only performed once in triplicates, these observations need to be validated.

Susceptibility profile of the double- and triple-knockouts:

In the next step the susceptibility towards negamycin was tested (Figure 38). MICs were performed in M9 and 0.5% PP.

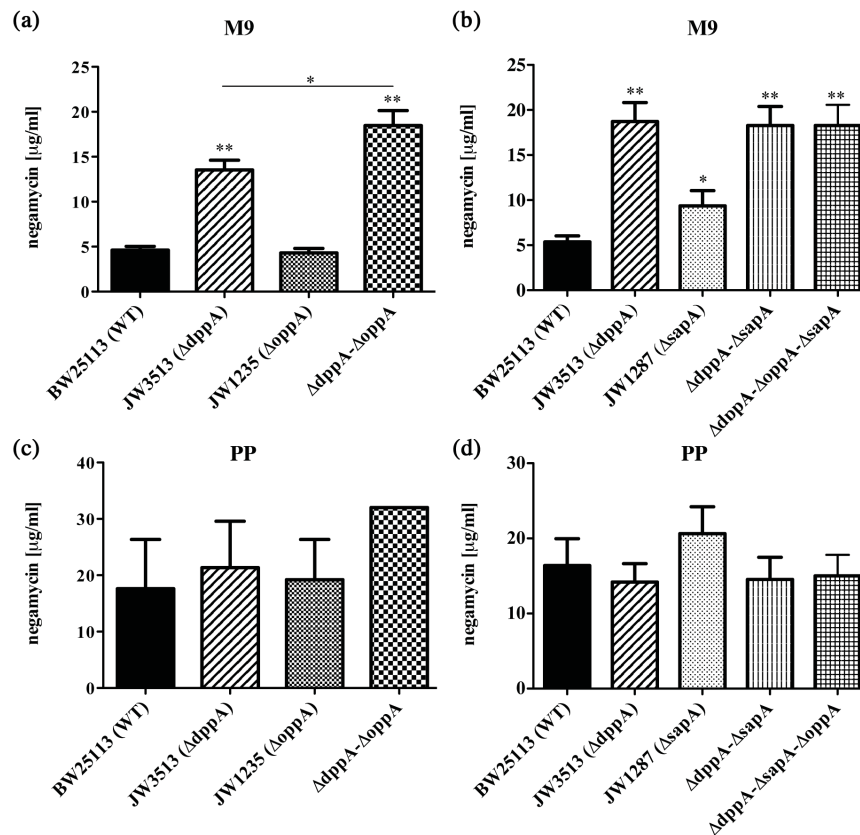


Figure 38: Negamycin susceptibility of the periplasmic binding protein- single- double and triple-knockout *E. coli* strains in (a, b) M9 and (c, d) PP. (n*=p<0.05, n= p<0.01)**

As shown before (Table 6) the knockout of the dipeptide permease leads to a highly significant decrease in susceptibility in M9 (Figure 38 a). The knockout strain is four-times more resistant than the wildtype. The single-knockout of the periplasmic binding protein of the oligopeptide transporter Opp did not have a substantial effect in M9 and PP (Figure 38 a, c), whereas the double knockout strain of *dppA* and *oppA* significantly decreased the susceptibility towards negamycin compared to the single *dppA*-knockout in M9 (Figure 38 a), even though the MIC values were only slightly different (16 µg/ml vs. 20 µg/ml). On the contrary the double-knockout of *sapA* and *dppA* did not have any additional effect on negamycin resistance. The double-knockout showed the same MIC values as the single *dppA*-knockout in M9. The single knockout of *sapA* was significantly more resistant to negamycin than the wildtype in M9 (Figure 38 b). The triple-knockout of the three periplasmic binding proteins also did not have any additional beneficial effect on the susceptibility compared to the single *dppA* knockout in this experiment (Figure 38 b). It should be considered that the determined MIC-value of the *dppA*-single knockout in the

experiment depicted in Figure 38 b was higher than in the experiment depicted in Figure 38 a. Therefore the resistance-effect of the triple-knockout might not be seen, when it only differs slightly, as seen for the *dppA-oppA*-double knockout. In PP, none of the periplasmic binding protein knockouts changed the negamycin susceptibility compared to the wildtype (Figure 38 c, d).

In summary the double knockout of *dppA* and *oppA* seemed to bring a beneficial effect for resistance of negamycin, which could be shown in 13 independent experiments. As there was only a very slight effect, Opp is probably only involved in negamycin uptake to a small extent. The double knockout of *dppA* and *sapA*, and the triple-knockout of *dppA*, *sapA* and *oppA*, had the same MIC-profile as the single *dppA* knockout. Even though a beneficial effect of the triple-knockout cannot be excluded, as some trends were seen in the experiments, a significant relevance could not be shown.

Excursus: Susceptibility of $\Delta dppA$ - $\Delta oppA$ and $\Delta dppA$ - $\Delta sapA$ - $\Delta oppA$ towards bialaphos

For comparison the susceptibilities of the *dppA*- and *oppA* knockouts, towards bialaphos, were tested in (2.4.1). The knockout of *dppA* did not have any effect on bialaphos susceptibility. When *oppA* was mutated, the bialaphos MIC strongly increased (Figure 28 (a)). To see whether the double-knockout of *dppA* and *oppA* or the triple-knockout of *dppA*, *sapA* and *oppA* led to a change in susceptibility compared to the single *oppA* knockout, the MIC was determined (Figure 39).

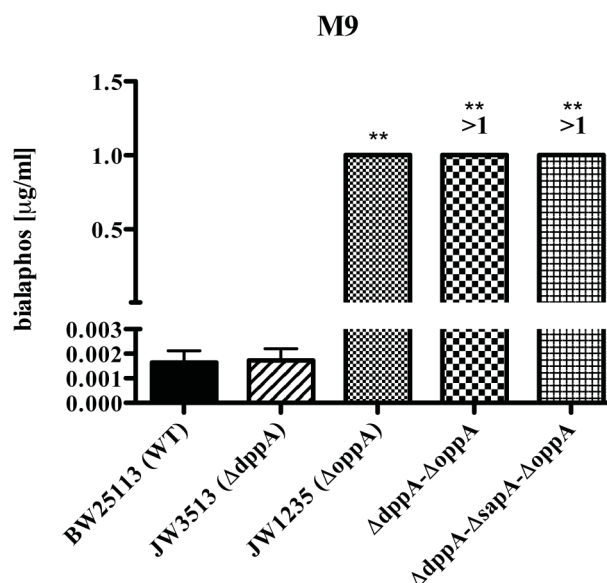


Figure 39: Bialaphos susceptibility in different *E. coli* knockout strains.
(n**=p<0.01)

In alignment with the MIC determination that was shown before (Figure 28) the single knockout of *dppA* did not have any effect on bialaphos susceptibility (Figure 39). When the periplasmic binding protein of the oligopeptide permease Opp was deleted, the MIC

increased from 0.0015 to 1 $\mu\text{g/ml}$. The double- and triple-knockout strains $\Delta dppA-\Delta oppA$, $\Delta dppA-\Delta sapA-\Delta oppA$ were even more resistant to bialaphos with an MIC of $>1 \mu\text{g/ml}$. This result shows that Opp seems to be the main entry route for bialaphos, but the other peptide transporter, at least Dpp, are involved in the uptake as well.

2.4.1.4 Comparison of strains with intact and deleted resistance cassette

Comparison of susceptibility-profile of strains with intact and deleted resistance cassette

In the next step it was investigated whether the insertion of the selection marker had a downstream effect, which might have a pinfluence on negamycin susceptibility. Therefore the susceptibility profile of the strains, carrying the antibiotic resistance-cassette, and the strains with the deleted cassette were compared in M9 (Figure 40).

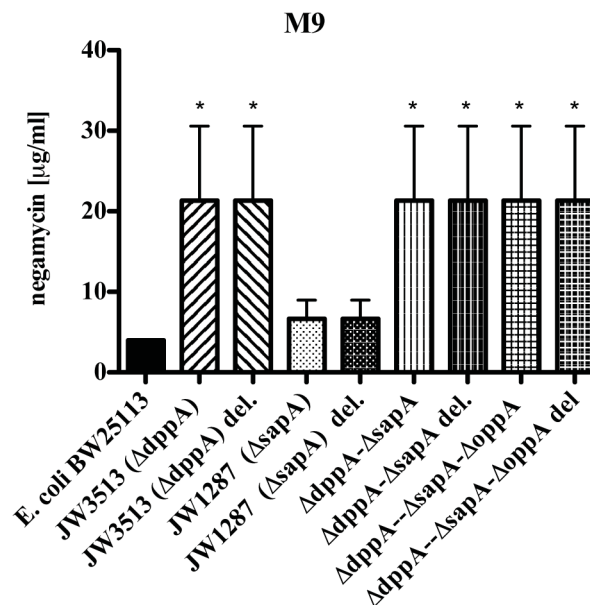


Figure 40: Comparison of the negamycin susceptibility of the *E. coli* knockout strains with intact and deleted resistance-cassette.

($n^*=p<0.05$)

The strains carrying the antibiotic resistance cassette and the strains with the deleted cassette showed the same susceptibility towards negamycin. Therefore the deletion of the selection marker did not affect the MIC of the strains.

Comparison of expression profile of strains with intact and deleted resistance cassette

DppA-F is encoded in one operon (Figure 41). The promoter is located in front of *dppA* and the whole operon is transcribed as one transcription unit.

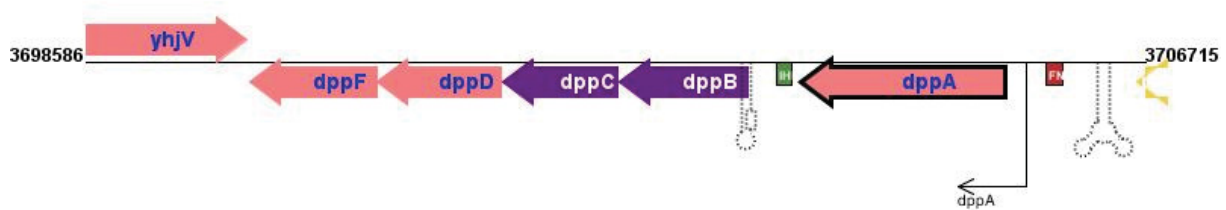


Figure 41: Transcription unit *dppABCDF*. The transcription starts in front of *dppA* (source: ecoliwiki)

The strain JW3513 ($\Delta dppA$) has a kanamycin resistance cassette inserted in *dppA*. The cassette carries a stop codon, which allows the assumption that the translation stops after the cassette and the mRNA of the other genes in the operon is not translated. In the strain JW3513 ($\Delta dppA$) del., in which the resistance cassette was deleted, *dppBCDF* could be translated. To investigate if the knockout of the *dppA* had an influence on the expression of the other genes in the knockout the gene expressions of *dppA-F* were measured in JW3513 ($\Delta dppA$) and JW3513 ($\Delta dppA$) del., and compared to the expression determined in the wildtype strain BW25113 (Figure 42). The expression of *dppA-F* in the wildtype was set as 1.

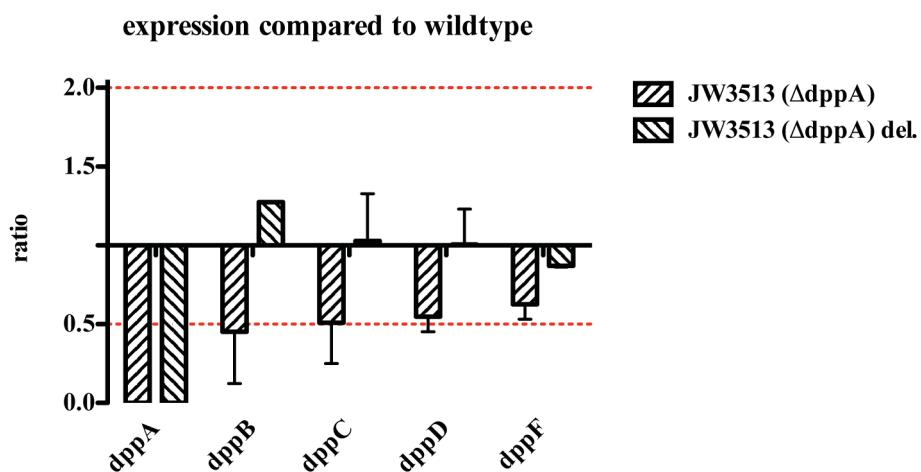


Figure 42: Gene expression of *dppA-F* in JW3513 ($\Delta dppA$) and JW3513 ($\Delta dppA$) del. compared to the expression in BW25113

DppA was, as expected, not expressed in either of the two strains (Figure 42). The other four genes *dppB-F* showed, in contrary to *dppA*, a low expression in JW3513 ($\Delta dppA$). Compared to the wildtype the expression is reduced to half. This expression-reduction could be explained through a negative autoregulation. As *dppB-F* are not translated, the expression might be downregulated. In JW3513 ($\Delta dppA$) del. the expressions of *dppBCDF* are comparable to the wildtype. This result shows that the kanamycin resistance-cassette was

inserted behind the promoter area and only affected *dppA*. When the cassette was deleted the expression of *dppB-F* could take place.

2.4.1.5 Expression of different ABC transporter periplasmic-binding proteins in *E. coli* JW3513 ($\Delta dppA$), JW1235 ($\Delta oppA$), JW1287 ($\Delta sapA$)

DppA, SapA, and OppA share a high similarity (2.4.1.2). Thus, it was investigated if cross-talk, of these periplasmic binding proteins might take place. One could hypothesize that the knockout of one of the periplasmic binding proteins could lead to an increased expression of another periplasmic binding protein that could then interact with the membrane-standing components of its cognate or a non-cognate transporter. To investigate possible transcriptional cross-talk between the ABC transporters, the gene expression levels of the genes encoding the different periplasmic binding proteins were measured by qPCR in the single-knockout strains ($\Delta dppA$, $\Delta oppA$, $\Delta sapA$) and in the double-knockout strain $\Delta dppA$ - $\Delta sapA$ (Figure 43). The expression was compared to the wildtype expression, which was set to 1.

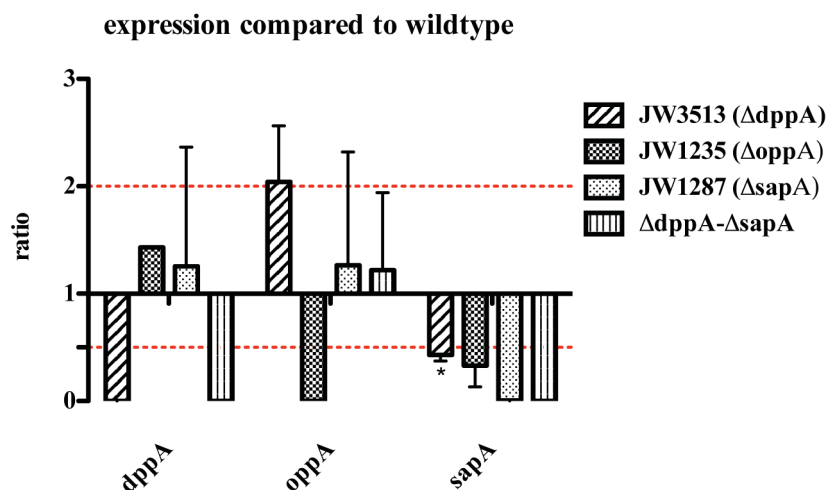


Figure 43: Expression of the periplasmic binding proteins *dppA*, *oppA* and *sapA* in JW3513 ($\Delta dppA$), JW1235 ($\Delta oppA$), JW1287 ($\Delta sapA$) and $\Delta dppA$ - $\Delta sapA$.

The expression was compared to the wildtype. ($n^*=p<0.05$)

As expected, no *dppA* expression was detected in JW3513 ($\Delta dppA$) and $\Delta dppA$ - $\Delta sapA$ (Figure 43). The expression levels of *dppA* in JW1235 ($\Delta oppA$) and JW1287 ($\Delta sapA$) were comparable to the wildtype levels. *OppA* was not expressed in the *oppA*-knockout strain, which confirmed the knockout of this gene. In the other strains, no significant change in *oppA* expression was seen. The periplasmic binding protein *sapA* was not expressed in the single *sapA* knockout strain and the double knockout strain $\Delta dppA$ - $\Delta sapA$. The reason is that a

resistance cassette is inserted into this gene. The *sapA* expression in the $\Delta dppA$ strain was significantly down regulated. In the single $\Delta oppA$ knockout the same trend was seen, but this was not significant, as the standard deviation between the different experiments was high.

The qPCR results showed that the knockout of one or two of these genes encoding the periplasmic binding proteins did not lead to an increased expression of the gene encoding the other binding proteins, therefore no compensation of the periplasmic binding proteins on transcriptional level took place. The knockout of *dppA* had even the opposite effect on *sapA*, as its the expression was significantly down regulated. In summary no cross-talk could be shown on the transcription level. These results are underlined by the fact that JW3513 ($\Delta dppA$) del., which has a intact SapA, and $\Delta dppA$ - $\Delta sapA$ did not show a difference in susceptibility (Figure 40). This observation indicates that SapA does not interact with Dpp in negamycin uptake.

2.4.2 Uptake of negamycin via lysine-uptake systems

Negamycin and the basic amino acid lysine have structural similarities (Figure 44) and they may compete for uptake by a so far elusive transporter. Uehara *et al.* even proposed an active negamycin uptake via a lysine-permeation system [120], but this hypothesis was not proven.

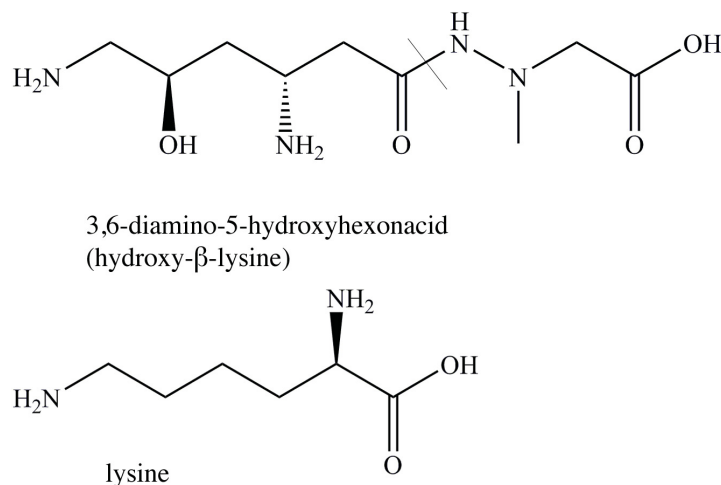


Figure 44: Comparison of negamycin (3,6-diamino-5-hydroxyhexonacid) and lysine structures

To test whether negamycin is competing with lysine or other basic amino acids for uptake, increasing lysine and arginine/histidine concentrations were added to M9. The negamycin MIC was then determined (Figure 45).

The addition of lysine to M9 showed that with increasing concentration the susceptibility towards negamycin is decreasing. In M9 the measured negamycin MIC was around 5 µg/ml. At a concentration of 0.5 mM lysine, up to 10 mM, the susceptibility drops to 16 µg/ml (Figure 45 a). This result indicates that negamycin is competing for uptake with lysine. This

effect is specific for lysine and does not occur with other basic amino acids, such as arginine and histidine (Figure 45 b).

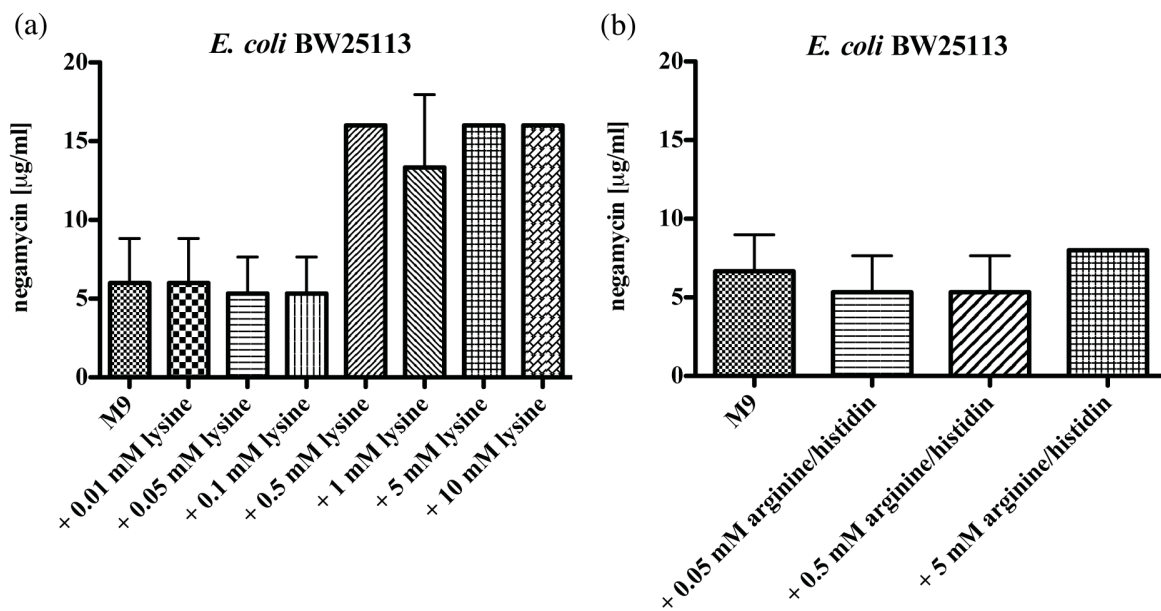


Figure 45: Addition of increasing concentrations of lysine or arginine/histidin to M9. Negamycin MIC was determined in *E. coli* BW25113 (WT).

As lysine and negamycin compete for uptake, they might use the same uptake system. In the next step the negamycin MIC was determined in different lysine transporter knockout strains. LysP is a lysine permease, which negatively regulates *cadBA* in the absence of lysine [142]. CadB is part of the *cadBA* operon, which encodes a cadaverine transporter [143]. It can act as a cadaverine-uptake transporter, which is dependent on the pmf, or as a cadaverine excretion system. The excretion system is based on a cadaverine-lysine antiporter activity, and the expression is induced by lysine [144]. Furthermore, the knockouts of different compartments of the lysine/arginine/ornithine and histidine ABC-transporter were tested (LAO-system *argT-hisJQMP*). *HisP* encodes an ATP-binding domain, and *hisM* and *hisQ* encode the integral membrane components. This transporter has multiple functions and is used for lysine/arginine/ornithine as well as for histidine transport [145]. The functional difference of the two transporter systems is based on the different binding proteins. ArgT binds arginine, lysine and ornithine whereas HisJ specifically binds histidine.

The knockout of different lysine and amino acid transporter-systems did not result in a decrease in negamycin susceptibility (Figure 46). In contrary, the knockout of *cadB* made the strain slightly more susceptible towards negamycin compared to the wildtype. The effect of the *hisM* knockout was even more significant. The knockout of the transmembrane domain, led to two to three fold increase in susceptibility. The knockout of the lysine permease *lysP* and the other compartments of the ABC transporter did not have any significant effect.

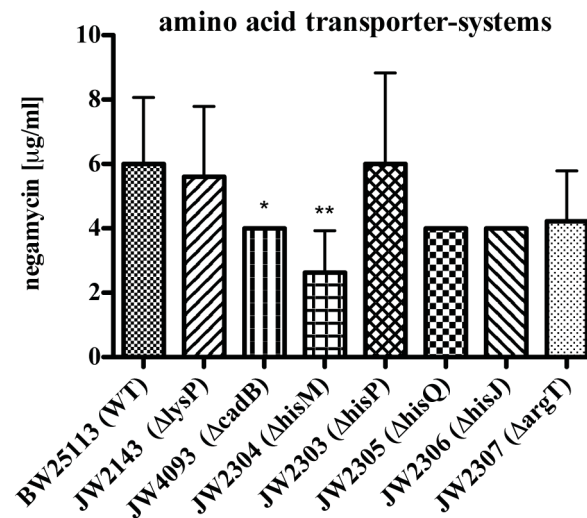


Figure 46: Negamycin susceptibility in different amino acid transporter-system knockouts.
(n*=p<0.05, n**= p<0.01)

A reason for these observations might be that lysine is competing for uptake across the outer membrane and not across the cytoplasmic membrane. This should be investigated in further experiments.

2.4.3 Isolation and characterization of negamycin resistant clones

In order to investigate the resistance-profiles of negamycin the resistance rate was determined. Negamycin resistant clones were isolated from M9- and PP-agar and further characterized.

In the first step the minimal inhibition concentration was determined on agar. The negamycin MIC on M9-agar was 8 µg/ml and the MIC on PP agar was 2 µg/ml (Table 2). Spontaneous mutants were identified on M9 by plating 1.8×10^9 CFU of *E. coli* BW25113 on plates containing different negamycin concentrations. The following resistance rates were determined:

1 x MIC: resistance rate: 1.1×10^{-9} (2 colonies)

0.75 x MIC: resistance rate: 3.9×10^{-9} (7 colonies)

0.5 x MIC: resistance rate: 8.4×10^{-8} (151 colonies)

At 2x MIC no colonies grew. Here, the resistance rate was $<5.55 \times 10^{-10}$. 10 colonies were isolated from the M9-plates and characterized. The same experiment was performed with the $\Delta dppA$ strain JW3513. No single colonies could be isolated, as a bacterial lawn was found on all plates.

On PP agar, containing 2x respectively 4x negamycin MIC, 4.3×10^9 CFU of *E. coli* BW25113 were plated. The following resistance rates were determined:

2 x MIC: resistance rate: 1.2×10^{-9} (5 colonies after 24)

4 x MIC: resistance rate: 1.4×10^{-9} (after 24 h no colonies, after 48 h 8 colonies, two of which turned out to be fully susceptible in later MIC determinations)

The colonies PP-1-5 were isolated on the plate which contained 2 x MIC, and the clones PP-6-8 were isolated on 4 x MIC plates.

In summary resistant clones were raised at a low frequency with 1.1×10^{-9} at 1x MIC on M9 and 1.4×10^{-9} at 4x MIC on polypeptone.

2.4.3.1 Susceptibility profile

In the next step the susceptibility towards negamycin of the isolated mutants was determined by broth microdilution (Table 8).

Table 8: Negamycin susceptibility of isolated resistant clones in M9 and PP.
(n*=p<0.05, n**= p<0.01)

<i>E. coli</i> strain	MIC [$\mu\text{g/ml}$]	
	M9	PP
BW25113	4	16
JW3513 ($\Delta dppA$)	16**	16
M9-1	16**	16
M9-2	16**	16
M9-3	16**	16
M9-4	16**	16
M9-5	16**	16
M9-6	16**	16
M9-7	16**	16
M9-8	16**	16
M9-9	16**	16
M9-10	16**	16

Table 8: Negamycin susceptibility of isolated resistant clones in M9 and PP (continued)

<i>E. coli</i> strain	MIC [$\mu\text{g/ml}$]	
	M9	PP
PP-1	4	32*
PP-2	4	32(64)*
PP-3	4	8
PP-4	4	32*
PP-5	4	8
PP-6	n.g.	32*
PP-7	1*	32*
PP-8	n.g.	32*

The mutants isolated on M9 showed low-level resistance to negamycin in M9 but no change of MIC in PP, similar as it was seen for JW3513 ($\Delta dppA$) (Table 8). The mutants generated on PP showed a low level of resistance to negamycin too, which occurred only in this medium and not in M9. Exceptions were the clones PP-6, PP-7 and PP-8. PP-6 and PP-8 did not grow in M9. The clone PP-7 did not grow well in the plates in M9 too, and was more susceptible to negamycin, which could be due to the weak growth. The isolated colonies PP-3 and PP-5 did not display a significant resistance towards negamycin and were not further investigated after the determination of the MIC against different aminoglycosides.

In the next step the cross-resistance to different antibiotics was investigated. First the MICs of aminoglycosides were determined in M9 and PP (Table 9, Table 10).

Table 9: Aminoglycoside susceptibility of isolated resistant clones in M9. (n*=p<0.05, n= p<0.01, n.g.: no growth, n.d.: not determined)**

<i>E. coli</i> strain	MIC in M9 [$\mu\text{g/ml}$]				
	negamycin	kanamycin	gentamicin	streptomycin	neomycin
BW25113	4	1	0.031 (0.0625)	2	0.5
JW3513 ($\Delta dppA$) del.	16**	1	0.0625	2	0.5
M9-1	16**	1	0.0625	2	0.5
M9-2	16**	1	0.0625	2	0.5

Table 9: Aminoglycoside susceptibility of isolated resistant clones in M9. (continued)

<i>E. coli</i> strain	MIC in M9 [$\mu\text{g/ml}$]				
	negamycin	kanamycin	gentamicin	streptomycin	neomycin
M9-3	16**	1	0.0625	2	0.5
M9-4	16**	1	0.0625	2	0.5
M9-5	16**	1	0.0625	2	0.5
M9-6	16**	1	0.0625	2	0.5
M9-7	16**	1	0.0625	2	0.5
M9-8	16**	1	0.0625	2	0.5
M9-9	16**	1	0.0625	2	0.5
M9-10	16**	1	0.0625	2	0.5
PP-1	4	3*	0.125**	2 (4)	1 (2)*
PP-2	4	3*	0.125**	4*	1 (2)*
PP-3	4	1 (2)	0.0625	2	0.5 (1)
PP-4	4	2*	0.0625	4 (8)*	0.5 (1)
PP-5	4	4*	0.125**	4	2*
PP-6	n.g.	n.g.	n.g.	n.g.	n.g.
PP-7	1*	n.d.	n.d.	n.d.	n.d.
PP-8	n.g.	n.g.	n.g.	n.g.	n.g.

Table 10: Aminoglycoside susceptibility of isolated resistant clones in PP.
(n*=p<0.05, n**= p<0.01)

<i>E. coli</i> strain	MIC in PP [$\mu\text{g/ml}$]				
	negamycin	kanamycin	gentamicin	streptomycin	neomycin
BW25113	16	0.0625	0.0625	0.03125 (0.0625)	0.125
JW3513 (ΔdppA) del.	16	0.125	0.0625	0.0625	0.125
M9-1	16	0.0625/0.125	0.0625	0.0625	0.125
M9-2	16	0.0625/0.125	0.0625	0.0625	0.125

Table 10: Aminoglycoside susceptibility of isolated resistant clones in PP. (continued)

<i>E. coli</i> strain	MIC in PP [$\mu\text{g/ml}$]				
	negamycin	kanamycin	gentamicin	streptomycin	neomycin
M9-3	16	0.0625/0.125	0.0625	0.0625	0.125
M9-4	16	0.0625/0.125	0.0625	0.0625	0.125
M9-5	16	0.0625	0.0625	0.0625	0.125
M9-6	16	0.0625/0.125	0.0625	0.0625	0.125
M9-7	16	0.0625/0.125	0.0625	0.0625	0.125
M9-8	16	0.0625/0.125	0.0625	0.0625	0.125
M9-9	16	0.0625/0.125	0.0625	0.0625	0.125
M9-10	16	0.0625/0.125	0.0625	0.0625	0.125
PP-1	32*	0.5**	0.25**	0.25**	0.25 (0.5)*
PP-2	32(64)*	0.5**	0.25 (0.5)**	0.5**	0.25 (0.5)*
PP-3	8	0.125	0.125	0.0625	0.5**
PP-4	32*	0.5**	0.25*	0.25*	0.125 (0.25)
PP-5	8	0.5**	0.25*	0.125 (0.25)**	0.5**
PP-6	32*	0.125**	0.125**	0.125*	0.25 (0.5)**
PP-7	32*	0.125**	0.125**	0.0625	0.25 (0.5)**
PP-8	32*	0.25**	0.125**	0.125**	0.5**

The susceptibilities to aminoglycosides of the wildtype, all the negamycin resistant mutants and JW3513 ($\Delta dppA$) del. were determined. The MICs were performed in M9 and PP. Only the polypeptone mutants showed cross-resistance to aminoglycosides (Table 9, Table 10). All M9-clones behaved comparable to the JW3513 ($\Delta dppA$) del. strain (Table 9). PP-6, PP-7 and PP-8 did not grow, or grew only weak, in the 96-well plates in M9, therefore no MIC could be determined. PP-1 and PP-2 showed cross-resistance towards all tested aminoglycosides in M9. PP-4 was only cross-resistant to kanamycin and streptomycin in this medium. The susceptibility profile in PP of the M9-isolated clones was comparable to the wildtype BW25113 and JW3513 ($\Delta dppA$) del. (Table 10). No cross-resistance was detected. In contrast the polypeptone-clones showed low-level cross-resistance towards kanamycin, gentamicin, streptomycin and neomycin, therefore to all aminoglycosides tested. Only two exceptions

were observed. PP-4 did not show a significant MIC difference towards neomycin, compared to the wildtype, and PP-7 was not more resistant to streptomycin.

If this observed cross-resistance of the PP-isolated clones is specific to aminoglycosides, or whether it is also the case for other antibiotics was investigated next. MIC determinations were performed with tetracycline and ciprofloxacin (Table 11).

Table 11: Tetracycline and ciprofloxacin susceptibilities of isolated resistant clones in M9 and PP. (n*=p<0.05, n**= p<0.01, n.g.: no growth, n.d.: not determined)

<i>E. coli</i> strain	MIC in M9 (µg/ml)		MIC in PP (µg/ml)	
	tetracycline	ciprofloxacin	tetracycline	ciprofloxacin
BW25113 (WT)	4 (8)	0.0078	4	0.00391 (0.0078)
PP-1	4	0.0078	4	0.0078
PP-2	4	0.00391 (0.0078)	2 (4)	0.00391 (0.0078)
PP-4	4	0.0078	4	0.0078
PP-6	n.g.	n.g.	4	0.00195*
PP-7	n.d.	n.d.	16**	0.03125*
PP-8	n.g.	n.g.	4	0.00391

The tetracycline and ciprofloxacin susceptibilities of the wildtype and the negamycin resistant clones, which were isolated on PP, were measured. In M9 no cross-resistance could be detected. As PP-6 to -8 were not growing at all in M9, or only slightly no MIC values could be determined. In PP only PP-7 showed highly significant cross-resistance towards tetracycline and ciprofloxacin. PP-6 was slightly more susceptible towards ciprofloxacin.

2.4.3.2 Growth and morphology studies

To determine the fitness of the different isolated resistant mutants, growth and morphology studies were performed.

Growth curves:

The different strains were grown in flasks. Every hour 100 µl culture were taken, and OD₆₀₀ was measured in the microplate reader (Tecan). The OD₆₀₀ was measured until strains entered the stationary phase (10 respectively 15 hours). The growth curves of the clones

isolated from M9 were measured in M9, and accordingly the strains isolated on PP were grown in PP broth (Figure 47).

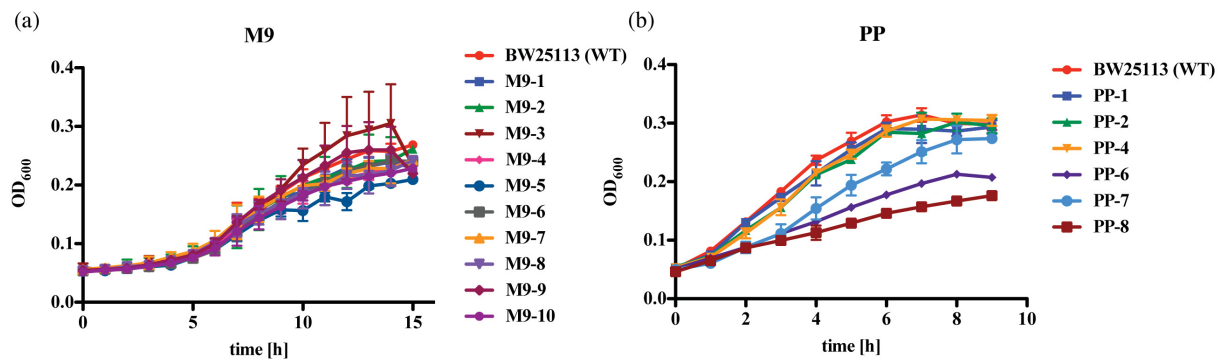


Figure 47: Growth curves at 37°C of BW25113 (WT) and M9-1 to M9-10 in M9 (a) and BW25113 (WT), PP-1, PP-2, PP-4, PP-6, PP-7 and PP-8 in PP(b).

The isolated M9-resistant clones grew comparable to the wildtype in M9 (Figure 47 a). After 6 hours they entered the exponential phase and became stationary after 14 hours at an OD₆₀₀ of 0.2. In contrast some of the PP-clones showed growth-deficiencies. The three strains, which were isolated from the plate containing 4x MIC negamycin, grew slower than the wildtype (Figure 47 b). They entered the stationary phase two hours later (8 hours compared to 6 hours of growth) and reached lower ODs. PP-6 reached an OD₆₀₀ of 0.2, PP-7 of almost 0.3 and PP-8 only of 0.17. The maximal wildtype OD₆₀₀ was 0.32. PP-1, PP-2, PP-4 showed similar growth patterns as the wildtype.

As PP-6, PP-7 and PP-8 showed growth deficiencies, which might be due to energy depletions or ribosomal mutations. These strains were further investigated and morphology studies were performed.

Colony morphology studies:

The colony-morphologies of the wildtype, PP-6, PP-7 and PP-8 were compared to each other. For comparison the membrane-energy-mutant AN66 (*ΔubiD*) and the isolated negamycin-resistant mutant PP-2, which grew comparable to the wildtype, were included in the experiment. The colony diameters of the different strains were measured and compared to each other (Figure 48). The cells were grown overnight on PP-agar and measured after 24 hours. When the strains were incubated longer, the ratio remained the same.

The membrane-energy-mutant AN66 showed slightly smaller colonies as the wildtype (Figure 48 a, b). PP-2 and PP-8 showed two types of colonies, smaller and bigger ones. However, separating the colonies only worked for the PP-8 mutant. PP-2 showed in the average smaller colonies than the wildtype. The same was seen for PP-6, PP-7 and PP-8.

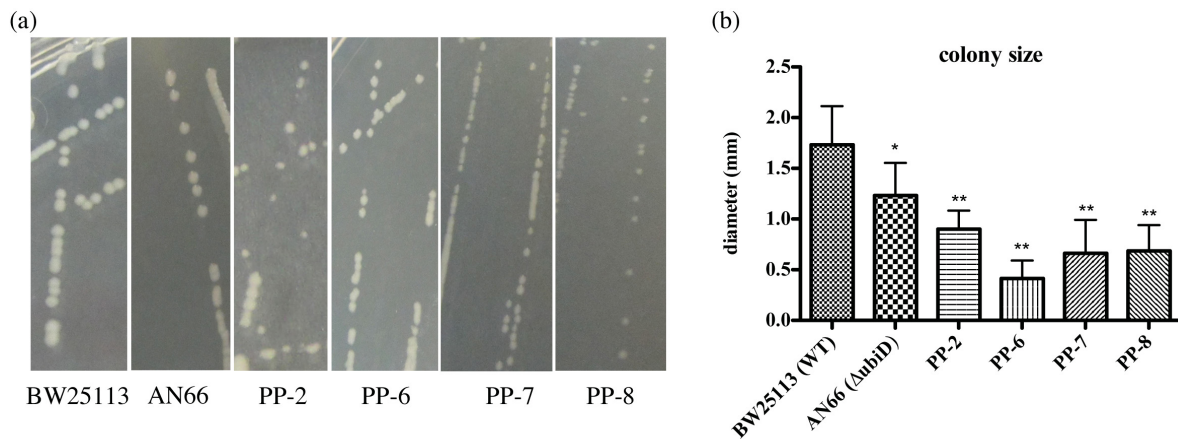


Figure 48: (a) Colony-morphologies of the wildtype BW25113, the membrane-energy-mutant AN66 ($\Delta ubiD$) and PP-2, PP-6, PP-7 and PP-8 on PP-agar. (b) Cells were grown on PP and the diameters of the colonies were determined.

($n^*=p<0.05$, $n^{**}=p<0.01$)

This observation underlines the assumption that these isolated negamycin-resistant clones may have an energy-depletion. Even though other mutations, as for example ribosomal-mutations, can lead to a similar phenotype. The negamycin susceptibilities of the two different colony-types were determined again.

Negamycin susceptibilities of small and big PP-8 colonies

PP-8 showed two different colony-types. These were separated from each other, and the negamycin susceptibility was tested (Figure 49).

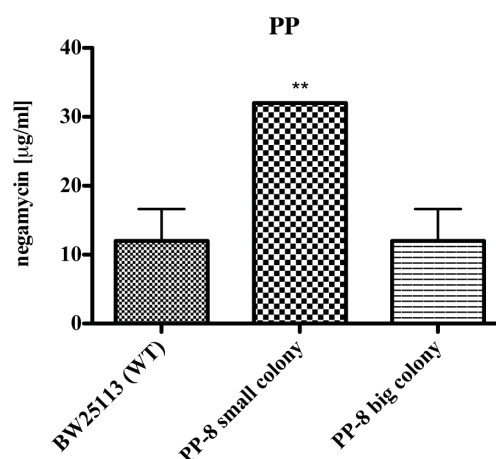


Figure 49: Negamycin susceptibilities of the E. coli strains BW25113 (WT), PP-8 small colony and PP-8 big colony. The MIC was determined in PP.

($n^{**}=p<0.01$)

The MIC-assay showed that the big colonies of PP-8 showed the same susceptibility profile as the wildtype. The PP-8 small-colony was 2-4 times more susceptible. Most likely a mixed culture was obtained while isolating the negamycin-resistant mutants from the plate.

2.4.3.3 Sequencing of the *dpp*-operon

As mentioned before, Dpp was identified as an important entry route of negamycin in M9. Therefore the *dpp*-operon of the sustained negamycin resistant clones was amplified and sequenced.

Many different primer combinations were tested for amplifying the *dppA* gene alone and the whole *dpp*-operon of the M9-resistant clones. Only the amplification of *dppA* in M9-8 succeeded and a mutation from tyrosine to cysteine was found (Figure 50).

M9-8 AA alignment *dppA*

<i>dppA</i>	301	mriskkksgmlklglslvamtvaasvqaktlvycsegspgfnpqlftsg
M9-8 <i>dppA</i> 1	186	mriskkksgmlklglslvamtvaasvqaktlvycsegspgfnpqlftsg
M9-8 <i>dppA</i> lm		-----
M9-8 <i>dppA</i> rev		-----
<i>dppA</i>	451	ttydassvplynrlvefkigttevipglaekwevsedgktytfhlrkgvk
M9-8 <i>dppA</i> 1	336	ttydassvplynrlvefkigttevipglaekwevsedgktytfhlrkgvk
M9-8 <i>dppA</i> lm		-----
M9-8 <i>dppA</i> rev	3	---gsavpr-----*pg-----
<i>dppA</i>	601	whdnkefkptrelnaddvvfsfdrqnaq---npyhkvsggsyeyfegm
M9-8 <i>dppA</i> 1	486	whdnkefkptrelnaddvvfsfdrqnaq---npyhkvsggsyeyfegm
M9-8 <i>dppA</i> lm		-----
M9-8 <i>dppA</i> rev	30	-----nglrlf--qknmlmr**kpvhrknwts---tqse
<i>dppA</i>	739	glpelisevkkvddntvqfvltrpeapfladlamdfasilskeyadamnk
M9-8 <i>dppA</i> 1	624	glpelisevkkvddntvqfvltrpeapfladlamdfasilskeyadamnk
M9-8 <i>dppA</i> lm		-----
M9-8 <i>dppA</i> rev	123	pvrssysisikkipvsatk-----rlma
<i>dppA</i>	889	agtpekldlnpigtgpfqlqqyqkdsrirykafdgywgtkpqidtlvfsi
M9-8 <i>dppA</i> 1	774	agtpekldlnpigtgpfqlqqyqkdsrirykafdgywgtkpqidtlvfsi
M9-8 <i>dppA</i> lm		-----
M9-8 <i>dppA</i> rev	189	tgapnrrsir-----w-----fsl
<i>dppA</i>	1039	tp-dasvryaklqkneqcvmypnpadiarmkqdksinlmempglnvgyl
M9-8 <i>dppA</i> 1	924	tp-dasvryaklqkneqcvmypnpadiarmkqdksin-----
M9-8 <i>dppA</i> lm	2	-----pypnpadiarmkqdksinlmempglnvgyl
M9-8 <i>dppA</i> rev	231	lppdasvryaklqkneqcvmypnpadiarmkqdksinlmempglnvgyl
<i>dppA</i>	1186	synvqkkplddvkvrqaltyavnkdaiikavyqqagvsaknlipptmwgy
M9-8 <i>dppA</i> 1		-----
M9-8 <i>dppA</i> lm	92	synvqkkplddvkvrqaltyavnkdaiikavyqqagvsaknlipptmwgy
M9-8 <i>dppA</i> rev	381	synvqkkplddvkvrqaltyavnkdaiikavyqqagvsaknlipptmwgy
<i>dppA</i>	1336	nddvqdytydpekakallkeaglekgfsidlwampvqrpnpnarremaem
M9-8 <i>dppA</i> 1		-----
M9-8 <i>dppA</i> lm	242	nddvqdytydpekakallkeaglekgfsidlwampvqrpnpnarremaem
M9-8 <i>dppA</i> rev	531	nddvqdytydpekakallkeaglekgfsidlwampvqrpnpnarremaem

Tyr → Cys

<i>dppA</i>	1486	iqadwakvgvqakivtyewgeylkrakdgehqtvmmgwtgdngdpdnffa
M9-8 <i>dppA</i> l	1035	-----pd-----
M9-8 <i>dppA</i> lm	392	iqadwakvgvqakivtyewgeylkrakdgehqtvmmgwtgdngdpdnffa
M9-8 <i>dppA</i> re	681	iqadwakvgvqakivtyewgeylkrakdgehqtvmmgwtgdngdpdnffa
<i>dppA</i>	1636	tlfscaaseqgsnyskwcykpfedliqparatddhnkrvelykqaqvvmh
M9-8 <i>dppA</i> l		-----
M9-8 <i>dppA</i> lm	542	tlfscaaseqgsnyskwcykpfedliqparatddhnkrvelykqaqvvmh
M9-8 <i>dppA</i> re	831	tlfscaaseqgsnyskwcykpfedliqparatddhnkrvelykqaqvvmh
<i>dppA</i>	1786	dqapaliiiahstvfepvrkevkgyvvdplgkhhfenvsie*lkaiqd*wq
M9-8 <i>dppA</i> l		-----
M9-8 <i>dppA</i> lm	692	dqapaliiiahstvfepvrkevkgyvvdplgkhhfenvsie*lkaiqd*w-
M9-8 <i>dppA</i> rev	981	dqapaliiiahstvfepvrkevkgyvvdplgkhhskt-----
<i>dppA</i>	1936	rqkclmrsayqayensamy*ictil*ag*gvnra--sginkahfvnnlyt
M9-8 <i>dppA</i> l	1041	-----gnrg*tsvis-----
M9-8 <i>dppA</i> lm		-----
M9-8 <i>dppA</i> rev		-----
<i>dppA</i>	2080	rwrcasacsairqqyfipcpiragidl*aiqtrssrlrvvtien
M9-8 <i>dppA</i> l	1074	-----rit-----
M9-8 <i>dppA</i> lm		-----
M9-8 <i>dppA</i> rev		-----

Figure 50: Alignment of *dppA* of the wildtype and M9-8.

Three different primers; *dppA* l, *dppA* lm and *dppA* rev were used. The sequences were aligned to the *dppA* sequence from the database, which is shown in the first row of the alignment. The other three rows show the M9-8 sequences obtained with the different primers.

The size of the complete *dpp*-operon is 6006 bp. As different primer combinations within the operon did not lead to any product in the M9-clones, besides for M9-8, primers were used that were far outside of the Dpp encoding region. The results observed with two primer sets are shown in Figure 51 as an example. With the primer set *dppA*-F-5/*dppA*-F rev4 a product of 10694 bp was expected. The primer combination *dppA*-F-2/*dppA*-F rev2 amplified a region of 8455 bp.

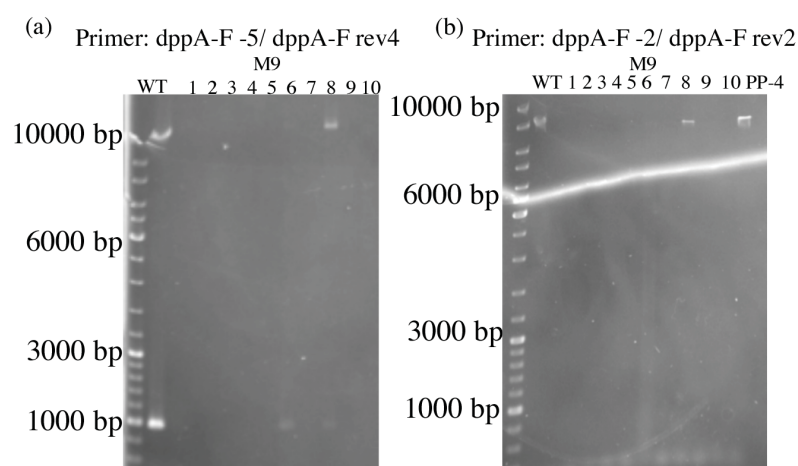


Figure 51: PCR with the primer set *dppA*-F-5/*dppA*-F rev4 (a) and *dppA*-F-2/*dppA*-F rev2 (b).

PCR was done in the wildtype and the M9-1 to M9-10 clones and the second primer set was tested in PP-4 too.

The size of the PCR-product in the wildtype with the primer combination dppA-F-5/dppA-F rev4 was slightly above 10000 bp (Figure 51 a). This product aligns with the expected size of 10694 bp. A second small product with the size of 1000 bp was seen. The same product of 10000 bp was seen in the strain M9-8. All other PCRs, which were performed with the DNA of the other M9-resistant clones, did not yield in any product. A similar picture was seen with the primer combination dppA-F-2/dppA-F rev2. A product was seen with a size of around 8000 bp for the wildtype, the clone M9-8 and the clone PP-4. This product corresponds to the expected size of 8455 bp.

None of the other tested primer combinations yielded in a product for M9-1, M9-2, M9-3, M9-4, M9-5, M9-6, M9-7, M9-9 and M9-10. As there was always a product for the wildtype, M9-8 and the polypeptone clones, a failure of the PCR-reactions can be excluded. This observation indicates that all the M9-clones have a change in the DNA-region of the *dpp*-operon. For M9-8 the region seemed to be intact, but a mutation in *dppA* was found. The complete *dpp*-operons of the polypeptone clones PP-1, PP-2 and PP-4 were sequenced, and no mutations were found (used primers are listed in Table 22). They showed 100% sequence identity with the wildtype.

To analyze which mutations occurred in the PP-clones and to see what happened to the *dpp*-region in the M9 clone, the strains BW25113 (WT), M9-2 as well as PP-2, PP-6, PP-8 were sent for whole genome sequencing. The results of the sequencing were not obtained and analyzed in the time course of this work.

2.5 Influence of salts on negamycin activity

Salts can play an important role in the uptake of antibiotics, as shown for tetracyclines [101] and quinolones [109] and in the activity of antibiotics as known for daptomycin [146] and empedopeptin [147]. Negamycin itself carries a carboxyl group (Figure 12), which could possibly chelate cations. Based on this it was investigated whether salts have an influence on negamycin activity. (Table 12). The results are presented in this chapter.

Table 12: salt effect on negamycin activity in PP.
(n*=p<0.05, n**= p<0.01, n.g.: no growth, n.d.: not determined)

salt conc.	MIC in PP (µg/ml)			
	CaCl ₂ (µg/ml)	MgCl ₂ (µg/ml)	NaCl (µg/ml)	KCl (µg/ml)
0 mM	16			
0.5 mM	4**	16	16	n.d.
2.5 mM	1**	8	16	n.d.
5.0 mM	4**	8	16	n.d.

Table 12: salt effect on negamycin activity in PP (continued).

salt conc.	MIC in PP ($\mu\text{g/ml}$)			
	CaCl_2 ($\mu\text{g/ml}$)	MgCl_2 ($\mu\text{g/ml}$)	NaCl ($\mu\text{g/ml}$)	KCl ($\mu\text{g/ml}$)
10 mM	4**	8	16	n.d.
25 mM	8	16	32*	32*
50 mM	16	16	64**	64**
100 mM	32*	16	64 (>64)**	>64**

When Ca^{2+} and Mg^{2+} were added to PP, a positive effect on negamycin activity was seen and the effect of Ca^{2+} was significantly stronger compared to Mg^{2+} (Table 12). The most effective concentration of CaCl_2 on negamycin activity was 2.5 mM. At a high concentration of 100 mM, calcium had an inhibiting effect. The addition of the monovalent cations, NaCl and KCl , led to a decrease of negamycin activity. From a concentration of 25 mM on, the MIC got higher with increasing salt concentrations.

In the next part it was investigated whether negamycin is able to chelate cations, and if this might explain the effect it has on the activity.

2.5.1 Complexation of divalent cations

As mentioned before, negamycin carries a carboxyl group, which might chelate cations. To investigate whether it forms complexes with Ca^{2+} , Mg^{2+} or Na^+ thin layer chromatographies (TLC) were done (Figure 52 a and b). The salts CaCl_2 , MgCl_2 and NaCl were added in different molar ratios to negamycin. In a second step negamycin was titrated with CaCl_2 using isothermal titration calorimetry (ITC) (Figure 52c).

The TLC-results proved a complexation of negamycin with Mg^{2+} and Ca^{2+} , but not with the monovalent cation Na^+ (Figure 52 a). When Mg^{2+} and Ca^{2+} were added in increasing concentrations the retardation factor (R_f) values decreased (Table 13).

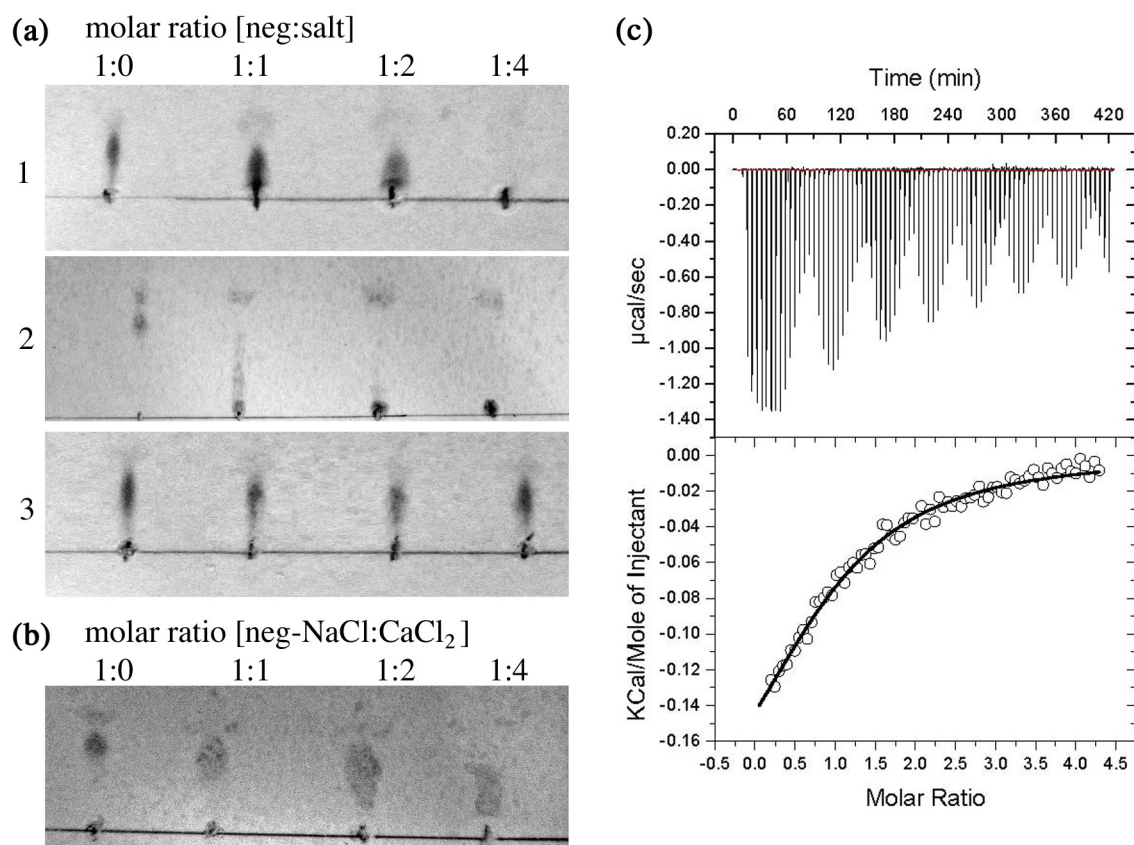


Figure 52: (a) Thin layer chromatography (TLC) analysis of complex formation of negamycin with CaCl₂ (1), MgCl₂ (2) and NaCl (3). (b) TLC of negamycin mixed with NaCl in a molar ratio of 1:10. CaCl₂ was added in increasing molar ratios. (c) Isothermal titration calorimetry (ITC) of negamycin titrated with CaCl₂. The upper thermogram panel shows the observed heat for each injection of CaCl₂ after baseline correction. The lower panel depicts the binding enthalpies against Ca²⁺/negamycin molar ratio. ITC data was fitted to the one-site binding model.

Table 13: Rf values of TLC with negamycin and different concentrations of CaCl₂, MgCl₂ and NaCl

negamycin	Ratio of negamycin:salt	Rf values			
		Rf values + CaCl ₂	Rf values + MgCl ₂	Rf values + NaCl	CaCl ₂ + NaCl (1:10)
0	0	0.12	0.15	0.13	0.17
6.226 mM	1:1	0.06	0.06	0.12	0.125
12.452 mM	1:2	0.05	0.02	0.12	0.12
24.905	1:4	0	0	0.13	0.08

To visualize the complexation better, the % migration was drawn against the molar ratio (Figure 53).

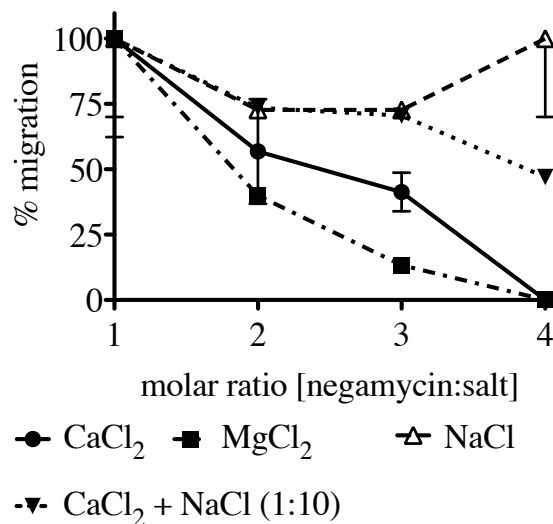


Figure 53: Negamycin migration upon salt-addition

Already at a molar ratio of 1:1 (negamycin:salt) the R_f value was reduced about 50%. It is likely that this is caused by a complexation with divalent cations. At a negamycin:salt ratio of 1:4, negamycin did not at all (MgCl₂ and CaCl₂) move on the TLC plate. The addition of NaCl did have a small effect on the R_f values. It was seen before that the addition of sodium to the medium had an inhibiting effect in negamycin activity (Table 12). To rule out that Na⁺ inhibits the complex formation of Ca²⁺ and negamycin, another TLC was performed. Na⁺ was added to negamycin in a molar ratio of 1:10, and Ca²⁺ was added to this solution in different concentrations (Figure 52 b). A slight inhibition of the complexation was seen (Figure 53).

ITC studies implied a 1:1 binding of negamycin and calcium (Figure 52 c), which is represented by a stoichiometry factor of 1.02 ± 0.07 . In comparison the control experiment of assay buffer and CaCl₂ shows 4 times less heat release as well as a linear behavior, which clearly results from dilution heats. After subtracting of the control experiment the curve reaches a defined saturation state which indicates an interaction between negamycin and CaCl₂. The method based limitations especially regarding high peptide concentrations do not allow to determine a precise K_D value. Nevertheless an interaction is proven by this experiment and furthermore an affinity in the low micro-molar range is suggested.

These observations indicate that the complex formation, especially of negamycin and Ca²⁺, lead to an increase in negamycin-activity. This could be due to an improved uptake rate or to a higher activity on the target.

2.5.2 Localization of the Ca²⁺-effect

To localize the effect of calcium an *in vitro* transcription-translation assay was performed to investigate the effect on the target. Calcium was added in different concentrations and the IC₅₀ value was determined. The intracellular Ca²⁺ concentration in *E. coli* is tightly regulated

and ranges from 0.1-1 μM [148-150]. Therefore CaCl_2 was added in low molecular concentrations to the *in vitro* transcription translation assay (Table 14). If calcium would increase the activity on the target a decrease of the IC_{50} values would be expected.

Table 14: Influence of Ca^{2+} on the negamycin activity in an *in vitro* transcription translation assay

	IC_{50}
w/o CaCl_2	0.3965
+ 1 μM CaCl_2	0.45
+ 2 μM CaCl_2	0.58
+ 4 μM CaCl_2	0.522
+ 8 μM CaCl_2	0.38

The addition of CaCl_2 did not have an effect on negamycin activity on the target (Table 14). The IC_{50} of negamycin without CaCl_2 was 0.3965 $\mu\text{g}/\text{ml}$. When increasing concentration of CaCl_2 were added to the assay the IC_{50} increased slightly to 0.58 $\mu\text{g}/\text{ml}$, but this effect was not significant. In summary this result points to a possible influence of calcium on the negamycin uptake, either across the outer membrane or the cytoplasmic membrane. To localize the effect, cells were treated with PMBN, to impair the outer membrane, and it was analyzed whether the Ca^{2+} -effect was still seen (Figure 54 a). Furthermore the effect of calcium was tested in Gram-positive strains, too, which lack the outer membrane (Figure 54b).

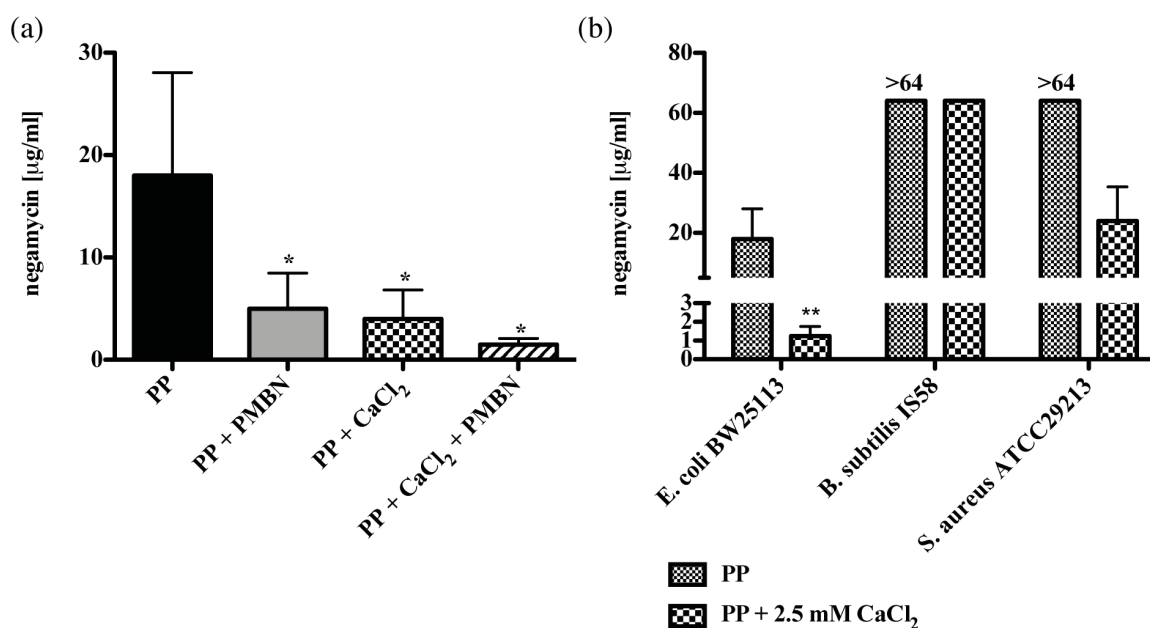


Figure 54: (a) CaCl_2 effect on negamycin activity in *E. coli* BW25113 after treatment with 15 $\mu\text{g}/\text{ml}$ PMBN (+ PMBN). MIC was determined in cells only treated with 15 $\mu\text{g}/\text{ml}$ PMBN (+ PMBN), treated with 2.5 mM CaCl_2

or treated with PMBN (15 $\mu\text{g/ml}$) and CaCl_2 (2.5 mM). (b) Effect of 2.5 mM CaCl_2 in *E. coli* BW25113 and the Gram-positive strains *B. subtilis* IS58 and *S. aureus* ATCC29213. (n*=p<0.05, n**= p<0.01)

In PMBN treated cells with an impaired outer membrane, the addition of CaCl_2 still showed a positive effect on negamycin activity (Figure 54 a). The measured MIC of cells treated only with PMBN was 4 $\mu\text{g/ml}$. When calcium was added to the PMBN pre-treated cells the MIC was 1 $\mu\text{g/ml}$. The cells showed the same increased susceptibility, compared to the ones, which were not treated with PMBN. In Gram-positive bacteria, such as *B. subtilis* and *S. aureus*, the addition of CaCl_2 had a beneficial effect on negamycin activity too (Figure 54 b). In PP the measured MIC in these two strains was >64 $\mu\text{g/ml}$. The addition of 2.5 mM CaCl_2 led to an increased negamycin activity, and the MIC in *B. subtilis* was 64 $\mu\text{g/ml}$ and the one in *S. aureus* 16 (32) $\mu\text{g/ml}$. These results suggest that the calcium effect cannot, at least not only, take place at the outer membrane, but more likely at the cytoplasmic membrane.

2.6 Influence of pH on negamycin activity

Not only salts, but also the pH can have an impact on antibiotic activity, as e.g. described for aminoglycosides [93-95]. This chapter represents the results on the pH effect on negamycin activity.

To investigate whether the pH influences negamycin activity, MIC determinations were done in media with different pH (Figure 55 a). In a further step the effect of pH and calcium in combination was tested (Figure 55 b).

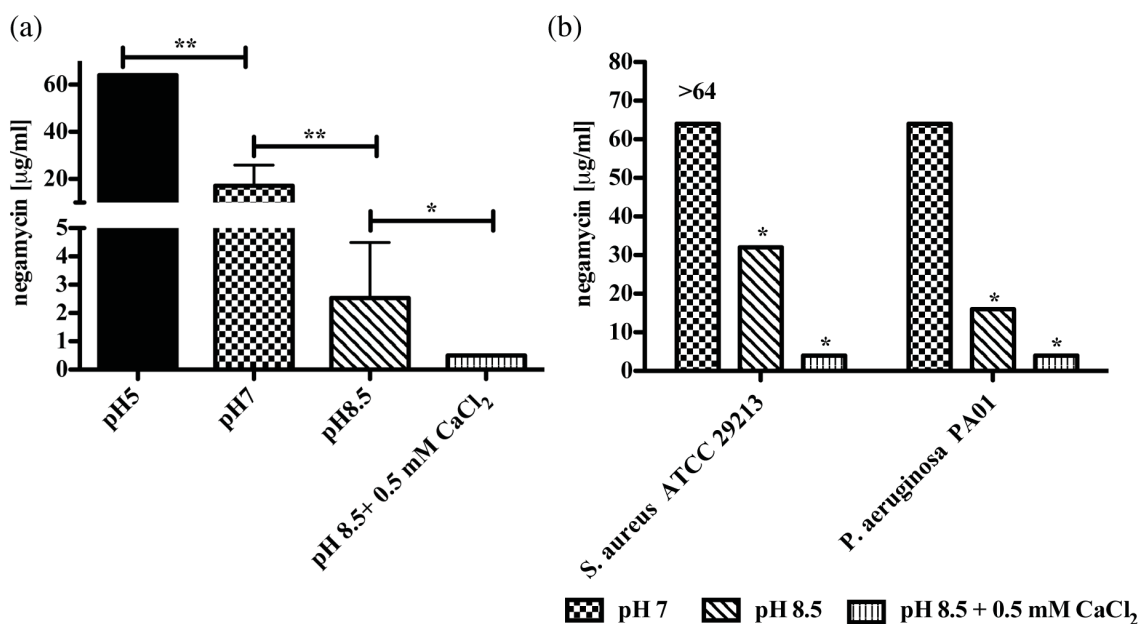


Figure 55: (a) Negamycin MIC of *E. coli* BW25113 in PP adjusted to different pH values, and effect of CaCl_2 addition. (b) Effect of alkaline pH and additional supplementation with CaCl_2 in *S. aureus* and *P. aeruginosa*. (n*=p<0.05, n**= p<0.01)

The MIC-assays showed that an acidic pH led to a drop in negamycin activity and under alkaline conditions negamycin was more active (Figure 55 a). The combination of both beneficial conditions, calcium and basic pH led to a 32-fold MIC improvement compared to the MIC measured at pH 7. The optimal CaCl_2 concentration was 0.5 mM, as higher concentrations precipitated under basic pH conditions. This effect was seen in other pathogens too. Under the optimized condition pH 8.5 + 0.5 mM CaCl_2 *P. aeruginosa* and *S. aureus* showed a negamycin MIC of 4 $\mu\text{g}/\text{ml}$ (Figure 55 b), implying a highly improved negamycin activity. Since alkaline pH and the addition of calcium have an effect in Gram-positive and Gram-negative bacteria, it seems to play a role at the cytoplasmic membrane. The increased activity at pH 8.5 in PP might be due to facilitated uptake of negamycin. However, as decreased fitness could also play a role, the growth rate was also determined.

2.6.1 Growth of *E. coli* BW25113 under different pH conditions

In the next step it was investigated whether a change to alkaline pH affects growth of *E. coli* BW25113 (WT) (Figure 56). The strain was grown in PP adjusted to pH 7 or pH 8.5. The cells were grown at 37°C in flasks with shaking and the OD_{600} as well as the pH were monitored over the time course of 12 hours.

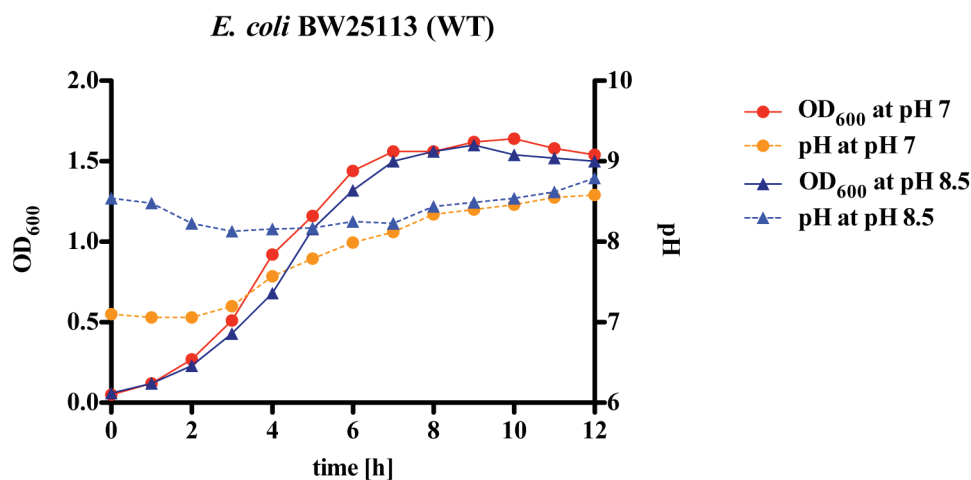


Figure 56: Growth of *E. coli* BW25113 (WT) in PP adjusted to pH 7 and pH 8.5.

The OD_{600} is displayed on the left y-axis (red and dark blue) and the pH is displayed on the right y-axis (orange and light blue).

E. coli BW25113 grew similarly in the medium adjusted to pH 7 and pH 8.5 (red and dark blue). The change to alkaline pH did not affect the fitness of the cells. After 2-3 hours *E. coli* entered the exponential phase and after 6 hours the stationary phase. Over time the pH was monitored. In the medium, which was adjusted to pH 8.5, the pH remained rather stable

(light blue). In the medium adjusted to pH 7, the medium got alkaline over the time and reached a pH of 8.6 after 12 hours.

Looking at the published pKAs, negamycin is zwitterionic and therefore net neutral at pH 8.5 (Figure 12). This might facilitate a passive uptake of negamycin across the cytoplasmic membrane. Therefore the killing in a medium, which is adjusted to pH 8.5, may be faster. This hypothesis was further investigated by performing killing curves under different pH conditions.

2.6.2 Negamycin killing in relation to pH

To investigate whether negamycin kills faster at pH 8.5, killing curves with *E. coli* BW25113 (WT) were performed in PP pH 7 and PP pH 8.5 (Figure 57). The cells were treated with $\frac{1}{8}$, $\frac{1}{4}$, $\frac{1}{2}$ and 1 x negamycin MIC.

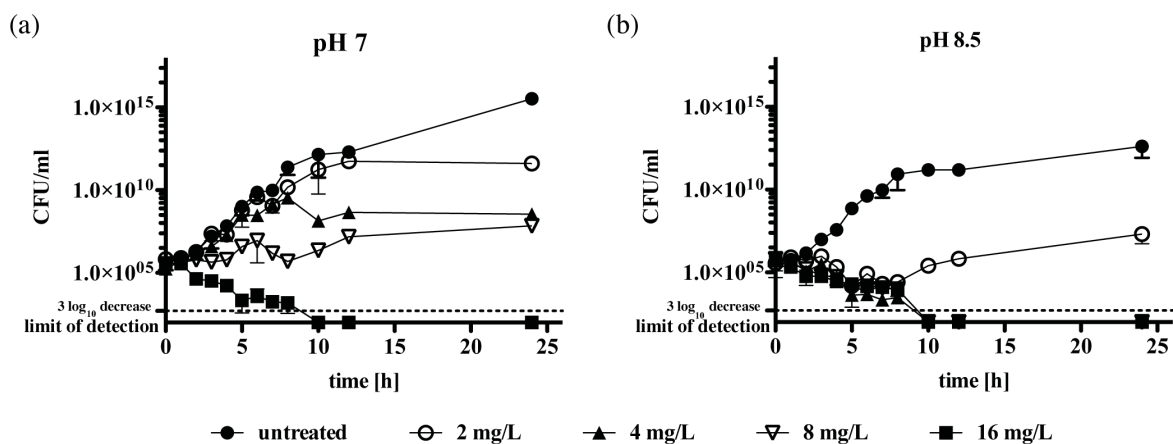


Figure 57: Killing curves of *E. coli* BW25113 in PP in the presence of different negamycin concentrations at (a) pH 7 and (b) pH 8.5.

The killing curves, at pH 7 and pH 8.5, showed that cells are not dying faster at pH 8.5 (Figure 57). After 10 hours no growth was detected anymore when 16 $\mu\text{g}/\text{ml}$ negamycin were added. This curve-development was seen for both pH conditions. However the antibacterial activity at pH 8.5 was better (Figure 57 b). Already a concentration of 4 $\mu\text{g}/\text{ml}$ led to a killing of the cells.

Another explanation for the increased activity at pH 8.5 might be an improved passage across the membrane, based on a change in pmf. A pH effect is well described for aminoglycoside-activity. The driving force of the uptake of this antibiotic class is the pmf [88] (1.3.1.1). A change in the pH affects the pmf and therefore the uptake of aminoglycosides [93-95]. One could assume that the change of the pH might have a similar effect on the negamycin uptake, if it is comparable to aminoglycosides. Therefore membrane-energy

mutants, which are described as being more resistant to aminoglycosides [92], were tested for cross-resistance.

2.6.3 Negamycin distribution between charged and uncharged species depending on pH

Negamycin carries a carboxyl-, two amine- and a alcohol group, which are, depending on the pH, protonated or deprotonated (Figure 12). The pKa-values for these groups were first published by Kondo *et al.* [151] and updated by McKinney *et al.* [114].

To calculate how many species are charged and how much uncharged at different pH, the Henderson–Hasselbalch equation was used.

$$pH = pKa + \log_{10} \left(\frac{[A^-]}{[HA]} \right)$$

pH 5

NH₃⁺-moiety:

$$5 = 9.6 + \log_{10} \left(\frac{[NH_2]}{[NH_3^+]} \right) \rightarrow -4.6 = \log_{10} \left(\frac{[NH_2]}{[NH_3^+]} \right) \rightarrow 0.000025 = \left(\frac{[NH_2]}{[NH_3^+]} \right)$$

$$\frac{[NH_3^+]}{[NH_3^+] + [NH_2]} = \frac{1}{\frac{[NH_3^+] + [NH_2]}{[NH_3^+]}} = \frac{1}{1 + \frac{[NH_2]}{[NH_3^+]}} = \frac{1}{1 + 0.000025} = \frac{1}{1.000025} = 0.99998 = \mathbf{99.998\%}$$

COO⁻-moiety:

$$5 = 3.2 + \log_{10} \left(\frac{[COO^-]}{[COOH]} \right) \rightarrow 1.8 = \log_{10} \left(\frac{[COO^-]}{[COOH]} \right) \rightarrow 63.1 = \left(\frac{[COO^-]}{[COOH]} \right)$$

$$\frac{[COO^-]}{[COO^-] + [COOH]} = \frac{1}{\frac{[COO^-] + [COOH]}{[COO^-]}} = \frac{1}{1 + \frac{[COOH]}{[COO^-]}} = \frac{1}{1 + \frac{1}{63.1}} = \frac{1}{1 + \frac{1}{63.1}} = 0.9844 = \mathbf{COO^-: 98.44\%}$$

β-NH₃⁺-moiety:

$$5 = 8.0 + \log_{10} \left(\frac{[NH_2]}{[NH_3^+]} \right) \rightarrow -3 = \log_{10} \left(\frac{[NH_2]}{[NH_3^+]} \right) \rightarrow 0.001 = \left(\frac{[NH_2]}{[NH_3^+]} \right) \rightarrow \frac{0.1}{100} \rightarrow$$

$$\frac{[NH_3^+]}{[NH_3^+] + [NH_2]} = \frac{1}{\frac{[NH_3^+] + [NH_2]}{[NH_3^+]}} = \frac{1}{1 + \frac{[NH_2]}{[NH_3^+]}} = \frac{1}{1 + 0.001} = \frac{1}{1.001} = 0.99899 = \mathbf{99.899\%}$$

To estimate 1) the number of molecules, where all three of these groups are charged versus 2) the number of molecules that occur in the zwitterionic state, the values were multiplied. As the interactions within the molecule are very complex and influencing each other, this approach is a highly simplified equation and only serves as a vague estimation.

Percentage of molecules with all three groups charged at pH 5:

$$P_{3x \text{ charged}} = P(\text{NH}_3^+) * P(\text{COO}^-) * P(\beta\text{-NH}_3^+) = 0.99998 * 0.9844 * 0.998999 = 0.983 \rightarrow \mathbf{98.3\%}$$

98.3% of molecules are charged at the carboxy as well as both amino-moieties at pH 5.

Percentage of zwitterionic molecules at pH 5:

$$P(\text{NH}_3^+) = 0.99998 \quad P(\text{NH}_2) = 1 - 0.99998 = 0.00002$$

$$P(\text{COO}^-) = 0.9844 \quad P(\text{COOH}) = 1 - 0.9844 = 0.0156$$

$$P(\beta\text{-NH}_3^+) = 0.9990 \quad P(\beta\text{-NH}_2) = 1 - 0.9990 = 0.001$$

$$P_{\text{zwitter}} = P(\text{COO}^-) * P(\text{NH}_3^+) * P(\beta\text{-NH}_2) + P(\text{COO}^-) * P(\text{NH}_2) * P(\beta\text{-NH}_3^+)$$

$$= 0.9844 * 0.99998 * 0.001 + 0.9844 * 0.00002 * 0.9990$$

$$= 0.9844 * (0.99998 * 0.001 + 0.00002 * 0.9990)$$

$$= 0.9844 * (0.00099998 + 0.00001998) = 0.001$$

0.1% of molecules are in the zwitterionic state at pH 5.

pH 7

NH₃⁺-moiety:

$$7 = 9.6 + \log_{10} \left(\frac{[\text{NH}_2]}{[\text{NH}_3^+]} \right) \rightarrow -2.6 = \log_{10} \left(\frac{[\text{NH}_2]}{[\text{NH}_3^+]} \right) \rightarrow 0.0025 = \left(\frac{[\text{NH}_2]}{[\text{NH}_3^+]} \right)$$

$$\frac{[\text{NH}_3^+]}{[\text{NH}_3^+] + [\text{NH}_2]} = \frac{1}{\frac{[\text{NH}_3^+] + [\text{NH}_2]}{[\text{NH}_3^+]}} = \frac{1}{1 + \frac{[\text{NH}_2]}{[\text{NH}_3^+]}} = \frac{1}{1 + 0.0025} = \frac{1}{1.0025} = 0.9975 = \mathbf{99.75\%}$$

COO⁻-moiety:

$$7 = 3.2 + \log_{10} \left(\frac{[\text{COO}^-]}{[\text{COOH}]} \right) \rightarrow 3.8 = \log_{10} \left(\frac{[\text{COO}^-]}{[\text{COOH}]} \right) \rightarrow 6309.57 = \left(\frac{[\text{COO}^-]}{[\text{COOH}]} \right)$$

$$\frac{[\text{COO}^-]}{[\text{COO}^-] + [\text{COOH}]} = \frac{1}{\frac{[\text{COO}^-] + [\text{COOH}]}{[\text{COO}^-]}} = \frac{1}{1 + \frac{[\text{COOH}]}{[\text{COO}^-]}} = \frac{1}{1 + \frac{1}{6309.57}} = \frac{1}{1 + 0.000158} = 0.9998 = \mathbf{COO^- : 99.98\%}$$

β -NH₃⁺-moiety:

$$7 = 8.0 + \log_{10} \left(\frac{[NH_2]}{[NH_3^+]} \right) \rightarrow -1.0 = \log_{10} \left(\frac{[NH_2]}{[NH_3^+]} \right) \rightarrow 0.1 = \left(\frac{[NH_2]}{[NH_3^+]} \right)$$

$$\frac{[NH_3^+]}{[NH_3^+] + [NH_2]} = \frac{1}{\frac{[NH_3^+] + [NH_2]}{[NH_3^+]}} = \frac{1}{1 + \frac{[NH_2]}{[NH_3^+]}} = \frac{1}{1 + 0.1} = \frac{1}{1.1} = 0.9090 = \mathbf{90.9\%}$$

To estimate 1) the number of molecules, where all three of these groups are charged versus 2) the number of molecules that occur in the zwitterionic state, the values were multiplied. As the interactions within the molecule are very complex and influencing each other, this approach is a highly simplified equation and only serves as a vague estimation.

Percentage of molecules with all three groups charged at pH 7:

$$NH_3^+ * COO^- * \beta-NH_3^+ = 0.9275 * 0.9998 * 0.9901 = 0.918 \rightarrow \mathbf{91.8\%}$$

Percentage of zwitterionic molecules at pH 7:

$$P_{\text{zwitter}} = P(COO^-) * P(NH_3^+) * P(\beta-NH_2) + P(COO^-) * P(NH_2) * P(\beta-NH_3^+)$$

$$= 0.9998 * 0.9975 * 0.091 + 0.9998 * 0.0025 * 0.9090$$

$$= 0.9998 * (0.9975 * 0.091 + 0.0025 * 0.9090)$$

$$= 0.9999 * (0.0908 + 0.0023) = 0.093$$

9.3 % of molecules are in the zwitterionic state at pH 7.

pH 8.5

NH₃⁺-moiety:

$$8.5 = 9.6 + \log_{10} \left(\frac{[NH_2]}{[NH_3^+]} \right) \rightarrow -1.1 = \log_{10} \left(\frac{[NH_2]}{[NH_3^+]} \right) \rightarrow 0.079 = \left(\frac{[NH_2]}{[NH_3^+]} \right)$$

$$\frac{[NH_3^+]}{[NH_3^+] + [NH_2]} = \frac{1}{\frac{[NH_3^+] + [NH_2]}{[NH_3^+]}} = \frac{1}{1 + \frac{[NH_2]}{[NH_3^+]}} = \frac{1}{1 + 0.079} = \frac{1}{1.079} = 0.9268 = \mathbf{92.68\%}$$

COO⁻-moiety:

$$8.5 = 3.2 + \log_{10} \left(\frac{[COO^-]}{[COOH]} \right) \rightarrow 5.3 = \log_{10} \left(\frac{[COO^-]}{[COOH]} \right) \rightarrow 199526.2 = \left(\frac{[COO^-]}{[COOH]} \right)$$

$$\frac{[COO^-]}{[COO^-]+[COOH]} = \frac{1}{\frac{[COO^-]+[COOH]}{[COO^-]}} = \frac{1}{1 + \frac{[COOH]}{[COO^-]}} = \frac{1}{1 + \frac{1}{\frac{[COOH]}{[COO^-]}}} = \frac{1}{1 + \frac{1}{199526.2}} = 0.9999 = COO^- : \mathbf{99.99\%}$$

β -NH₃⁺-moiety:

$$8.5 = 8.0 + \log_{10} \left(\frac{[NH_2]}{[NH_3^+]} \right) \rightarrow 0.5 = \log_{10} \left(\frac{[NH_2]}{[NH_3^+]} \right) \rightarrow 3.16 = \left(\frac{[NH_2]}{[NH_3^+]} \right)$$

$$\frac{[NH_3^+]}{[NH_3^+]+[NH_2]} = \frac{1}{\frac{[NH_3^+]+[NH_2]}{[NH_3^+]}} = \frac{1}{1 + \frac{[NH_2]}{[NH_3^+]}} = \frac{1}{1 + 3.16} = \frac{1}{4.16} = 0.2402 = \mathbf{24.04\%}$$

To estimate 1) the number of molecules, where all three of these groups are charged versus 2) the number of molecules that occur in the zwitterionic state, the values were multiplied. As the interactions within the molecule are very complex and influencing each other, this approach is a highly simplified equation and only serves as a vague estimation.

Percentage of molecules with all three groups charged at pH 8.5:

$$NH_3^+ * COO^- * \beta-NH_3^+ = 0.9268 * 0.9999 * 0.2404 = 0.2228 \rightarrow \mathbf{22.28\%}$$

Percentage of zwitterionic molecules at pH 8.5:

$$P_{\text{zwitter}} = P(COO^-) * P(NH_3^+) * P(\beta-NH_2) + P(COO^-) * P(NH_2) * P(\beta-NH_3^+)$$

$$= 0.9999 * 0.9268 * 0.7596 + 0.9999 * 0.0732 * 0.2404$$

$$= 0.9999 * (0.9268 * 0.7596 + 0.0732 * 0.2404)$$

$$= 0.9999 * (0.70399 + 0.01759) = 0.7215$$

72.15 % of molecules are in the zwitterionic state at pH 8.5.

2.6.4 Influence of CCCP on negamycin activity

The pH has a huge influence on negamycin activity, as shown in the previous chapters. At a pH of 8.5 a considerably higher proportion of negamycin molecules are in the zwitterionic state compared to pH 5 (72.15 % vs. 0.1%). As zwitterions are in equilibrium with the uncharged state and as small, uncharged molecules can pass the membrane often passively [2], it is likely that a certain proportion of negamycin might passively diffuse under these

conditions. To investigate this assumption, cells were treated with carbonyl cyanide m-chlorophenylhydrazone (CCCP), an inhibitor of the oxidative phosphorylation [152] (Figure 58). CCCP uncouples the proton gradient and energy-consuming activities cannot take place, as for example active transportation. If negamycin can passively enter the cell, the CCCP-treated cells should still be susceptible. In the first step the MIC of CCCP was determined in PP.

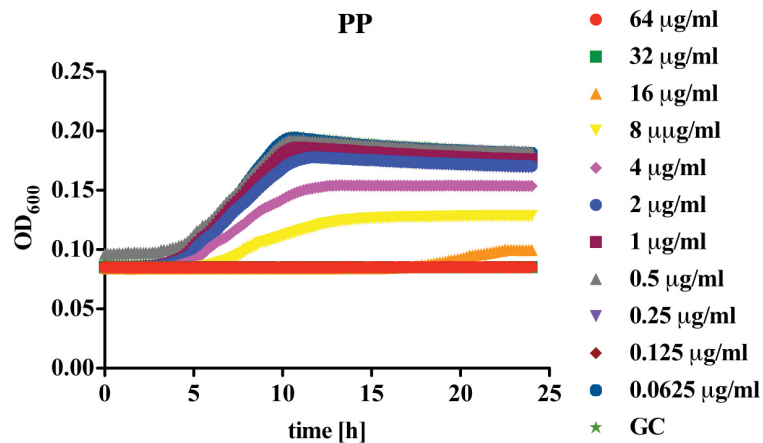


Figure 58: Determination of CCCP-susceptibility of *E. coli* BW25113 in PP.
The cells were grown for 24 hours and OD₆₀₀ was detected using the infinite M200 microplate reader

The determined MIC of CCCP in *E. coli* BW25113 was 32 µg/ml, whereas a strong inhibition was seen at 16 µg/ml. At a concentration of 2 µg/ml no effect was seen on the growth of the cells. Therefore this concentration was used in the next experiment.

To investigate the effect of CCCP on the negamycin activity, the cells were treated with 2 µg/ml and the growth was monitored to determine a change in negamycin susceptibility (Figure 59).

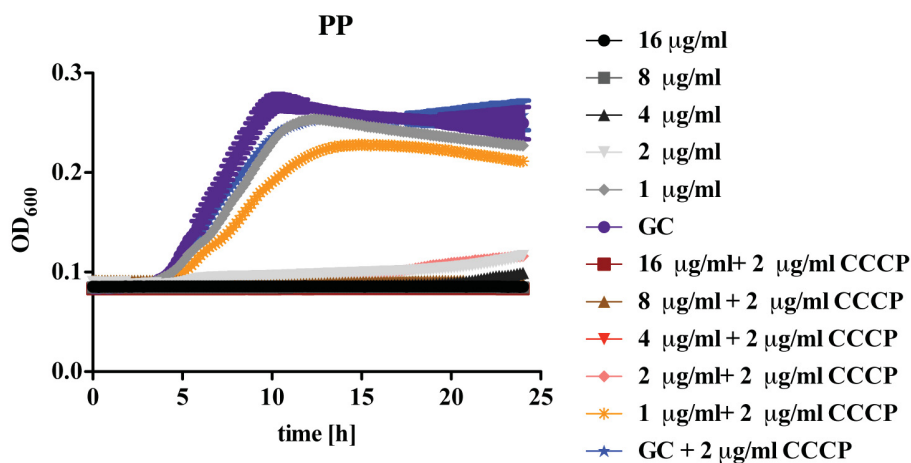


Figure 59: Growth curve in the presence of different negamycin concentrations of *E. coli* BW25113 with and without addition of 2 µg/ml CCCP.

The addition of 2 µg/ml CCCP did not affect the susceptibility of *E. coli* BW25113 towards negamycin. Under both conditions, with and without CCCP, the MIC was 2 µg/ml. This MIC differs from the determined MIC in PP, which is 16 µg/ml. This is due to the different inoculation. The MIC determination is performed with 5×10^5 CFU. The inoculum of this growth curve was 1×10^4 CFU. Therefore fewer cells were used, this might explain the higher susceptibility to the drug.

CCCP alone had already a small inhibitory effect on the growth, which can be seen comparing the purple (GC) and the blue (GC + 2 µg/ml CCCP) growth curves to each other. The addition of negamycin had a small additive effect on the growth inhibition, which was caused by CCCP. As the addition of CCCP to the negamycin MIC determination did only have a small effect on the susceptibility to negamycin, negamycin can most likely enter the cell via passive diffusion too and is not only transported via active uptake. An effect would be probably seen when higher concentrations of CCCP would be used, but as already 4 µg/ml had a higher inhibitory effect on the growth (Figure 58), it would be hard to distinguish between the negamycin and the CCCP effect. Furthermore this experiment needs to be done with a control antibiotic, as for example aminoglycosides, to validate the effect of CCCP.

2.6.5 Negamycin activity in membrane energy mutants

To determine the negamycin activity in membrane energy mutants MICs in PP were performed (Table 15).

Table 15: Negamycin and aminoglycoside MICs of different *E. coli* membrane-energy mutants in PP.
(n*=p<0.05, n**= p<0.01, n.d.: not determined)

<i>E. coli</i> strain	MIC in PP (µg/ml)		
	negamycin	kanamycin	streptomycin
BW25113	16	0.125	0.03125 (0.0625)
AN66 ($\Delta ubiD$)	16	8**	0.03125
GR75N (<i>cydA2</i>)	16/32	1**	8**
JW0723 ($\Delta cydB$)	16	n.d.	n.d.

AN66 (ubiquinone deficient [153]) and GR75N (*cydA* mutant [154]) showed moderate- up to high-level resistance to kanamycin. The resistance-profile was not equal for all aminoglycosides. AN66 did not show a change of susceptibility to streptomycin compared to the BW25113 wildtype. It should be taken in account that AN66 was received from another strain, therefore the strain background is not the same. GR75N was highly resistant to aminoglycosides. Only the *cydA*-mutant was slightly less susceptible to negamycin. AN66 and

the *cydB*-knockout strain JW0723 showed the same negamycin-profile as the *E. coli* wildtype BW25113.

At an alkaline pH the membrane potential is changing and increasing. To investigate which effect this change of pH has on the negamycin susceptibility in the membrane-energy mutants MICs were determined (Figure 60). Furthermore it was compared to the behavior of the isolated-resistant clones on PP, which showed small colony size, which could be due to energy depletion. PP-2 and PP-6 showed a very weak growth at PP pH 8.5 and were excluded from the experiment. From PP-8 the small colony form was used in this experiment.

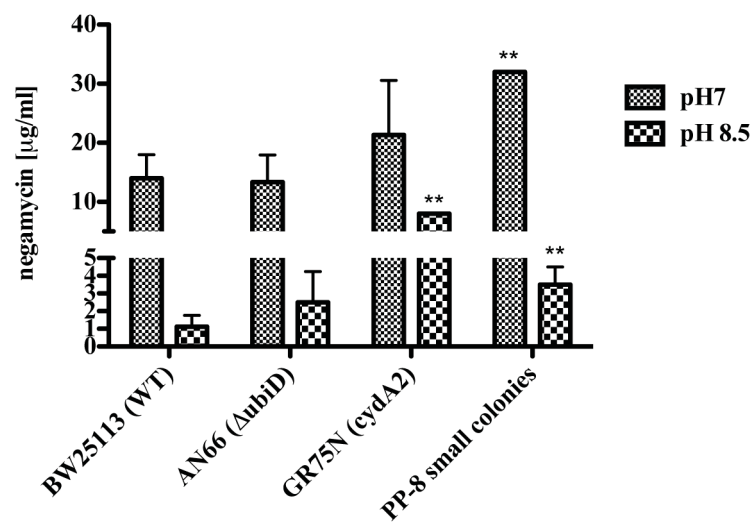


Figure 60: Negamycin susceptibility in energy mutants and PP-8 (small colony) in dependency on the pH in PP.
(n**= p<0.01)

At pH 7 only the strain PP-8 small colonies was significantly less susceptible towards negamycin compared to the wildtype (Figure 60). This was already shown in Figure 49. At pH 8.5 all tested strains BW25113, AN66, GR75N and PP-8 were more susceptible towards negamycin than at pH 7. AN66 did not show a difference compared to the wildtype, but GR75N and PP-8 did. They both were significantly less susceptible to negamycin compared to the wildtype. At a pH 8.5 both strains were less susceptible. These observations could imply again that PP-8 has some kind of energy-mutation, as it behaves similar to the *cydA*-mutant.

Unfortunately, the experiments could only be performed with energy-mutants, which did not have an isogenic strain background. This probably explains the fact that AN66 is behaving similar to the Keio-wildtype and did not show any change, besides for kanamycin, in streptomycin and negamycin susceptibility, even though it was described before [92, 126]. This might be due to the fact that it is not a Keio-strain. Nevertheless, effects for kanamycin and streptomycin could be seen and also for negamycin small effects could be detected. Therefore the membrane potential seems to play a role in negamycin uptake, even though to a smaller extent compared to aminoglycosides.

2.7 Negamycin as a possible efflux-substrate

Besides understanding how negamycin is entering the cell, it is crucial to investigate how negamycin is leaving the cell. This chapter focuses on this question.

One well-described drug secretion system, in *E. coli*, is AcrAB-TolC. It consists of three components, the cytoplasmic transporter, a membrane-fusion protein and the outer membrane factor (comparable to Figure 8). Mutations in this efflux system confer resistance towards a variety of antibiotics [155, 156].

To investigate whether negamycin is a substrate of this efflux system too, the knockout strains of *acrA*-, *acrB*- and *tolC* of the Keio-collection were tested for negamycin susceptibility in M9 and PP (Figure 61). As a positive control the antibiotic tetracycline, a described substrate of AcrAB-TolC, was used. As a negative control the drug meropenem.

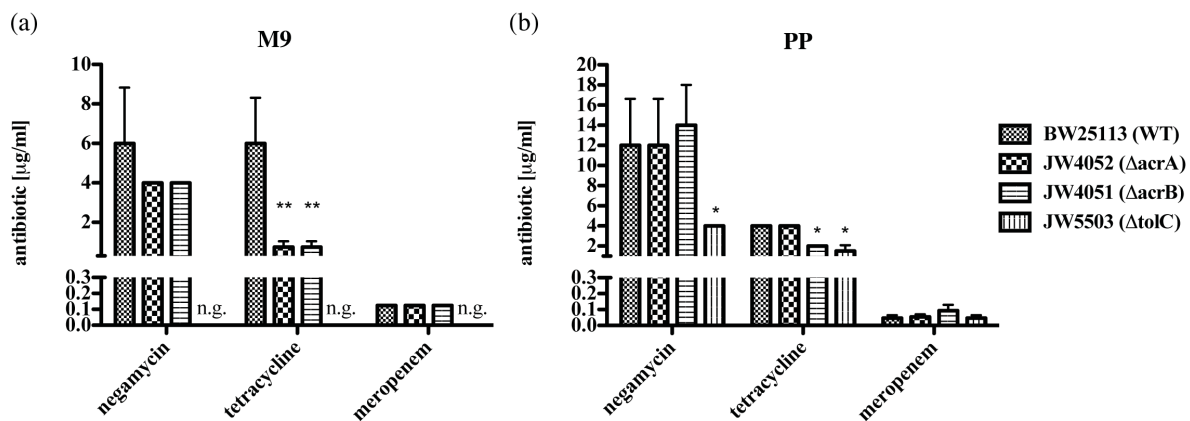


Figure 61: Negamycin, tetracycline and meropenem susceptibility in knockouts of AcrAB-tolC. The knockouts JW4052 (Δ acrA), JW4051 (Δ acrB) and JW5503 (Δ tolC) were tested in (a) M9 and (b) PP. (n*=p<0.05, n= p<0.01, n.g.: no growth)**

The Δ tolC strain did not grow in M9, so no MIC determination could be done. The other strains, JW4052 (Δ acrA) and JW4051 (Δ acrB) did not show a significant change in negamycin susceptibility compared to the wildtype (Figure 61 a). For the positive control, tetracycline, the MIC dropped highly significantly in M9, when *acrA* or *acrB* were knocked out. The treatment with meropenem, the negative control, yielded in the same MIC in all strains. In PP the knockout of *acrA* and *acrB* did not have any effect on negamycin sensitivity. In contrary the knockout of *tolC* led to a significantly more susceptible strain. Tetracycline was more active in the Δ acrB and the Δ tolC strain. The single knockout of *acrA* did not lead to a change in MIC compared to the wildtype. For meropenem the same MIC was determined in all four strains.

These results indicate that negamycin might be a substrate of TolC, even though the knockout of the AcrAB subunit did not reveal any susceptibility change compared to the wildtype. But TolC can interact with other inner membrane proteins, as for example the translocase HlyB and HlyD, which is involved in haemolysin export [157]. The positive

control, tetracycline, showed the expected results, besides the fact that in polypeptone the single knockout *acrA* strain was as sensitive as the wildtype.

3 Discussion

3.1 Negamycin and sperabillin activity

Negamycin and sperabillins share structural similarities as they are both positively charged pseudopeptides with a 3,6-diamino-5-hydroxyhexonicacid (Figure 14). One of the aims of this thesis was to investigate and compare the antimicrobial activity of these two pseudopeptides. The presented data demonstrate that both, negamycin and sperabillin, are active against Gram-positive and Gram-negative bacteria, with negamycin showing a higher potency in Gram-negative bacteria (Table 2, Table 4, [4, 131]). Discovering and developing novel antibiotics against Gram-negative bacteria is even more problematic than for Gram-positive bacteria. The main reason is that, besides presenting a cytoplasmic membrane, a characteristic shared with Gram-positive bacteria, Gram-negative bacteria also feature an additional barrier, the outer membrane. Antibiotics active against Gram-positive bacteria are often inactive against Gram-negative bacteria, only due to the incapacity of penetrating this additional barrier [2]. Both membranes have opposing penetration requirements, as described in 1.2. In this context, there is currently an urgent need to find antibiotics able to cross both of these diverse barriers, and therefore enabling the treatment of infections mediated by Gram-negative bacteria. One appealing approach is to learn from nature the characteristics that a drug needs to bring. In this respect, sperabillins and negamycin are very interesting candidates for further investigations aimed at addressing this question. The activity of both antibiotics showed striking media dependency (Table 2, Table 4), a characteristic previously described for sperabillin [127]. Negamycin did not show growth inhibition in rich media up to 64 µg/ml, and only showed moderate activity in minimal media, which either contained only peptides (PP) or only salts and glucose (M9) (Table 2). The differences in negamycin activity in different media point to distinct entry routes into the bacterial cytoplasm. Different derivatisation-approaches aimed at improving the activity of negamycin were attempted, but resulted in either a decreased or complete loss of activity [116-119]. Only recently, McKinney *et al.* published a new negamycin analogue, N6-(3-aminopropyl)-negamycin, which is showing a 4-fold improvement of antibacterial activity [121].

The derivative azidonegamycin (Figure 15) was synthesized by a cooperation partner, Dr. Glüsenkamp (Squarix GmbH), and tested in the course of this work for its anti-bacterial activity against a range of strains. Azidonegamycin did not show any activity, neither in Gram-positive nor in Gram-negative bacteria (Table 3). These findings align with previous observations [116], and support the assumption that the basicity of the N-terminal amino-group is critical for activity. As the azido group of azidonegamycin does not provide this requirement, the activity gets lost.

The mode of action of negamycin was described previously. Although the details of the mechanism of action need still to be elucidated, negamycin has been shown to target the

protein biosynthesis [158] through inhibition of ribosome translocation, polysome stabilization and miscoding [6-13]. Recent studies showed that negamycin binds to 9 independent sites at the ribosome, which are distributed over the large and small subunit [13]. The main binding site is located at the 16S rRNA in the vicinity of the conserved h34. This binding site overlaps with the tetracycline-binding site. Here, negamycin interacts also with the tRNA, and stabilizes the binding of the aminoacyl-tRNA to the ribosome. This leads to an inhibition of translocation, and stimulates miscoding [12, 13].

Additionally negamycin inhibits the termination step by binding, most likely irreversibly, to polysomal ribosomes and inhibits the release of the peptides [10, 11].

The ribosome was also identified as the target of azidonegamycin in this work. Although azidonegamycin inhibited the protein-synthesis only in a cell-free transcription-translation assay (Figure 17). This was only seen when azidonegamycin was applied in high concentrations. Accordingly, azidonegamycin has an IC_{50} of 32.6 $\mu\text{g/ml}$, compared to negamycin with an IC_{50} of 0.692 $\mu\text{g/ml}$, which explains the loss of antibacterial activity.

Sperabillins present stringent structure-activity relationships too. When the amidino moiety was modified the resulting compounds lost their activity [131]. Two sperabillins derivatives were investigated in this work: sperabillin C and hexadecyl-sperabillin. No antimicrobial activity was seen for sperabillin C up to a concentration of 64 $\mu\text{g/ml}$. Only hexadecyl-sperabillin showed a moderate activity against Gram-positive and Gram-negative bacteria (Table 4). The mode of action of sperabillin is not yet understood, and only preliminary data are available in the literature and inhibition of all biosynthesis-pathways (RNA-, DNA-, protein- and cell-wall) was seen [127]. Consequently, both derivatives were tested in an *in vitro* promoter assay. Sperabillin C induced the reporters for cell-envelope, RNA- and DNA-damage slightly, albeit only concentrations higher than 100 $\mu\text{g/ml}$ (Figure 19).

In addition, sperabillin C showed a slight effect on transcription and translation (Figure 20). However, even high conc did not prevent more than 50% of ribosome function. In contrast, Hexadecyl-sperabillin induced selectively the promoter for cell-envelope damage (Figure 19). This induction might be evoked by the hexadecyl moiety, and might not be based on the sperabillin moiety itself. In order to further investigate the mode of action of sperabillins, more active derivatives, such as sperabillin A, should be studied, as the promoter induction that was seen for sperabillin C and hexadecyl-sperabillin were only very small. Using a more potent derivate, promoter assay and an incorporation assay, as previously described in literature [127], should be performed, but taking samples not only at one single timepoint, but over a course of time.

3.2 Passage of negamycin across the outer membrane

The presented data show that the uptake mechanism of negamycin into the bacterial cell is very complex. Negamycin enters the cell using different uptake routes, which reduces the risk of developing resistance by mutating a single transporter. Negamycin is a positively

charged pseudopeptide, which most likely supports the initial interaction with and electrostatic binding to the outer membrane.

In mutants displaying the “rough phenotype” due to the mutation in *rfaG*, the negative charge of the inner core lies open and is accessible (Figure 23), which could support the initial binding of the positively charged antibiotic. The strain was even more susceptible towards negamycin and other cationic antibiotics (Figure 24). Hypersensitivity towards detergents and hydrophobic compounds was described for this phenotype before [159]. However, the effect was stronger in M9 than in PP. This could be due to the weaker growth in this minimal medium (Figure 25), as the mutant is also more sensitive to the non-cationic antibiotics (tetracycline and ciprofloxacin) (Figure 24). But also in PP a trend for negamycin was seen, even though the trend was reversed for the other antibiotics.

It was shown in this project that negamycin uses the porin OmpN to cross the outer membrane (Table 5). A porin-mediated uptake route was proposed before [114], but never proven.

In general small, charged and hydrophilic molecules (<600 Da), as negamycin, can pass the bacterial membrane through water filled channels, the porins [28]. Negamycin shows a higher affinity to the minor porin OmpN than to the main *E. coli* porins, OmpF, OmpC and PhoE, and the minor porins YbfM, OmpA, OmpG and OmpL (Table 5). So far OmpN was not described for the uptake of the main antibiotic classes. In fact the overexpression of OmpN did not have any effect on the susceptibility to a wide range of antibiotics, as for example tetracycline and ciprofloxacin [160]. These antibiotics use preferably one of the main above mentioned porins [35, 36, 101]. Tetracycline, for example, uses OmpF as the main entry route. The knockout of this porin leads to a twofold decrease of susceptibility [101, 161, 162], similar as it was seen for negamycin and OmpN. Additionally to OmpF, the antibiotic tetracycline can use OmpC as an uptake route too. This cannot be seen in the single *ompC* knockout, which shows the same susceptibility as the wildtype strain, but is manifested in the double *ompF* and *ompC* knockout [101]. A similar occurrence could also apply to negamycin, which might use, besides OmpN, one or more additional porins for crossing the outer membrane. Strains with several combined porin knockouts should be tested for change in negamycin susceptibility, to determine which other porins are involved in the uptake.

The involvement of OmpN in negamycin uptake was only detected in the peptide-free medium M9. Under this condition the outer membrane is not rate-limiting for the uptake of negamycin (Figure 21). In the *ompN*-knockout, in contrary, it becomes a rate-limiting barrier, as negamycin cannot use its preferred route to enter the cell (Figure 22). In PP, where peptides are present, negamycin has to compete with them for uptake through OmpN and further potential porins (Figure 27), and also here the outer membrane is a rate-limiting factor for the antimicrobial activity. As the knockout of OmpN does not lead to a complete loss of negamycin activity, it seems likely that negamycin can cross the outer membrane also via an alternative way. One option could be other porins, either such that were not tested so far or porins among the list of tested ones, which individually make minor contributions but

collectively cause a notable effect. As mentioned before, the susceptibility of different double- and triple porin- knockouts should be determined. Another possibility could be a non-porin-mediated uptake.

For tetracycline and quinolones for example, a porin-mediated and a lipid-mediated pathway is described. They both cross through porins in the chelated form [35, 36, 101]. In the uncharged form they enter the cell by passive diffusion, more specifically, by porin independent diffusion, through the outer membrane [101, 103, 163].

A similar mechanism by negamycin seems possible. Macroscopic constant calculation showed that approximately 9.3 % of negamycin are zwitterionic at a neutral pH (2.6.3) and to a small extent negamycin will be uncharged and can passively diffuse, in this form, over the outer membrane.

Also, an aminoglycoside-like-approach over the outer membrane cannot be excluded. Aminoglycosides cross the outer membrane by self-promoted uptake [32]. They carry 3-6 positive charges, which support the initial interaction with the negatively charged outer membrane. Subsequently, they bind to the outer membrane and act as permeabilizer, even though this effect is relatively weak compared to PMBN [32, 90, 91]. Finally, they are able to disrupt the Mg^{2+} bridges between the lipopolysaccharide (LPS) molecules, and promote their own uptake. Negamycin has only one single net positive charge at neutral pH. Consequently, the initial binding to the negatively charged outer membrane could be expected not as strong as for the aminoglycosides, which carry 3-6 positive charges. However, considering that complexed Ca^{2+} neutralizes the negative carboxyl group of negamycin (see below), generating a negamycin species with two protonated, positively charged amino groups, it cannot be excluded that also this route contributes to the overall negamycin uptake over the outer membrane to a small percentage. This point is supported by the description of Silver *et al.* of the drugs belonging to the class: “extracytoplasmic and transported drugs”, as aminoglycosides do. This class of drugs is much more polar and is mainly charged at neutral pH [2]. These characterisations are true for negamycin too, as it has two positive centers.

3.3 Passage of negamycin across the cytoplasmic membrane

The second barrier an antibiotic has to cross, if its target is located in the cytoplasm, is the cytoplasmic membrane. The physicochemical characteristics of negamycin, a charged and hydrophilic molecule, predestines it for entry mediated by active uptake [2]. Negamycin uses an energy-dependent uptake mechanism as an entry route, the dipeptide permease Dpp (Table 6). Here, my results confirm the data reported by Rafanan *et al.*, who suggested this permease as a possible negamycin transporter [126], and the recently published data of McKinney *et al.* [114]. The complementation of *dppA* verified the knockout as the cause for the increased resistance, and excluded a random downstream effect (Figure 32). Ten isolated resistance mutants in M9 showed either a *dpp*-mutation or –deletion, and confirmed this permease as the main entry route in M9 (Figure 50, Figure 51). Interestingly,

resistant mutants generated on PP did not show a mutation in Dpp (2.4.3.3). This is in agreement with the observation that negamycin is only using this entry route in M9 (Table 6), not in PP, even though peptide transporters are more highly expressed in PP (Figure 26). An explanation for this is that negamycin has to compete with peptides for uptake at Dpp in PP, as it is the case for the passage across the outer membrane. Adding peptides, casein or amino acids, in increasing concentrations to M9, led to reduced negamycin activity (Figure 27). A similar effect was seen for bialaphos (Figure 28), a described substrate of Dpp and Opp [64].

M9 lacks any peptides. Thus, it was tested, if the pseudopeptide negamycin, even though present only in μM amount, might be recognized as a peptide-source, and hence induces the expression of peptide transporters in this medium. After 30 minutes of negamycin treatment, transporter expression was down-regulated (Figure 30). This observation shows that negamycin does not induce peptide transporter expression in the minimal medium M9. On the contrary, it even seems to inhibit the expression of these transporters. This suggests that the cell recognizes negamycin as a harmful substance, and consequently inhibits the expression of different peptide transporters, which can be uptake routes of the peptide-like antibiotic. This is seen at least after a time course of 30 minutes. This observation does not exclude that right up on negamycin treatment, the transporter expression might still be induced. But as the loss of function of Dpp does not lead to complete insusceptibility, negamycin must use other routes besides the dipeptide permease.

Interestingly, in peptide-rich PP, but not in M9, the knockout of the POT transporter YbgH, showed reduced susceptibility to negamycin (Table 6). YbgH is one of the four POTs in *E. coli*, which are described to transport di- and tripeptides [82, 83]. YbgH itself has an affinity to dipeptides [87], which makes negamycin a suitable substrate. However, the deletion of YbgH resulted only in a twofold loss of susceptibility. Therefore the pseudopeptide must use additional routes in PP. Transport might occur via a collective peptide transporter uptake. Many transporters share a high similarity, and therefore have a similar and overlapping substrate-spectrum, as described for some ABC-transporters [60, 68, 73]. As mentioned before YbgH did not have an effect in M9. To investigate this aspect further, transcription-analysis should be performed, to see if this transporter is, for example, not expressed in the minimal medium M9.

Screening additional transporters, it was observed that also SapA, the periplasmic binding protein of the Sap transporter (sensitive to antimicrobial peptides), plays a role in negamycin uptake, even though, astonishingly, knockouts of the membran components of the Sap transporter did not show reduced susceptibility (Table 6). The Sap-transporter shows the same structural organisation as Dpp and Opp, and shares a high similarity with these peptide transporters, as described in 1.2.2.2.3 [78]. The Sap-transporter was described as being involved in resistance to antimicrobial drugs [78], heme utilization [81] and K^+ -transport via the uptake system TrkH and TrkG [79]. The uptake of further substrates was not described so far.

As the periplasmic binding proteins of the main ABC-peptide transporters (DppA, OppA) share high similarity with SapA in *E. coli* (54.7% and 41.1%), a cross-talk between transporter

and the binding of the same substrates could in principle occur. This would implicate that the loss of one periplasmic binding protein could be compensated by the others. This was investigated by creating a double knockout of DppA plus SapA, DppA plus OppA and a triple knockout of DppA, SapA and OppA. However, the knockouts did not have a strong additional effect on negamycin-resistance compared to the single *dppA*-knockout (Figure 38). On the basis of the number of MIC determinations performed in this work, OppA might be involved in negamycin uptake to a small extent, similar to the uptake of bialaphos. For bialaphos, the main uptake transporter is Opp, and Dpp is just involved to a small extent [64]. The double-knockout $\Delta dppA\text{-}\Delta oppA$ is more resistant to bialaphos as JW1235 ($\Delta oppA$), even though the single *dppA*-knockout did not show any effect on bialaphos-susceptibility (Figure 39).

In this work the single knockout of each compartment of the Dpp-transporter resulted in a increased resistance towards negamycin, which was also shown recently by others [114]. The knockout of one compartment of the ABC transporters Dpp or Opp results in a complete loss of function of these transporters [62, 71]. As Sap shares a high similarity with the two ABC-transporters, the same can be assumed for this transporter, even though it was not described so far.

The promoter lies in front of the genes *dppA*, *oppA* and *sapA*, and the transcription terminator is located behind *dppF*, *oppF* and *sapF* (Figure 41 [71]). As no other promoters are found in the operon, the insertion of the resistance-cassette in *dppA*, *sapA* or *oppA* leads, for each transporter, to a complete loss of function. It was shown that the removal of the resistance cassette in *dppA* resulted in the expression of the other four transporter domains, which was comparable to the wildtype level (Figure 42). Nevertheless this strain, with the deleted cassette, was still as resistant to negamycin as the strain containing the cassette (Figure 40). This implies that the periplasmic binding proteins of the other ABC-transporters cannot compensate the loss of DppA via cross-talk with the remaining domains of the dipeptide permease. Expression studies showed further that the knockout of one periplasmic binding protein did not result in an increased expression of the others (Figure 43). However, it should be considered that the possibility of cross-talk between the transporters cannot be completely excluded, as the qPCR shows only the expression levels, which does not allow us to take any conclusions on the status on protein level.

The observation that even the triple knockout in *dppA*, *oppA* and *sapA* is affected by negamycin, indicates that there must be further uptake routes not involving these ABC transporters. Uehara *et al.* proposed negamycin uptake via a lysine-permeation system [120]. Negamycin and lysine share structural similarities (Figure 44), and it was shown, in this work, that they compete for uptake (Figure 45). However, no tested lysine permeation system could be identified as a negamycin uptake-route (Figure 46). This observation could indicate that the competition for uptake between lysine and negamycin does not take place at the cytoplasmic membrane, but at the outer membrane. This hypothesis needs to be investigated in follow-up studies.

The negamycin uptake through peptide transporter in *S. aureus* [164] was investigated too, but a strong involvement in minimal medium could not be shown (Table 7).

The results on the negamycin uptake via peptide transporter suggest that negamycin can use additional ways to enter the cell, as none of the tested and created knockouts resulted in a complete resistance towards this pseudopeptide. Investigations on the negamycin resistant clones, which were isolated on PP showed that they display a low-level cross-resistance with aminoglycosides (Table 9, Table 10). A cross-resistance of negamycin and aminoglycosides was described in literature, too [114, 165].

Aminoglycosides enter the cell via a self-promoted uptake [88]. The first step of this process is based on rapid electrostatic binding. In this phase the positive aminoglycosides bind to the negatively charged sides (lipopolysaccharides) of the outer membrane [89]. The uptake across the cytoplasmic membrane is energy-dependent and driven by the pmf. They cross the plasma membrane in response to the membrane potential, in the so called EDPI (energy-dependent-phase-1) [92]. In the second step (EDPII), aminoglycosides cross the cytoplasmic membrane at a linear rate. This process is energized by energy from electron transport and possibly from ATP-hydrolyses [99]. Rafanan *et al.* described mutants deficient in components of the electron transport, which displayed a low level resistance to negamycin, too [165]. The EDPI of aminoglycosides is rate limiting, and changes in the membrane potential, as for example caused by low pH, inhibit this phase [166]. Membrane-energy-mutants show a lower susceptibility to aminoglycosides [92]. A similar uptake mechanism might be possible for negamycin. The resistant mutants selected on PP showed growth deficiencies (Figure 47, Figure 48), which were not detected in the M9-isolated resistant mutants (Figure 47). One possible explanation for the slower growth might be that the mutants display energy-depletions. McKinney *et al.* isolated membrane energy mutants and suggested an uptake driven by the membrane potential [114]. Negamycin might use this route, driven by the membrane potential, in peptide-rich medium, where peptide transporters are occupied.

Membrane-energy mutants, which are described as being more resistant to aminoglycosides [92], were tested for cross resistance to negamycin in this work. The strain AN66 (ubiquinone deficient [153]) was described before to be more resistant to aminoglycosides [165]. In this work the resistance-profile was not equal for all aminoglycosides, but a resistance towards kanamycin was shown (Table 15). However, the *ubiD*-knockout did not show a significant effect on streptomycin and negamycin resistance, even though it was described before [92, 126]. This could be due to the fact that the strain is not a Keio-strain and was derived from another parent strain. Therefore it was not compared to its isogenic parent strain. However, recent studies described resistant negamycin mutants, which were isolated on M9, which showed mutations in several *ubi* genes [114]. Based on these facts one can assume that the comparison of a strain to a non-isogenic wildtype strain can only detect strong effects, as seen for kanamycin. A slight, not significant, effect was seen for negamycin too, which became more prominent at a pH 8.5 (Figure 60).

GR75N (*cydA* mutant [154]) showed moderate- to high-level resistance to kanamycin and streptomycin. This strain was slightly, but not significantly, less susceptible to negamycin

(Table 15). However, this strain has another strain background as well, as it is not originated from the wildtype BW25113. To verify this observation, the experiment would need to be repeated with the original parent strain. The *cydB*-knockout strain did not show any change in the negamycin susceptibility.

The results indicate that the membrane potential might play a small role in negamycin uptake. Unfortunately, the experiments could only be performed with energy-mutants, which did not have an isogenic strain background. Therefore the comparison to the Keio-strain has limited validity. Nevertheless, effects for kanamycin and streptomycin could be seen and also for negamycin small effects could be detected. Therefore the membrane potential seems to play a role in negamycin uptake, even though to a smaller extent compared to aminoglycosides.

Another potential uptake pathway might be a ciprofloxacin/tetracycline-like uptake. As described in 3.2, both antibiotics chelate magnesium and can pass in this form through porins across the outer membrane [35, 36, 101]. The complex dissociates again in the periplasm, and the uncharged molecule can diffuse through the lipid-bilayer of the cytoplasmic membrane [103, 104, 111, 167]. 9.3% of negamycin molecules are zwitterionic at neutral pH. A small amount of these species will be uncharged and might use this uptake route. Negamycin would then distribute across the membrane so that the concentration of uncharged species is identical on both sides of the membrane, as it is seen for the other antibiotics [103]. The uptake of e.g. tetracycline is driven by the Δ pH component of the proton motive force [103]. With increasing pH the complexation is favoured and therefore the change of pH can influence the uptake rate [108].

However, it should be taken into account that negamycin causes misreading, which leads most likely to the insertion of defective and incorrect membrane-proteins, which causes an increased permeability of the cytoplasmic membrane and an improved negamycin uptake. Therefore, after the initial transport of negamycin into the cell, the uptake should increase already based on this effect.

3.4 Ca^{2+} -complexation by negamycin

The calcium concentration within the cell is highly regulated [168, 169]. It plays an important role in different bacterial physiological processes, as for example the cell-cycle [170], motility [171], and spore formation [172].

When calcium was added to PP, the activity of negamycin increased significantly. This improvement could be based on either a target-related or an uptake-related effect. For other antibiotics both effects were described. For empedopeptin for example, the interaction with calcium lead to an improved interaction of the antibiotic with its membrane-standing target [147]. A similar effect was described for daptomycin as well. For

both antibiotics calcium is crucial to interact with the negatively charged phospholipids of the membrane [147, 173].

For negamycin a target-related effect could be excluded (Table 14). Therefore an uptake-related effect seems likely.

Other antibiotics, as e.g. tetracycline and ciprofloxacin, bind preferably another divalent cation, Mg^{2+} . Magnesium is crucial for many cellular processes, as for example stabilization of rRNA [174]. Tetracycline for example binds to the ribosome as a magnesium-tetracycline complex [167]. Mg^{2+} also plays a role in antibiotic uptake. Tetracycline and ciprofloxacin complex Mg^{2+} and bind to the negatively charged cell surface and cross the membrane [36, 101]. Both antibiotics release the cation in the periplasm and diffuse as uncharged molecules through the cytoplasmic membrane [104, 111]. Nevertheless, tetracycline cannot only complex Mg^{2+} , but also Ca^{2+} [175]. In this work it was shown that negamycin complexes, as tetracycline, both divalent cations Mg^{2+} and Ca^{2+} (Table 13, Figure 52). The ITC experiment of negamycin and $CaCl_2$ revealed that negamycin is interacting with Ca^{2+} in a 1:1 stoichiometry, which is represented by a stoichiometry factor of 1.02 ± 0.07 (Figure 52). Recent studies showed that negamycin complexes Mg^{2+} at the target too, which leads to a Mg^{2+} -mediated interaction with the 16S rRNA [13]. However, if Mg^{2+} was added to the MIC-assay the negamycin activity was not significantly improved (Table 12). The magnesium concentration is highly regulated in the cytoplasm [174, 176, 177]. The external addition of Mg^{2+} probably does not improve the target binding of negamycin, as the concentration in the cytoplasm is most likely already very high. It can be assumed that Mg^{2+} does not, in contrary to Ca^{2+} , improve the membrane binding in the chelated-form. For aminoglycosides it was described that high concentrations of divalent cations inhibit the activity of aminoglycosides. This is due to a competition of binding to the negatively charged binding sites of the cell surface [92]. High concentrations of Mg^{2+} do not have the same effect on negamycin activity, this lets one assume that it the uptake via self-promoted uptake, as it is described for aminoglycosides, is not one of the main routes for negamycin.

Monovalent cations, as Na^+ and K^+ , inhibit negamycin activity (Table 12). Na^+ and negamycin do not form a complex. It was shown that Na^+ rather inhibits complex formation between Ca^{2+} and negamycin (Figure 52, Figure 53). Furthermore, Na^+ might bind to the negatively charged phospholipids, and prevent the positively charged chelate-complex from binding to the cell surface. In a next step the effect of the monovalent and divalent cations on negamycin interaction with the membrane needs to be elucidated. Surface-acoustic-wave (SAW) experiments were initiated, and performed by a cooperation partner at the University of Bonn. These experiments were not finished in the time course of this thesis.

The effect of Ca^{2+} occurs on the cytoplasmic membrane as it was also detected in Gram-positive bacteria, which lack an outer membrane, and in PMBN treated cells (Figure 54). However, an additional effect on the outer membrane cannot be excluded.

3.5 Alkaline pH increases negamycin activity

Not only salts, but also the pH can have an impact on antibiotic activity, as described for example for aminoglycosides [93-95]. The pH effect is well described for aminoglycoside-activity. The driving force of the uptake of this antibiotic class is the pmf [88]. A change in the pH affects the pmf, and consequently the uptake of aminoglycosides [93-95]. When the membrane potential is low, less aminoglycosides can enter the cell. This phenomenon is seen at acidic pH. In contrary, since at high pH (pH 8.5) the membrane potential is higher, more aminoglycosides enter the cell, and therefore the activity increases [94]. Negamycin resistant-mutants, with growth deficiencies, share cross-resistance with aminoglycosides. One could assume that the change of the pH might have a similar effect on the negamycin uptake, if it is comparable to aminoglycosides. An acidic pH led to a drop in negamycin activity, whereas a basic pH of 8.5 increased the activity (Figure 55). McKinney *et al.* tested the pH effect in cation-adjusted MH, and could also observe a negative effect of acidic pH on the antimicrobial activity, but could not see the beneficial effect of alkaline pH in this medium [114]. The beneficial effect of alkaline pH was also seen in membrane-energy mutants. The isolated negamycin-resistant clone PP-8 showed the same phenotype as the *cydA*-mutant, as they were both significantly less susceptible to negamycin compared to the wildtype at pH 8.5. This underlines again the assumption that this strain has mutations, which influence the energy-household of the cell. The beneficial effect of alkaline pH was also seen for Gram-positive bacteria, which implies an effect on the cytoplasmic membrane (Figure 55). One potential option for an increased activity at pH 8.5 could be faster killing. Killing curves, at pH 7 and pH 8.5, showed that the killing event is not increased in speed, but occurs at lower negamycin concentrations (Figure 57). Interestingly, the pH in PP pH 7 became more alkaline over time (Figure 56). After 7 hours the pH reached a value of 8.5. At pH 8.5 negamycin is partially net neutral (2.6.3), and a lower proportion of the molecules is net charged. It is reasonable to assume that more negamycin can enter the cell passively at pH 8.5 than at pH 7. Under this condition, a ciprofloxacin/tetracycline-like uptake might be possible (as described above). The ciprofloxacin-Mg²⁺ complex dissociates in the periplasm, and the uncharged species diffuses through the cytoplasmic membrane [111]. The same mechanism is seen for tetracycline [103, 104, 111, 167]. If negamycin enters the cell under alkaline conditions, in a similar way as ciprofloxacin and tetracycline, it could enter the cell by passive diffusion, as discussed in 3.2. It was shown that the addition of CCCP, an uncoupler of the proton-gradient [178] did not significantly affect negamycin susceptibility (Figure 59). The protonophor was added in low concentrations, but a shift of susceptibility might have been expected if negamycin would only enter the cell via active transportation. However, this experiment should be repeated and performed with a control antibiotic. For further confirmation, uptake studies with a radioactive labeled negamycin should be performed. The labeling of the compound was already initiated, but so far it was not successful.

However, the combination of both beneficial conditions (i.e. the presence of Ca^{2+} and basic pH) led to a 32-fold MIC improvement compared to PP (pH 7) (Figure 55). The optimal CaCl_2 concentration at pH 8.5 was 0.5 mM, as higher concentrations precipitated under alkaline pH. This effect was seen in other pathogens, too. Under the optimized condition pH 8.5 + 0.5 mM CaCl_2 *P. aeruginosa* and *S. aureus* showed a MIC of 4 $\mu\text{g/ml}$ (Figure 6 b). Basic pH and the addition of calcium have therefore an effect in Gram-positive and Gram-negative bacteria. An explanation might be a combination of improved binding capacity of negamycin to the membrane due to calcium binding, and an improved passage through the membrane based on a change in pmf and negamycin charge.

3.6 Negamycin: a substrate of the TolC-efflux pump

Bacterial resistance to antibiotics is often based on an efflux of the compound out of the bacterial cell [179-181]. Drug-specific efflux has been described e.g. for tetracycline [182], but multidrug efflux pumps have been described as well, and they play an important role in the development of resistance in Gram-negative and Gram-positive bacteria [155, 156, 181, 183]. One of the major drug-efflux systems in *E. coli* is the pump AcrAB-TolC [184, 185]. It consists of three components: AcrB, a resistance-modulation division (RND) protein [186], AcrA, a membrane fusion protein [187], and the outer membrane channel TolC [157]. As an efflux of negamycin could be a possible resistance mechanism in bacteria, it was tested whether negamycin is a substrate of the AcrAB-TolC efflux-pump.

Preliminary results suggested that negamycin might be a substrate of TolC (Figure 61), while knockout of the subunit AcrAB did not reveal any susceptibility change compared to the wildtype. But TolC can interact with other inner membrane proteins, as for example the translocase HlyB and HlyD, which is involved in haemolysin export [157]. In the next step knockouts of additional interaction-partners of TolC should be tested for negamycin sensitivity, as well as further efflux-systems.

4 Conclusion and proposed negamycin uptake-model

The data presented in this work show that negamycin has multiple ways to enter the cell, which reduces the risk of developing resistance by mutating a single transporter. The proposed model for the uptake is summarized in Figure 62 and Figure 63.

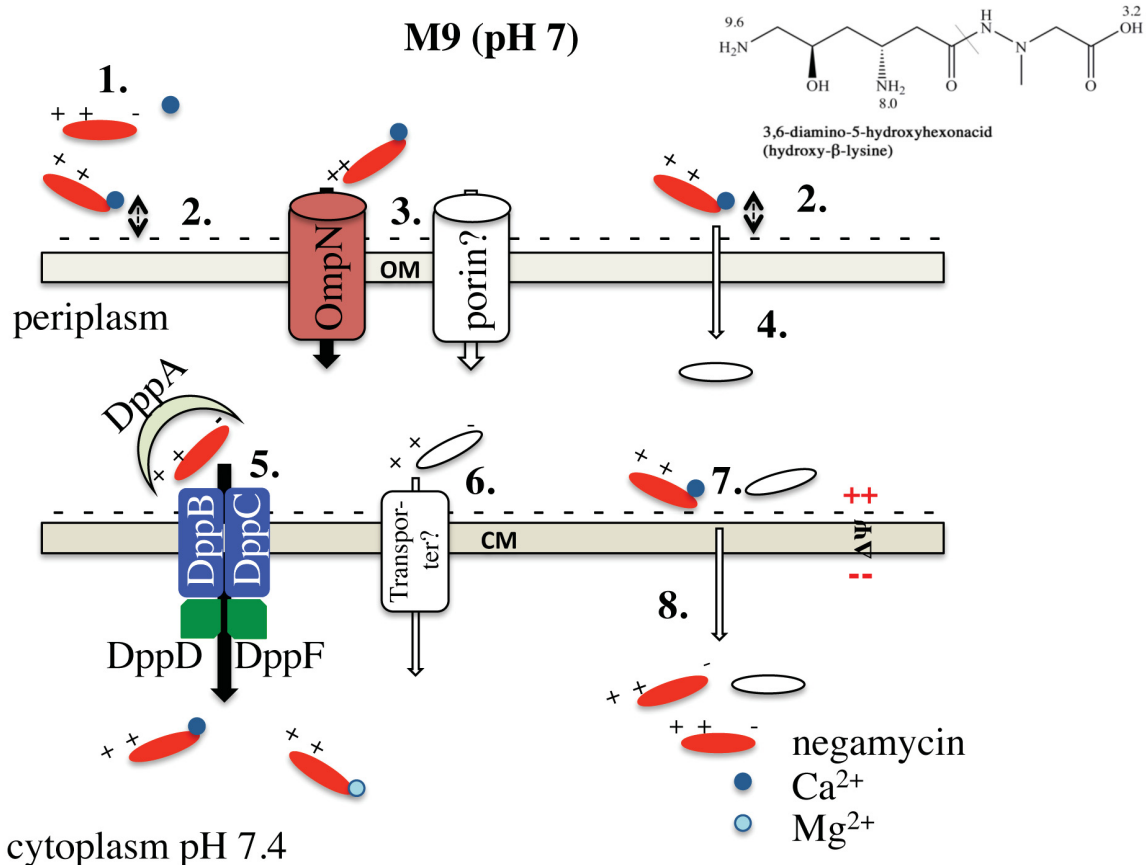


Figure 62: Proposed model of negamycin uptake in M9.

The different steps of negamycin uptake are explained in the text. Impact of the coloured steps was demonstrated in this work. Contribution of the uncoloured steps is not experimentally proven, so far.

M9 medium contains salts and glucose but no peptides and has a pH of 7. At this pH the majority of negamycin is present as a positively charged species (protonated $\alpha\text{-NH}_3^+$, $\beta\text{-NH}_3^+$ and deprotonated COO^-). In M9 the negatively charged carboxyl group of negamycin is able to complex the divalent cation Ca^{2+} (1). Calcium complexation shields the negative carboxyl moiety and facilitates initial interactions with, and electrostatic binding to, the negatively charged LPS of the outer membrane (2.).

The negamycin- Ca^{2+} complex is in equilibrium with the unchelated species. The majority of negamycin enters via the porin OmpN, and probably further porins. In M9, the passage of negamycin is not hampered by competing nutrient peptides (3.). Porin-mediated uptake is efficient under these conditions and the outer membrane is no rate-limiting barrier.

To a smaller extent negamycin can probably also cross the outer membrane independently of porins (4.). As negamycin has two positive centers and is a polar, small molecule, self-promoted uptake, as described for aminoglycosides [31, 32], might also take place, although it is not the main uptake route across the outer membrane in M9. In addition, a small portion of negamycin is zwitterionic at pH 7 (protonated $\alpha\text{-NH}_3^+$, deprotonated $\beta\text{-NH}_2$ and deprotonated COO^-) and to an even smaller extent it will be uncharged (deprotonated $\alpha\text{-NH}_2$, deprotonated $\beta\text{-NH}_2$ and protonated COOH) at neutral pH. Once Ca^{2+} is released, the uncharged form is able to pass the outer membrane by passive diffusion. However, this is also a minor route at pH 7. In the periplasm, reversible dissociation of the chelate releases negamycin. The periplasmic binding protein DppA binds the compound and leads it to the cytoplasmic membrane, where negamycin is transported via the ABC transporter Dpp into the cytoplasm (5.). It is not known yet if this energy consuming transport of negamycin is taking place in the chelated form or not. It is likely that one or more additional peptide transporters (6.), besides Dpp, are involved in negamycin uptake in M9, but as Dpp is such a strong route in M9, they could not be unambiguously identified in this work. Calcium facilitates also the interaction of negamycin with the phospholipids of the cytoplasmic membrane (7.). A small proportion of negamycin might enter the cytoplasm independently of peptide transporters (8). An aminoglycoside-like uptake across the cytoplasmic membrane cannot be excluded, but as the tested electron transport mutations had only a weak effect on negamycin activity, its contribution to negamycin uptake cannot be large under the conditions employed in this work. Negamycin in its uncharged form could cross the cytoplasmic membrane by passive diffusion, but this is also only a minority at pH7. In the cytoplasm, negamycin can chelate Ca^{2+} or other divalent cations and binds to its target, the ribosome. The ribosome acts like a scavenger, which promotes the uptake of further negamycin molecules across the cytoplasmic membrane. Furthermore the misreading, caused by negamycin, leads most likely to the insertion of defective and incorrect membrane-proteins, which might result in an increased permeability of the cell envelope and facilitated negamycin uptake.

The proposed model for negamycin-uptake in polypeptone is presented in Figure 63.

a. As described for the uptake model in M9, the negatively charged carboxyl group of negamycin complexes Ca^{2+} (1.). Consequently, the negative charge of the carboxyl group is shielded, and at pH 7 the majority of negamycin carries two positive charges, one at each aminogroup. In the chelated form the interaction with, and electrostatic binding to, the outer membrane increases (2.). In polypeptone negamycin can use the porin route (3.) less efficiently than in M9. As the porins also transport nutrient peptides (orange circles), which form the sole carbon and energy source in this medium, negamycin has to compete with them for uptake. Passage across the outer membrane becomes a rate-limiting step in the uptake. As in M9, some negamycin might cross the outer membrane independently of porins (4.), either via self-promoted uptake and with respect to the minority of uncharged

negamycin, by passive diffusion. In the periplasm negamycin and negamycin- Ca^{2+} associate and dissociate in equilibrium. The compound interacts with the negatively charged cytoplasmic membrane, as soon as it is in vicinity to it (5.). A minority of negamycin might cross the cytoplasmic membrane by passive diffusion (6.). In PP negamycin competing peptides obstruct Dpp as an uptake route. One transporter was identified as an uptake route in PP, the POT transporter YbgH (7.). Most likely the uptake in PP over the cytoplasmic membrane occurs via a collective peptide transporter uptake.

As mentioned before, an aminoglycoside-like-uptake cannot be excluded (8.). The driving force is the pmf. This becomes particularly relevant at pH 8.5, where the membrane potential increases and will be described in section b.

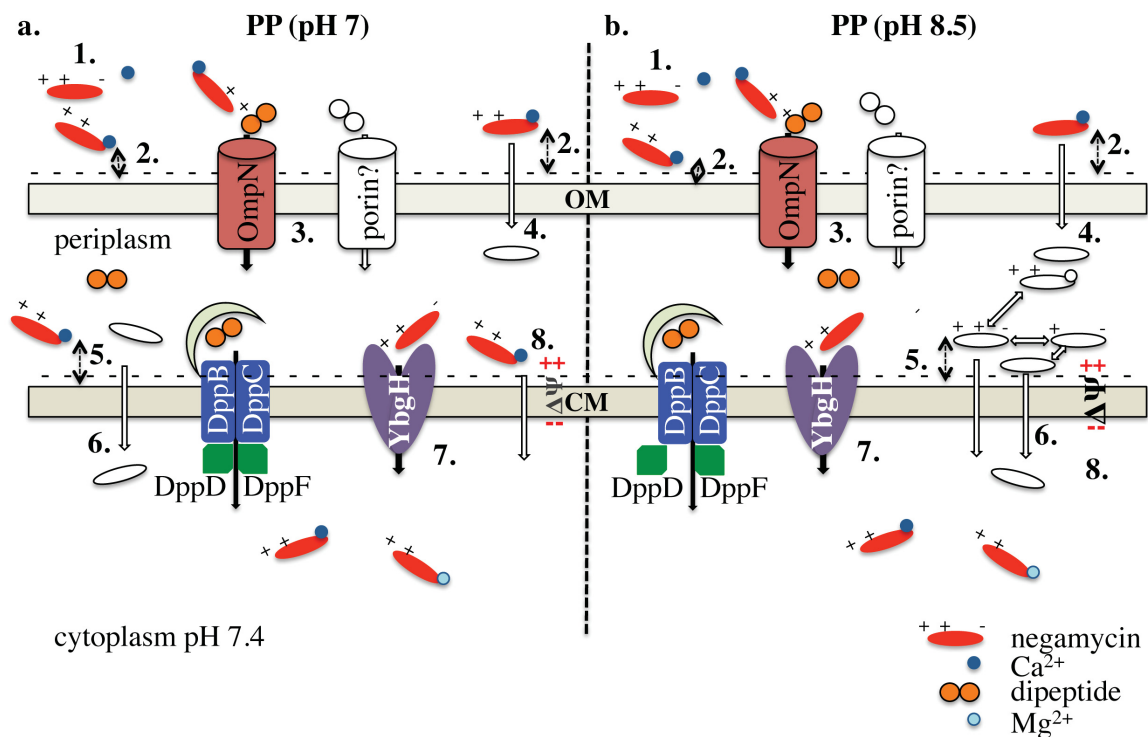


Figure 63: Proposed model of negamycin uptake in PP at pH 7 (a) and pH 8.5 (b).

The different steps of negamycin uptake are explained in the text. Impact of the coloured steps was demonstrated in this work. Contribution of the uncoloured steps is not experimentally proven, so far.

b. At pH 8.5 a substantial proportion negamycin species is zwitterionic and also the proportion of uncharged negamycin is increased compared to pH 7. Negamycin can still complex at the carboxyl group the divalent cation Ca^{2+} (1.) and interacts with the negatively charged LPS (2.). The remaining charged species can still use porins as an uptake route, where they have to compete with peptides in PP (3.). The uncharged form may passively diffuse through the outer membrane (4.). In the periplasm negamycin and negamycin- Ca^{2+} associate and dissociate in equilibrium. The compound interacts with the negatively charged cytoplasmic membrane (5.). As the proportion of uncharged negamycin is increased, more molecules can cross the cytoplasmic membrane passively (6.) Negamycin also crosses via

YbgH (7.). The change of external pH has a huge impact on ΔpH and therefore on the membrane potential component of the pmf (ΔpH is lower at pH 8.5 compared to pH 7, while $\Delta\Psi$ rises accordingly, see Figure 5). Some negamycin might pass the cytoplasmic membrane in response to the membrane potential (comparable to EDPI in aminoglycosides) (8.). For aminoglycosides EDPI is rate limiting. Here, changes in $\Delta\Psi$ have a strong effect on the uptake rate already at pH 7. In the case of negamycin, electron-transport mutants were only slightly less susceptible than the wildtype at pH 7, but the effect increased at pH 8.5. At elevated pH the transmembrane force is raised, which leads to a stronger inwards pull for negamycin. These observations suggest that although $\Delta\Psi$ contributes to negamycin uptake, uptake of the pseudopeptide is less strongly driven by the membrane potential than the uptake of aminoglycosides.

5 Material and Methods

5.1 Material

5.1.1 Chemicals

Table 16: Chemicals

Chemicals	Supplier
6 x loading dye	Thermo Scientific
Agarose	AppliChem
Alanine	AppliChem
Ammonium acetate	AppliChem
Ammonium chloride	AppliChem
Ammonium sulfate	AppliChem
Arginine	AppliChem
Asparagine monohydrate	AppliChem
Aspartic acid	AppliChem
Adenosine triphosphate (ATP)	Roth
Bacto Agar	BD
Bovine serum albumin (BSA)	Sigma Aldrich
Calcium chloride di-hydrate	AppliChem
Citric acid	Grüssing
Coenzyme A	AppliChem
Creatine phosphokinase	Sigma Aldrich
Cytidine triphosphate (CTP)	Roth
Cysteine HCl monohydrate	AppliChem
D-Luciferin	Iris Biotech
D(+)-Glucose monohydrate	Caelo
Di-potassiumhydrogenphosphate	Grüssing

Table 16: Chemicals (continued)

Chemicals	Supplier
Di-sodiumhydrogenphosphate di-hydrate	Grüssing
Bis-(1,3-dibutylbarbituric acid) trimethine oxonol (DiBAC₄(3))	AAT Bioquest
Dimethyl sulfoxide (DMSO)	VWR
Dithiothreitol (DTT)	Invitrogen
EDTA	Merck
Ethanol, p.a.	VWR
Glutamate	Sigma Aldrich
Glutamic acid	Acros
Glutamine	AppliChem
Glycerol	Roth
Glycine	AppliChem
Guanosine triphosphate (GTP)	Roth
Histidine	AppliChem
Iron (II) sulfate heptahydrate	Acros Organics
Isoleucine	AppliChem
L-Tryptophane	AppliChem
Leucine	Merck
Lysine	AppliChem
Magnesium acetate	AppliChem
Magnesium chloride	Grüssing
Magnesium sulfate heptahydrate	AppliChem
Manganese sulfate hydrate	AppliChem
Meat extract	Fluka
Methionine	AppliChem
Milli-Q water	Merck Millipore
MOPS	Sigma

Table 16: Chemicals (continued)

Chemicals	Supplier
Mueller-Hinton-broth	Difco
Ninhydrin	Fluka
Nutrient broth	BD
Peptone from meat	BD
Peptone tryptic digest	Roth
Peptone water	BD
Phenylalanine	AppliChem
Phosphocreatine disodium salt hydrate	Sigma Aldrich
Phosphoenolpyruvate	Sigma Aldrich
PMSF (phenylmethanesulfonylfluoride)	AppliChem
Polyethylene glycol 6000	AppliChem
Polypeptone (BBL Polypeptone™ Peptone)	BD
Potassium acetate	Grüssing
Potassium chloride	AppliChem
Potassium sulfate	Merck
Potassium-dihydrogenphosphate	Grüssing
Proline	AppliChem
Putrescine (PUT)	Sigma Aldrich
Pyruvate kinase	Sigma Aldrich
RNA protect	Qiagen
RNase away	Molecular Bioproducts
Scintillation fluid-Ultima Gold	Perkin Elmer
Serine	AppliChem
Sodium chloride, p.a.	VWR
Spermidine	Sigma Aldrich

Table 16: Chemicals (continued)

Chemicals	Supplier
Tetraphenylphosphonium bromide, [phenyl-3H]; (specific activity 40 Ci/mmol)- 0.05 mCi; conc. (1mCi/ml)	Hartmann Analytic
Threonine	AppliChem
TraceSELECT® H₂O	Fluka
Tricine	Sigma-Aldrich
Triethanolamine	Roth
Tris-HCl	Roth
Trisodium citrate	Alfa Aesar
Tyrosine	AppliChem
Uridine triphosphate (UTP)	Roth
Valine	AppliChem
Yeast extract	BD

5.1.2 Antibiotics

Table 17: Antibiotics

Antibiotics	Supplier
Ampicillin sodium salt	Roth
Anhydrotetracycline hydrochloride	Cayman Chemical Company
Azidonegamycin	Squarix GmbH
Chloramphenicol	Sigma-Aldrich
Ciprofloxacin hydrochloride	AppliChem
Erythromycin (free base)	AppliChem
Hexadecyl-Sperabillin	Squarix GmbH
Kanamycin sulfate	Roth
Negamycin	Squarix GmbH

Table 17: Antibiotics (continued)

Antibiotics	Supplier
Rifampicin (>97%, HPLC)	Sigma-Aldrich
Sperabillin C	Squarix GmbH
Streptomycin sulfate	AppliChem
Tetracycline	Sigma-Aldrich
Vancomycin hydrochloride	AppliChem

5.1.3 Kits

Table 18: Kits

Kit	Supplier
AffinityScript cDNA Synthesis Kit	Agilent
Brilliant III Ultra-Fast SYBR Green QPCR Master Mix	Agilent
High Pure RNA Isolation Kit	Roche
InnuPREP Bacteria DNA Kit	Analytik Jena
InnuPREP DNase I Digest Kit	Analytik Jena
InnuPREP Double pure Kit	Analytik Jena
InnuPREP Miniprep Kit	Analytik Jena
InnuPREP RNA Mini Kit	Analytik Jena
RNeasy Mini Kit	Qiagen

5.1.4 Enzymes

Table 19: Enzymes

Enzymes	Supplier
DNase I, RNase free	Qiagen
DreamTaq Polymerase	Thermo Scientific

Table 19: Enzymes (continued)

Enzymes	Supplier
Fast alkaline phosphatase	Thermo Scientific
Fast digest <i>NcoI</i>	Thermo Scientific
Fast digest <i>XbaI</i>	Thermo Scientific
Fast digest <i>XhoI</i>	Thermo Scientific
Fast digest <i>NotI</i>	Thermo Scientific
Fast digest <i>Clal</i>	Thermo Scientific
Lysozyme	Thermo Scientific
Phusion Polymerase	Thermo Scientific
Proteinase K	Analytik Jena
Q5 Polymerase	NEB
RNase A	Peqlab
T4-Ligase	Thermo Scientific

5.1.5 DNA-Ladder

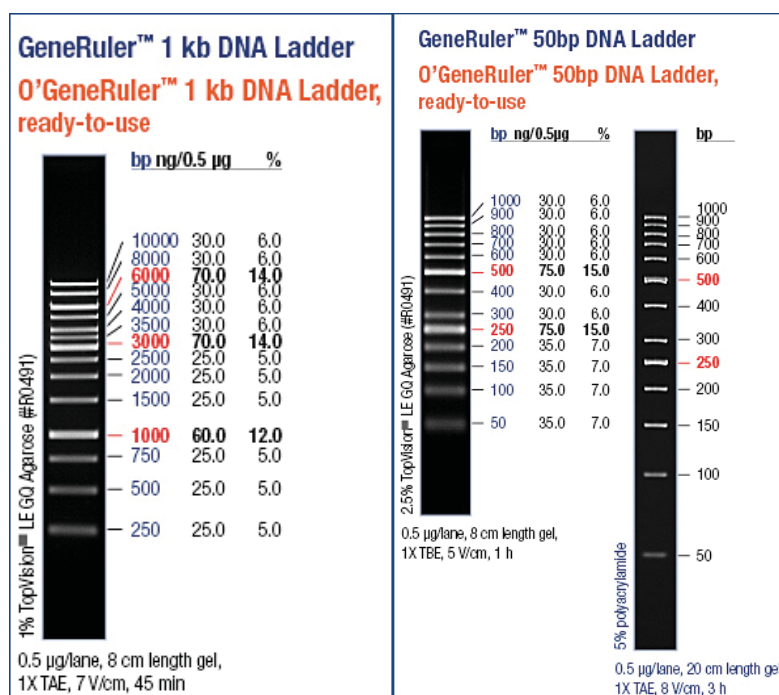


Figure 64: DNA-ladder

5.1.6 Bacterial Strains

Table 20: Bacterial strains

Species	Strain	Genotype and comments	Reference
<i>B. subtilis</i>	<i>trpC2</i>	<i>trpC2</i>	Anagnostopoulos et al., 1961 [188]
<i>B. subtilis</i>	1S34 pS63 MH124	<i>trpC2</i> , Spo-, pS63	Piggot, 1973; Urban et al., 2007 [140, 189]
<i>B. subtilis</i>	1S34 pS130	<i>trpC2</i> , Spo-, pS130	Piggot, 1973 [189]
<i>B. subtilis</i>	1S34 pS77	<i>trpC2</i> , Spo-, pS77	Piggot, 1973; Urban et al., 2007 [140, 189]
<i>B. subtilis</i>	1S34 pS72	<i>trpC2</i> , Spo-, pS72	Piggot, 1973; Urban et al., 2007 [140, 189]
<i>B. subtilis</i>	1S34 pS107	<i>trpC2</i> , Spo-, pS107	Piggot, 1973; Urban et al., 2007 [140, 189]
<i>B. subtilis</i>	IS58	<i>trpC2</i> , <i>lys-3</i>	Smith et al., 1980 [190]
<i>E. coli</i>	BW25113	F-, $\Delta(\text{araD-araB})567$, $\Delta\text{lacZ4787}(\text{:rrnB-3})$, λ -, & <i>rph-1</i> , $\Delta(\text{rhaD-rhaB})568$, <i>hsdR514</i>	Baba et al., 2006; Datsenko et al. 2000 [141, 191]
<i>E. coli</i>	K12	F+, λ +	Gray et al., 1944 [192]
<i>E. coli</i>	ATCC25922		CLSI, 2006 [193]
<i>E. coli</i>	MRE600	F-, <i>rna</i> -	Branlant et al., 1981 [194]
<i>E. coli</i>	BW25113 pBestluc-mut	F-, DE(<i>araD-araB</i>)567, <i>lacZ4787</i> (del):: <i>rrnB-3</i> , LAM-, <i>rph-1</i> , DE(<i>rhaD-rhaB</i>)568, <i>hsdR514</i>	Dr. Anne Berscheid, Brötz-Oesterhelt lab
<i>E. coli</i>	AN66 (ΔubiD)	Hfr(PO13), <i>thr-1</i> , <i>leuB6</i> (Am), <i>lacZ4</i> , <i>glnV44</i> (AS), P1+?, <i>rpsL8</i> , <i>ubiD410</i>	Cox et al., 1969 [195]
<i>E. coli</i>	GR75N (<i>cydA2</i>)	F-, <i>cydA2</i> , <i>nadA50::Tn10</i> , λ -, <i>relA1?</i> , <i>rpsE2130</i> (SpcR)	Green et al., 1984 [196]
<i>E. coli</i>	JW0723 (ΔcydB)	F-, $\Delta(\text{araD-araB})567$, $\Delta\text{lacZ4787}(\text{:rrnB-3})$, $\Delta\text{cydB782::kan}$, λ -, <i>rph-1</i> , $\Delta(\text{rhaD-rhaB})568$, <i>hsdR514</i>	Baba et al., 2006; Datsenko et al. 2000 [141, 191]

Table 20: Bacterial strains (continued)

Species	Strain	Genotype and comments	Reference
<i>E. coli</i>	JW3710 ($\Delta atpD$)	F-, $\Delta(araD-araB)567$, $\Delta lacZ4787(::rrnB-3)$, λ -, $\Delta atpD761::kan$, <i>rph-1</i> , $\Delta(rhaD-rhaB)568$, <i>hsdR514</i>	Baba <i>et al.</i> , 2006; Datsenko <i>et al.</i> 2000 [141, 191]
<i>E. coli</i>	JW3513 ($\Delta dppA$)	F-, $\Delta(araD-araB)567$, $\Delta lacZ4787(::rrnB-3)$, &lambda-, $\Delta dppA728::kan$, <i>rph-1</i> , $\Delta(rhaD-rhaB)568$, <i>hsdR514</i>	Baba <i>et al.</i> , 2006; Datsenko <i>et al.</i> 2000 [141, 191]
<i>E. coli</i>	JW3513 ($\Delta dppA$)- <i>del.</i>	F-, $\Delta(araD-araB)567$, $\Delta lacZ4787(::rrnB-3)$, &lambda-, $\Delta dppA728$, <i>rph-1</i> , $\Delta(rhaD-rhaB)568$, <i>hsdR514</i>	this work
<i>E. coli</i>	JW3512 ($\Delta dppB$)	F-, $\Delta(araD-araB)567$, $\Delta lacZ4787(::rrnB-3)$, &lambda-, $\Delta dppB726::kan$, <i>rph-1</i> , $\Delta(rhaD-rhaB)568$, <i>hsdR514</i>	Baba <i>et al.</i> , 2006; Datsenko <i>et al.</i> 2000 [141, 191]
<i>E. coli</i>	JW3511 ($\Delta dppC$)	F-, $\Delta(araD-araB)567$, $\Delta lacZ4787(::rrnB-3)$, &lambda-, $\Delta dppC725::kan$, <i>rph-1</i> , $\Delta(rhaD-rhaB)568$, <i>hsdR514</i>	Baba <i>et al.</i> , 2006; Datsenko <i>et al.</i> 2000 [141, 191]
<i>E. coli</i>	JW3510 ($\Delta dppD$)	F-, $\Delta(araD-araB)567$, $\Delta lacZ4787(::rrnB-3)$, &lambda-, $\Delta dppD724::kan$, <i>rph-1</i> , $\Delta(rhaD-rhaB)568$, <i>hsdR514</i>	Baba <i>et al.</i> , 2006; Datsenko <i>et al.</i> 2000 [141, 191]
<i>E. coli</i>	JW3509 ($\Delta dppF$)	F-, $\Delta(araD-araB)567$, $\Delta lacZ4787(::rrnB-3)$, &lambda-, $\Delta dppF723::kan$, <i>rph-1</i> , $\Delta(rhaD-rhaB)568$, <i>hsdR514</i>	Baba <i>et al.</i> , 2006; Datsenko <i>et al.</i> 2000 [141, 191]
<i>E. coli</i>	JW3513 <i>del.</i> pASK- <i>dppA</i>	F-, $\Delta(araD-araB)567$, $\Delta lacZ4787(::rrnB-3)$, &lambda-, $\Delta dppA728$, <i>rph-1</i> , $\Delta(rhaD-rhaB)568$, <i>hsdR514</i>	Dr. Anne Berscheid, Brötz-Oesterhelt lab
<i>E. coli</i>	JW3513 <i>del.</i> pASK-empty	F-, $\Delta(araD-araB)567$, $\Delta lacZ4787(::rrnB-3)$, &lambda-, $\Delta dppA728$, <i>rph-1</i> , $\Delta(rhaD-rhaB)568$, <i>hsdR514</i>	Dr. Anne Berscheid, Brötz-Oesterhelt lab
<i>E. coli</i>	JW1287 ($\Delta sapA$)	F-, $\Delta(araD-araB)567$, $\Delta lacZ4787(::rrnB-3)$, λ -, $\Delta sapA730::kan$, <i>rph-1</i> , $\Delta(rhaD-rhaB)568$, <i>hsdR514</i>	Baba <i>et al.</i> , 2006; Datsenko <i>et al.</i> 2000 [141, 191]
<i>E. coli</i>	JW1286 ($\Delta sapB$)	F-, $\Delta(araD-araB)567$, $\Delta lacZ4787(::rrnB-3)$, λ -, $\Delta sapB729::kan$, <i>rph-1</i> , $\Delta(rhaD-rhaB)568$, <i>hsdR514</i>	Baba <i>et al.</i> , 2006; Datsenko <i>et al.</i> 2000 [141, 191]
<i>E. coli</i>	JW1285 ($\Delta sapC$)	F-, $\Delta(araD-araB)567$, $\Delta lacZ4787(::rrnB-3)$, λ -, $\Delta sapC728::kan$, <i>rph-1</i> , $\Delta(rhaD-rhaB)568$, <i>hsdR514</i>	Baba <i>et al.</i> , 2006; Datsenko <i>et al.</i> 2000 [141, 191]

Table 20: Bacterial strains (continued)

Species	Strain	Genotype and comments	Reference
<i>E. coli</i>	JW1284 ($\Delta sapD$)	F-, $\Delta(araD-araB)567$, $\Delta lacZ4787(::rrnB-3)$, λ -, $\Delta sapD727::kan$, <i>rph-1</i> , $\Delta(rhaD-rhaB)568$, <i>hsdR514</i>	Baba <i>et al.</i> , 2006; Datsenko <i>et al.</i> 2000 [141, 191]
<i>E. coli</i>	JW1283 ($\Delta sapF$)	F-, $\Delta(araD-araB)567$, $\Delta lacZ4787(::rrnB-3)$, λ -, $\Delta sapF726::kan$, <i>rph-1</i> , $\Delta(rhaD-rhaB)568$, <i>hsdR514</i>	Baba <i>et al.</i> , 2006; Datsenko <i>et al.</i> 2000 [141, 191]
<i>E. coli</i>	JW1287 ($\Delta sapA$)-del.	F-, $\Delta(araD-araB)567$, $\Delta lacZ4787(::rrnB-3)$, λ -, $\Delta sapA730$, <i>rph-1</i> , $\Delta(rhaD-rhaB)568$, <i>hsdR514</i>	this work
<i>E. coli</i>	JW1235 ($\Delta oppA$)	F-, $\Delta(araD-araB)567$, $\Delta lacZ4787(::rrnB-3)$, λ -, $\Delta oppA750::kan$, <i>rph-1</i> , $\Delta(rhaD-rhaB)568$, <i>hsdR514</i>	Baba <i>et al.</i> , 2006; Datsenko <i>et al.</i> 2000 [141, 191]
<i>E. coli</i>	JW1236($\Delta oppB$)	F-, $\Delta(araD-araB)567$, $\Delta lacZ4787(::rrnB-3)$, λ -, $\Delta oppB751::kan$, <i>rph-1</i> , $\Delta(rhaD-rhaB)568$, <i>hsdR514</i>	Baba <i>et al.</i> , 2006; Datsenko <i>et al.</i> 2000 [141, 191]
<i>E. coli</i>	JW1237($\Delta oppC$)	F-, $\Delta(araD-araB)567$, $\Delta lacZ4787(::rrnB-3)$, λ -, $\Delta oppC752::kan$, <i>rph-1</i> , $\Delta(rhaD-rhaB)568$, <i>hsdR514</i>	Baba <i>et al.</i> , 2006; Datsenko <i>et al.</i> 2000 [141, 191]
<i>E. coli</i>	JW1238($\Delta oppD$)	F-, $\Delta(araD-araB)567$, $\Delta lacZ4787(::rrnB-3)$, λ -, $\Delta oppD753::kan$, <i>rph-1</i> , $\Delta(rhaD-rhaB)568$, <i>hsdR514</i>	Baba <i>et al.</i> , 2006; Datsenko <i>et al.</i> 2000 [141, 191]
<i>E. coli</i>	JW1239($\Delta oppF$)	F-, $\Delta(araD-araB)567$, $\Delta lacZ4787(::rrnB-3)$, λ -, $\Delta oppF754::kan$, <i>rph-1</i> , $\Delta(rhaD-rhaB)568$, <i>hsdR514</i>	Baba <i>et al.</i> , 2006; Datsenko <i>et al.</i> 2000 [141, 191]
<i>E. coli</i>	JW1235($\Delta oppA$)-del.	F-, $\Delta(araD-araB)567$, $\Delta lacZ4787(::rrnB-3)$, λ -, $\Delta oppA750$, <i>rph-1</i> , $\Delta(rhaD-rhaB)568$, <i>hsdR514</i>	this work
<i>E. coli</i>	JW1626 ($\Delta tppB$)	F-, $\Delta(araD-araB)567$, $\Delta lacZ4787(::rrnB-3)$, λ -, $\Delta tppB784::kan$, <i>rph-1</i> , $\Delta(rhaD-rhaB)568$, <i>hsdR514</i>	Baba <i>et al.</i> , 2006; Datsenko <i>et al.</i> 2000 [141, 191]
<i>E. coli</i>	$\Delta dppA-\Delta sapA$	F-, $\Delta(araD-araB)567$, $\Delta lacZ4787(::rrnB-3)$, λ -, $\Delta dppA728::kan$, $\Delta sapA::cm$, <i>rph-1</i> , $\Delta(rhaD-rhaB)568$, <i>hsdR514</i>	Melanie Dostert, Brötz-Oesterhelt lab
<i>E. coli</i>	$\Delta dppA-\Delta sapA$ -del.	F-, $\Delta(araD-araB)567$, $\Delta lacZ4787(::rrnB-3)$, λ -, $\Delta dppA728$, $\Delta sapA$, <i>rph-1</i> , $\Delta(rhaD-rhaB)568$, <i>hsdR514</i>	Melanie Dostert, Brötz-Oesterhelt lab

Table 20: Bacterial strains (continued)

Species	Strain	Genotype and comments	Reference
<i>E. coli</i>	$\Delta dppA\text{-}\Delta oppA$	F-, $\Delta(\text{araD-araB})567$, $\Delta lacZ4787(::rrnB\text{-}3)$, $\&\lambda$ -, $\Delta dppA728::kan$, $\Delta oppA::cm$, <i>rph-1</i> , $\Delta(\text{rhaD-rhaB})568$, <i>hsdR514</i>	this work
<i>E. coli</i>	$\Delta dppA\text{-}\Delta oppA\text{-}del.$	F-, $\Delta(\text{araD-araB})567$, $\Delta lacZ4787(::rrnB\text{-}3)$, $\&\lambda$ -, $\Delta dppA728$, $\Delta oppA$, <i>rph-1</i> , $\Delta(\text{rhaD-rhaB})568$, <i>hsdR514</i>	this work
<i>E. coli</i>	$\Delta dppA\text{-}\Delta sapA\text{-}\Delta oppA$	F-, $\Delta(\text{araD-araB})567$, $\Delta lacZ4787(::rrnB\text{-}3)$, $\&\lambda$ -, $\Delta dppA728$, $\Delta sapA$, $\Delta oppA::cm$, <i>rph-1</i> , $\Delta(\text{rhaD-rhaB})568$, <i>hsdR514</i>	this work
<i>E. coli</i>	$\Delta dppA\text{-}\Delta sapA\text{-}\Delta oppA\text{-}del.$	F-, $\Delta(\text{araD-araB})567$, $\Delta lacZ4787(::rrnB\text{-}3)$, $\&\lambda$ -, $\Delta dppA728$, $\Delta sapA$, $\Delta oppA$, <i>rph-1</i> , $\Delta(\text{rhaD-rhaB})568$, <i>hsdR514</i>	this work
<i>E. coli</i>	JW0699 ($\Delta ybgH$)	F-, $\Delta(\text{araD-araB})567$, $\Delta lacZ4787(::rrnB\text{-}3)$, λ -, $\Delta ybgH759::kan$, <i>rph-1</i> , $\Delta(\text{rhaD-rhaB})568$, <i>hsdR514</i>	Baba <i>et al.</i> , 2006; Datsenko <i>et al.</i> 2000 [141, 191]
<i>E. coli</i>	JW5240 ($\Delta ddpA$)	F-, $\Delta(\text{araD-araB})567$, $\Delta lacZ4787(::rrnB\text{-}3)$, λ -, $\Delta ddpA780::kan$, <i>rph-1</i> , $\Delta(\text{rhaD-rhaB})568$, <i>hsdR514</i>	Baba <i>et al.</i> , 2006; Datsenko <i>et al.</i> 2000 [141, 191]
<i>E. coli</i>	JW1480 ($\Delta ddpC$)	F-, $\Delta(\text{araD-araB})567$, $\Delta lacZ4787(::rrnB\text{-}3)$, λ -, $\Delta ddpC778::kan$, <i>rph-1</i> , $\Delta(\text{rhaD-rhaB})568$, <i>hsdR514</i>	Baba <i>et al.</i> , 2006; Datsenko <i>et al.</i> 2000 [141, 191]
<i>E. coli</i>	JW4091 ($\Delta yjdL$)	F-, $\Delta(\text{araD-araB})567$, $\Delta lacZ4787(::rrnB\text{-}3)$, λ -, $\Delta yjdL757::kan$, <i>rph-1</i> , $\Delta(\text{rhaD-rhaB})568$, <i>hsdR514</i>	Baba <i>et al.</i> , 2006; Datsenko <i>et al.</i> 2000 [141, 191]
<i>E. coli</i>	JW3463 ($\Delta yhiP$)	F-, $\Delta(\text{araD-araB})567$, $\Delta lacZ4787(::rrnB\text{-}3)$, λ -, $\Delta yhiP752::kan$, <i>rph-1</i> , $\Delta(\text{rhaD-rhaB})568$, <i>hsdR514</i>	Baba <i>et al.</i> , 2006; Datsenko <i>et al.</i> 2000 [141, 191]
<i>E. coli</i>	JW1322 ($\Delta mppA$)	F-, $\Delta(\text{araD-araB})567$, $\Delta lacZ4787(::rrnB\text{-}3)$, λ -, $\Delta mppA767::kan$, <i>rph-1</i> , $\Delta(\text{rhaD-rhaB})568$, <i>hsdR514</i>	Baba <i>et al.</i> , 2006; Datsenko <i>et al.</i> 2000 [141, 191]
<i>E. coli</i>	JW2988 ($\Delta ygiS$)	F-, $\Delta(\text{araD-araB})567$, $\Delta lacZ4787(::rrnB\text{-}3)$, λ -, $\Delta ygiS790::kan$, <i>rph-1</i> , $\Delta(\text{rhaD-rhaB})568$, <i>hsdR514</i>	Baba <i>et al.</i> , 2006; Datsenko <i>et al.</i> 2000 [141, 191]
<i>E. coli</i>	JW2800 ($\Delta ygdQ$)	F-, $\Delta(\text{araD-araB})567$, $\Delta lacZ4787(::rrnB\text{-}3)$, λ -, $\Delta ygdQ757::kan$, <i>rph-1</i> , $\Delta(\text{rhaD-rhaB})568$, <i>hsdR514</i>	Baba <i>et al.</i> , 2006; Datsenko <i>et al.</i> 2000 [141, 191]

Table 20: Bacterial strains (continued)

Species	Strain	Genotype and comments	Reference
<i>E. coli</i>	JW2304 ($\Delta hisM$)	F-, $\Delta(araD-araB)567$, $\Delta lacZ4787(::rrnB-3)$, λ -, $\Delta hisM779::kan$, <i>rph-1</i> , $\Delta(rhaD-rhaB)568$, <i>hsdR514</i>	Baba <i>et al.</i> , 2006; Datsenko <i>et al.</i> 2000 [141, 191]
<i>E. coli</i>	JW2303 ($\Delta hisP$)	F-, $\Delta(araD-araB)567$, $\Delta lacZ4787(::rrnB-3)$, λ -, $\Delta hisP778::kan$, <i>rph-1</i> , $\Delta(rhaD-rhaB)568$, <i>hsdR514</i>	Baba <i>et al.</i> , 2006; Datsenko <i>et al.</i> 2000 [141, 191]
<i>E. coli</i>	JW2305 ($\Delta hisQ$)	F-, $\Delta(araD-araB)567$, $\Delta lacZ4787(::rrnB-3)$, λ -, $\Delta hisQ780::kan$, <i>rph-1</i> , $\Delta(rhaD-rhaB)568$, <i>hsdR514</i>	Baba <i>et al.</i> , 2006; Datsenko <i>et al.</i> 2000 [141, 191]
<i>E. coli</i>	JW2306 ($\Delta hisJ$)	F-, $\Delta(araD-araB)567$, $\Delta lacZ4787(::rrnB-3)$, λ -, $\Delta hisJ730::kan$, <i>rph-1</i> , $\Delta(rhaD-rhaB)568$, <i>hsdR514</i>	Baba <i>et al.</i> , 2006; Datsenko <i>et al.</i> 2000 [141, 191]
<i>E. coli</i>	JW2307 ($\Delta argT$)	F-, $\Delta(araD-araB)567$, $\Delta lacZ4787(::rrnB-3)$, λ -, $\Delta argT721::kan$, <i>rph-1</i> , $\Delta(rhaD-rhaB)568$, <i>hsdR514</i>	Baba <i>et al.</i> , 2006; Datsenko <i>et al.</i> 2000 [141, 191]
<i>E. coli</i>	JW2143 ($\Delta lysP$)	F-, $\Delta(araD-araB)567$, $\Delta lacZ4787(::rrnB-3)$, λ -, $\Delta lysP783::kan$, <i>rph-1</i> , $\Delta(rhaD-rhaB)568$, <i>hsdR514</i>	Baba <i>et al.</i> , 2006; Datsenko <i>et al.</i> 2000 [141, 191]
<i>E. coli</i>	JW4093($\Delta cadB$)	F-, $\Delta(araD-araB)567$, $\Delta lacZ4787(::rrnB-3)$, λ -, <i>rph-1</i> , $\Delta(rhaD-rhaB)568$, $\Delta cadB759::kan$, <i>hsdR514</i>	Baba <i>et al.</i> , 2006; Datsenko <i>et al.</i> 2000 [141, 191]
<i>E. coli</i>	JW3600 ($\Delta rfaY$)	F-, $\Delta(araD-araB)567$, $\Delta lacZ4787(::rrnB-3)$, λ -, $\Delta rfaY736::kan$, <i>rph-1</i> , $\Delta(rhaD-rhaB)568$, <i>hsdR514</i>	Baba <i>et al.</i> , 2006; Datsenko <i>et al.</i> 2000 [141, 191]
<i>E. coli</i>	JW3605 ($\Delta rfaP$)	F-, $\Delta(araD-araB)567$, $\Delta lacZ4787(::rrnB-3)$, λ -, $\Delta rfaP741::kan$, <i>rph-1</i> , $\Delta(rhaD-rhaB)568$, <i>hsdR514</i>	Baba <i>et al.</i> , 2006; Datsenko <i>et al.</i> 2000 [141, 191]
<i>E. coli</i>	JW3606 ($\Delta rfaG$)	F-, $\Delta(araD-araB)567$, $\Delta lacZ4787(::rrnB-3)$, λ -, $\Delta rfaG742::kan$, <i>rph-1</i> , $\Delta(rhaD-rhaB)568$, <i>hsdR514</i>	Baba <i>et al.</i> , 2006; Datsenko <i>et al.</i> 2000 [141, 191]
<i>E. coli</i>	JW1371($\Delta ompN$)	F-, $\Delta(araD-araB)567$, $\Delta lacZ4787(::rrnB-3)$, λ -, $\Delta ompN740::kan$, <i>rph-1</i> , $\Delta(rhaD-rhaB)568$, <i>hsdR514</i>	Baba <i>et al.</i> , 2006; Datsenko <i>et al.</i> 2000 [141, 191]
<i>E. coli</i>	JW0231 ($\Delta phoE$)	F-, $\Delta(araD-araB)567$, $\Delta lacZ4787(::rrnB-3)$, λ -, $\Delta phoE759::kan$, <i>rph-1</i> , $\Delta(rhaD-rhaB)568$, <i>hsdR514</i>	Baba <i>et al.</i> , 2006; Datsenko <i>et al.</i> 2000 [141, 191]

Table 20: Bacterial strains (continued)

Species	Strain	Genotype and comments	Reference
<i>E. coli</i>	JW0667 (Δ ybfM)	F-, Δ (araD-araB)567, Δ lacZ4787(::rrnB-3), λ -, Δ ybfM729::kan, rph-1, Δ (rhaD-rhaB)568, hsdR514	Baba <i>et al.</i> , 2006; Datsenko <i>et al.</i> 2000 [141, 191]
<i>E. coli</i>	JW0940 (Δ ompA)	F-, Δ (araD-araB)567, Δ lacZ4787(::rrnB-3), λ -, Δ ompA772::kan, rph-1, Δ (rhaD-rhaB)568, hsdR514	Baba <i>et al.</i> , 2006; Datsenko <i>et al.</i> 2000 [141, 191]
<i>E. coli</i>	JW0912 (Δ ompF)	F-, Δ (araD-araB)567, Δ lacZ4787(::rrnB-3), λ -, Δ ompF746::kan, rph-1, Δ (rhaD-rhaB)568, hsdR514	Baba <i>et al.</i> , 2006; Datsenko <i>et al.</i> 2000 [141, 191]
<i>E. coli</i>	JW1312 (Δ ompG)	F-, Δ (araD-araB)567, Δ lacZ4787(::rrnB-3), λ -, Δ ompG756::kan, rph-1, Δ (rhaD-rhaB)568, hsdR514	Baba <i>et al.</i> , 2006; Datsenko <i>et al.</i> 2000 [141, 191]
<i>E. coli</i>	JW2203 (Δ ompC)	F-, Δ (araD-araB)567, Δ lacZ4787(::rrnB-3), λ -, Δ ompC768::kan, rph-1, Δ (rhaD-rhaB)568, hsdR514	Baba <i>et al.</i> , 2006; Datsenko <i>et al.</i> 2000 [141, 191]
<i>E. coli</i>	JW3846 (Δ ompL)	F-, Δ (araD-araB)567, Δ lacZ4787(::rrnB-3), λ -, Δ ompL737::kan, rph-1, Δ (rhaD-rhaB)568, hsdR514	Baba <i>et al.</i> , 2006; Datsenko <i>et al.</i> 2000 [141, 191]
<i>E. coli</i>	JW0452 (Δ acrA)	F-, Δ (araD-araB)567, Δ lacZ4787(::rrnB-3), Δ acrA748::kan, λ -, rph-1, Δ (rhaD-rhaB)568, hsdR514	Baba <i>et al.</i> , 2006; Datsenko <i>et al.</i> 2000 [141, 191]
<i>E. coli</i>	JW0451 (Δ acrB)	F-, Δ (araD-araB)567, Δ lacZ4787(::rrnB-3), Δ acrB747::kan, λ -, rph-1, Δ (rhaD-rhaB)568, hsdR514	Baba <i>et al.</i> , 2006; Datsenko <i>et al.</i> 2000 [141, 191]
<i>E. coli</i>	JW5503 (Δ tolC)	F-, λ -, Δ (araD-araB)567, Δ lacZ4787(::rrnB-3), Δ tolC732::kan, rph-1, Δ (rhaD-rhaB)568, hsdR514	Baba <i>et al.</i> , 2006; Datsenko <i>et al.</i> 2000 [141, 191]
<i>E. faecalis</i>	ATCC29212		Kim <i>et al.</i> , 2012 [197]
<i>P. aeruginosa</i>	PAOI		Holloway, 1955 [198]
<i>A. baumannii</i>	09987	clinical isolate	university hospital Bonn
<i>S. aureus</i>	ATCC29213		CLSI, 2006 [193]

Table 20: Bacterial strains (continued)

Species	Strain	Genotype and comments	Reference
<i>S. aureus</i>	ATCC13709		Rogers <i>et al.</i> , 1960 [199]
<i>S. aureus</i>	WT		Hiron <i>et al.</i> , 2007 [164]
<i>S. aureus</i>	$\Delta opp1$	oligopeptide transport system 1, organized in one operon <i>oppABCDF</i>	Hiron <i>et al.</i> , 2007 [164]
<i>S. aureus</i>	$\Delta opp2$	oligopeptide transport system 2, organized in one operon <i>oppABCDF</i>	Hiron <i>et al.</i> , 2007 [164]
<i>S. aureus</i>	$\Delta opp3$	oligopeptide transport system 3, organized in one operon <i>oppABCDF</i>	Hiron <i>et al.</i> , 2007 [164]
<i>S. aureus</i>	$\Delta opp4$	oligopeptide transport system 4, organized in one operon <i>oppABCDF</i>	Hiron <i>et al.</i> , 2007 [164]
<i>S. aureus</i>	$\Delta dtpT$	proton-driven di- and tripeptide permease	Hiron <i>et al.</i> , 2007 [164]
<i>S. aureus</i>	$\Delta opp1234$	knock-out of all four oligopeptide transport systems	Hiron <i>et al.</i> , 2007 [164]
<i>S. aureus</i>	$\Delta dtpT-opp1234$	knock-out of all four oligopeptide transport systems and the proton-driven di- and tripeptide permease	Hiron <i>et al.</i> , 2007 [164]
<i>S. aureus</i>	133		DSM strain collection, Braunschweig, Germany (number DSM 11832)

Table 21: isolated negamycin resistant *E. coli* strains

Species	Strain	Comment	Reference
<i>E. coli</i>	M9-1	low-level negamycin resistance in M9	this work
<i>E. coli</i>	M9-2	low-level negamycin resistance in M9	this work
<i>E. coli</i>	M9-3	low-level negamycin resistance in M9	this work
<i>E. coli</i>	M9-4	low-level negamycin resistance in M9	this work
<i>E. coli</i>	M9-5	low-level negamycin resistance in M9	this work
<i>E. coli</i>	M9-6	low-level negamycin resistance in M9	this work

Table 21: isolated negamycin resistant *E. coli* strains (continued)

Species	Strain	Comment	Reference
<i>E. coli</i>	M9-7	low-level negamycin resistance in M9	this work
<i>E. coli</i>	M9-8	low-level negamycin resistance in M9	this work
<i>E. coli</i>	M9-9	low-level negamycin resistance in M9	this work
<i>E. coli</i>	M9-10	low-level negamycin resistance in M9	this work
<i>E. coli</i>	PP-1	low-level negamycin resistance in PP	this work
<i>E. coli</i>	PP-2	low-level negamycin resistance in PP	this work
<i>E. coli</i>	PP-3	no change in negamycin resistance in PP	this work
<i>E. coli</i>	PP-4	low-level negamycin resistance in PP	this work
<i>E. coli</i>	PP-5	no change in negamycin resistance in PP	this work
<i>E. coli</i>	PP-6	low-level negamycin resistance in PP	this work
<i>E. coli</i>	PP-7	low-level negamycin resistance in PP	this work
<i>E. coli</i>	PP-8	low-level negamycin resistance in PP	this work

5.1.7 Synthetic Oligonucleotides

Table 22: Primer

Name	Sequence (5'-3')	Application	Expected PCR product size
<i>dppA fwd del</i>	TGGAGGATCCGCACTGTTAC	Control of Kan-resistance cassette deletion	JW3513: 1800 bp JW3513-del: 500 bp
<i>dppA rev del</i>	GCCACCGGTATAACAGATTG	Control of Kan-resistance cassette deletion	JW3513: 1800 bp JW3513-del: 500 bp
<i>dppA-F</i> -5	CGACGATTCGTCAGCCAGAG	primer for sequencing of the Dpp-operon	
<i>dppA-F</i> -4	CGTCTGGAAAGGCATTTCTG	primer for sequencing of the Dpp-operon	

Table 22: Primer (continued)

Name	Sequence (5'-3')	Application	Expected PCR product size
<i>dppA-F</i> -2	TGACAACCTCGGTGACCTATG	primer for sequencing of the Dpp-operon	
<i>dppA-F</i> -1	GATTGACGAGGGCGTATCTG	primer for sequencing of the Dpp-operon	
<i>dppA-F</i> 0	CCGCCTTATTCGACCTACAC	primer for sequencing of the Dpp-operon	
<i>dppA-F</i> 1	CTCACCGTTGGTGAAATCC	primer for sequencing of the Dpp-operon	
<i>dppA-F</i> 2	AAGGCATGGGCTTCCAGAG	primer for sequencing of the Dpp-operon	
<i>dppA-F</i> 3	GCTGAAAGAAGCGGGTCTGG	primer for sequencing of the Dpp-operon	
<i>dppA-F</i> 4	CCATCCGGCAGCAATACTTC	primer for sequencing of the Dpp-operon	
<i>dppA-F</i> 5	CCGTCGCCATATGATCTTG	primer for sequencing of the Dpp-operon	
<i>dppA-F</i> 6	ATGTGCTGTCGCGCTGATG	primer for sequencing of the Dpp-operon	
<i>dppA-F</i> 7	GCATTTGGCGACGAAAGCG	primer for sequencing of the Dpp-operon	
<i>dppA-F</i> 8	CGCGTCACCCGTATACTCAG	primer for sequencing of the Dpp-operon	
<i>dppA-F</i> 9	CGAGCACTATGACCGCTATC	primer for sequencing of the Dpp-operon	
<i>dppA-F</i> PP4 pw2	TTTGCCGACAGGCAATCGC	primer for sequencing of the Dpp-operon in PP-4	
<i>dppA-F</i> PP4 pw3	GTACCTCAAGCGTGCGAAAG	primer for sequencing of the Dpp-operon in PP-4	
<i>dppA-F</i> PP4 pw 4 rev	GGCAAGGCAACGAAGGTCAG	primer for sequencing of the Dpp-operon in PP-4	
<i>dppA-F</i> PP4 pw5	TTGAGTCATCGAGGAACAC	primer for sequencing of the Dpp-operon in PP-4	

Table 22: Primer (continued)

Name	Sequence (5'-3')	Application	Expected PCR product size
<i>dppA-F rev</i>	ATTGTGTCGTGCCTCATTCC	primer for sequencing of the Dpp-operon	
<i>dppA-F rev pw1</i>	CCTGCTGCAAATCCATCATC	primer for sequencing of the Dpp-operon	
<i>dppA-F rev1</i>	GCGGATAAAGTACTGGCAAC	primer for sequencing of the Dpp-operon	
<i>dppA-F rev2</i>	GCAGCGATCATTGCTTATCC	primer for sequencing of the Dpp-operon	
<i>dppA-F rev3</i>	TGCCGTTTACACGCTACGAC	primer for sequencing of the Dpp-operon	
<i>dppA-F rev4</i>	TGGTGTGTCAGGTGCATAC	primer for sequencing of the Dpp-operon	
<i>dppOgap1</i>	CTGCGTAAAGGTGTGAAGTG	primer for sequencing of the Dpp-operon	
<i>dppOgap2</i>	CTGATCCCGCCAACCATGTG	primer for sequencing of the Dpp-operon	
<i>dppOgap3</i>	TGATGCGCTCCGCTTATCAG	primer for sequencing of the Dpp-operon	
<i>dppOgap4</i>	TGACGCGCTCGATCCCAAAC	primer for sequencing of the Dpp-operon	
<i>dppA-XbaI_for</i>	TTGGTCTAGATTGGAGCAGAAT AATGCGTA	primer for <i>dppA</i> complementation	1682 bp
<i>dppA-XhoI_rev</i>	TTGCCTCGAGTTGCCTTTGCCA TCAGTCTT	primer for <i>dppA</i> complementation	1682 bp
<i>etpB rev</i>	GGTCACCGAGTTGTCATAGG	primer for sequencing of the Dpp-operon/upstream gene	
<i>gapDH fwd</i>	ACTTACGAGCAGATCAAAGC	primer for qPCR-amplification of <i>gapDH</i> (reference gene)	BW25113: 170 bp
<i>gapDH rev</i>	AGTTTCACGAAGTTGTCGTT	primer for qPCR-amplification of <i>gapDH</i> (reference gene)	BW25113: 170 bp

Table 22: Primer (continued)

Name	Sequence (5'-3')	Application	Expected PCR product size
<i>oppA</i>- fwd	CAGAAAGTCTCCGAGCCTGTG	Amplification of the Cm-resistance-cassette in <i>oppA</i>	BW25113: 1851 bp JW3513- <i>oppA</i> : 1370 bp
<i>oppA</i>-rev	GTCGGAATCGCTTCCAGACAG	Amplification of the Cm-resistance-cassette in <i>oppA</i>	BW25113: 1851 bp JW3513- <i>oppA</i> :1370 bp
<i>oppA1</i>-H1-P1	H1 AGAGAAGTTTAGTAGCAGCTG GCGTTCTGGCTGCGCTAATGGT <u>GTAGGCTGGAGCTGCTTC</u> P1	Primer for <i>oppA</i> -knockout, amplification of Cm-resistance cassette; Primer is homolog to P1 of the resistance cassette and homolog to <i>oppA</i> (H1)	1094 bp
<i>oppA2</i>-H2-P2	H2 CCGGGTATAGGTATTATCCAGC GGATCTTTGCCGTATAGCCAT <u>ATGAATATCCTCCTTAG</u> P2	Primer for <i>oppA</i> -knockout, amplification of Cm-resistance cassette; Primer is homolog to P2 of the resistance cassette and homolog to <i>oppA</i> (H2)	1094 bp
<i>qargT</i> rev	CTAGCCAGGTCTCGTTAGC	primer for qPCR-amplification of <i>argT</i>	BW25113: 358bp
<i>qargT</i> fwd	CCTACGCACCGTTCTCATCG	primer for qPCR-amplification of <i>argT</i>	BW25113: 358bp
<i>qcadB</i> rev	AGTGGTTAAACGGCTTACCC	primer for qPCR-amplification of <i>cadB</i>	BW25113: 291bp
<i>qcadB</i> fwd	TCGCTGGCGTATGTATATGC	primer for qPCR-amplification of <i>cadB</i>	BW25113: 291 bp
<i>qdppA</i> fwd	TCCATCTGCGTAAAGGTGTG	primer for qPCR-amplification of <i>dppA</i>	BW25113: 276 bp
<i>qdppA</i> rev	ATAGAGGCGAAGTCCATTGC	primer for qPCR-amplification of <i>dppA</i>	BW25113: 276 bp
<i>qdppB</i> fwd	TGCCTTTGTCCACATGATCC	primer for qPCR-amplification of <i>dppB</i>	BW25113: 373 bp

Table 22: Primer (continued)

Name	Sequence (5'-3')	Application	Expected PCR product size
<i>qdppB rev</i>	CCACCAGAAGATAGGCATTG	primer for qPCR-amplification of <i>dppB</i>	BW25113: 373 bp
<i>qdppC fwd</i>	CCTATAACCCGGCGGAACAG	primer for qPCR-amplification of <i>dppC</i>	BW25113: 230 bp
<i>qdppC rev</i>	GACCAGGCCGCCAAAGTAAC	primer for qPCR-amplification of <i>dppC</i>	BW25113: 230 bp
<i>qdppD fwd</i>	CGCTCGATCCCAAAGTGAAG	primer for qPCR-amplification of <i>dppD</i>	BW25113: 219 bp
<i>qdppD rev</i>	GCCCGGATAATCAATCAGCC	primer for qPCR-amplification of <i>dppD</i>	BW25113: 219 bp
<i>qdppF fwd</i>	GCCGGAACGTCTGGTTAAAG	primer for qPCR-amplification of <i>dppF</i>	BW25113: 253 bp
<i>qdppF rev</i>	CGGATTCAGCGAACCGTAAG	primer for qPCR-amplification of <i>dppF</i>	BW25113: 253 bp
<i>qhisJ rev</i>	TTTCGCCACCACCAAACGAG	primer for qPCR-amplification of <i>hisJ</i>	BW25113: 307 bp
<i>qhisJ fwd</i>	TGCGGCGTTTGCTGCGATTC	primer for qPCR-amplification of <i>hisJ</i>	BW25113: 307 bp
<i>qhisM fwd</i>	GCTGTTTCTGGCGATTGGTC	primer for qPCR-amplification of <i>hisM</i>	BW25113: 373 bp
<i>qhisM rev</i>	GTTGCTGTATGCCGGTAACG	primer for qPCR-amplification of <i>hisM</i>	BW25113: 373 bp
<i>qhisP fwd</i>	TGCGCTGCATTAATTCTC	primer for qPCR-amplification of <i>hisP</i>	BW25113: 344 bp
<i>qhisP rev</i>	AGAAACACGCTGTTGCTGAC	primer for qPCR-amplification of <i>hisP</i>	BW25113: 344 bp
<i>qhisQ fwd</i>	CTGTAGTGCTCGCTGTAATC	primer for qPCR-amplification of <i>hisQ</i>	BW25113: 312 bp
<i>qhisQ rev</i>	CCGCCTCTATATGTCCTTTC	primer for qPCR-amplification of <i>hisQ</i>	BW25113: 312 bp
<i>qlysP rev</i>	TTCGCCGGATCTTCGGACTC	primer for qPCR-amplification of <i>lysP</i>	BW25113: 344 bp
<i>qlysP fwd</i>	AGCTGGTGGTCCCGGATAC	primer for qPCR-amplification of <i>lysP</i>	BW25113: 344 bp
<i>qoppA fwd</i>	CGCTAATGGCAGGGAATGTC	primer for qPCR-amplification of <i>oppA</i>	BW25113: 359 bp

Table 22: Primer (continued)

Name	Sequence (5'-3')	Application	Expected PCR product size
<i>qoppA rev</i>	TGGCATACGGAGAAGCAGTG	primer for qPCR-amplification of <i>oppA</i>	BW25113: 359 bp
<i>qsapA fwd</i>	CCGGAACCTTGCCGAAAGCTG	primer for qPCR-amplification of <i>sapA</i>	BW25113: 189 bp
<i>qsapA rev</i>	GCTGCCGTTGACGTTATGCC	primer for qPCR-amplification of <i>sapA</i>	BW25113: 189 bp
<i>qsapD fwd</i>	CGGTGATGAGTGGGTTAAAG	primer for qPCR-amplification of <i>sapD</i>	BW25113: 279 bp
<i>qsapD rev</i>	ACACGTTCTGAAGGGTCAAG	primer for qPCR-amplification of <i>sapD</i>	BW25113: 279 bp
<i>qtppB fwd</i>	ACAACCGAAGGCGTTCTATC	primer for qPCR-amplification of <i>tppB</i>	BW25113: 335 bp
<i>qtppB rev</i>	TTAAACAGGCCGTTACCGAC	primer for qPCR-amplification of <i>tppB</i>	BW25113: 335 bp
<i>qygdQ rev</i>	GATAGCGCCGAGGAATGATG	primer for qPCR-amplification of <i>ygdQ</i>	BW25113: 330 bp
<i>qygdQ fwd</i>	CTGCTGGAGATCGTTCTTGG	primer for qPCR-amplification of <i>ygdQ</i>	BW25113: 330 bp
<i>sapA fwd</i>	AACCACACGGCCCTCATTAC	Amplification of the Cm-resistance-cassette in <i>sapA</i> ; Control of Cm-resistance cassette deletion	BW25113: 1813 bp JW3513- <i>sapA</i> : 1370 bp JW3513- <i>sapA</i> del.: 500 bp
<i>sapA rev</i>	CTGAAGCCAACGAAGGTCAG	Amplification of the Cm-resistance-cassette in <i>sapA</i> ; Control of Cm-resistance cassette deletion	BW25113: 1813 bp JW3513- <i>sapA</i> : 1370 bp JW3513- <i>sapA</i> del.: 500 bp

Table 22: Primer (continued)

Name	Sequence (5'-3')	Application	Expected PCR product size
<i>sapA</i>-H2-P2	H2 CCAGCAAAGGAGGCGTTACCA AACGGGCTAAGTACCAGACCA <u>TATGAATATCCTCCTTAG</u> P2	Primer for <i>sapA</i> -knockout, amplification of Cm-resistance cassette; Primer is homolog to P2 of the resistance cassette and homolog to <i>sapA</i> (H2)	1094 bp
<i>sapA</i>-H1-P1	H1 TGAATCTCCCCGCATGCTGAT ATCCGCGACAGCGTTTTGGTG <u>TAGGCTGGAGCTGCTTC</u> P1	Primer for <i>sapA</i> -knockout, amplification of Cm-resistance cassette; Primer is homolog to P1 of the resistance cassette and homolog to <i>sapA</i> (H1)	1094 bp
<i>yhjV</i> fwd	ATGCCGTACAGCAGAATCAG	primer for sequencing of the Dpp-operon/downstream gene	

5.1.8 Plasmids

Table 23: Plasmids

Vectors	Resistance marker	Description	Reference
pASK-<i>dppA</i>	Amp ^R	plasmid pASK- <i>dppA</i> for the complementation of DppA	<i>this work</i> , Dr. Anne Berscheid
pASK-IBA 5 plus	Amp ^R	empty vector control	IBA GmbH
pBestluc-mut	Amp ^R	pBESTluc-mut harbors a mutation in the luciferase gene leading to a Stop codon at amino acid position 31 in the protein (K31STOP)	Dr. Anne Berscheid, Brötz-Oesterhelt lab
pBESTluc	Amp ^R	contains the firefly luciferase gene under the control of the <i>Escherichia coli</i> tac promoter	Promega
pCP 20	Amp ^R Cm ^R	contains yeast Flp recombinase gene, temperature sensitive replication.	Datsenko <i>et al.</i> , 2000 [141]
pET14b-luc	Amp ^R	firefly (<i>Photinus pyralis</i>) luciferase gene under control of T7 promoter in the pET14b vector	Dr. Anne Berscheid, Brötz-Oesterhelt lab

Table 23: Plasmids (continued)

Vectors	Resistance marker	Description	Reference
pKD 3	Cm ^R	template plasmid for <i>frt</i> -flanked <i>cat</i> cassette. FRT sites create an identical scar that has stop codons in all six reading frames. The scar has an idealized ribosome binding site and start codon for downstream (rightward) gene expression	Datsenko <i>et al.</i> , 2000 [141]
pKD 46	Amp ^R	temperature sensitive promoter (<i>repA101ts</i>); encodes λ red genes (<i>exo</i> , <i>bet</i> , <i>gam</i>); native terminator (tL3) after <i>exo</i> gene; arabinose-inducible promoter for expression (P_{araB}); encodes <i>araC</i> for repression of P_{araB} promoter	Datsenko <i>et al.</i> , 2000 [141]
pS107	Ery ^R	<i>ypuA</i> promoter-sequence upstream of firefly luciferase-gene original plasmid: pHT304	Piggot, 1973; Urban <i>et al.</i> , 2007 [140, 189]
pS130	Ery ^R	<i>yvqI</i> promoter-sequence upstream of firefly luciferase-gene original plasmid: pHT304	Piggot, 1973 [189]
pS63	Ery ^R	<i>yvgS</i> promoter-sequence upstream of firefly luciferase-gene original plasmid: pHT304	Piggot, 1973; Urban <i>et al.</i> , 2007 [140, 189]
pS72	Ery ^R	<i>yheI</i> promoter-sequence upstream of firefly luciferase-gene original plasmid: pHT304	Piggot, 1973; Urban <i>et al.</i> , 2007 [140, 189]
pS77	Ery ^R	<i>yorB</i> promoter-sequence upstream of firefly luciferase-gene original plasmid: pHT304	Piggot, 1973; Urban <i>et al.</i> , 2007 [140, 189]

5.1.9 Media

Belitzky minimal-medium

Table 24: Belitzky stock medium

Ingredients	g/l
0.015 M (NH ₄) ₂ SO ₄	2
0.008 M MgSO ₄ x 7H ₂ O	2
0.027 M KCl	2
0.007 M Na ₃ citrat x 2H ₂ O	2
0.05 M Tris	6.06

pH was adjusted to 7.5 using 5 M HCl and with dH₂O added up to 1 liter. Stock-medium was sterilized using sterile filtration. To 100 ml stock medium the following supplements were added:

Table 25: Belitzky-Supplements

Supplements	Conc.	Form of sterilization	Volume
0.2 M KH₂PO₄	1.35g / 50ml	autoclaved	0.3 ml
1 M CaCl₂ x 2H₂O	7.35g / 50ml	autoclaved	0.2 ml
0.5 M FeSO₄ x 7H₂O	6.95mg / 50ml	sterile filtration	0.2 ml
0.025 M MnSO₄ x H₂O	0.211g / 50ml	sterile filtration	0.04 ml
0.5 M Glutamic acid	7.36g / 100ml	sterile filtration	0.9 ml
0.039 M L-Tryptophan	8mg / ml	sterile filtration	2 ml
20% Glucose	20g / 100ml	sterile filtration	1 ml

CYG

Table 26: CYG growth medium

Ingredients	g/l
Glucose	5.0
Yeast extract	5.0
Casein hydrolysate	5.0

Medium was autoclaved for 20 minutes at 121°C.

E. coli MRE600 growth medium

Table 27: MRE600 growth medium

Ingredients	g/l
Bacto Tryptone	9
Yeast extract	0.8
NaCl	5.6
1 N NaOH	1 ml/l

The medium was autoclaved and 20% sterile glucose (sterile filtration) was added (4 ml/l).

Lysogeny Broth

Table 28: Lysogeny Broth (LB)

Ingredients	g/l
NaCl	5
Tryptone	10
Yeast extract	5
if required Agar	15

LB medium was autoclaved for 20 minutes at 121°C and a pressure of 2 bar. If required the medium was cooled down to 50°C after sterilization and supplemented with antibiotics for selection.

Mueller Hinton Broth

Table 29: Mueller Hinton Broth

Ingredients	g/l
Beef infusion solids	2
Casein hydrolysate	17.5
starch	1.5
if required Agar	15

21 g of medium were dissolved in distilled water and autoclaved for 20 minutes at 121°C. If required the medium was cooled down to 50°C after sterilization and supplemented with antibiotics for selection.

M9-broth

Table 30: M9-broth

Ingredients	g/l	Final concentration
M9 salts		
Na₂HPO₄ x 2 H₂O	19.0997	28.5 mM
KH₂PO₄	15	22.04 mM

Table 30: M9-broth (continued)

Ingredients	g/l	Final concentration
M9 salts		
NaCl	2.5	8.556 mM
NH₄Cl	5	18.7 mM
MgSO₄	0.4814	2 mM
Glucose	4.0	0.4%
CaCl₂	11.098	100 μ M

The components of M9-salts were mixed and stirred in distilled H₂O until they were dissolved. The volume was adjusted to 1000 ml and sterilized by autoclaving for 20 minutes at 121°C. 200 ml of autoclaved M9 salts, 2 ml of MgSO₄ (sterile), 20 ml of 20% glucose (sterile), 100 μ l of 1M CaCl₂ (sterile) were added and adjusted to 1000 ml with distilled H₂O.

M9-Agar:

1.5% agar for final volume in distilled water (amount needed for final volume) was prepared and autoclaved. The agar was equilibrated to 45-50°C then the other components of M9 (pre warmed to 45°C in waterbath) were added.

Nutrient broth

Table 31: Nutrient broth growth medium

Ingredients	g/l
Meat extract	3.0
Peptone	5.0

The components of the medium were dissolved in distilled water and autoclaved for 20 minutes at 121°C.

Peptone (meat)**Table 32: peptone meat**

Ingredients	g/l
peptone meat	5

5 g of medium were dissolved in distilled water. Medium was autoclaved for 20 minutes at 121°C.

Peptone water (monopeptone)**Table 33: Peptone water growth medium**

Ingredients	g/l
Peptone	10.0
NaCl	5.0

Medium was autoclaved for 20 minutes at 121°C.

PP**Table 34: PP**

Ingredients	g/l
polypeptone	5

5 g of medium were dissolved in distilled water. If required salts were added or pH was adjusted to 7, 8.5 or 5 and medium was autoclaved for 20 minutes at 121°C. If required the medium was cooled down to 50°C after sterilization and supplemented with antibiotics for selection.

5.1.10 Solutions and Buffers**KPO₄ Buffer****Table 35: KPO₄ buffer**

Ingredients	
KPO ₄	50 mM

pH was adjusted to 7 and after filter sterilization the buffer was stored at 4°C.

TE Buffer

Table 36: TE Buffer

Ingredients	
Tris Base	10 mM
EDTA	1 mM

The components were dissolved in distilled H₂O and pH was adjusted to 8 with 1 M HCl. Distilled H₂O was added to 1000 ml.

10x PBS-Buffer

Table 37: 10x PBS

Ingredients	g/l
NaCl	80
KCl	2
Na ₂ HPO ₄ -7H ₂ O	26.8
KH ₂ PO ₄	2.4

pH was adjusted to 7.4 with HCl and the volume was adjusted to 1000 ml with distilled H₂O. The buffer was sterilized by autoclaving for 20 minutes at 121°C

50x TAE Buffer

Table 38: 50x TAE Buffer

Ingredients	
Tris Base	242 g/l
EDTA 0.5 M	100 ml
glacial acetic acid	57.1 ml

pH was adjusted to 8 with NaOH and distilled H₂O was added to 1000 ml.

5.1.11 Laboratory equipment

Table 39: Laboratory equipment

Device	Supplier
Agarose gel electrophoresis apparatus	PeqLab
Analytical scale XA105DU, Dual Range	Mettler
C Mag HS7 magnetic stirrer	IKA
Centrifuge Avanti JE	Beckmann Coulter
Clean bench safe2020	Thermo Scientific
CO 8000 cell density meter	WPA biowave
External microscope lamp HBO 100	Zeiss
Geldoc Gel documentation system	Biorad
Incubator Celsius 10.0	Memmert
Infinite M200 Microtiterplate reader	Tecan
Inverse microscope AE31	Motic
Membrane vacuum pump	Vakubrand
Microscope axio scope A1	Zeiss
Mikro pulser electroporation apparatus	Biorad
Milli-Q water reference system	Merck-Millipore
Multifuge X1R	Thermo Scientific
MxP 3005 Cycler for qPCR	Agilent
NanoDrop 2000c Spectrophotometer	Peqlab
Peqpower 300 power supply	Peqlab
Peqstar 2x Gradient Thermocycler	Peqlab
pH meter seven easy	Mettler toledo
Power pack power supply	Biorad

Table 39: Laboratory equipment (continued)

Device	Supplier
Scout pro scale	Haus
Shaker Ecotron	Infors
Shaking Waterbath 1083	GFL
Table centrifuge 5414R	Eppendorf
Table centrifuge 5418	Eppendorf
Table centrifuge minister	VWR
Thermomixer comfort	Eppendorf
Vortex REAX 2000	Heidolph
Water bath WNB 7	Memmert

5.1.11.1 Software

Table 40: Software

Software	Application	Supplier
Chromas 2	DNA sequence analysis	Technelysium
Clone Manager suite 7	DNA sequence analysis	Sci-Ed software
GraphPad Prism 6	graphs and data analysis	GraphPad Software, inc.
Icontrol	programming and set-up for microtiterplate assays-	Tecan
Image Lab 3.0.1	gel documentation	Biorad
Image plus 2.0	inverse microscopy	Motic
Mx 2005 P™	set-up and analysis of qPCR data	Agilent
EndNote X7	Bibliography management	Thomson Reuters
ZEN	Phasecontrast- and fluorescence microscopy	Zeiss

5.2 Methods

5.2.1 Microbiology methods

5.2.1.1 Culturing of bacteria

E. coli was grown overnight, shaking (220 rpm) at 37°C. Growth and cell density were monitored by determination of the extinction at $\lambda=600$ nm (OD_{600}). If required for selection an antibiotic was added to the cultures. For long-term storage, glycerol-stocks (50% glycerol + 50% stationary culture) were prepared and stored at -80°C.

5.2.1.2 Minimal inhibition concentration (MIC) determination

5.2.1.2.1 Broth Microdilution method

The bacterial isolates were streaked onto Mueller-Hinton (MH) agar plates and incubated for 18-24 h at 37°C. On the next day 3-5 morphologically similar colonies were selected and transferred into an eppi tube containing sterile saline solution (500 μ l 0.9% saline). The suspension was adjusted to an OD_{600} of 0.1 (diluted with broth) and further diluted with broth to achieve an inoculum of 1×10^6 in 5 ml. A suspension of an $OD_{600} = 0.1$ in Mueller-Hinton broth contains the following CFUs: *E. coli* ATCC 25922: 1.4×10^8 CFU/ml; *E. coli* K12: 1.1×10^8 CFU/ml; *B. subtilis* 168: 1.9×10^7 CFU/ml; *S. aureus* ATCC 29213: 1.5×10^8 CFU/ml; *Enterococcus faecalis* ATCC 29212: 6.3×10^7 CFU/ml; *P. aeruginosa* PAO1: 1.1×10^8 CFU/ml

A stock-solution of negamycin was prepared in DMSO with the concentration of 10 mg/ml. The solution was stored at -20°C.

To prepare the antibiotic dilution series, a serial twofold dilution of the antibiotic from 64 μ g/ml to 0.0625 μ g/ml in medium was prepared. 100 μ l of the stock solution (128 μ g/ml: 2x concentrated) were added into the first well of a 96-well round bottom microplate. 50 μ l of medium were added into the wells 2-12. 50 μ l of the first well were taken and mixed with the second one, and so on. After dilution each well contained 50 μ l of antibiotic solution at twice the desired final concentration. In the next step each well of the microdilution tray was inoculated with 50 μ l of bacterial suspension to yield a final concentration of 5×10^5 CFU/ml in a final volume of 100 μ l. Two different controls were prepared (GC: growth control (broth with bacterial inoculum, no antibiotic) 100 μ l and SC: sterility control (broth only) 100 μ l. A 10 μ l sample of the growth control was removed immediately after inoculating the plate and pipetted into 990 μ l broth. It was mixed and one further dilution (1:10) of this suspension was made. 100 μ l of the final dilution were plated on Mueller Hinton agar plates to validate the number of colony forming units in the assay.

Microtiter plates and agar plates were incubated for 16-24 h at 37°C. When MIC determinations were performed in PP the plates were incubated for 20 hours. When M9 was used, the plates were incubated for 24 hours. The MIC, as the lowest concentration of the

antibacterial agent that inhibited visible bacterial growth, was read. Colonies were counted on agar plates to verify that the right number of CFUs was used.

5.2.1.2.2 Agar dilution method

The bacterial isolates were streaked out onto Mueller-Hinton (MH) agar plates and incubated for 18-24 h at 37°C. On the next day 3-5 morphologically similar colonies were selected and transferred into an eppi tube containing sterile saline solution (500 µl 0.9% saline). The suspension was adjusted to an OD₆₀₀ of 0.1 (diluted with broth) and diluted with broth to achieve an inoculum of 1×10^7 in 5 ml.

The agar medium was equilibrated in a water bath to 45-50°C and the appropriate dilutions of negamycin (64 to 0.03 µg/ml) were added. To ensure that there was no contamination one drug-free plate each was inoculated.

The components were mixed thoroughly and the agar was poured immediately into petri dishes to yield an agar depth of 3-4 mm (10 ml in small petri dishes). The plates solidified at room temperature (they were always used the same day).

Within 15 minutes after the inoculum had been standardized, 1 µl (10^4 CFU) was spotted onto each agar plate (in triplicates). The inoculation started with the plate that contained the lowest concentration of the antibacterial and proceeded to the highest. After inoculation, the plates stood at room temperature for up to 30 min until the inoculum spots were absorbed by the agar.

To validate the inoculum 10 µl sample of the bacterial suspension, which was adjusted to 10^7 CFU/ml, was removed immediately after inoculating the plate and pipetted into 990 µl broth. It was mixed and two further 1/10 dilutions of this were made. 50 µl of each dilution were plated on small MH plates.

Unless otherwise indicated agar plates were incubated bottom-up for 16 to 20 h at 37°C in ambient air. The MIC was read on a dark non-reflecting surface as the lowest concentration of antibacterial agent that completely inhibited visible bacterial growth.

5.2.1.3 Growth curves

E. coli strains were inoculated in 5 ml of desired medium (M9 or PP) and incubated for 18-24 h at 37°C shaking (220 rpm). The OD₆₀₀ was measured on the next day and 20 ml M9 or PP were inoculated to an OD₆₀₀ of 0.05 in 100 ml flasks. The OD₆₀₀ was measured every 30 min. If negamycin was added: Cells were grown to an OD₆₀₀ 0.2-0.5. The culture was split in two times 10 ml aliquots and negamycin was added to one of them. The OD₆₀₀ was measured every 30 min.

5.2.1.4 Killing curves

E. coli strains were inoculated in PP and incubated for 18-24 h at 37°C shaking (220 rpm). On the next day 10 ml of PP were inoculated with 100 µl of the overnight-culture, and cells were grown to an OD₆₀₀ 0.5. The OD₆₀₀ was adjusted to 0.1 in 1 ml broth.

A suspension of an OD₆₀₀ = 0.1 in Mueller-Hinton broth contains the following CFUs: *E. coli* K12: 1.1 x 10⁸ CFU/ml (Inoculum was adjusted to 5 x 10⁵ cells/ml). Negamycin was added at the desired concentration. Cells were incubated at 37°C in small tubes (no shaking!) and samples were taken over a time course of 24 hours. At every time point 25 µl were taken, diluted and plated on 0.5% polypeptone agar plates. Colonies were counted after incubating for 24 hours at 37°C.

5.2.1.5 Resistance rate determination

The bacterial isolates were streaked out onto Mueller-Hinton agar and incubated for 18-24 h at 37°C. On the next day 3-5 morphologically similar colonies were isolated and transferred into an eppi tube containing sterile saline solution (500 µl 0.9% saline). The suspension was adjusted to an OD₆₀₀ of 2 (diluted with M9/PP).

A suspension of an OD₆₀₀ = 2 in Mueller-Hinton broth contains the following CFUs: *E. coli* K12: 2.2 x 10⁹ CFU/ml. The agar plates were prepared and antibiotic was added in the desired concentration. To ensure that there was no contamination one drug-free plate each was inoculated. Furthermore a dilution series was plated. Within 15 minutes after the inoculum had been standardized 5x10⁸: 227.25 µl of the solution (2.2 x 10⁹) were plated. After inoculation, the plates stood at room temperature for up to 30 min until the inoculum was absorbed by the agar. Colonies were counted after 24 or 48 hours.

5.2.2 Molecular Biology Methods

5.2.2.1 DNA isolation

The genomic DNA was isolated with innuPREP bacteria DNA Kit from Analytik Jena. The isolation was performed as described in the manual of the manufacturer. This kit combines an initial lysis step and a proteolytic digestion step with a selective and reversible binding to a silica membrane.

5.2.2.2 Plasmid isolation

Plasmids were isolated using the innuPREP Plasmid Miniprep Kit from Analytik Jena. This kit combines a modified alkaline denaturation with selective and reversible DNA binding to a silica membrane. The manufacturer's manual was followed for plasmid isolation.

5.2.2.3 DNA sequencing

DNA was sequenced using the Sanger chain-termination method [200]. This method involves *in vitro* DNA synthesis using synthetic oligonucleotides as primers. The integration of dideoxynucleotides leads to termination of the growing nucleotide chain. Four parallel reactions, each containing one of four dideoxynucleotides (ddATP, ddGTP, ddCTP or ddTTP) and all four deoxynucleotides allow the formation of chain termination products of various lengths. Electrophoretic separation of the termination products allows the sequence to be determined by the comparison of the various fragments.

DNA was sequenced at LGC genomics. Samples were supplied at a concentration of 20-100 ng/ μ l, according to the company's recommendations.

5.2.2.4 Computer supported sequence analysis

DNA sequence data was analyzed and processed using the program Clone Manager suite 7 (Sci-Ed software). Clone Manager suite 7 was also used for primer design, planning of cloning strategies and finding of restriction sites as well as the managing of plasmid sequence data.

5.2.2.5 DNA amplification via the Polymerase Chain Reaction (PCR)

PCR [201] allows the *in vitro* amplification of a specific DNA fragment. The starting points for synthesis by a heat-stable DNA polymerase are given by synthetic oligonucleotide primers. These primers flank the desired sequence and are complementary to the respective strand of the template DNA. Site-specific mutations may be introduced by one or more base exchanges in the primer sequence. This allows the generation and integration of desired restriction endonuclease sites.

In the first step the template DNA and the primers were denatured (as shown in Table 42). During the subsequent cooling phase, the primers were able to bind their complementary

sequence on the single stranded DNA template. During the elongation step, DNA polymerase then synthesized the new DNA strand (complementary to the template). The desired DNA fragment is thus, in theory, exponentially amplified by the repetition of these three steps (denaturing, primer annealing and elongation). In this work either the Phusion–polymerase (proof reading function) or the DreamTaq polymerase (no proof reading function) from Thermo Scientific, or the Q5 polymerase (proof reading function) from NEB were used. The concentrations of the different PCR components were used as described in the manufacturer’s manual (Table 41). Every reaction contained the following reagents:

Table 41: Composition of the PCR reactions

Reagent	Final concentration
10x buffer	1x
template-DNA	0.1 – 10 ng
10 mM dNTPs	200 μ M
Polymerase	0.02 U/ μ l
fwd primer	0.5 μ M
rev primer	0.5 μ M
dH₂O	to 50 μ l

The cycling conditions were used as recommended by the manufacturer (Table 42). The annealing temperature was adjusted to the different primers according to their melting temperatures (T_m) and optimized by using a temperature gradient in the PCR program.

Table 42: Cycle conditions

Cycle Step	Temperature			Time			Cycles		
	Dream Taq	Phusion	Q5	Dream Taq	Phusion	Q5	Dream Taq	Phusion	Q5
initial Denaturation	95°C	98°C	98°C	1-3 min	30 sec	30 sec	1	1	1
Denaturation	95°C	98°C	98°C	30 sec	5-10sec	5-10sec	25-40	25-35	25-35
Annealing	T_m-5°	T_m+3°	50-72°C	30 sec	10-30 sec	10-30sec			

Table 42: Ccle condition (continued)

Cycle Step	Temperature			Time			Cycles		
Extension	72°C	72°C	72°C	1 min/kb	15-30sec/kb	20-30sec/kb			
Final extension	72°C	72°C	72°C	5-15 min	5-10 min	2 min	1	1	1
Final hold	4°C	4°C	4°C	∞	∞	∞			

5.2.2.6 Purification of PCR products

PCR products destined for cloning were purified using the innuPREP double pure kit of Analytik Jena. The manufacturer's manual was followed for purification.

5.2.2.7 DNA digest with restriction endonucleases

Plasmid and PCR Products were cut with restriction endonucleases in order to perform an analytic or preparative digest. For an analytic digest smaller amounts of plasmid DNA were digested to determine the restriction pattern of isolated plasmids. This provides a first indication of the construct's correctness. For cloning a preparative digest with larger amounts of DNA was done. The digest was performed as indicated in the manual (Table 43).

Table 43: Composition of DNA digest

Reagent	Volume (μl)
DNA	500 ng – 2 μg
Buffer (10x)	2
Restriction enzyme	1
dH₂O	add up to 20

For analytic purposes 2 μl of the reaction mixture were loaded onto a 1% agarose gel.

5.2.2.8 Agarose gel electrophoresis

DNA fragments were separated via agarose gel electrophoresis. By applying an electric field, the negatively charged DNA can be separated in the agarose matrix according to its size. Small molecules are able to move faster and therefore further through the pores of the gel. 1 % agarose was boiled in 1x TAE Buffer until it was completely dissolved. After cooling down the solution was poured into the gel tray. Before loading the samples to the gel, they were mixed with the appropriate amount of 6x loading dye. To determine later the sizes and concentration of the DNA fragments standardized digested DNA (“DNA-ladders”) were added (Figure 64). The separation of the fragments took place at 100-120 V for 1-2 hours. Afterwards the gel was stained in an ethidiumbromide-bath (0.1% EtBr in H₂O) for 20-30 minutes. The ethidiumbromide intercalates into the DNA. The absorption of the ethidiumbromide can then be analyzed under UV-light (320 nm) using a gel documentation system.

If the gel was needed for preparative purposes, it was analyzed 320 nm UV-Screen and the bands were selected for excision.

5.2.2.9 Gel purification

To isolate and purify DNA fragments or PCR-products, the DNA was loaded onto a 1%-agarose gel and separated as described in 5.2.2.8. The band of interest was excised with a sharp, clean scalpel. The isolation was performed using the InnuPREP Double Pure Kit from Analytik Jena.

5.2.2.10 Dephosphorylation of vectors

Linearized plasmid-DNA was dephosphorylated using the fast alkaline phosphatase (FAST AP) of Thermo Scientific. The protocol of the manufacturer was followed (Table 44)

Table 44: Composition of vector dephosphorylation

Reagent	Volume (μl)
DNA (linearized)	1 μg
10X Thermo Scientific FastDigest Buffer (1U/μl)	2
FastAP Thermosensitive Alkaline Phosphatase	1
dH₂O	add up to 20

The mixture was incubated for 45 minutes at 37°C. The reaction was stopped by incubation at 65°C for 15 minutes.

5.2.2.11 Ligation of two DNA Fragments

To ligate two DNA fragments with each other, such as a vector and a PCR product, the enzyme T4 DNA Ligase (Thermo Scientific) was used. This enzyme catalyses the formation of new phosphodiester bonds between the 5'-phosphate and the 3'-hydroxyl ends of DNA. The molar ratio of vector to insert was 1:3. The amount of DNA that should be added to the reaction was determined using the following equation:

$$V_{\text{Insert}} = (c_{\text{Vector}} \times \text{length}_{\text{Insert}} \times A) / (\text{length}_{\text{Vector}} \times c_{\text{Insert}} \times B)$$

The ratio of A/B defines how many molecules of insert should be added to one molecule of vector.

Reactions were run over night at room temperature.

5.2.2.12 Preparation of electrocompetent cells

500 ml LB medium were inoculated with 500 µl over night culture of *E. coli* and incubated with shaking (200 rpm) at 37°C to an OD₆₀₀ of 0.5. The cells were cooled on ice for 30 min and then spun down (15 min, 6000 rpm, 4°C). Cells were washed first with 500 ml ice-cold sterile water, then with 250 ml and finally with 10 ml ice-cold 10% glycerol. The pellet was resuspended in 800 µl 10% glycerol. 60 µl aliquots were stored at -80°C.

5.2.2.13 Transformation of electrocompetent cells

E. coli was transformed by electroporation. 50 µl of competent cells were thawed on ice. Up to 3 µl of the DNA were added to the cells and incubated for 30 minutes on ice. The suspension was then transferred to an electroporation cuvette (2 mm). The electroporation took place a voltage of 2.5 kV, a capacity of 25 µF and a resistance of 1000 Ω. The optimal time constant under these conditions is 2.5 ms. After the pulse, 1 ml of LB medium was added to the cells. After one hour incubation (37°C, 200 rpm) different dilutions were plated on LB-agar, containing an antibiotic for selection.

5.2.2.14 Single-gene knockout (Datsenko & Wanner)

To knockout a single gene in the *E. coli* Keio strains the method of Datsenko and Wanner was used [141]. In the first steps an antibiotic resistance cassette was inserted in the gene of interest. Most of the gene was therefore deleted and only some basepairs at the start and end of the gene were left. When needed the cassette was eliminated and only a scar region was left. This could be achieved in a several-step procedure (Figure 65).

Step 1: The template plasmid pKD3 was isolated from *E. coli* BW25141 pKD3. Using the restriction enzymes *Cla*I and *Not*I, the resistance cassette (1700 bp) was cut out and purified using gel-extraction.

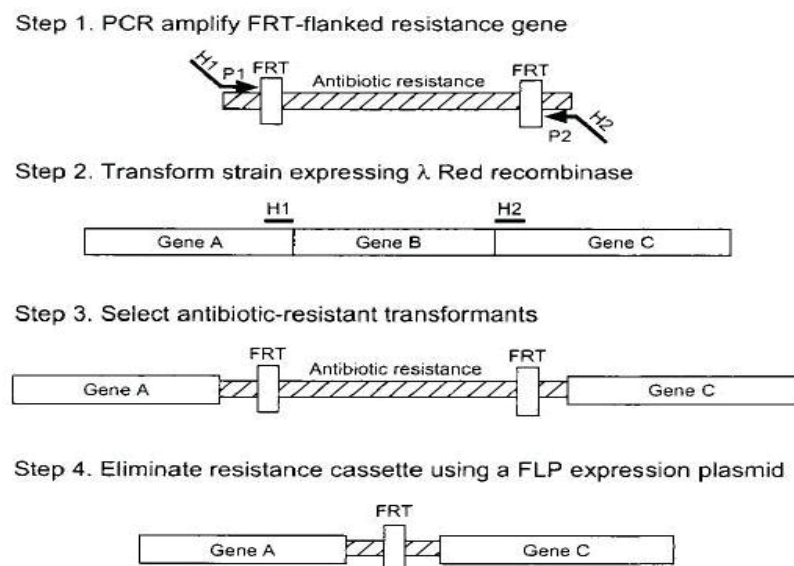


Figure 65: Gene disruption strategy by Datsenko & Wanner [141]

Step 2: Primer design

Primers were designed which contained homologous parts to P1 and P2 of the resistance cassette and homologous sequences to the gene that should be deleted (homolog to H1 and H2)

Step 3: Amplification

A PCR with the purified chloramphenicol (Cm) resistance cassette as a template and the designed primers was performed. The PCR-product was then purified.

Step 4: Transformation with pKD46

Electrocompetent cells of the strain in which the knock-out should take place were prepared. This strain was transformed with the helper plasmid pKD46 and plated on LB-Amp, as pKD46 carries an ampicillin (Amp)-resistance cassette, and grown overnight at 30°C. 10 ml

LB-Amp containing 10 mM arabinose (for induction of λ red genes) was inoculated with the grown colonies, and electrocompetent cells were prepared.

Step 5: Transformation with the amplified cassette

The strain containing the pKD46 helper plasmid was transformed with the purified PCR product of the extended resistance cassette, and cells were plated on LB-Amp agar plates and were grown for 48 hours at 30°C.

Step 6: PCR/Sequencing of possible knockouts

The genomic DNA was isolated and amplified using primers flanking the gene of interest. To verify the insertion of the resistance cassette, the DNA was sequenced.

Step 7: Elimination of pKD46

The strain carrying both selection markers, the Amp-marker in pKD46 and the Cm-marker in the gene that was knocked out, was grown on LB (no selection) overnight at 43°C. The sensitivity was then tested on LB-Amp and LB-Cm plates. When the strain grew only on LB-Cm and not on LB-Amp, the temperature-sensitive plasmid pKD46 was eliminated, and therefore the strain was not ampicillin resistant anymore.

Step 8: Deletion of resistance cassette

To delete the resistance cassette, electrocompetent cells of the mutants were prepared and transformed with pCP20 (temperature-sensitive replication and thermal induction of FLP synthesis, amp-resistance cassette) and incubated for 48 hours at 30°C. Due to the thermal induction FLP is expressed and binds to the FRT-sequence. FRT-mediated cleavage occurs. After removing the cassette only a scar region was left. Ampicillin-resistant transformants were selected and incubated at 43°C, to loose the plasmids, which carry a temperature-sensitive replicon. Afterwards the strains were tested for loss of all antibiotic resistances.

5.2.2.15 RNA isolation

10 ml of M9 or PP were inoculated with an overnight-culture to an OD_{600} of 0.02. Cells were grown under continuous shaking (200 rpm, 37°C) until they reached an OD_{600} of 0.5. When required, cells were treated with antibiotics for a certain amount of time. Two volumes of RNAprotect™ were added to 6-8 ml of culture and incubated for 5 minutes at 37°C. Cells were spun down (10 min, 8000 rpm, RT) and RNA was isolated using either the High Pure RNA Isolation Kit (Roche) or the innuPREP RNA Mini Kit (Analytik Jena AG) combined with innuPREP DNase I Digest Kit (Analytik Jena AG). The manufacturers instructions were followed. The RNA concentration was measured using the Nanodrop spectrophotometer. To determine the quality of the RNA and to exclude that the RNA was degraded an analytic 1.2% agarose gel was prepared. The RNA was stored at -80°C.

5.2.2.16 cDNA synthesis

In order to use RNA for qRT-PCR the RNA must be transcribed into single stranded cDNA. The enzyme used for this purposes is called reverse transcriptase, an RNA-dependent DNA polymerase isolated from a retrovirus. The AffinityScript cDNA Synthesis Kit from Agilent was used. For each RNA sample one no-RT control (sample without reverse transcriptase) was included to detect any DNA contamination in the RNA-sample. The reaction was set up as shown in Table 45 and Table 46.

Table 45: Step 1 cDNA-Synthesis

Reagent	Volume
RNA	0.5 µg
10x RT random primers	3 µl
RNase free H ₂ O	17.5 µl

The sample was incubated for 3 minutes at 65°C, followed by 10 minutes at room temperature to let the primer anneal. Afterwards the following reagents were added:

Table 46: Step 2 cDNA-Synthesis

Reagent	Volume
dNTPs	0.8 µl
10x RT buffer	2 µl
RNase blocker	0.5 µl
Reverse transcriptase (not in no-RT samples)	1 µl
RNase free H ₂ O	20 µl

Samples were incubated for 10 min at 25°C, followed by 60 minutes at 55°C and 15 minutes at 70°C. The resulting cDNA samples were 10-fold diluted and stored at -20°C.

5.2.2.17 Quantitative real-time-PCR (qPCR)

qPCR is used to amplify and simultaneously quantify a targeted DNA template. Besides the general procedure of the PCR, the qPCR has the key feature to detect the amplified DNA while the reaction is ongoing in real time. The qPCR products were detected using a fluorescent dye (SYBR Green I), that is able to intercalate into the DNA.

The qPCR was performed using Brilliant III Ultra-Fast SYBR Green qPCR Master Mix Kit (Agilent). SYBR Green is the reporter dye the fluorescence signal of which increases with the rising amount of DNA during amplification. The fluorescence reference dye Rox was used as internal standard to normalize well-to-well fluorescence detection differences. As Rox does not bind to DNA its signal remains constant throughout the cycles. The specificity of the primers was validated by a melting curve of each primer set. Several controls were used in the qPCR assay. Each plate of samples included no-reverse transcription controls (no-RT) and no-template controls (no-TC). Through the no-RTs genomic DNA contamination was detected. The no-TCs detected general PCR contaminations and were also able to distinguish between unintended amplification products such as primer-dimers. Every sample was at least run in duplicates. To normalize the cellular mRNA data, the stably expressed *gapDH* gene (housekeeping gene) was used as a reference gene and therefore included as an internal control on the plate.

The setup of the plate was performed using the software Mx 2005 PTM (Agilent). The reaction was set up as shown in Table 47.

Table 47: qPCR composition

reagent	volume (μ l)
SYBR Green QPCR master mix	10
Rox	0.3
Primermix (fwd/rev)	2
cDNA (1:10-dilution)	2
RNase free H₂O	5.7

A master mix containing RNase free H₂O, the primers and the SYBR Green qPCR master mix was prepared. 18 μ l of the master mix and 2 μ l of the cDNA were pipetted into one well of the 96-well PCR plate. The wells were sealed and the samples were spun down for 30 sec at 150 rpm. The qPCR was run as shown in Table 48.

Table 48: qPCR cycle condition

temperature ($^{\circ}$ C)	time	cycles
95	3 min	1
95	20 sec	40
60	20 sec	

Table 48: qPCR cycle condition (continued)

temperature (°C)	time	cycles
Melting curve		
95	1 min	1
45	30 sec	
95	30 sec	

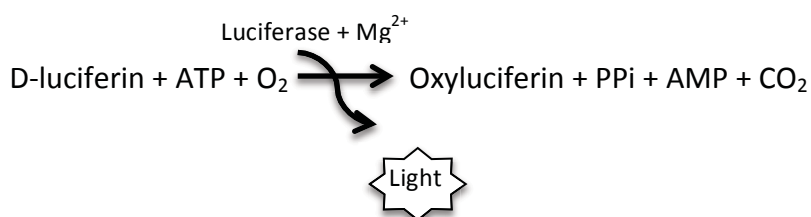
In the end of every qPCR a melting curve was calculated for each product. The product always showed only one single peak, which was expected as only one specific product was amplified.

qPCR analysis was performed using the $\Delta\Delta C(t)$ -method (Livak and Schmittgen, 2001 [202]). The $\Delta\Delta C(t)$ -method is an approximation method and is based on normalization to a single reference gene. The difference in $C(t)$ values between the target gene and the reference gene is calculated, and the $C(t)$ s of the different samples are compared directly. It is important that the different genes are amplified with comparable efficiencies for this comparison to be accurate.

5.2.3 *in vitro* Assays

5.2.3.1 Promoter assay (Urban *et al.*)

Antibiotics generally target different bacterial biosynthesis pathways. Urban *et al.* [140] showed that interference with different biosynthesis pathways in *B. subtilis* activates certain promoters. These reporters are suitable as screening tools to generate first hints on the target area of antibacterial agents. Urban *et al.* generated five *B. subtilis* promoters fused to the firefly luciferase reporter gene. If a compound targets one of the biosynthesis pathways, the promoter is activated, the luciferase is expressed, and the luminescence can be detected after adding D-luciferin as a substrate (Figure 66).

**Figure 66: Luciferase reaction**

strains: *B. subtilis* 1S34 pS63 MH124 (yvgS)

B. subtilis 1S34 pS130 (yvql)

B. subtilis 1S34 pS72 (yhel)

B. subtilis 1S34 pS77 (yorB)

B. subtilis 1S34 pS107 (ypuA)

In using these strains in the course of this work, the procedure of Urban et al. (167) was followed.

5.2.3.2 *Miscoding assay*

To determine if an antibiotic causes misreading, a miscoding assay was performed. Therefore a strain was used, carrying the pBestluc-mut plasmid, which has a stop-codon in the luciferase gene leading to a truncated, non-functional enzyme. If a compound causes misreading, the stop-codon is read through and a functional luciferase is expressed. Therefore a luminescence signal can be detected.

E. coli pBestluc-mut was grown in M9 or 0.5% until exponential phase and treated with streptomycin (positive control), tetracycline (negative control) or negamycin in different concentrations (0.5-4 µg/ml).

streptomycin: (MIC in 0.5% polypeptone: 0.0625 µg/ml; M9: 4 µg/ml)

tetracycline: (MIC: ca. 4 µg/ml in M9 and 0.5% polypeptone)

negamycin (MIC: ca. 4 µg/ml in M9 and 16 µg/ml in 0.5% polypeptone)

Cells were incubated under continuous shaking (220 rpm) at 37°C for 2.5 hours (0.5% polypeptone) or for 5 hours (M9) and chemoluminescence was read in a M200 Microtiterplate reader Pro.

5.2.3.3 *Transcription-translation assay (TraLa-Assay)*

The coupled transcription-translation assay is used to screen for inhibitors of these steps in the protein-biosynthesis in a cell-free approach. The assay is performed *in vitro* with an *E. coli* S30 extract and uses the firefly (*Photinus pyralis*) luciferase gene as a reporter. If the tested compound targets protein synthesis, the expression of the firefly luciferase is inhibited and the reaction, catalyzed by the luciferase, is taking place to a lower extent (Figure 66). A protocol was used as described in the following publications [203-205]. To distinguish whether the transcription or the translation is targeted by the antibiotic, an uncoupled T7/translation assay was performed. In this assay the luciferase was expressed from a T7-promoter. The T7 polymerase from the T7 bacteriophage is highly promoter specific and only transcribes DNA downstream of a T7 promoter. If a compound targets the

bacterial transcription the luminescence will be stable, as it only inhibits the bacterial polymerase and not the T7 polymerase. If a compound targets the translation, the signal will decrease. Chemoluminescence was read in a M200 Microtiterplate reader Pro.

5.2.4 Analytical methods

5.2.4.1 *Thin layer chromatography (TLC)*

TLC was used to determine whether negamycin forms a complex with different salts. Negamycin was solved in 100% methanol in a concentration of 10 mg/ml and diluted to 1 mg/ml in TraceSELECT® H₂O (Fluka). CaCl₂, NaCl or MgCl₂ was added in a molar ratio 1:1, 1:2 or 1:4. 6 µl of each sample was applied to the adsorbent layer. TLC was carried out with chloroform-methanol-25% aqueous ammonia (2:2:1) as mobile phase in a TLC chamber, using TLC silicagel 60 F₂₅₄ (Merck) The developed plates were dried at 37°C and treated with ninhydrin. The retardation factor (R_f-value) was determined for each sample.

5.2.4.2 *Isothermal titration calorimetry (ITC)*

Isothermal titration calorimetry is used to characterise the binding and interaction of two molecules. It is a quantitative technique to determine the thermodynamic parameters of an interaction in solution. To analyse the binding capacity of negamycin to calcium, a 5 mM negamycin solution in 200 mM MOPS (pH7) was prepared from a 20 mg/ml negamycin stock solution in DMSO. The resulting negamycin solution contained 8% DMSO and 300 µl were added to the sample chamber. 100 mM CaCl₂ was dissolved in 200 mM MOPS (pH 7) + 8% DMSO. This calcium solution was added in 80 injections of 0.5 µl resulting in 340 µl total volume in the sample chamber. The control experiment was performed by titrating CaCl₂ into the corresponding buffer without negamycin by the same ITC setup. Subsequently, the first point of the isotherm as well as a control experiment were subtracted from the isotherm before data evaluation. All ITC experiments were performed with a Microcal ITC 200 from GE Healthcare at 37 °C, a stirring speed of 1000 rpm and 80 injections of 0.5 µL. All other experimental details were defined as follows: Filter periode: 5 seconds, Feedbackmode: high and spacing between each injection: 300 seconds. The resulting isotherm was manually integrated and fitted with the OneSites binding site model of the corresponding Microcal Software Package based on Origin.

List of Tables

Table 1: Antibiotic discovery and evolution of resistance	16
Table 2: Negamycin MICs in Gram-positive and Gram-negative bacteria under different test conditions	35
Table 3: Azidonegamycin activity in Gram-negative and Gram-positive bacteria.....	37
Table 4: Sperabillin MICs in Gram-negative and Gram-positive bacteria under different test conditions.....	40
Table 5: MIC of different porin-knockout-strains in PP and M9.....	45
Table 6: Negamycin MICs of different <i>E. coli</i> transporter mutants in M9 and PP media.	48
Table 7: Negamycin susceptibility in different <i>S. aureus</i> transporter mutants in <i>S. aureus</i> minimal medium. 50	
Table 8: Negamycin susceptibility of isolated resistant clones in M9 and PP.	70
Table 9: Aminoglycoside susceptibility of isolated resistant clones in M9.	71
Table 10: Aminoglycoside susceptibility of isolated resistant clones in PP.	72
Table 11: Tetracycline and ciprofloxacin susceptibilities of isolated resistant clones in M9 and PP.	74
Table 12: salt effect on negamycin activity in PP.....	79
Table 13: RF values of TLC with negamycin and different concentrations of CaCl ₂ , MgCl ₂ and NaCl.....	81
Table 14: Influence of Ca ²⁺ on the negamycin activity in an <i>in vitro</i> transcription translation assay	83
Table 15: Negamycin and aminoglycoside MICs of different <i>E. coli</i> membrane-energy mutants in PP.	92
Table 16: Chemicals.....	111
Table 17: Antibiotics.....	114
Table 18: Kits.....	115
Table 19: Enzymes	115
Table 20: Bacterial strains	117
Table 21: isolated negamycin resistant <i>E. coli</i> strains.....	123
Table 22: Primer	124
Table 23: Plasmids.....	130
Table 24: Belitzky stock medium	131
Table 25: Belitzky-Supplements.....	132
Table 26: CYG growth medium	132
Table 27: MRE600 growth medium.....	132
Table 28: Lysogeny Broth (LB).....	133
Table 29: Mueller Hinton Broth	133
Table 30: M9-broth	133
Table 31: Nutrient broth growth medium.....	134
Table 32: peptone meat	135
Table 33: Peptone water growth medium	135
Table 34: PP	135
Table 35: KPO ₄ buffer	135
Table 36: TE Buffer	136
Table 37: 10x PBS	136
Table 38: 50x TAE Buffer.....	136
Table 39: Laboratory equipment	137
Table 40: Software	138
Table 41: Composition of the PCR reactions	143
Table 42: Cycle conditions	143
Table 43: Composition of DNA digest	144
Table 44: Composition of vector dephosphorylation	145
Table 45: Step 1 cDNA-Synthesis	149
Table 46: Step 2 cDNA-Synthesis	149

Table 47: qPCR composition150
Table 48: qPCR cycle condition150

List of Figures

Figure 1: Timeline of the discovery of new antibiotic classes.	16
Figure 2: Cell-envelope of Gram-positive and Gram-negative bacteria [25].....	18
Figure 3: Structure of the OmpF trimer [33].....	19
Figure 4: (a) Different types of membrane transport [50] (b) Relative permeability of a pure phospholipid bilayer to various molecules (Lodish 4 th edition [51]).....	20
Figure 5: PMF-the electrochemical gradient of H ⁺	21
Figure 6: (a) pH-homeostasis for acidophile, neutrophile and alkaliphile bacteria. (b) Pattern of $\Delta\Psi$, ΔpH and cytoplasmic pH plotted over a range of external pH values for acidophilic, neutralophilic and alkaliphilic bacteria [53].....	22
Figure 7: General ABC transporter architecture in <i>E. coli</i>	23
Figure 8: Schematic model of the molecular construction of the ABC-type macrolide-specific drug exporter MacA-MacB system complex with TolC in <i>E. coli</i>	24
Figure 9: Structure of the <i>E. coli</i> POT YbgH.....	26
Figure 10: Model for proton-driven peptide symport by PepT _{St} [84]	26
Figure 11: Passage of tetracycline across the bacterial cytoplasmic membrane and accumulation within the cytoplasm	29
Figure 12: Structure of negamycin with previously published pKa's [114].	30
Figure 13: Structure of Sperabillin A, B, C, D and Hexadecyl-Sperabillin.	32
Figure 14: Structure-comparison of sperabillin and negamycin.	33
Figure 15: Comparison of the chemical structures of negamycin and azidonegamycin	37
Figure 16: Bactericidal activity of negamycin in PP	38
Figure 17: <i>in vitro</i> coupled transcription/translation assay with (a) azidonegamycin, (b) negamycin and (c) uncoupled T7/translation assay with negamycin	39
Figure 18: Miscoding-Assay in M9 with negamycin, streptomycin (pos. control) and tetracycline (neg. control)	40
Figure 19: <i>in vitro</i> promoter assay with (a) sperabillin C and (b) hexadecyl-sperabillin	42
Figure 20: <i>in vitro</i> transcription-translation assay with sperabillin C	43
Figure 21: (a) Negamycin and (b) vancomycin and erythromycin activity in M9 and PP with addition of 15 $\mu\text{g/ml}$ PMBN (+ PMBN, or +) in <i>E. coli</i> BW25113.	44
Figure 22: Negamycin activity in JW1371 ($\Delta ompN$) with addition of 15 mg/L PMBN (+ PMBN).	45
Figure 23: Outer membrane structure of <i>E. coli</i> BW25113 and JW3606 ($\Delta rfaG$).	46
Figure 24: Antibiotic susceptibility of the “deep-rough phenotype” strain JW3606 ($\Delta rfaG$) compared to the wildtype (BW25113) in (a) M9 and (b) PP.	46
Figure 25: Growth curves of the <i>E. coli</i> strains BW25113 (wildtype) and JW3606 (<i>rfaG</i> -knockout) in M9 over 24 hours	47
Figure 26: Transporter expression in 0.5 % polypeptone compared to M9 in <i>E. coli</i> BW25113.	51
Figure 27: Determination of <i>E. coli</i> BW25113 (WT) MICs in M9 with the addition of different concentrations of (a) polypeptone, (b) casein and (c) aminoacid-mix. (d) Transporter expression after 30 minutes treatment with 0.1 mM amino acid-mix (AA-mix) compared to no treatment (M9).	52
Figure 28: (a) MIC determination of bialaphos in <i>E. coli</i> BW25113, $\Delta dppA$ and $\Delta oppA$. (b) Bialaphos MIC determination in M9 with the addition of different concentrations of polypeptone	53
Figure 29: Growth curves of treated and untreated <i>E. coli</i> BW25113 (WT) in (a) M9 and (b) PP.	54
Figure 30: Transporter expression in M9 after 30 minutes treatment with $\frac{1}{2}$ MIC negamycin (2 $\mu\text{g/ml}$).	54
Figure 31: Determination of ATc-concentration for induction of <i>dppA</i> -expression in pASK- <i>dppA</i>	55
Figure 32: Negamycin susceptibility in BW25113 (WT), the <i>dppA</i> -knockout strain JW3513 ($\Delta dppA$) del., the complemented strain JW3513 del. pASK- <i>dppA</i> and JW3513 del.-pASK-empty.	56

Figure 33: PCR confirmation of the <i>oppA</i> -knockout (a) and the <i>sapA</i> -knockout (b) in <i>E. coli</i> JW3513:	57
Figure 34: Sequencing result and alignment of the plasmid pKD3 (sequence from database) with obtained sequences with the primers <i>oppA fwd</i> and <i>oppA rev</i>	58
Figure 35: Sequencing result and alignment of the plasmid pKD3 (sequence from database) with obtained sequences with the primers <i>sapA fwd</i> and <i>sapA rev</i>	59
Figure 36: PCR confirmation of the <i>oppA</i> -knockout in <i>E. coli</i> $\Delta dppA$ - $\Delta sapA$ del.	60
Figure 37: Growth curves of the periplasmic binding protein-single, double- and triple-knockout strains in (a) M9 and (b) PP.	61
Figure 38: Negamycin susceptibility of the periplasmic binding protein- single- double and triple-knockout <i>E. coli</i> strains in (a, b) M9 and (c, d) PP.	62
Figure 39: Bialaphos susceptibility in different <i>E. coli</i> knockout strains.	63
Figure 40: Comparison of the negamycin susceptibility of the <i>E. coli</i> knockout strains with intact and deleted resistance-cassette.	64
Figure 41: Transcription unit <i>dppABCDF</i> . The transcription starts in front of <i>dppA</i> (source: ecoliwiki).....	65
Figure 42: Gene expression of <i>dppA-F</i> in JW3513 ($\Delta dppA$) and JW3513 ($\Delta dppA$) del. compared to the expression in BW25113	65
Figure 43: Expression of the periplasmic binding proteins <i>dppA</i> , <i>oppA</i> and <i>sapA</i> in JW3513 ($\Delta dppA$), JW1235 ($\Delta oppA$), JW1287 ($\Delta sapA$) and $\Delta dppA$ - $\Delta sapA$	66
Figure 44: Comparison of negamycin (3,6-diamino-5-hydroxyhexonacid) and lysine structures	67
Figure 45: Addition of increasing concentrations of lysine or arginine/histidin to M9.	68
Figure 46: Negamycin susceptibility in different amino acid transporter-system knockouts.	69
Figure 47: Growth curves at 37°C of BW25113 (WT) and M9-1 to M9-10 in M9 (a) and BW25113 (WT), PP-1, PP-2, PP-4, PP-6, PP-7 and PP-8 in PP(b).	75
Figure 48: (a) Colony-morphologies of the wildtype BW25113, the membrane-energy-mutant AN66 (<i>DubiD</i>) and PP-2, PP-6, PP-7 and PP-8 on PP-agar. (b) Cells were grown on PP and the diameters of the colonies were determined.	76
Figure 49: Negamycin susceptibilities of the <i>E. coli</i> strains BW25113 (WT), PP-8 small colony and PP-8 big colony. The MIC was determined in PP.	76
Figure 50: Alignment of <i>dppA</i> of the wildtype and M9-8.	78
Figure 51: PCR with the primer set <i>dppA-F-5/dppA-F rev4</i> (a) and <i>dppA-F-2/dppA-F rev2</i> (b).	78
Figure 52: (a) Thin layer chromatography (TLC) analysis of complex formation of negamycin with CaCl ₂ (1), MgCl ₂ (2) and NaCl (3). (b) TLC of negamycin mixed with NaCl in a molar ratio of 1:10. CaCl ₂ was added in increasing molar ratios. (c) Isothermal titration calorimetry (ITC) of negamycin titrated with CaCl ₂	81
Figure 53: Negamycin migration upon salt-addition	82
Figure 54: (a) CaCl ₂ effect on negamycin activity in <i>E. coli</i> BW25113 after treatment with 15 µg/ml PMBN (+ PMBN). MIC was determined in cells only treated with 15 µg/ml PMBN (+ PMBN), treated with 2.5 mM CaCl ₂ or treated with PMBN (15 µg/ml) and CaCl ₂ (2.5 mM). (b) Effect of 2.5 mM CaCl ₂ in <i>E. coli</i> BW25113 and the Gram-positive strains <i>B. subtilis</i> IS58 and <i>S. aureus</i> ATCC29213.	83
Figure 55: (a) Negamycin MIC of <i>E. coli</i> BW25113 in PP adjusted to different pH values, and effect of CaCl ₂ addition. (b) Effect of alkaline pH and additional supplementation with CaCl ₂ in <i>S. aureus</i> and <i>P. aeruginosa</i>	84
Figure 56: Growth of <i>E. coli</i> BW25113 (WT) in PP adjusted to pH 7 and pH 8.5.	85
Figure 57: Killing curves of <i>E. coli</i> BW25113 in PP in the presence of different negamycin concentrations at (a) pH 7 and (b) pH 8.5.	86
Figure 58: Determination of CCCP-susceptibility of <i>E. coli</i> BW25113 in PP.	91
Figure 59: Growth curve in the presence of different negamycin concentrations of <i>E. coli</i> BW25113 with and without addition of 2 µg/ml CCCP.	91
Figure 60: Negamycin susceptibility in energy mutants and PP-8 (small colony) in dependency on the pH in PP.	93
Figure 61: Negamycin, tetracycline and meropenem susceptibility in knockouts of AcrAB-tolC. The knockouts JW4052 ($\Delta acrA$), JW4051 ($\Delta acrB$) and JW5503 ($\Delta tolC$) were tested in (a) M9 and (b) PP.	94

Figure 62: Proposed model of negamycin uptake in M9.....	107
Figure 63: Proposed model of negamycin uptake in PP at pH 7 (a) and pH 8.5 (b).	109
Figure 64: DNA-ladder	116
Figure 65: Gene disruption strategy by Datsenko & Wanner [141].....	147

Bibliography

1. WHO, *The European health report 2012 : charting the way to well-being*. 2012, UN City, Marmorvej 51: Copenhagen, Denmark.
2. Silver LL. Challenges of antibacterial discovery. *Clin.Microbiol.Rev.* 2011; **24**: 71-109.
3. Walsh C. Where will new antibiotics come from? *Nat Rev Microbiol* 2003; **1**: 65-70.
4. Hamada M, Takeuchi T, Kondo S *et al.* A new antibiotic, negamycin. *J Antibiot (Tokyo)* 1970; **23**: 170-1.
5. Guo J, Miele EW, Chen A *et al.* Pharmacokinetics of the natural antibiotic negamycin. *Xenobiotica* 2015: 1-9.
6. Uehara Y, Kondo S, Umezawa H *et al.* Negamycin, a miscoding antibiotic with a unique structure. *J Antibiot (Tokyo)* 1972; **25**: 685-8.
7. Mizuno S, Nitta K, Umezawa H. Mechanism of action of negamycin in Escherichia coli K12. I. Inhibition of initiation of protein synthesis. *J Antibiot (Tokyo)* 1970; **23**: 581-8.
8. Mizuno S, Nitta K, Umezawa H. Mechanism of action of negamycin in Escherichia coli K12. II. Miscoding activity in polypeptide synthesis directed by synthetic polynucleotide. *J Antibiot (Tokyo)* 1970; **23**: 589-94.
9. Uehara Y, Hori M, Umezawa H. Negamycin inhibits termination of protein synthesis directed by phage f2 RNA in vitro. *Biochim Biophys Acta* 1974; **374**: 82-95.
10. Uehara Y, Hori M, Umezawa H. Inhibitory effect of negamycin on polysomal ribosomes of Escherichia coli. *Biochim Biophys Acta* 1976; **447**: 406-12.
11. Uehara Y, Hori M, Umezawa H. Specific inhibition of the termination process of protein synthesis by negamycin. *Biochim Biophys Acta* 1976; **442**: 251-62.
12. Olivier NB, Altman RB, Noeske J *et al.* Negamycin induces translational stalling and miscoding by binding to the small subunit head domain of the Escherichia coli ribosome. *Proc Natl Acad Sci U S A* 2014; **111**: 16274-9.
13. Polikanov YS, Szal T, Jiang F *et al.* Negamycin Interferes with Decoding and Translocation by Simultaneous Interaction with rRNA and tRNA. *Mol Cell* 2014; **56**: 541-50.
14. Fabrega A, Rosner JL, Martin RG *et al.* SoxS-dependent coregulation of ompN and ydbK in a multidrug-resistant Escherichia coli strain. *FEMS Microbiol.Lett.* 2012; **332**: 61-67.
15. Walsh C, *Antibiotics: Actions, origins, resistance*. Vol. 1 edition 2003, Washington, DC: ASM Press. 335.
16. Waksman SA. What is an antibiotic or an antibiotic substance? *Mycologia* 1947; **39**: 565-9.
17. Duchesne E, *Contribution à l'étude de la concurrence vitale chez les micro-organismes: antagonisme entre les moisissures et les microbes*, in *L'Ecole du Service de Santé Militaire de Lyon*. 1897.
18. Lloyd NC, Morgan HW, Nicholson BK *et al.* The composition of Ehrlich's salvarsan: resolution of a century-old debate. *Angew Chem Int Ed Engl* 2005; **44**: 941-4.
19. Fleming A. Classics in infectious diseases: on the antibacterial action of cultures of a penicillium, with special reference to their use in the isolation of B. influenzae by Alexander Fleming, Reprinted from the British Journal of Experimental Pathology 10:226-236, 1929. *Rev Infect Dis* 1980; **2**: 129-39.

20. Spellberg B, Taylor-Blake B. On the exoneration of Dr. William H. Stewart: debunking an urban legend. *Infect Dis Poverty* 2013; **2**: 3.
21. Walsh CT, Wencewicz TA. Prospects for new antibiotics: a molecule-centered perspective. *J Antibiot (Tokyo)* 2014; **67**: 7-22.
22. WHO, *European strategic action plan on antibiotic resistance*. 2011, Baku, Azerbaijan: Copenhagen, Denmark.
23. Franklin TJ, Snow GD, *Biochemistry and Molecular Biology of Antimicrobial Drug Action*. 6 ed. 2005, Cheshire England: Springer Science + Business Media, Inc. 182.
24. Madigan MT, Martinko JN, *Brock Microbiology*. 11 ed. 2006: Pearson Studium. 1203.
25. Murphy K, Travers P, Walport M, *Janeway's Immunobiology*. 7 ed. 2007, New York: Garland Science. 928.
26. Nikaido H. Molecular basis of bacterial outer membrane permeability revisited. *Microbiol.Mol.Biol.Rev.* 2003; **67**: 593-656.
27. Vaara M. Agents that increase the permeability of the outer membrane. *Microbiol Rev* 1992; **56**: 395-411.
28. Nikaido H. Porins and specific diffusion channels in bacterial outer membranes. *J.Biol.Chem.* 1994; **269**: 3905-3908.
29. Braun V, Hancock RE, Hantke K *et al.* Functional organization of the outer membrane of escherichia coli: phage and colicin receptors as components of iron uptake systems. *J Supramol Struct* 1976; **5**: 37-58.
30. Di Masi DR, White JC, Schnaitman CA *et al.* Transport of vitamin B12 in Escherichia coli: common receptor sites for vitamin B12 and the E colicins on the outer membrane of the cell envelope. *J Bacteriol* 1973; **115**: 506-13.
31. Hancock RE. Aminoglycoside uptake and mode of action-with special reference to streptomycin and gentamicin. II. Effects of aminoglycosides on cells. *J Antimicrob Chemother* 1981; **8**: 429-45.
32. Hancock RE, Farmer SW, Li ZS *et al.* Interaction of aminoglycosides with the outer membranes and purified lipopolysaccharide and OmpF porin of Escherichia coli. *Antimicrob Agents Chemother* 1991; **35**: 1309-14.
33. Yamashita E, Zhálnina MV, Zakharov SD *et al.* Crystal structures of the OmpF porin: function in a colicin translocon. *Embo j* 2008; **27**: 2171-80.
34. Jeanteur D, Lakey JH, Pattus F. The bacterial porin superfamily: sequence alignment and structure prediction. *Mol Microbiol* 1991; **5**: 2153-64.
35. Mortimer PG, Piddock LJ. The accumulation of five antibacterial agents in porin-deficient mutants of Escherichia coli. *J Antimicrob Chemother* 1993; **32**: 195-213.
36. Hirai K, Aoyama H, Irikura T *et al.* Differences in susceptibility to quinolones of outer membrane mutants of Salmonella typhimurium and Escherichia coli. *Antimicrob Agents Chemother* 1986; **29**: 535-8.
37. Ziervogel BK, Roux B. The binding of antibiotics in OmpF porin. *Structure* 2013; **21**: 76-87.
38. Tommassen J, Lugtenberg B. PHO-regulon of Escherichia coli K12: a minireview. *Ann Microbiol (Paris)* 1982; **133**: 243-9.
39. Samartzidou H, Delcour AH. Distinct sensitivities of OmpF and PhoE porins to charged modulators. *FEBS Lett* 1999; **444**: 65-70.
40. Johnson CL, Ridley H, Marchetti R *et al.* The antibacterial toxin colicin N binds to the inner core of lipopolysaccharide and close to its translocator protein. *Mol Microbiol* 2014; **92**: 440-52.

41. Lee SY, Xu Z, Choi JH, *Expression vectors encoding Escherichia coli OmpC as a cell surface anchoring motif*. 2001, Google Patents.
42. Delcour AH. Outer membrane permeability and antibiotic resistance. *Biochim Biophys Acta* 2009; **1794**: 808-16.
43. Huang H, Hancock RE. Genetic definition of the substrate selectivity of outer membrane porin protein OprD of *Pseudomonas aeruginosa*. *J Bacteriol* 1993; **175**: 7793-800.
44. Nestorovich EM, Sugawara E, Nikaido H *et al*. *Pseudomonas aeruginosa* porin OprF: properties of the channel. *J Biol Chem* 2006; **281**: 16230-7.
45. Prilipov A, Phale PS, Koebnik R *et al*. Identification and characterization of two quiescent porin genes, nmpC and ompN, in *Escherichia coli* BE. *J. Bacteriol.* 1998; **180**: 3388-3392.
46. Hong H, Patel DR, Tamm LK *et al*. The outer membrane protein OmpW forms an eight-stranded beta-barrel with a hydrophobic channel. *J Biol Chem* 2006; **281**: 7568-77.
47. Arora A, Rinehart D, Szabo G *et al*. Refolded outer membrane protein A of *Escherichia coli* forms ion channels with two conductance states in planar lipid bilayers. *J Biol Chem* 2000; **275**: 1594-600.
48. Harder KJ, Nikaido H, Matsushashi M. Mutants of *Escherichia coli* that are resistant to certain beta-lactam compounds lack the ompF porin. *Antimicrob Agents Chemother* 1981; **20**: 549-52.
49. Goldstein FW, Gutmann L, Williamson R *et al*. In vivo and in vitro emergence of simultaneous resistance to both beta-lactam and aminoglycoside antibiotics in a strain of *Serratia marcescens*. *Ann Microbiol (Paris)* 1983; **134a**: 329-37.
50. Encyclopædia, Britannica, *Different types of membrane transport*. 2008.
51. Lodish H, Berk A, Zipursky L *et al.*, *Molecular Cell Biology* 4ed. 2000, New York: W. H. Freeman. 1184
52. Ehrenberg B, Montana V, Wei MD *et al*. Membrane potential can be determined in individual cells from the nernstian distribution of cationic dyes. *Biophys J* 1988; **53**: 785-94.
53. Krulwich TA, Sachs G, Padan E. Molecular aspects of bacterial pH sensing and homeostasis. *Nat Rev Microbiol* 2011; **9**: 330-43.
54. Mitchell P. Chemiosmotic coupling in oxidative and photosynthetic phosphorylation. *Biol Rev Camb Philos Soc* 1966; **41**: 445-502.
55. Padan E, Bibi E, Ito M *et al*. Alkaline pH homeostasis in bacteria: new insights. *Biochim Biophys Acta* 2005; **1717**: 67-88.
56. Maurer LM, Yohannes E, Bondurant SS *et al*. pH regulates genes for flagellar motility, catabolism, and oxidative stress in *Escherichia coli* K-12. *J Bacteriol* 2005; **187**: 304-19.
57. Schuldiner S, Agmon V, Brandsma J *et al*. Induction of SOS functions by alkaline intracellular pH in *Escherichia coli*. *J Bacteriol* 1986; **168**: 936-9.
58. Davidson AL, Dassa E, Orelle C *et al*. Structure, function, and evolution of bacterial ATP-binding cassette systems. *Microbiol Mol Biol Rev* 2008; **72**: 317-64, table of contents.
59. Linton KJ, Higgins CF. The *Escherichia coli* ATP-binding cassette (ABC) proteins. *Mol Microbiol* 1998; **28**: 5-13.

60. Doeven MK, Kok J, Poolman B. Specificity and selectivity determinants of peptide transport in *Lactococcus lactis* and other microorganisms. *Mol Microbiol* 2005; **57**: 640-9.
61. Kuhnau S, Reyes M, Sievertsen A *et al.* The activities of the *Escherichia coli* MalK protein in maltose transport, regulation, and inducer exclusion can be separated by mutations. *J Bacteriol* 1991; **173**: 2180-6.
62. Andrews JC, Short SA. Genetic analysis of *Escherichia coli* oligopeptide transport mutants. *J.Bacteriol.* 1985; **161**: 484-492.
63. Naider F, Becker JM. Multiplicity of oligopeptide transport systems in *Escherichia coli*. *J Bacteriol* 1975; **122**: 1208-15.
64. Abouhamad WN, Manson M, Gibson MM *et al.* Peptide transport and chemotaxis in *Escherichia coli* and *Salmonella typhimurium*: characterization of the dipeptide permease (Dpp) and the dipeptide-binding protein. *Mol.Microbiol.* 1991; **5**: 1035-1047.
65. Kobayashi N, Nishino K, Yamaguchi A. Novel macrolide-specific ABC-type efflux transporter in *Escherichia coli*. *J Bacteriol* 2001; **183**: 5639-44.
66. Tikhonova EB, Devroy VK, Lau SY *et al.* Reconstitution of the *Escherichia coli* macrolide transporter: the periplasmic membrane fusion protein MacA stimulates the ATPase activity of MacB. *Mol Microbiol* 2007; **63**: 895-910.
67. Hiles ID, Gallagher MP, Jamieson DJ *et al.* Molecular characterization of the oligopeptide permease of *Salmonella typhimurium*. *J Mol Biol* 1987; **195**: 125-42.
68. Klepsch MM, Kovermann M, Low C *et al.* *Escherichia coli* peptide binding protein OppA has a preference for positively charged peptides. *J Mol Biol* 2011; **414**: 75-85.
69. Goodell EW, Higgins CF. Uptake of cell wall peptides by *Salmonella typhimurium* and *Escherichia coli*. *J Bacteriol* 1987; **169**: 3861-5.
70. Maqbool A, Levdikov VM, Blagova EV *et al.* Compensating stereochemical changes allow murein tripeptide to be accommodated in a conventional peptide-binding protein. *J.Biol.Chem.* 2011; **286**: 31512-31521.
71. Abouhamad WN, Manson MD. The dipeptide permease of *Escherichia coli* closely resembles other bacterial transport systems and shows growth-phase-dependent expression. *Mol.Microbiol.* 1994; **14**: 1077-1092.
72. Olson ER, Duniak DS, Jurss LM *et al.* Identification and characterization of dppA, an *Escherichia coli* gene encoding a periplasmic dipeptide transport protein. *J.Bacteriol.* 1991; **173**: 234-244.
73. Weinberg MV, Maier RJ. Peptide transport in *Helicobacter pylori*: roles of dpp and opp systems and evidence for additional peptide transporters. *J.Bacteriol.* 2007; **189**: 3392-3402.
74. Manson MD, Blank V, Brade G *et al.* Peptide chemotaxis in *E. coli* involves the Tap signal transducer and the dipeptide permease. *Nature* 1986; **321**: 253-6.
75. Letoffe S, Delepelaire P, Wandersman C. The housekeeping dipeptide permease is the *Escherichia coli* heme transporter and functions with two optional peptide binding proteins. *Proc.Natl.Acad.Sci.U.S.A* 2006; **103**: 12891-12896.
76. Wick LM, Quadroni M, Egli T. Short- and long-term changes in proteome composition and kinetic properties in a culture of *Escherichia coli* during transition from glucose-excess to glucose-limited growth conditions in continuous culture and vice versa. *Environ Microbiol* 2001; **3**: 588-99.
77. Easton JA, Thompson P, Crowder MW. Time-dependent translational response of *E. coli* to excess Zn(II). *J Biomol Tech* 2006; **17**: 303-7.

78. Parra-Lopez C, Baer MT, Groisman EA. Molecular genetic analysis of a locus required for resistance to antimicrobial peptides in *Salmonella typhimurium*. *EMBO J.* 1993; **12**: 4053-4062.
79. Harms C, Domoto Y, Celik C *et al.* Identification of the ABC protein SapD as the subunit that confers ATP dependence to the K⁺-uptake systems Trk(H) and Trk(G) from *Escherichia coli* K-12. *Microbiology* 2001; **147**: 2991-3003.
80. Schlosser A, Meldorf M, Stumpe S *et al.* TrkH and its homolog, TrkG, determine the specificity and kinetics of cation transport by the Trk system of *Escherichia coli*. *J Bacteriol* 1995; **177**: 1908-10.
81. Mason KM, Raffel FK, Ray WC *et al.* Heme utilization by nontypeable *Haemophilus influenzae* is essential and dependent on Sap transporter function. *J Bacteriol* 2011; **193**: 2527-35.
82. Steiner HY, Naider F, Becker JM. The PTR family: a new group of peptide transporters. *Mol.Microbiol.* 1995; **16**: 825-834.
83. Zhao Y, Mao G, Liu M *et al.* Crystal structure of the *E. coli* peptide transporter YbgH. *Structure* 2014; **22**: 1152-60.
84. Solcan N, Kwok J, Fowler PW *et al.* Alternating access mechanism in the POT family of oligopeptide transporters. *Embo j* 2012; **31**: 3411-21.
85. Harder D, Stolz J, Casagrande F *et al.* DtpB (YhiP) and DtpA (TppB, YdgR) are prototypical proton-dependent peptide transporters of *Escherichia coli*. *FEBS J.* 2008; **275**: 3290-3298.
86. Ernst HA, Pham A, Hald H *et al.* Ligand binding analyses of the putative peptide transporter YjdL from *E. coli* display a significant selectivity towards dipeptides. *Biochem.Biophys.Res.Commun.* 2009; **389**: 112-116.
87. Casagrande F, Harder D, Schenk A *et al.* Projection structure of DtpD (YbgH), a prokaryotic member of the peptide transporter family. *J Mol Biol* 2009; **394**: 708-17.
88. Taber HW, Mueller JP, Miller PF *et al.* Bacterial uptake of aminoglycoside antibiotics. *Microbiol.Rev.* 1987; **51**: 439-457.
89. Andry K, Bockrath RC. Dihydrostreptomycin accumulation in *E. coli*. *Nature* 1974; **251**: 534-6.
90. Hancock RE, Bell A. Antibiotic uptake into gram-negative bacteria. *Eur.J.Clin.Microbiol.Infect.Dis.* 1988; **7**: 713-720.
91. Vaara M, Vaara T. Polycations sensitize enteric bacteria to antibiotics. *Antimicrob Agents Chemother* 1983; **24**: 107-13.
92. Bryan LE, Van Den Elzen HM. Effects of membrane-energy mutations and cations on streptomycin and gentamicin accumulation by bacteria: a model for entry of streptomycin and gentamicin in susceptible and resistant bacteria. *Antimicrob.Agents Chemother.* 1977; **12**: 163-177.
93. Bryan LE, Kwan S. Roles of ribosomal binding, membrane potential, and electron transport in bacterial uptake of streptomycin and gentamicin. *Antimicrob.Agents Chemother.* 1983; **23**: 835-845.
94. Damper PD, Epstein W. Role of the membrane potential in bacterial resistance to aminoglycoside antibiotics. *Antimicrob.Agents Chemother.* 1981; **20**: 803-808.
95. Eisenberg ES, Mandel LJ, Kaback HR *et al.* Quantitative association between electrical potential across the cytoplasmic membrane and early gentamicin uptake and killing in *Staphylococcus aureus*. *J Bacteriol* 1984; **157**: 863-7.
96. Schlessinger D. Failure of aminoglycoside antibiotics to kill anaerobic, low-pH, and resistant cultures. *Clin.Microbiol.Rev.* 1988; **1**: 54-59.

97. Kashiwagi K, Miyaji A, Ikeda S *et al.* Increase of sensitivity to aminoglycoside antibiotics by polyamine-induced protein (oligopeptide-binding protein) in *Escherichia coli*. *J.Bacteriol.* 1992; **174**: 4331-4337.
98. Kashiwagi K, Tsuchioka MH, Sakata K *et al.* Relationship between spontaneous aminoglycoside resistance in *Escherichia coli* and a decrease in oligopeptide binding protein. *J.Bacteriol.* 1998; **180**: 5484-5488.
99. Bryan LE, Van den Elzen HM. Streptomycin accumulation in susceptible and resistant strains of *Escherichia coli* and *Pseudomonas aeruginosa*. *Antimicrob Agents Chemother* 1976; **9**: 928-38.
100. Busse HJ, Wostmann C, Bakker EP. The bactericidal action of streptomycin: membrane permeabilization caused by the insertion of mistranslated proteins into the cytoplasmic membrane of *Escherichia coli* and subsequent caging of the antibiotic inside the cells due to degradation of these proteins. *J.Gen.Microbiol.* 1992; **138**: 551-561.
101. Thanassi DG, Suh GS, Nikaido H. Role of outer membrane barrier in efflux-mediated tetracycline resistance of *Escherichia coli*. *J Bacteriol* 1995; **177**: 998-1007.
102. Chopra I, Hawkey PM, Hinton M. Tetracyclines, molecular and clinical aspects. *J Antimicrob Chemother* 1992; **29**: 245-77.
103. Nikaido H, Thanassi DG. Penetration of lipophilic agents with multiple protonation sites into bacterial cells: tetracyclines and fluoroquinolones as examples. *Antimicrob.Agents Chemother.* 1993; **37**: 1393-1399.
104. Argast M, Beck CF. Tetracycline diffusion through phospholipid bilayers and binding to phospholipids. *Antimicrob Agents Chemother* 1984; **26**: 263-5.
105. Yamaguchi A, Ohmori H, Kaneko-Ohdera M *et al.* Delta pH-dependent accumulation of tetracycline in *Escherichia coli*. *Antimicrob.Agents Chemother.* 1991; **35**: 53-56.
106. Wilks JC, Slonczewski JL. pH of the cytoplasm and periplasm of *Escherichia coli*: rapid measurement by green fluorescent protein fluorimetry. *J Bacteriol* 2007; **189**: 5601-7.
107. Slonczewski JL, Rosen BP, Alger JR *et al.* pH homeostasis in *Escherichia coli*: measurement by ³¹P nuclear magnetic resonance of methylphosphonate and phosphate. *Proc Natl Acad Sci U S A* 1981; **78**: 6271-5.
108. Carlotti B, Cesaretti A, Elisei F. Complexes of tetracyclines with divalent metal cations investigated by stationary and femtosecond-pulsed techniques. *Phys Chem Chem Phys* 2012; **14**: 823-34.
109. Lecomte S, Baron MH, Chenon MT *et al.* Effect of magnesium complexation by fluoroquinolones on their antibacterial properties. *Antimicrob Agents Chemother* 1994; **38**: 2810-6.
110. Cohen SP, Hooper DC, Wolfson JS *et al.* Endogenous active efflux of norfloxacin in susceptible *Escherichia coli*. *Antimicrob Agents Chemother* 1988; **32**: 1187-91.
111. Piddock LJ, Jin YF, Ricci V *et al.* Quinolone accumulation by *Pseudomonas aeruginosa*, *Staphylococcus aureus* and *Escherichia coli*. *J.Antimicrob.Chemother.* 1999; **43**: 61-70.
112. Kondo S, Yoshida K, Ikeda T *et al.* 3-epi-deoxynegamycin and leucyl-3-epi-deoxynegamycin produced by *Streptomyces*. *J Antibiot (Tokyo)* 1977; **30**: 1137-9.
113. Maehr H, Smallheer J, Chin M *et al.* Microbial products. III Epi-deoxynegamycin from a *Micromonospora*. *J Antibiot (Tokyo)* 1979; **32**: 531-2.
114. McKinney DC, Bezdenezhnik-Snyder N, Farrington K *et al.* Illicit Transport via the Dipeptide Transporter Dpp is Irrelevant to Efficacy of Negamycin in Mouse Thigh Models of *Escherichia coli* Infection. *ACS Infectious Diseases* 2015.

115. Chen D, Tembe V, Press B *et al.*, *F-1683 In Vivo Evaluation of VRC4219, A New Bactericidal Protein Synthesis Inhibitor Antibiotic*, in ICAAC. 2003: Chicago.
116. Raju B, Mortell K, Anandan S *et al.* N- and C-terminal modifications of negamycin. *Bioorg Med Chem Lett* 2003; **13**: 2413-8.
117. Raju B, Anandan S, Gu S *et al.* Conformationally restricted analogs of deoxynegamycin. *Bioorg Med Chem Lett* 2004; **14**: 3103-7.
118. Raju B, Gu S, Gómez M *et al.*, *F-1686 Fluorinated Deoxynegamycin Analogs: Synthesis and Antimicrobial Properties*, in ICAAC. 2003: Chicago.
119. Streicher W, Reinshagen H, Turnowsky F. Total synthesis of rac. negamycin and of negamycin analogs. *J Antibiot (Tokyo)* 1978; **31**: 725-8.
120. Uehara Y, Hori M, Kondo S *et al.* Structure-activity relationships among negamycin analogs. *J Antibiot (Tokyo)* 1976; **29**: 937-43.
121. McKinney DC, Basarab GS, Cocozaki AI *et al.* Structural Insights Lead to a Negamycin Analogue with Improved Antimicrobial Activity against Gram-Negative Pathogens. *ACS Med Chem Lett* 2015; **6**: 930-5.
122. Schroeder SJ, Blaha G, Moore PB. Negamycin binds to the wall of the nascent chain exit tunnel of the 50S ribosomal subunit. *Antimicrob Agents Chemother* 2007; **51**: 4462-5.
123. Arakawa M, Shiozuka M, Nakayama Y *et al.* Negamycin restores dystrophin expression in skeletal and cardiac muscles of mdx mice. *J Biochem* 2003; **134**: 751-8.
124. Mendell JT, Dietz HC. When the message goes awry: disease-producing mutations that influence mRNA content and performance. *Cell* 2001; **107**: 411-4.
125. Floquet C, Rousset JP, Bidou L. Readthrough of premature termination codons in the adenomatous polyposis coli gene restores its biological activity in human cancer cells. *PLoS One* 2011; **6**: e24125.
126. Rafanan N, Margolis P, Kubo A *et al.*, *F-1682 Resistance to VRC4219 in Escherichia coli*, in ICAAC 2003: Chicago.
127. Katayama N, Nozaki Y, Tsubotani S *et al.* Sperabillins, new antibacterial antibiotics with potent in vivo activity. Taxonomy, fermentation, isolation and biological activity. *J Antibiot (Tokyo)* 1992; **45**: 10-9.
128. Harada S, Ono H, *Antibiotic tan-749, production and use thereof*. 1992, Google Patents.
129. Hida T, Tsubotani S, Funabashi Y *et al.* Structures of New Pseudo-Peptide Antibiotics, Sperabillins. *Bulletin of the Chemical Society of Japan* 1993; **66**: 863-869.
130. Hashiguchi S, Kawada A, Natsugari H. Stereoselective synthesis of sperabillins and related compounds. *Journal of the Chemical Society, Perkin Transactions 1* 1991: 2435-2444.
131. Hida T, Tsubotani S, Katayama N *et al.* Synthesis and antimicrobial activity of sperabillin derivatives. *J Antibiot (Tokyo)* 1993; **46**: 803-12.
132. Takizawa M, Hida T, Harada S *et al.* Augmentation of host defense mechanisms against tumor by sperabillin polymers, new basic peptidyl biopolymers, in mice. *Int J Immunopharmacol* 1994; **16**: 67-74.
133. Hida T, Tsubotani S, Hori A *et al.* Chemistry and anti-tumor activity of sperabillin polymers. *Chem Pharm Bull (Tokyo)* 1993; **41**: 889-93.
134. Shulman ST, Friedmann HC, Sims RH. Theodor Escherich: the first pediatric infectious diseases physician? *Clin Infect Dis* 2007; **45**: 1025-9.
135. Reece JB, *Campbell Biology (9th Edition)*. Campbell Biology, ed. B. Wilbur. Vol. 9. 2010, Glenview, United States: Benjamin Cummings. 1464.

136. Bentley R, Meganathan R. Biosynthesis of vitamin K (menaquinone) in bacteria. *Microbiol Rev* 1982; **46**: 241-80.
137. Kaper JB, Nataro JP, Mobley HL. Pathogenic Escherichia coli. *Nat Rev Microbiol* 2004; **2**: 123-40.
138. Schultsz C, Geerlings S. Plasmid-mediated resistance in Enterobacteriaceae: changing landscape and implications for therapy. *Drugs* 2012; **72**: 1-16.
139. Blattner FR, Plunkett G, 3rd, Bloch CA *et al*. The complete genome sequence of Escherichia coli K-12. *Science* 1997; **277**: 1453-62.
140. Urban A, Eckermann S, Fast B *et al*. Novel whole-cell antibiotic biosensors for compound discovery. *Appl Environ Microbiol* 2007; **73**: 6436-43.
141. Datsenko KA, Wanner BL. One-step inactivation of chromosomal genes in Escherichia coli K-12 using PCR products. *Proc.Natl.Acad.Sci.U.S.A* 2000; **97**: 6640-6645.
142. Neely MN, Dell CL, Olson ER. Roles of LysP and CadC in mediating the lysine requirement for acid induction of the Escherichia coli cad operon. *J Bacteriol* 1994; **176**: 3278-85.
143. Soksawatmaekhin W, Kuraishi A, Sakata K *et al*. Excretion and uptake of cadaverine by CadB and its physiological functions in Escherichia coli. *Mol Microbiol* 2004; **51**: 1401-12.
144. Neely MN, Olson ER. Kinetics of expression of the Escherichia coli cad operon as a function of pH and lysine. *J Bacteriol* 1996; **178**: 5522-8.
145. Moussatova A, Kandt C, O'Mara ML *et al*. ATP-binding cassette transporters in Escherichia coli. *Biochim.Biophys.Acta* 2008; **1778**: 1757-1771.
146. Straus SK, Hancock RE. Mode of action of the new antibiotic for Gram-positive pathogens daptomycin: comparison with cationic antimicrobial peptides and lipopeptides. *Biochim Biophys Acta* 2006; **1758**: 1215-23.
147. Muller A, Munch D, Schmidt Y *et al*. Lipodepsipeptide empedopeptin inhibits cell wall biosynthesis through Ca²⁺-dependent complex formation with peptidoglycan precursors. *J Biol Chem* 2012; **287**: 20270-80.
148. Tisa LS, Adler J. Cytoplasmic free-Ca²⁺ level rises with repellents and falls with attractants in Escherichia coli chemotaxis. *Proc Natl Acad Sci U S A* 1995; **92**: 10777-81.
149. Watkins NJ, Knight MR, Trewavas AJ *et al*. Free calcium transients in chemotactic and non-chemotactic strains of Escherichia coli determined by using recombinant aequorin. *Biochem J* 1995; **306 (Pt 3)**: 865-9.
150. Norris V, Grant S, Freestone P *et al*. Calcium signalling in bacteria. *J.Bacteriol.* 1996; **178**: 3677-3682.
151. Kondo S, Shibahara S, Takahashi S *et al*. Negamycin, a novel hydrazide antibiotic. *J Am Chem Soc* 1971; **93**: 6305-6.
152. Diez-Gonzalez F, Russell JB. Effects of carbonylcyanide-m-chlorophenylhydrazone (CCCP) and acetate on Escherichia coli O157:H7 and K-12: uncoupling versus anion accumulation. *FEMS Microbiol Lett* 1997; **151**: 71-6.
153. Cox GB, Young IG, McCann LM *et al*. Biosynthesis of ubiquinone in Escherichia coli K-12: location of genes affecting the metabolism of 3-octaprenyl-4-hydroxybenzoic acid and 2-octaprenylphenol. *J Bacteriol* 1969; **99**: 450-8.
154. Green GN, Kranz RG, Lorence RM *et al*. Identification of subunit I as the cytochrome b558 component of the cytochrome d terminal oxidase complex of Escherichia coli. *J Biol Chem* 1984; **259**: 7994-7.

155. Elkins CA, Nikaido H. Substrate specificity of the RND-type multidrug efflux pumps AcrB and AcrD of *Escherichia coli* is determined predominantly by two large periplasmic loops. *J Bacteriol* 2002; **184**: 6490-8.
156. de Cristobal RE, Vincent PA, Salomon RA. Multidrug resistance pump AcrAB-TolC is required for high-level, Tet(A)-mediated tetracycline resistance in *Escherichia coli*. *J Antimicrob Chemother* 2006; **58**: 31-6.
157. Wandersman C, Delepelaire P. TolC, an *Escherichia coli* outer membrane protein required for hemolysin secretion. *Proc Natl Acad Sci U S A* 1990; **87**: 4776-80.
158. !!! INVALID CITATION !!!
159. Parker CT, Kloser AW, Schnaitman CA *et al.* Role of the rfaG and rfaP genes in determining the lipopolysaccharide core structure and cell surface properties of *Escherichia coli* K-12. *J Bacteriol* 1992; **174**: 2525-38.
160. Fabrega A, Rosner JL, Martin RG *et al.* SoxS-dependent coregulation of ompN and ydbK in a multidrug-resistant *Escherichia coli* strain. *FEMS Microbiol Lett* 2012; **332**: 61-7.
161. Cohen SP, McMurry LM, Hooper DC *et al.* Cross-resistance to fluoroquinolones in multiple-antibiotic-resistant (Mar) *Escherichia coli* selected by tetracycline or chloramphenicol: decreased drug accumulation associated with membrane changes in addition to OmpF reduction. *Antimicrob Agents Chemother* 1989; **33**: 1318-25.
162. Agafitei O, Kim JE, Maguire T *et al.* The role of *Escherichia coli* porins OmpC and OmpF in antibiotic cross resistance induced by sub-inhibitory concentrations of kanamycin. *Journal of Experimental Microbiology and Immunology (JEMI)* 2010; **14**: 34-39.
163. Piddock LJ. Mechanism of quinolone uptake into bacterial cells. *J Antimicrob Chemother* 1991; **27**: 399-403.
164. Hiron A, Borezee-Durant E, Piard JC *et al.* Only one of four oligopeptide transport systems mediates nitrogen nutrition in *Staphylococcus aureus*. *J. Bacteriol.* 2007; **189**: 5119-5129.
165. Rafanan N, Margolis P, Kubo A *et al.*, *Resistance to VRC4219 in Escherichia coli*, . 2003, Versicor: ICAAC Poster Versicor; . p. F-1682.
166. Mingeot-Leclercq MP, Glupczynski Y, Tulkens PM. Aminoglycosides: activity and resistance. *Antimicrob Agents Chemother* 1999; **43**: 727-37.
167. Chopra I, Roberts M. Tetracycline antibiotics: mode of action, applications, molecular biology, and epidemiology of bacterial resistance. *Microbiol Mol Biol Rev* 2001; **65**: 232-60 ; second page, table of contents.
168. Jones HE, Holland IB, Baker HL *et al.* Slow changes in cytosolic free Ca²⁺ in *Escherichia coli* highlight two putative influx mechanisms in response to changes in extracellular calcium. *Cell Calcium* 1999; **25**: 265-274.
169. Holland IB, Jones HE, Campbell AK *et al.* An assessment of the role of intracellular free Ca²⁺ in *E. coli*. *Biochimie* 1999; **81**: 901-7.
170. Norris V, Seror SJ, Casaregola S *et al.* A single calcium flux triggers chromosome replication, segregation and septation in bacteria: a model. *J Theor Biol* 1988; **134**: 341-50.
171. Tisa LS, Olivera BM, Adler J. Inhibition of *Escherichia coli* chemotaxis by omega-conotoxin, a calcium ion channel blocker. *J Bacteriol* 1993; **175**: 1235-8.
172. O'Hara MB, Hageman JH. Energy and calcium ion dependence of proteolysis during sporulation of *Bacillus subtilis* cells. *J Bacteriol* 1990; **172**: 4161-70.

173. Jung D, Rozek A, Okon M *et al.* Structural transitions as determinants of the action of the calcium-dependent antibiotic daptomycin. *Chem Biol* 2004; **11**: 949-57.
174. Hurwitz C, Rosano CL. The intracellular concentration of bound and unbound magnesium ions in *Escherichia coli*. *J Biol Chem* 1967; **242**: 3719-22.
175. Jin L, Amaya-Mazo X, Apel ME *et al.* Ca²⁺ and Mg²⁺ bind tetracycline with distinct stoichiometries and linked deprotonation. *Biophys.Chem.* 2007; **128**: 185-196.
176. Kung FC, Raymond J, Glaser DA. Metal ion content of *Escherichia coli* versus cell age. *J.Bacteriol.* 1976; **126**: 1089-1095.
177. Gangola P, Rosen BP. Maintenance of intracellular calcium in *Escherichia coli*. *J.Biol.Chem.* 1987; **262**: 12570-12574.
178. Ghouil M, Pommepuy M, Moillo-Batt A *et al.* Effect of carbonyl cyanide m-chlorophenylhydrazone on *Escherichia coli* halotolerance. *Appl.Environ.Microbiol.* 1989; **55**: 1040-1043.
179. Zgurskaya HI, Nikaido H. Multidrug resistance mechanisms: drug efflux across two membranes. *Mol Microbiol* 2000; **37**: 219-25.
180. Li XZ, Livermore DM, Nikaido H. Role of efflux pump(s) in intrinsic resistance of *Pseudomonas aeruginosa*: resistance to tetracycline, chloramphenicol, and norfloxacin. *Antimicrob Agents Chemother* 1994; **38**: 1732-41.
181. Li XZ, Nikaido H. Efflux-mediated drug resistance in bacteria. *Drugs* 2004; **64**: 159-204.
182. Speer BS, Shoemaker NB, Salyers AA. Bacterial resistance to tetracycline: mechanisms, transfer, and clinical significance. *Clin Microbiol Rev* 1992; **5**: 387-99.
183. Markham PN, Neyfakh AA. Efflux-mediated drug resistance in Gram-positive bacteria. *Curr Opin Microbiol* 2001; **4**: 509-14.
184. Ma D, Cook DN, Alberti M *et al.* Genes *acrA* and *acrB* encode a stress-induced efflux system of *Escherichia coli*. *Mol Microbiol* 1995; **16**: 45-55.
185. Nikaido H, Zgurskaya HI. AcrAB and related multidrug efflux pumps of *Escherichia coli*. *J Mol Microbiol Biotechnol* 2001; **3**: 215-8.
186. Saier MH, Jr., Tam R, Reizer A *et al.* Two novel families of bacterial membrane proteins concerned with nodulation, cell division and transport. *Mol Microbiol* 1994; **11**: 841-7.
187. Dinh T, Paulsen IT, Saier MH, Jr. A family of extracytoplasmic proteins that allow transport of large molecules across the outer membranes of gram-negative bacteria. *J Bacteriol* 1994; **176**: 3825-31.
188. Anagnostopoulos C, Spizizen J. REQUIREMENTS FOR TRANSFORMATION IN *BACILLUS SUBTILIS*. *J Bacteriol* 1961; **81**: 741-6.
189. Piggot PJ. Mapping of asporogenous mutations of *Bacillus subtilis*: a minimum estimate of the number of sporeulation operons. *J Bacteriol* 1973; **114**: 1241-53.
190. Smith I, Pares P, Cabane K *et al.* Genetics and physiology of the *rel* system of *Bacillus subtilis*. *Mol Gen Genet* 1980; **178**: 271-9.
191. Baba T, Ara T, Hasegawa M *et al.* Construction of *Escherichia coli* K-12 in-frame, single-gene knockout mutants: the Keio collection. *Mol Syst Biol* 2006; **2**: 2006.0008.
192. Gray CH, Tatum EL. X-Ray Induced Growth Factor Requirements in Bacteria. *Proc Natl Acad Sci U S A* 1944; **30**: 404-10.
193. CLSI, *Performance standards for antimicrobial disk susceptibility tests: approved standard (M2-A9) in Performance Standards for Antimicrobial Disk Susceptibility Tests; Approved Standard -*. 2006, Clinical and Laboratory Standards Institute (CLSI): Wayne, Pennsylvania.

194. Branlant C, Krol A, Machatt MA *et al.* Primary and secondary structures of *Escherichia coli* MRE 600 23S ribosomal RNA. Comparison with models of secondary structure for maize chloroplast 23S rRNA and for large portions of mouse and human 16S mitochondrial rRNAs. *Nucleic Acids Res* 1981; **9**: 4303-24.
195. Cox GB, Young IG, McCann LM *et al.* Biosynthesis of ubiquinone in *Escherichia coli* K-12: location of genes affecting the metabolism of 3-octaprenyl-4-hydroxybenzoic acid and 2-octaprenylphenol. *J.Bacteriol.* 1969; **99**: 450-458.
196. Green GN, Kranz RG, Lorence RM *et al.* Identification of subunit I as the cytochrome b558 component of the cytochrome d terminal oxidase complex of *Escherichia coli*. *J.Biol.Chem.* 1984; **259**: 7994-7997.
197. Kim EB, Kopit LM, Harris LJ *et al.* Draft genome sequence of the quality control strain *Enterococcus faecalis* ATCC 29212. *J Bacteriol* 2012; **194**: 6006-7.
198. Holloway BW. Genetic recombination in *Pseudomonas aeruginosa*. *J Gen Microbiol* 1955; **13**: 572-81.
199. Rogers DE, Melly MA. Further observations on the behavior of staphylococci within human leukocytes. *J Exp Med* 1960; **111**: 533-58.
200. Sanger F, Nicklen S, Coulson AR. DNA sequencing with chain-terminating inhibitors. *Proc Natl Acad Sci U S A* 1977; **74**: 5463-7.
201. Mullis KB, Faloona FA. Specific synthesis of DNA in vitro via a polymerase-catalyzed chain reaction. *Methods Enzymol* 1987; **155**: 335-50.
202. Livak KJ, Schmittgen TD. Analysis of relative gene expression data using real-time quantitative PCR and the 2(-Delta Delta C(T)) Method. *Methods* 2001; **25**: 402-8.
203. Cammack KA, Wade HE. The sedimentation behaviour of ribonuclease-active and -inactive ribosomes from bacteria. *Biochem J* 1965; **96**: 671-80.
204. Wade HE, Robinson HK. Magnesium ion-independent ribonucleic acid depolymerases in bacteria. *Biochem J* 1966; **101**: 467-79.
205. Wade HE, Robinson HK. The distribution of ribosomal ribonucleic acids among subcellular fractions from bacteria and the adverse effect of the membrane fraction on the stability of ribosomes. *Biochem J* 1965; **96**: 753-65.


```

# Gaps:          18/550 (3.3%)
# Score: 939.5
#
#
#=====
SapA          1 MRQVL--SLLLVIAGLVSGQAIAPESPAPHADIRDSGFVYCVSQVNTFN      48
|.|.| |.:|.:|.:|.:|.:|.:|.:|.:|.:|.:|.:|.:|.:|.:|.:|
DppA          1 MRISLKKSGMLKLGSLVAMTVA-----ASVQAKTLVYCSEGSPEGFN      43

SapA          49 PSKASSGLIVDTLAAQFYDRLLDVPYTYRLMPELAESWEVLDNGATYRF      98
|.:|.:|.:|.:|.:|.:|.:|.:|.:|.:|.:|.:|.:|.:|.:|
DppA          44 PQLFTSGTTYDASSVPLYNRLVEFKIGTTEVIPGLAEKWEVSEDGKTYTF      93

SapA          99 HLRRDVPFQKTDWFTPTRKMNADDVVFTFQRFDRNNPWHNVNGSNFPYF     148
|.|.:|.:|.:|.:|.:|.:|.:|.:|.:|.:|.:|.:|.:|.:|.:|
DppA          94 HLRKGVKWHDNKEFKPTRELNADDVVFSDRQKNAQNPYHKVSGGSYEYF     143

SapA          149 DSLQFADNVKSVRKLDNHTVEFRLAQPDAFLWHLATHYASVMSAEYARK     198
.:|.:|.:|.:|.:|.:|.:|.:|.:|.:|.:|.:|.:|.:|.:|
DppA          144 EGMGLPELISEVKKVDDNTVQFVLTREAPFLADLAMDFASILSKEYADA     193

SapA          199 LEKEDRQEQQLDRQPVGTGQPYQLSEYRAGQFIRLQRHDDFWRGKPLMPQVV   248
.:|.:|.:|.:|.:|.:|.:|.:|.:|.:|.:|.:|.:|.:|.:|
DppA          194 MMKAGTPEKLDLNPIGTGPFQQLQYQKDSRIRYKAFDGYWGTQPKQIDTLV   243

SapA          249 VDLGSGGTGRSLKLLTGECVDLAWPAASQLSILRDDPRLRLTLRPGMNVA     298
.:|.:|.:|.:|.:|.:|.:|.:|.:|.:|.:|.:|.:|.:|.:|
DppA          244 FSITPDASVRYAKLQKNECQVMPYPNPADIARMKQDKSINLMEMPGLNVG     293

SapA          299 YLAFNTAKPPLNNPAVRHALALAINNQRLMQSIYYGTAETAASILPRASW     348
|.:|.:|.:|.:|.:|.:|.:|.:|.:|.:|.:|.:|.:|.:|.:|
DppA          294 YLSYNVQKKPLDDVKVRQALTYAVNKDAIIKAVYQGAGVSAKNLIPTMW     343

SapA          349 AYDNEAKITEYNPAKSREQLKSLGLE-NLTLKLWVPTRSQAWNPSPLKTA     397
.:|.:|.:|.:|.:|.:|.:|.:|.:|.:|.:|.:|.:|.:|.:|
DppA          344 GYNDDVQDYTYDPEKAKALLKEAGLEKGFSIDLWAMPVQRPYNPNARRMA     393

SapA          398 ELIQADMAQVGVKVVIVPVEGRFQEARLMDMSHDLTSLGWATDSNDPDSF     447
|.:|.:|.:|.:|.:|.:|.:|.:|.:|.:|.:|.:|.:|.:|.:|
DppA          394 EMIQADWAKVGVQAKIVTYEWGEYLKRAKDGEHQTVMMGWTGDNGDPDNF     443

SapA          448 FRPLLSCAAIIHSQTNLAHWCDPKFDSVLRKALSSQQLAARIEAYDEAQS I     497
|.:|.:|.:|.:|.:|.:|.:|.:|.:|.:|.:|.:|.:|.:|.:|
DppA          444 FATLFSCAAASEQGSNYKWCYKPFEDLIQPARATDDHNKRVELYKQAQVV     493

SapA          498 LAQELPILPLASSRLQAYRYDIKGLVLSFPGNASFAGVYREKQDEVKPKP     547
.:|.:|.:|.:|.:|.:|.:|.:|.:|.:|.:|.:|.:|.:|.:|
DppA          494 MHDQAPALIIAHSTVFEPVRKEVKGYVVDPLGKHHFENVVSI-----     535

```

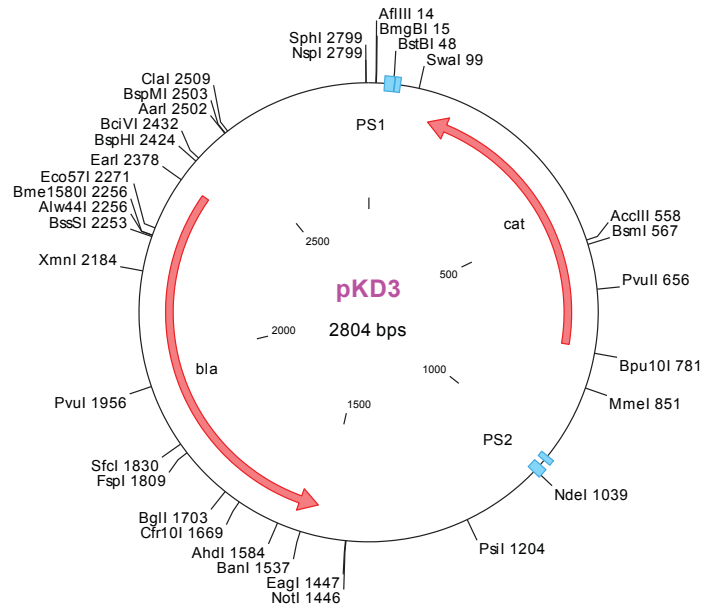
Alignment OppA and SapA

```

#####
# Program: needle
# Rundate: Wed 31 Jul 2013 11:44:25
# Commandline: needle
# -auto
# -stdout
# -asequence emboss_needle-I20130731-114424-0707-55783646-oy.asequence
# -bsequence emboss_needle-I20130731-114424-0707-55783646-oy.bsequence
# -datafile EBLOSUM62
# -gapopen 10.0
# -gapextend 0.5
# -endopen 10.0
# -endextend 0.5

```

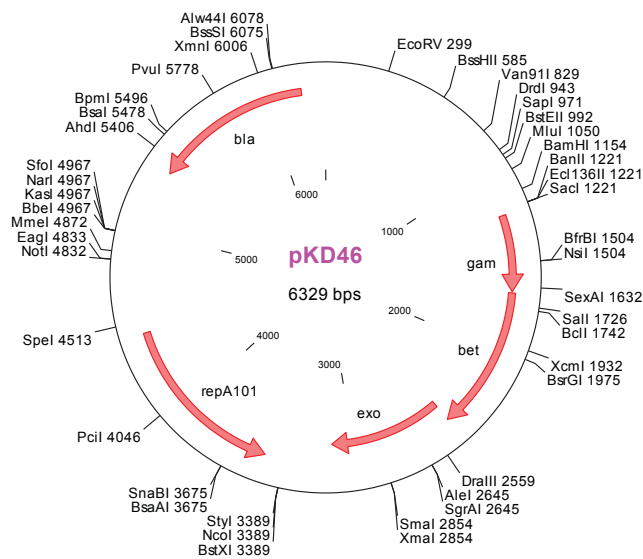

Plasmid-maps

pKD3

AGATTGCAGCATTACACGTCTTGAGCGATTGTGTAGGCTGGAGCTGCTTCGAAGTTCTATACTTTCTAGAGAATAGGAAC
TTCGGAATAGGAACTTCATTTAAATGGCGCGCCTTACGCCCCGCCCTGCCACTCATCGCAGTACTGTTGTATTCATTAAGCA
TCTGCCGACATGGAAGCCATCACAAACGGCATGATGAACCTGAATCGCCAGCGGCATCAGCACCTTGTCGCCTTGCGTATA
ATATTTGCCCATGGTAAAACGGGGCGAAGAAGTTGTCCATATTGGCCACGTTTAAATCAAACCTGGTGAACTCACCCA
GGGATTGGCTGAGACGAAAAACATATTCTCAATAAACCTTTAGGGAAATAGGCCAGGTTTTACCGTAACACGCCACATC
TTGCCAATATATGTGTAGAACTGCCGAAATCGTCGTGGTATTCACTCCAGAGCGATGAAAACGTTTCAGTTTGCTCATG
GAAAACGGTGAACAAGGGTGAACACTATCCCATATCACCAGCTCACCGTCTTTATTGCCATACGTAATTCGGATGAGC
ATTCATCAGGCGGGCAAGAATGTGAATAAAGGCCGATAAAACTTGTGCTTATTTTTCTTTACGGTCTTTAAAAAGGCCGT
AATATCCAGCTGAACGGTCTGGTTATAGGTACATTGAGCAACTGACTGAAATGCCTCAAATGTTCTTTACGATGCCATTG
GGATATATCAACGGTGGTATATCCAGTGATTTTTTTCTCATTTTAGCTTCCTTAGCTCCTGAAAATCTCGACAACTCAAAAA
ATACGCCCGGTAGTGATCTTATTTTATTATGGTGAAGTTGGAACCTTACGTGCCGATCAACGTCTCATTTCGCCAAAA
GTTGGCCAGGGCTTCCCGGTATCAACAGGGACACCAGGATTTATTTATTCTGCGAAGTGATCTTCCGTCACAGGTAGGCG
CGCCGAAGTTCCTATACTTTCTAGAGAATAGGAACTTCGGAATAGGAACTAAGGAGGATATTCATATGGACCATGGCTAAT
TCCATGTCAGCCGTTAAGTGTTCTGTGTCCTACTGAAAATTGCTTTGAGAGGCTCTAAGGGCTTCTCAGTGCGTTACATCCC
TGGCTTGTGTCACAACCGTTAAACCTTAAAAGCTTTAAAAGCCTTATATATTCTTTTTTTCTTATAAACTTAAAACCTTA
GAGGCTATTTAAGTTGCTGATTTATATTAATTTTATTGTTCAAACATGAGAGCTTAGTACGTGAAACATGAGAGCTTAGTAC
GTTAGCCATGAGAGCTTAGTACGTTAGCCATGAGGGTTTAGTTCGTTAAACATGAGAGCTTAGTACGTTAAACATGAGAG
CTTAGTACGTGAAACATGAGAGCTTAGTACGTAATCAACAGGTTGAACTGCGGATCTTGCGGCCGCAAAAATTAATAAAT
GAAGTTTTAAATCAATCTAAAGTATATATGAGTAACTTGGTCTGACAGTTACCAATGCTTAATCAGTGAGGCACCTATCTC
AGCGATCTGTCTATTTTCGTTTCATCCATAGTTGCCTGACTCCCCGTCGTGTAGATAACTACGATACGGGAGGGCTTACCATCT
GGCCCCAGTGCTGCAATGATACCGCGAGACCCACGCTCACCAGGCTCCAGATTTATCAGCAATAAACCAGCCAGCCGGAAG
GGCCGAGCGCAGAAGTGGTCTGCAACTTTATCCGCCTCCATCCAGTCTATTAATTGTTGCCGGAAGCTAGAGTAAGTAG
TTCGCCAGTTAATAGTTTGCACAACGTTGTTGCCATTGCTACAGGCATCGTGGTGTACGCTCGTCTTGGTATGGCTTCA

TTCAGCTCCGGTCCCAACGATCAAGGCGAGTTACATGATCCCCATGTTGTGCAAAAAAGCGGTTAGCTCCTTCGGTCCTC
 CGATCGTTGTCAGAAGTAAGTTGGCCGAGTGTATCACTCATGGTTATGGCAGCACTGCATAATTCTTACTGTCATGCC
 ATCCGTAAGATGCTTTTCTGTGACTGGTGAAGTACTCAACCAAGTATTCTGAGAATAGTGTATGCGGCGACCGAGTTGCTC
 TTGCCGCGGTCAATACGGGATAATACCGCGCCACATAGCAGAACTTTAAAAGTGCTCATCATTGGAAAACGTTCTTCGGG
 GCGAAAACCTCAAGGATCTTACCGCTGTTGAGATCCAGTTCGATGTAACCCACTCGTGCACCAACTGATCTTCAGCATCT
 TTTACTTTACCAGCGTTTCTGGGTGAGCAAAAACAGGAAGGCAAAATGCCGCAAAAAAGGGAATAAGGGCGACACGGA
 AATGTTGAATACTCATACTCTTCTTTTCAATATTATTGAAGCATTATCAGGGTATTGTCTCATGAGCGGATACATATT
 GAATGTATTAGAAAAATAACAAATAGGGGTTCCGCGCACATTTCCCGAAAAGTGCCACCTGCATCGATGGCCCCCGA
 TGGTAGTGTGGGGTCTCCCATGCGAGAGTAGGGAAGTCCAGGCATCAAATAAACGAAAAGGCTCAGTCGAAAGACTG
 GGCCTTCGTTTTATCTGTTGTTTGTGGTGAACGCTCTCTGAGTAGGACAAATCCGCCGGGAGCGGATTTGAACGTTGC
 GAAGCAACGGCCCGGAGGGTGGCGGGCAGGACGCCGCCATAAACTGCCAGGCATCAAATTAAGCAGAAGGCCATCTGC
 ACGGATGGCCTTTTTCGCTGGCCAGTGCCAAGCTTGCATGC

pKD46

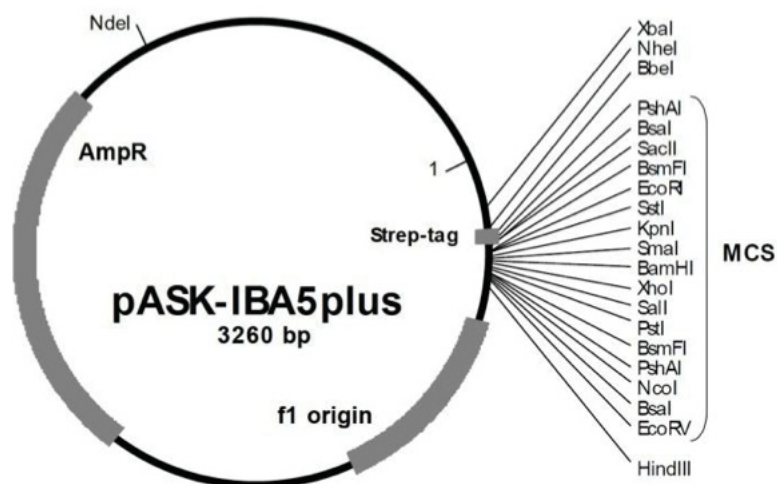


CATCGATTTATTATGACAACCTTGACGGCTACATCATTCACTTTTTCTTACAACCGGCACGGAACTCGCTCGGGCTGGCCCC
 GGTGCATTTTTTAAATACCCGCGAGAAATAGAGTTGATCGTCAAACCAACATTGCGACCGACGGTGGCGATAGGCATCC
 GGGTGGTGCTCAAAGCAGCTTCGCCTGGTGATACGTTGGTCTCGCGCCAGCTTAAGACGCTAATCCCTAACTGCTGGC
 GGAAAAGATGTGACAGACGCGACGGCGACAAGCAAACATGCTGTGCGACGCTGGCGATATCAAATTTGCTGTCTGCCAG
 GTGATCGCTGATGTAAGCAAGCCTCGGTACCCGATTATCCATCGGTGGATGGAGCGACTCGTTAATCGCTTCCATGCG
 CCGCAGTAAACAATTGCTCAAGCAGATTTATCGCCAGCAGCTCCGAATAGCGCCCTTCCCCTTGGCCGGCGTTAATGATTTGC
 CCAAACAGTTCGCTGAAATGCGGCTGGTGGCTTTCATCCGGGCGAAAGAACCCCGTATTGGCAAATATTGACGGCCAGTT
 AAGCCATTCATGCCAGTAGGCGCGCGGACGAAAGTAAACCCACTGGTGATACCATTGCGGAGCCTCCGGATGACGACCGT
 AGTGATGAATCTCTCTGGCGGGAACAGCAAATATCACCCGGTGGCAAACAAATTCTGTCCTGATTTTTACCACCCC
 CTGACCGCAATGGTGGAGATTGAGAATATAACCTTTTATTCCAGCGGTGGTGGATAAAAAAATCGAGATAACCGTTGG
 CCTCAATCGGCGTTAAACCCGCCACCAGATGGGCATTAACGAGTATCCCGGACGAGGGGATCATTTTTCGCTTACGCCA
 TACTTTTCACTCCCGCCATTAGAGAAGAAACCAATTGTCATATTGCATCAGACATTGCCGTCACTGCGTCTTTTACTGG
 CTCTTCTCGTAACCAAACCGGTAACCCGCTTATTAAGCATTCTGTAACAAAGCGGGACCAAAGCCATGACAAAAACG
 CGTAACAAAAGTGTCTATAATCACGGCAGAAAAGTCCACATTGATTATTTGCACGGCGTACACTTTTGTATGCCATAGCAT
 TTTTATCCATAAGATTAGCGGATCTACCTGACGCTTTTTATCGCAACTCTACTGTTTCTCCATACCCGTTTTTTGGGAAT

CCTATCTCAGCGATCTGTCTATTTGTTTCATCCATAGTTGCCTGACTCCCCGTCGTGTAGATAACTACGATACGGGAGGGCT
TACCATCTGGCCCCAGTGCTGCAATGATACCGCGAGACCCACGCTCACGGGCTCCAGATTTATCAGCAATAAACCAGCCAG
CCGGAAGGGCCGAGCGCAGAAGTGGTCTGCAACTTTATCCGCTCCATCCAGTCTATTAATTGTTGCCGGGAAGCTAGA
GTAAGTAGTTCGCCAGTTAATAGTTTGCGCAACGTTGTTGCCATTGCTACAGGCATCGTGGTGTACGCTCGTCGTTTGGT
ATGGCTTCATTCAGCTCCGGTCCCAACGATCAAGGCGAGTTACATGATCCCCATGTTGTGCAAAAAAGCGGTTAGCTCC
TTCGGTCTCCGATCGTTGTGAGAAGTAAGTTGGCCGAGTGTATCACTCATGGTTATGGCAGCACTGCATAATTCTCTTA
CTGTCATGCCATCCGTAAGATGCTTTTCTGTGACTGGTGAGTACTCAACCAAGTCATTCTGAGAATAGTGTATGCGGCGAC
CGAGTTGCTCTTGCCCGGCTCAATACGGGATAATACCGCGCCACATAGCAGAACTTTAAAAGTGCTCATCATTGGAAAAC
GTTCTTCGGGGCGAAAACCTCTCAAGGATCTTACCGCTGTTGAGATCCAGTTCGATGTAACCCACTCGTGCACCCAAGTAT
CTTCAGCATCTTTACTTTACCAGCGTTTCTGGGTGAGCAAAAACAGGAAGGCAAAATGCCGAAAAAAGGGAATAAGG
GCGACACGGAAATGTTGAATACTCATACTCTTCTTTTCAATATTATTGAAGCATTTATCAGGGTTATTGTCTCATGAGCG
GATACATATTTGAATGTATTTAGAAAAATAACAAATAGGGGTTCCGCGCACATTTCCCCGAAAAGTGCCACCTG

pASK-IBA5plus

The pASK-IBA5plus vector allows the expression of Strep-tag[®]-fusion-proteins in E.coli. pASK-IBA5plus carries inducible tetracycline promoter, which ensures a regulated expression of proteins. Furthermore it carries a Strep-tag[®] for N-terminal fusion to the recombinant protein and the Ampicillin Resistance cassette

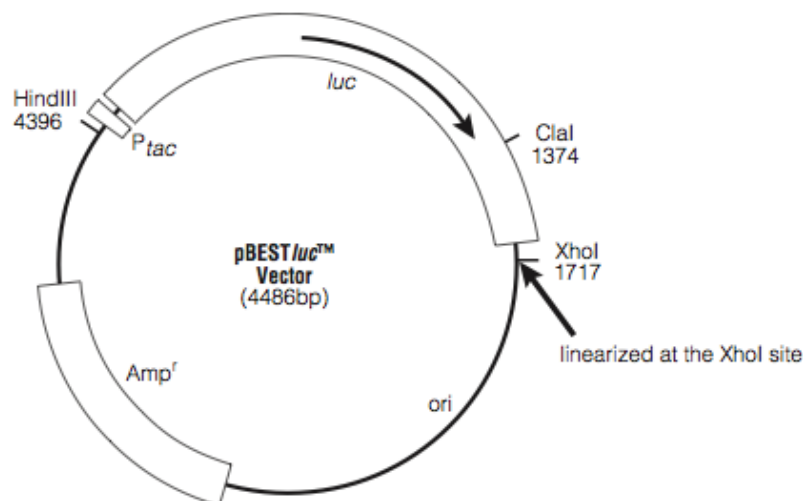


promoter from bp 37 to 72
forward primer binding site from bp 57 to 76
Strep -tag[®] from bp 160 to 192
multiple cloning site from bp 193 to 274
reverse primer binding site from bp 342 to 358
f1 origin from bp 371 to 809
AmpR resistance gene from bp 958 to 1818
tet-repressor from bp 1828 to 2451

CCATCGAATGGCCAGATGATTAATTCCTAATTTTTGTTGACACTCTATCATTGATAGAGTTATTTTACCACTCCCTATCAGTG
ATAGAGAAAAGTGAAATGAATAGTTCGACAAAAAATCTAGAAATAATTTGTTTAACTTTAAGAAGGAGATATCAAAATGG
CTAGCTGGAGCCACCCGAGTTCGAAAAAGGCGCGGAGACCGCGGTCCCGAATTCGAGCTCGGTACCCGGGGATCCCTCG
AGGTCGACCTGCAGGGGGACCATGGTCTCTGATATCTAACTAAGCTTGACCTGTGAAGTAAAAATGGCGCACATTGTGC
GACATTTTTTTTTGTCTGCCGTTTACCGTACTGCGTCACGGATCTCCACGCGCCCTGTAGCGGGCGATTAAGCGCGGGGG
TGTGGTGGTTACGCGCAGCGTGACCGCTACACTTGCCAGCGCCCTAGCGCCCGCTCCTTTCGCTTCTTCCCTTCTTTCTCG
CCACGTTCCGGGCTTTCCCGTCAAGCTCTAAATCGGGGGCTCCCTTTAGGGTTCGATTTAGTGCTTTACGGCACCTCGA

CCCCCAAAACCTTGATTAGGGTGATGGTTCACGTAGTGGGCCATCGCCCTGATAGACGGTTTTTCGCCCTTTGACGTTGGA
 GTCCACGTTCTTTAATAGTGGACTCTTGTCCAAACTGGAACAACACTCAACCCTATCTCGGTCTATTCTTTTGATTTATAAG
 GGATTTTGGCGATTTTCGGCCTATTGGTTAAAAAATGAGCTGATTTAACAAAAATTTAACCGGAATTTTAACAAAATATTAAC
 GCTTACAATTTTCAGGTGGCACTTTTCGGGGAAATGTGCGCGGAACCCCTATTGTTTATTTTTCTAAATACATTCAAATATGT
 ATCCGCTCATGAGACAATAACCCTGATAAATGCTTCAATAATATTGAAAAAGGAAGAGTATGAGTATTCACATTTCCGTG
 TCGCCCTTATCCCTTTTTTTCGGCATTTCCTTCTGTTTTGCTCACCCAGAAACGCTGGTGAAGTAAAAGATGCTGAA
 GATCAGTTGGGTGCACGAGTGGGTTACATCGAACTGGATCTCAACAGCGGTAAGATCCTTGAGAGTTTTTCGCCCCGAAGA
 ACGTTTTCCAATGATGAGCACTTTAAAGTTCTGCTATGTGGCGCGGTATTATCCCGTATTGACGCCGGGCAAGAGCAACT
 CGGTCGCCGCATACACTATTCTCAGAATGACTTGGTTGAGTACTCACCAGTCACAGAAAAGCATCTTACGGATGGCATGAC
 AGTAAGAGAATTATGCAGTGTGCCATAACCATGAGTGATAAACAACACTGCGGCCAACTTACTTCTGACAACGATCGGAGGAC
 CGAAGGAGCTAACCGCTTTTTTGCACAACATGGGGGATCATGTAACCTGCGCTTGATCGTTGGGAACCGGAGCTGAATGAA
 GCCATACCAAACGACGAGCGTGACACCAGATGCCTGTAGCAATGGCAACAACGTTGCGCAAATTAATACTGGCGAACT
 ACTTACTCTAGCTTCCCGCAACAATTGATAGACTGGATGGAGGCGGATAAAGTTGCAGGACCACTTCTGCGCTCGGCCCT
 TCCGGCTGGCTGGTTTATTGCTGATAAATCTGGAGCCGGTGAGCGTGGCTCTGCGGTATCATTGCAGCACTGGGGCCAG
 ATGGTAAGCCCTCCCGTATCGTAGTTATCTACACGACGGGGAGTCAGGCAACTATGGATGAACGAAATAGACAGATCGCT
 GAGATAGGTGCCTCACTGATTAAGCATTGGTAGGAATTAATGATGTCTCGTTTAGATAAAAAGTAAAGTGATTAACAGCGCA
 TTAGAGCTGCTTAATGAGGTGCGAATCGAAGGTTTAAACAACCCGTAACCTCGCCAGAAGCTAGGTGTAGAGCAGCCTAC
 ATTGTATTGGCATGTAAAAAATAAGCGGGCTTTGCTCGACGCCCTTAGCCATTGAGATGTTAGATAGGCACCATACTCACTT
 TTGCCCTTTAGAAGGGGAAAGCTGGCAAGATTTTTACGTAATAACGCTAAAAGTTTTAGATGTGCTTTACTAAGTCATCGC
 GATGGAGCAAAAGTACATTTAGGTACACGGCCTACAGAAAAACAGTATGAAACTCTCGAAAATCAATTAGCCTTTTTATGC
 CAACAAGTTTTTTCACTAGAGAATGCATTATATGCACTCAGCGCAGTGGGGCATTTTACTTTAGGTTGCGTATTGGAAGAT
 CAAGAGCATCAAGTCGCTAAAGAAGAAAGGGAAACACCTACTACTGATAGTATGCCGCCATTATTACGACAAGCTATCGA
 ATTATTTGATCACCAAGGTGCAGAGCCAGCCTTCTATTTCGGCCTTGAATTGATCATATGCGGATTAGAAAAACAACCTAAA
 TGTGAAAGTGGGTCTTAAAAGCAGCATAACCTTTTTCCGTGATGGTAACTTCACTAGTTTTAAAAGGATCTAGGTGAAGATC
 CTTTTGATAATCTCATGACCAAAATCCCTAACGTGAGTTTTGTTCCACTGAGCGTCAGACCCGTAGAAAAGATCAAAG
 GATCTTCTTGAGATCCTTTTTTCTGCGCGTAATCTGCTGCTGCAAACAAAAAACCCCGTACCAGCGGTGGTTTTGTTT
 GCCGGATCAAGAGCTACCAACTCTTTTTCCGAAGGTAAGTGGCTTCAGCAGAGCGCAGATACCAATACTGCTTCTAGT
 GTAGCCGTAGTTAGGCCACCCTCAAGAAGTCTGTAGCACCGCCTACATACCTCGCTGCTAATCCTGTTACCAAGTGGCT
 GCTGCCAGTGGCGATAAGTCGTGTCTTACCGGGTTGGACTCAAGACGATAGTTACCGGATAAGGCGCAGCGTCCGGCT
 GAACGGGGGGTTCGTGCACACAGCCAGCTTGGAGCGAACGACCTACACCGAACTGAGATACCTACAGCGTGAGCTATG
 AGAAAGCGCCACGCTTCCGAAGGGAGAAAGGCGGACAGGTATCCGGTAAGCGGCAGGGTCCGAACAGGAGAGCGCAC
 GAGGGAGCTTCCAGGGGAAACGCCTGGTATCTTTATAGTCTGTGCGGTTTTGCCACCTCTGACTTGAGCGTCGATTTTT
 GTGATGCTCGTCAGGGGGCGGAGCCTATGAAAAACGCCAGCAACGCGGCCCTTTTTACGGTCTTGCCCTTTTGTCTGGC
 CTTTTGCTCACATGACCCGACA

pBESTluc:

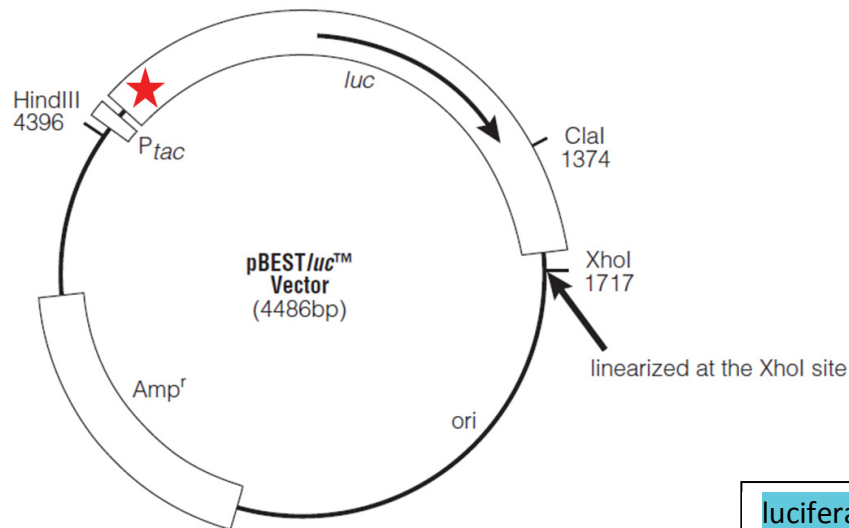


GGATCCAAATGGAAGACGCCAAAAACATAAAGAAAGGCCCGCGCCATTCTATCCTCTAGAGGATGGAACCGCTGGAGA
 GCAACTGCATAAGGCTATGAAGAGATACGCCCTGGTTCTGGAACAATTGCTTTTACAGATGCACATATCGAGGTGAACAT

CACGTACGCGAATACTTCGAAATGTCCGTTCCGGTTGGCAGAAGCTATGAAACGATATGGGCTGAATACAAATCACAGAA
TCGTCGTATGCAGTGAAAACCTCTTCAATTTATGCGCGTGGGCGCGTTATTTATCGGAGTTGCAGTTGCGCCCGC
GAACGACATTTATAATGAACGTGAATTGCTCAACAGTATGAACATTTGCGAGCCTACCGTAGTGTGTTGTTCCAAAAAGG
GTTGCAAAAAATTTGAACGTGCAAAAAAATTACCAATAATCCAGAAAATTATTATCATGGATTCTAAAACGGATTACCA
GGGATTTAGTCGATGTACACGTTTCGTCACATCTCATCTACCTCCCGGTTTAATGAATACGATTTTGTACCAGAGTCTTTG
ATCGTGACAAAAAATTGCACTGATAATGAATTCCTCTGGATCTACTGGTTACCTAAGGGTGTGGCCCTCCGCATAGAA
CTGCCTGCGTCAGATTCTCGCATGCCAGAGATCCTATTTTGGCAATCAAATCATTCCGGATACTGCGATTTAAGTGTGT
TCCATTCCATCACGGTTTTGGAATGTTTACTACACTCGGATATTTGATATGTGGATTTGAGTCGTCTTAATGTATAGATTTG
AAGAAGAGCTGTTTTACGATCCCTTCAGGATTACAAAATCAAAGTGCCTTGTAGTACCAACCTATTTTCATTCTTCGCC
AAAAGCACTCTGATTGACAAATACGATTTATCTAATTTACACGAAATTGCTTCTGGGGCGCACCTCTTCGAAAGAAGTC
GGGGAAGCGGTTGCAAAACGTTCCATCTTCAGGGATACGACAAGGATATGGGCTCACTGAGACTACATCAGCTATTCT
GATTACACCCGAGGGGATGATAAACCGGGCGCGGTGCGTAAAGTTGTTCCATTTTTGAAGCGAAGGTTGTGGATCTGG
ATACCGGAAAACGCTGGGCGTTAATCAGAGAGGCGAATTATGTGTAGAGGACCTATGATTATGTCCGTTATGTAAC
AATCCGGAAGCGACCAACGCTTGATTGACAAGGATGGATGGCTACATTCTGGAGACATAGCTTACTGGGACGAAGACGA
ACACTTCTCATAGTTGACCGCTTGAAGTCTTAAATTAATAACAAAGGATATCAGGTGGCCCCGCTGAATTGGAATCGATA
TTGTTACAACACCCCAACATCTTCGACGCGGGCGTGGCAGGTTCCCGACGATGACGCCGGTGAACCTCCGCGCCGTT
GTTGTTTTGGAGCACGGAAGACGATGACGGAAGAGATCGTGGATTACGTGGCCAGTCAAGTAACAACCGCGAAAA
AGTTGCGCGGAGGAGTTGTGTTTGTGGACGAAGTACCGAAAGTCTTACCGGAAAACCTGACGCAAGAAAAATCAGAGA
GATCCTATAAAGGCCAAGAAGGGCGGAAAGTCAAATTTGAAAATGTAAGTATTTCAGCGATGACGAAATTTAGCT
ATTGTAATCCTCCGAGGCCTCGAGGAATTCGACTCAATTAGTTCAGTCAGTTTCAGGATATTAGTCATCTACATTGATTA
TGAGTATTCAGAAATTCCTAAATATTCTGACAAATGCTTTCCCTAACTCCCCCATAAAAAACCCGCGAAGCGGGT
TTTTACGTTATTTGCGGATTAACGATTACTCGTTATCAGAACCGCCAGACCTGCGTTCAGCAGTTCTGCCAGGCTGGCAGA
TGCGTCTCCGAATTGATCCGTCGACCGATGCCCTTGAGAGCCTTCAACCCAGTCAGCTCCTTCCGGTGGGCGCGGGGCAT
GACTATCGTCGCCGCACTTATGACTGTCTTTATCATGCAACTCGTAGGACAGGTGCCGGCAGCGCTCTCCGTTCTC
GCTCACTGACTCGCTGCGCTCGGTCGTTCCGGTGCAGGAGCGGTATCAGCTCACTCAAAGGCGGTAATACGTTATCCAC
AGAATCAGGGGATAACGCGAGGAAAGCATGTGAGCAAAAGGCCAGCAAAAGGCCAGGAACCGTAAAAAGGCCGCGTT
GCTGGCGTTTTTCCATAGGCTCCGCCCTGACGAGCATCACAAAAATCGACGCTCAAGTCAGAGGTGGCGAAACCCGA
CAGGACTATAAAGATAACAGGCGTTTCCCCTGGAAGCTCCCTCGTGCCTCTCCTGTTCCGACCCTGCCGTTACCGGATA
CCTGTCCGCTTTCTCCCTTCGGAAGCGTGGCGCTTTCTCAATGCTCAGCTGTAGGTATCTCAGTTCGGTGTAGGTCGTT
CGCTCCAAGCTGGGCTGTGTGCACGAACCCCCGTTACGCCGACCGCTGCGCCTTATCCGGTAACTATCGTCTTGAGTCC
AACCCGTAAGACACGACTTATCGCCACTGGCAGCAGCCACTGGTAACAGGATTAGCAGAGCGAGGTATGTAGGCGGTG
CTACAGAGTTCTTGAAGTGGTGGCCTAACTACGGCTACACTAGAAGGACAGTATTTGGTATCTGCGCTCTGCTGAAGCCAG
TTACCTTCGAAAAAGAGTTGGTAGCTCTTGATCCGGCAAAACAAACCACCGCTGGTAGCGGTGGTTTTTTGTTGCAAGC
AGCAGATTACGCGCAGAAAAAAGGATCTCAAGAAGATCCTTTGATCTTTTCTACGGGGTCTGACGCTCAGTGAACGAA
AACTCACGTTAAGGGATTTTGGTCATGAGATTACAAAAAGGATCTTACCTAGATCCTTTAAATAAAAATGAAGTTTTA
AATCAATCTAAAGTATATATGAGTAAACTTGGTCTGACAGTTACCAATGCTTAATCAGTGAGGCACCTATCTCAGCGATCTG
TCTATTTGTTTCATCCATAGTTGCTGACTCCCCGTCGTGTAGATAACTACGATACGGGAGGGCTTACCATCTGGCCCCAGT
GCTGCAATGATACCGCGAGACCCAGCTCACCGGCTCCAGATTTATCAGCAATAAACCCAGCCAGCCGGAAGGGCCGAGCG
CAGAAGTGGTCTGCAACTTTATCCGCTCCATCCAGTCTATTAATTGTTGCCGGAAGCTAGAGTAAGTAGTTCGCCAGTT
AATAGTTTGCACAACGTTGTTGCCATTGCTACAGGCATCGTGGTGTACGCTCGTCGTTTGGTATGGCTTCATTAGCTCCG
GTTCCCAACGATCAAGGCGAGTTACATGATCCCCATGTTGTGCAAAAAAGCGGTTAGCTCCTTCGGTCTCCGATCGTTG
TCAGAAGTAAGTTGGCCGAGTGTATCACTCATGGTTATGGCAGCACTGCATAATTCTTACTGTCTGCTATCCGTAAG
ATGTTTTCTGTGACTGGTGAGTACTCAACCAAGTCACTTCTGAGAATAGTGTATGCGGCGACCGAGTTGCTCTTGGCCGGC
GTCAATACGGGATAATACCGCGCCACATAGCAGAATTTAAAAGTGTCTCATCTTGGAAAAAGTTCTTCGGGGCGAAAACT
CTCAAGGATCTTACCGCTGTTGAGATCCAGTTCGATGTAACCCACTCGTGCACCCAACTGATCTTTCAGCATCTTTACTTTCA
CCAGCGTTTCTGGGTGAGCAAAAAACAGGAAGGCAAAATGCCGAAAAAAGGGAATAAGGGCGACACGGAATGTTGAA
TACTCATACTCTTCTTTTTCAATATTATTGAAGCATTTATCAGGGTTATTGTCTCATGAGCGGATACATATTTGAATGTATTT
AGAAAAATAAACAAATAGGGGTTCCGCGCACATTTCCCCGAAAAGTGCCACCTGACGTCTAAGAAACCATTATTATCATGA
CATTAACTATAAAAAATAGGCGTATCACGAGGCCCTTTCGTTCTCAAGAATTCTGGCGAATCCTCTGACCAGCCAGAAAAAC
GACCTTTCTGTGGTGAACCGGATGCTGCAATTACAGAGCGGCAGCAAGTGGGGGACAGCAGAAGACCTGACCGCCGACG
AGTGGATGTTTGACATGGTGAAGACTATCGCACCATCAGCCAGAAAACCGAATTTGCTGGGTGGGCTAACGATATCCGC

CTGATGCGTGAACGTGACGGACGTAACCACGCGACATGTGTGTGCTGTTCCGCTGGGCATGCCAGGACAACCTTCTGGTC
CGGTAACGTGCTGAGCCCGCCAAGCTTACTCCCCATCCCCCTGTTGACAATTAATCATCGGCTCGTATAATGTGTGGAATT
GTGAGCGGATAACAATTTACACAGGAAACA*

pBESTluc-mut:

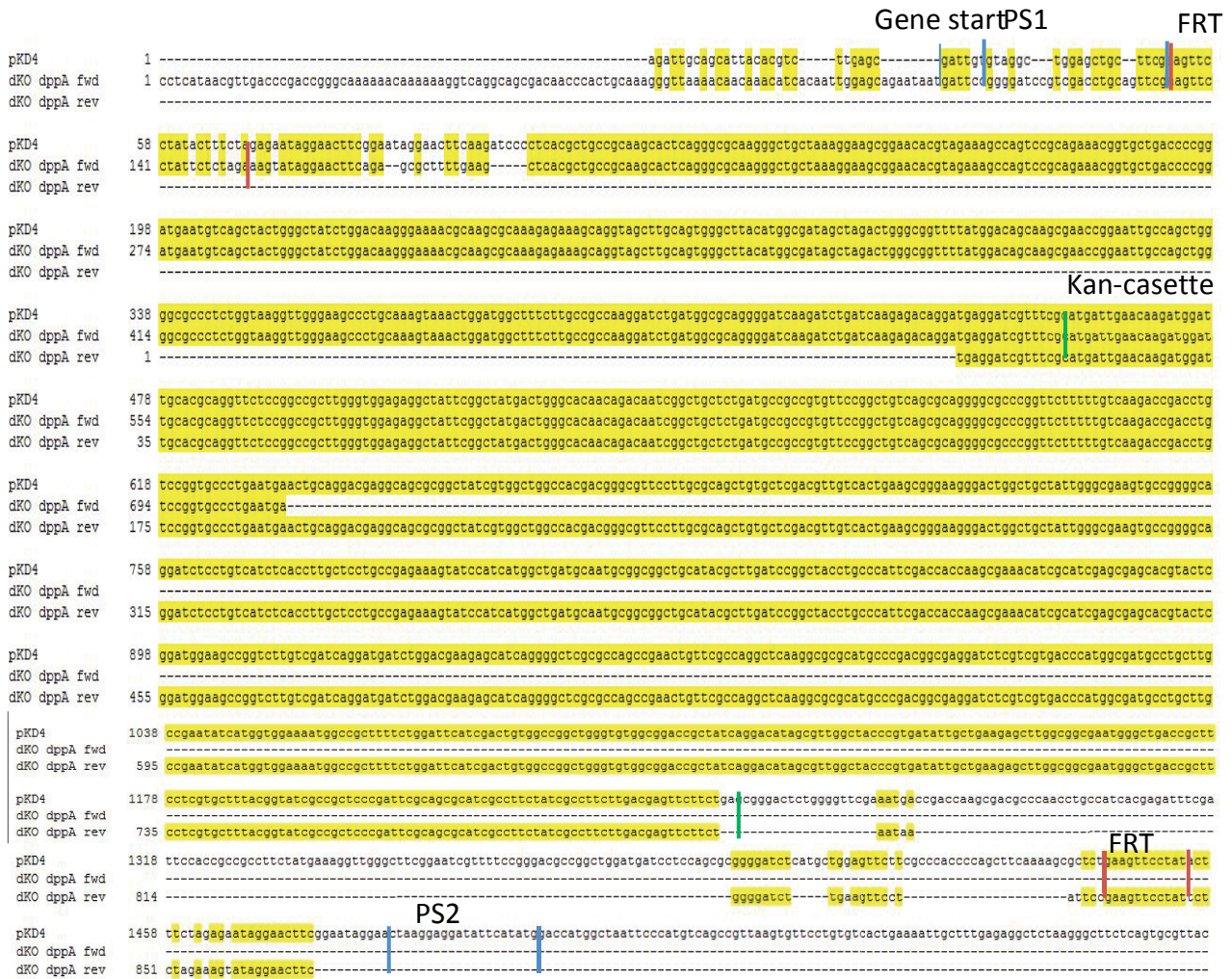
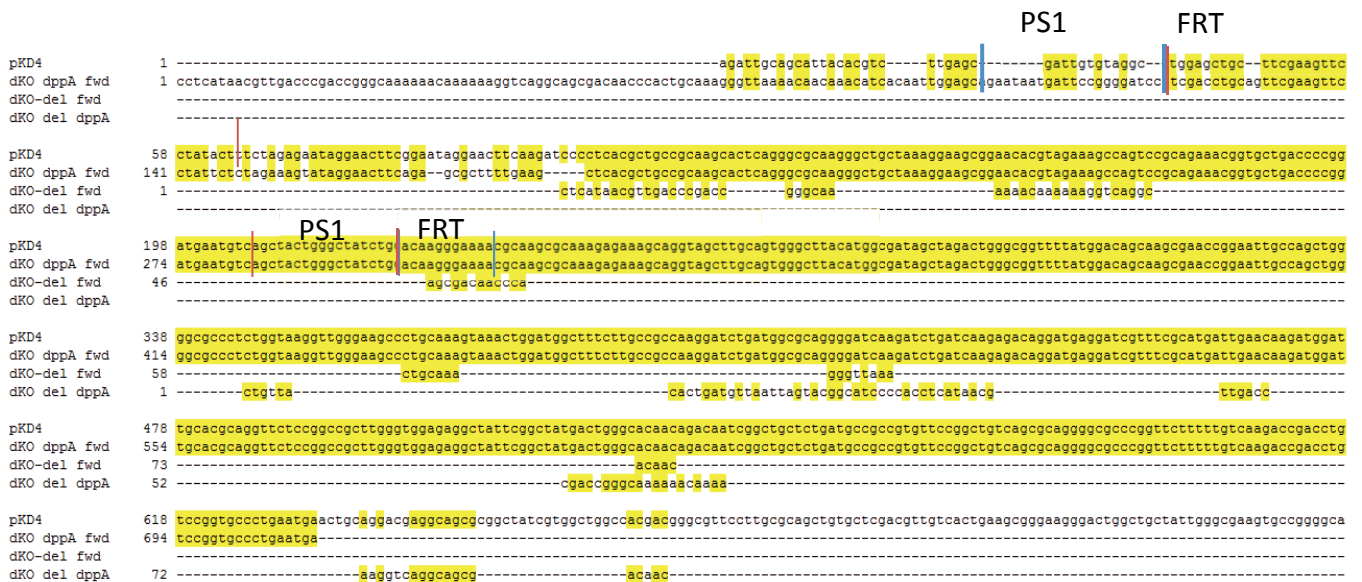


GGATCCAAATGGAAGACGCCAAAAACATAAAGAAAGGCCCGGCCATTCTATCCTCTAGAGGATGGAACCGCTGGAGA
GCAACTGCATAAGGCTATGAAAGATACGCCCTGGTTCTGGAACAATTGCTTTTACAGATGCACATATCGAGGTGAACAT
CACGTACGCGGAATACTTCGAAATGTCCGTTCCGTTGGCAGAGCTATGAAACGATATGGGCTGAATACAAATCACAGAA
TCGTCGTATGCAGTGAAGAACTCTTCAATTCTTTATGCCGGTGTGGGCGCGTTATTTATCGGAGTTGCAGTTGCGCCCGC
GAACGACATTTATAATGAACGTGAATTGCTCAACAGTATGAACATTCGCAGCCTACCGTAGTGTGTTGTTCCAAAAAGGG
GTTGCAAAAAATTTGAACGTGCAAAAAAATTACCAATAATCCAGAAAATTATTATCATGGATTCTAAAACGGATTACCA
GGGATTTCAAGTCGATGTACAGTTCGTCACATCTCATCTACCTCCCGTTTTAATGAATACGATTTTGTACCAGAGTCCTTTG
ATCGTGACAAAAAATTGCACTGATAATGAATTCCTCTGGATCTACTGGGTTACCTAAGGGTGTGGCCCTTCCGCATAGAA
CTGCCTGCGTCAGATTCTCGCATGCCAGAGATCTATTTTTGGCAATCAAATCATTCCGGATACTGCGATTTAAGTGTGT
TCCATTCCATCACGTTTTGGAATGTTTACTACACTCGGATATTTGATATGTGGATTTGAGTCGTCTTAATGTATAGATTTG
AAGAAGAGCTGTTTTACGATCCCTTCAGGATTACAAAATCAAAGTGCCTTGTAGTACCAACCCTATTTTCATTCTTCGCC
AAAAGCACTCTGATTGACAAATACGATTTATCTAATTTACACGAAATTGCTTCTGGGGGCGCACCTCTTTCGAAAGAAGTC
GGGGAAGCGGTTGCAAAACGCTTCCATCTTCCAGGGATACGACAAGGATATGGGCTCACTGAGACTACATCAGCTATTCT
GATTACACCCGAGGGGATGATAAACGGGCGCGGTCCGTTAAAGTTGTTCCATTTTTGAAGCGAAGGTTGTGGATCTGG
ATACCGGAAAAACGCTGGGCGTTAATCAGAGAGGCGAATTATGTGTCAGAGGACCTATGATTATGTCCGTTATGTAAC
AATCCGGAAGCGACCAACGCCTTGATTGACAAGGATGGATGGCTACATTCTGGAGACATAGCTTACTGGGACGAAGACGA
ACACTTCTCATAGTTGACCGCTTGAAGTCTTTAATTAATACAAAGGATATCAGGTGGCCCCGCTGAATTGGAATCGATA
TTGTTACAACACCCCAACATCTTCGACGCGGGCGTGGCAGGTCTTCCCGACGATGACGCCGGTGAACCTCCCGCCCGCTT
GTTGTTTTGGAGCACGGAAGACGATGACGAAAAAGAGATCGTGGATTACGTGGCCAGTCAAGTAACAACCGCGAAAA
AGTTGCGCGGAGGAGTTGTGTTGTGGACGAAGTACCGAAAGGCTTACCGGAAAACCTGACGCAAGAAAAATCAGAGA
GATCCTCATAAAGGCCAAGAAGGGCGGAAAGTCCAAATTGTAAATGTAAGTGTATTAGCGATGACGAAATTTAGCT
ATTGTAATCCTCCGAGGCCTCGAGGAATTCGACTCAATTAGTTCAGTCAGTTTCAGGATATTAGTCATCTCTACATTGATTA
TGAGTATTCAGAAAATTCCTAAATATTCTGACAAATGCTCTTCCCTAAACTCCCCCATAAAAAAACCGCCGAAGCGGGT
TTTTACGTTATTTGCGGATTAACGATTACTCGTTATCAGAACCGCCAGACCTGCGTTCAGCAGTTCTGCCAGGCTGGCAGA

TGCGTCTTCCGAATTGATCCGTCGACCGATGCCCTTGAGAGCCTTCAACCCAGTCAGCTCCTTCCGGTGGGCGCGGGGCAT
GACTATCGTCGCCGCACTTATGACTGTCTTCTTTATCATGCAACTCGTAGGACAGGTGCCGGCAGCGCTCTTCCGCTTCTC
GCTCACTGACTCGCTGCGCTCGGTCTGCTCGGCTGCGGCGAGCGGTATCAGCTCACTCAAAGGCGGTAATACGGTTATCCAC
AGAATCAGGGGATAACGCAGGAAAGAACATGTGAGCAAAAGGCCAGCAAAAGGCCAGGAACCGTAAAAAGGCCGCGTT
GCTGGCGTTTTTCCATAGGCTCCGCCCCCTGACGAGCATCACAAAAATCGACGCTCAAGTCAGAGGTGGCGAAACCCGA
CAGGACTATAAAGATAACCAGGCGTTTTCCCTGGAAGCTCCCTCGTGCCTCTCCTGTTCCGACCCTGCCGCTTACCGGATA
CCTGTCCGCTTTCTCCCTTCGGGAAGCGTGGCGCTTTCTCAATGCTCACGCTGTAGGTATCTCAGTTCGGTGTAGGTCGTT
CGCTCCAAGCTGGGCTGTGTGCACGAACCCCGTTCAGCCGACCGCTGCGCCTTATCCGGTAACTATCGTCTTGAGTCC
AACCCGGTAAGACACGACTTATCGCCACTGGCAGCAGCCACTGGTAAACAGGATTAGCAGAGCGAGGTATGTAGCGGGTG
CTACAGAGTCTTGAAGTGGTGGCCTAACTACGGCTACACTAGAAGGACAGTATTTGGTATCTGCGCTCTGCTGAAGCCAG
TTACCTTCGGAAAAAGAGTTGGTAGCTTTGATCCGGCAAAACAAACCACCGTGGTAGCGGTGGTTTTTTTGTGGAAGC
AGCAGATTACGCGCAGAAAAAAGGATCTCAAGAAGATCCTTTGATCTTTTCTACGGGGTCTGACGCTCAGTGGAACGAA
AACTCACGTTAAGGGATTTTGGTCATGAGATTATCAAAAAGGATCTTCACCTAGATCCTTTTAAATAAAAATGAAGTTTTA
AATCAATCTAAAGTATATATGAGTAACTTGGTCTGACAGTTACCAATGCTTAATCAGTGAGGCACCTATCTCAGCGATCTG
TCTATTTCTGTTTATCCATAGTTGCTGACTCCCCGTCGTGTAGATAACTACGATACGGGAGGGCTTACCATCTGGCCCCAGT
GCTGCAATGATACCGCGAGACCCACGCTCACCGGCTCCAGATTTATCAGCAATAAACCCAGCCAGCCGGAAGGGCCGAGCG
CAGAAGTGGTCTGCAACTTTATCCGCTCCATCCAGTCTATTAATTGTTGCCGGGAAGCTAGAGTAAGTAGTTCGCCAGTT
AATAGTTTGCACAACGTTGTTGCCATTGCTACAGGCATCGTGGTGTACGCTCGTCTGTTGGTATGGCTTATTAGCTCCG
GTTCCCAACGATCAAGGCGAGTTACATGATCCCCATGTTGTGCAAAAAGCGGTTAGCTCCTTCGGTCTCCGATCGTTG
TCAGAAGTAAGTTGGCCGAGTGTATCACTCATGGTTATGGCAGCACTGCATAATTCTTACTGTCATGCCATCCGTAAG
ATGCTTTTCTGTGACTGGTGAGTACTCAACCAAGTCACTTCTGAGAATAGTGTATGCGGCGACCGAGTTGCTCTTGCCCGC
GTCAATACGGGATAATACCGCGCCACATAGCAGAACTTTAAAAGTGTCTATCATTGGAAAACGTTCTTCGGGGCGAAAAC
CTCAAGGATCTTACCGCTGTTGAGATCCAGTTCGATGTAACCCACTCGTGCACCCAAGTATCTTACGATCTTTTACTTTCA
CCAGCGTTTCTGGGTGAGCAAAAACAGGAAGGCAAAATGCCGCAAAAAGGGAATAAGGGCGACACGGAAATGTTGAA
TACTCATACTCTTCTTTTCAATATTATTGAAGCATTTATCAGGGTTATTGTCTCATGAGCGGATAACATTTGAATGTATT
AGAAAAATAAACAAATAGGGGTTCCGCGCACATTTCCCGAAAAAGTGCCACCTGACGTCTAAGAAAACATTATTATCATGA
CATTAACTATAAAAATAGGCGTATCACGAGGCCCTTTCTGTTCAAGAATTCTGGCGAATCCTCTGACCAGCCAGAAAAC
GACCTTTCTGTGGTGAACCGGATGCTGCAATTCAGAGCGGCAGCAAGTGGGGGACAGCAGAAGACCTGACCGCCGAG
AGTGGATGTTTACATGGTGAAGACTATCGCACCATCAGCCAGAAAACCGAATTTGCTGGGTGGGCTAACGATATCCGC
CTGATGCGTGAACGTGACGCGACGTAACCACCGCGACATGTGTGTGCTGTTCCGCTGGGCATGCCAGGACAACCTTCTGGT
CGGTAACGTGCTGAGCCCGCCAAGCTTACTCCCATCCCTGTTGACAATTAATCATCGGCTCGTATAATGTGTGGAATT
GTGAGCGGATAACAATTTACACAGGAAACA*

pBestLuc is designed for efficient expression of firefly luciferase (*Photinus pyralis*) in *E. coli*. It contains a tac promoter, two tandem prokaryotic ribosome binding sites, and a transcriptional terminator down-stream of the luciferase gene. (Luciferase coding region: 9 - 1658, Amp resistance coding region: 3985 - 3038) The origin of replication is from pUC18.

Alignments of constructed knockouts

Sequencing results of *dppA*-knockout of JW3513Deletion of kan-cassette in the *dppA*- gene of the double knockout $\Delta dppA$ - $\Delta sapA$ 

Deletion of kan-cassette in the *sapA*- gene of the double knockout $\Delta dppA$ - $\Delta sapA$

sapA

```

del-resistan 1 -----agtaagatagcctctttacataaaaacccctaatattatggccagggtattatcgtctcttttgggtgattgctggaactgtgtgagtggtcaggc
del resistan 1 ttaagaccctgaacacaaaacgtaatggcaaatgcaaatgcaaatattatgtaagatagcctctttacataaaaacccctaatattatggccagggtattatcgtctcttttgggtgattgctggaactgtgtgagtggtcaggc
                                     PS1          FRT          FRT          PS2
del-resistan 94 aatcgccgcgctgaatctccccgcgatgctgatatccgcgacagcggtttctggttaggctggagctgcttcaagtccctatactttctagagaataggaaacttcggaataggaaataaggaggatattcatatgctc
del resistan 141 aatcgccgcgctgaatctccccgcgatgctgatatccgcgacagcggtttctggttaggctggagctgcttcaagtccctatactttctagagaataggaaacttcggaataggaaataaggaggatattcatatgctc
                                     PS1          FRT          FRT          PS2
del-resistan 234 tggtaacttagccggtttgtaacgcctcctcttctgctgggtgta-tccgagaaaaacaggatgaggtgaaaaaacctgattatcttccacctaacgcgcattttgttattgattgacacctgttctcctgctgacc
del resistan 281 tggtaacttagccggtttgtaacgcctcctcttctgctgggtgtaatcgc-----gaaagaaacagg-----

```

sapA stop

Deletion of cm-cassette in the *oppA* gene of the triple knockout $\Delta dppA$ - $\Delta sapA$ - $\Delta oppA$

```

oppA + 200 b 1 tgtgtctcgacaggggagacacagtcgaaatcgacataaagtgatgctgtaatcaccagaataaaatgctggtgatagtaatacgtaacgataaagtaacctgacagcagaaagtctccgagcctgtgcaggggtccc
tK01 oppA fw -----
oppA + 200 b 141 aatccgggattacacatgctggttaataaccagtaattataatgagggagtcocaaaaaacatgaccaatccaccaagagaagtttagtagcagctggcgttctggtctgcgtaatggcaggaatgctgcgctggcagc
tK01 oppA fw 1 -----tgctgggta-taccagtaattataatgagggagtcocaaaaaacatgaccaatccaccaagagaagtttagtagcagctggcgttctggtctgcgtaatgg-----
                                     start oppA
oppA + 200 b 281 tgatgtaccgcagggctcacactggcggaaaaaacaactggtacgtaacaatggttcagaagttcagtcattagatccgcacaaaaatgaagggtttccggagcttaataatcagccgagacctgttgaaggcttac
tK01 oppA fw 102 -----tgtaggg-----tggagctgcttogaagt-----tctatactt-----
oppA + 200 b 1679 taaagcagaacaacagctggataaggattcggccattgttctctgtttactacgtgaatgcgcgtctgtgaaaccgtgggttggtggctataccggcaaaagatccgctggataatacctataccoggaatgtgaca
tK01 oppA re 566 taagg-----agga-----tattcata-----tggctataccggcaaaagatccgctggataatacctataccoggaatgtgaca
                                     stop oppA
oppA + 200 b 1819 ttgtgaagcactatggcaatacgtggggcaggagtgctctgccaggtgctctgatttttatcgcattacaagaaggcagagccagaaggtagggcaatgttaaaattatctacgtcgtctctggaagcagctcc
tK01 oppA re 636 ttgtgaagcactaatggcaatacgtggggcaggagtgctctgccaggtgctctgatttttatcgcattacaagaaggcagagcc-----

```

Curriculum vitae

Education

- 02/2011-present** **PhD student and research assistant** at Heinrich-Heine-Universität Düsseldorf
- Titel: *Uptake of the dipeptide-like antibiotic negamycin into bacterial cells*
- Supervisor: Prof. Dr. Heike Brötz-Oesterhelt
- 02/2011-08/2014** **Scholarship** of the „Studienstiftung des deutschen Volkes“
- 01/2010 -12/2010** **Diplomathesis** at the University of British Columbia, Vancouver
- Titel: *FurA is a stress-sensor in Mycobacteria and is negatively regulated by WhiB7*
- Supervisor: Prof. Dr. Wolfgang Wohlleben (Universität Tübingen), Prof. Dr. Charles J. Thompson (University of British Columbia)
- 10/2005 - 12/2010** Diploma in Biology (Eberhard-Karls Universität, Tübingen)
- Degree **Diploma**; Final grade: 1.0
- 08/1996 - 06/2005** **High school degree**, Gymnasium Hochdahl, Erkrath
- Final grade: 1.9

Work experience and internships

- 08/2015-present** **Junior Product Manager VASC**, St. Jude Medical GmbH, Eschborn
- 02/2011-08/2014** **Teaching assistant** „Cytological and histological basics“ and „pharmaceutical Biology I“ for pharmacy-students, Heinrich-Heine-Universität Düsseldorf
- 07/2014-04/2015** **Internship in Therapeutic Value Management**, Janssen-Cilag GmbH, Neuss
- product management, communication, health outcome management
- 04/2007- 01/2009** **Teaching assistant** „Microbiology“, „Cell-biology“ and „Genetics“ for biology-students,

Eberhard-Karls-Universität Tübingen

01/2003-09/2005

Temporary work, NewLab BioQuality AG, Erkrath

- receptionist and accounting
- insights in lab work

01/2001-12/2002

volunteer experience, EJH Hochdahl

- leading and organizing a kids-group „Teenie-Club“

Additional skills

Advanced training

„Interdisciplinary Graduate and Research Academy
Düsseldorf“ (iGrad)

- „Introduction to good scientific practice“
- „Presenting Science 1“
- „Fundamentals of Project Management“
- „Career planning in business-How to shape up your future“

workshops of the **be.boosted-Shaping Future Global leaders** program

- “Effective negotiation”
- “Effective communication”

Languages

German: native speaker

English: fluent in spoken and written

Italian: intermediate

French: basic

Latin: degree: Latinum

Computer skills

MS Office, GraphPad Prism, Reference Manager, Endnote

Personal interests

Tennis, skiing, running, traveling, reading, meeting friends

Publications

- Paper:** Wenzel, M., Chiriac A. I., Otto, A., Zweytick D., May C., **Schumacher, C.**, Gust, R., Albada, H. B., Penkova, M., Krämer U., Erdmann, R., Mtzler-Nolte, N., Straus, S. K., Bremer, E., Becher, D., Brötz-Oesterhelt, H., Sahl, H.-G., Bandow, J. E. "Small cationic antimicrobial peptides delocalize peripheral membrane proteins" Proc Natl Acad Sci USA (2014), Epub 2014 March 25.
- Schumacher, C.**[§], Berscheid, A.[§], Zerfaß, I., Lampe, U., Abst, A., Frankenstein-Paul, H., Bendas, G., Glüsenkamp, K.-H., Brötz-Oesterhelt, H. „Negamycin enterst he bacterial cell via multiple uptake routes“ *in preperation*
- Poster:** **Schumacher, C.**, Zerfaß, I., Glüsenkamp, K.-H., Brötz-Oesterhelt, H. "Investigations on the molecular route of Negamycin uptake" 7. Joint Ph.D. Students Meeting, Freudenstadt, Germany, November 2012.
- Schumacher, C.**, Zerfaß, I., Glüsenkamp, K.-H., Brötz-Oesterhelt, H. "Investigations on the molecular route of Negamycin uptake" Jahrestagung der Vereinigung für Allgemeine und Angewandte Mikrobiologie (VAAM), Bremen, Germany, March 2013. Published in: Tagungsband BIOSpektrum (2013); S. 104. FTP065
- Schumacher, C., **Berscheid, A.**, Zerfaß, I., Glüsenkamp, K.-H., Brötz-Oesterhelt, H. "Negamycin enters the bacterial cell via multiple uptake routes" Gordon Research Conferences: New Antibacterial Discovery & Development, Ventura CA United States, March 2014
- Schumacher, C.**, Berscheid, A., Zerfaß, I., Glüsenkamp, K.-H., Brötz-Oesterhelt, H. "Uptake of the antibiotic negamycin into bacterial cells" 24th ECCMID, Barcelona Spain, May 2014
- Presentation:** **Schumacher, C.**, Zerfaß, I., Glüsenkamp, K.-H., Brötz-Oesterhelt, H. "Progress in the sperabillin project and the uptake of negamycin" InA (Innovative Antibiotika aus NRW) Progress-Meeting, Bochum, Germany, January 2013.
- Schumacher, C.**, Zerfaß, I., Glüsenkamp, K.-H., Brötz-Oesterhelt, H. "Untersuchungen zum molekularen Mechanismus der Aufnahme Peptid-haltiger Antibiotika in die Bakterienzelle" Herbsttagung der Doktorandenforen - Studienstiftung des deutschen Volkes, Köln, Deutschland, November 2013.

§ Both authors contributed equally to this work.

Schumacher, C., Zerfaß, I., Glüsenkamp, K.-H., Brötz-Oesterhelt, H. "Uptake of the antibiotic negamycin into bacterial cells" InA (Innovative Antibiotika aus NRW) Progress-Meeting, Mettmann, Germany, December 2013.

Acknowledgements

I thankfully acknowledge Prof. Heike Brötz-Oesterhelt for letting me carrying out my PhD-thesis in her laboratories, for her time, advice and support in my research. Furthermore I want to thank her for encouraging me to participate in different conferences and gaining experience in the pharmaceutical industry.

I want to thank Prof. Peter Proksch for his kind support and contribution to my thesis, by being my second supervisor.

To Prof. Reinhold Egger my “Vertrauensdozent” from the Studienstiftung des deutschen Volkes, who gave me advices during my PhD and was encouraging me at any time point. Furthermore I want to thank the “Studienstiftung des Deutschen Volkes” for supporting me during my PhD and for the great opportunities they offered.

I cannot thank enough my colleagues: my Postdoc Anne Berscheid, Peter Sass, Heike Goldbach-Gecke, Kirsten Famulla, Dhana Thomy, our adopted Lena Hammerschmidt, Imran Malik, Clemens Lux, Ilka Zerfaß and Katharina Arenz for supporting me, for cheering me up in times of “research-frustration” and for making the last years to such a precious experience.

Especially I want to thank Kirsten, Heike, Lena and Dhana who became very close friends and I really miss the chats, the laughter and coffee together. I cannot wait for the next girls-nights, dinners and trips to come. I want to thank Andy Marmann and Thomas Gecke, who quickly became good friends and part of our group and unforgettable BBQ-Parties too.

I want thank my other colleagues and friends: Ido, Alex and Christopher. We experienced so many thinks together in the last years, from Karneval and parties to cooking evenings.

I wish to thank my family: my parents, my siblings and David and Charlotte (and of course Amélie and Emil). You were always supporting me, giving me advices, cheering me up, encouraging me, cursing with me if I needed it and always believed in me, even when I had my doubts. Thank you so much for that!

To my close friends Nici, Moritz, Inga, Frank, Kathi, Elena, Anna and Julia, whom I always can count on no matter where I am. You were always interested in my PhD, and stayed next to me at any time.

And of course to my Blondie group: Henni, Jenny and Dani. They started the “research-path” with me and became amazing friends. Even though we are distributed all over Germany, you are always there for me, support me and I want to thank you for that.

To Emanuele Ciglia I want to give a special thanks. You were always there for me, supporting me, listening to my complains, you cheered me up, distracted me and you always believed in me. You stayed close to me even when I was frustrated and upset and you always had a good advice. We did the “project PhD” together and became an amazing team.